frontiers | Research Topics

Therapeutic relevance and mechanisms of neuro-immune communication in brain injury

Edited by
Yuchuan Ding, Feng Zhang, Zhang Pengyue, Xiangjian Zhang, Yunping Deng and Yulong Bai

Published in
Frontiers in Cellular Neuroscience

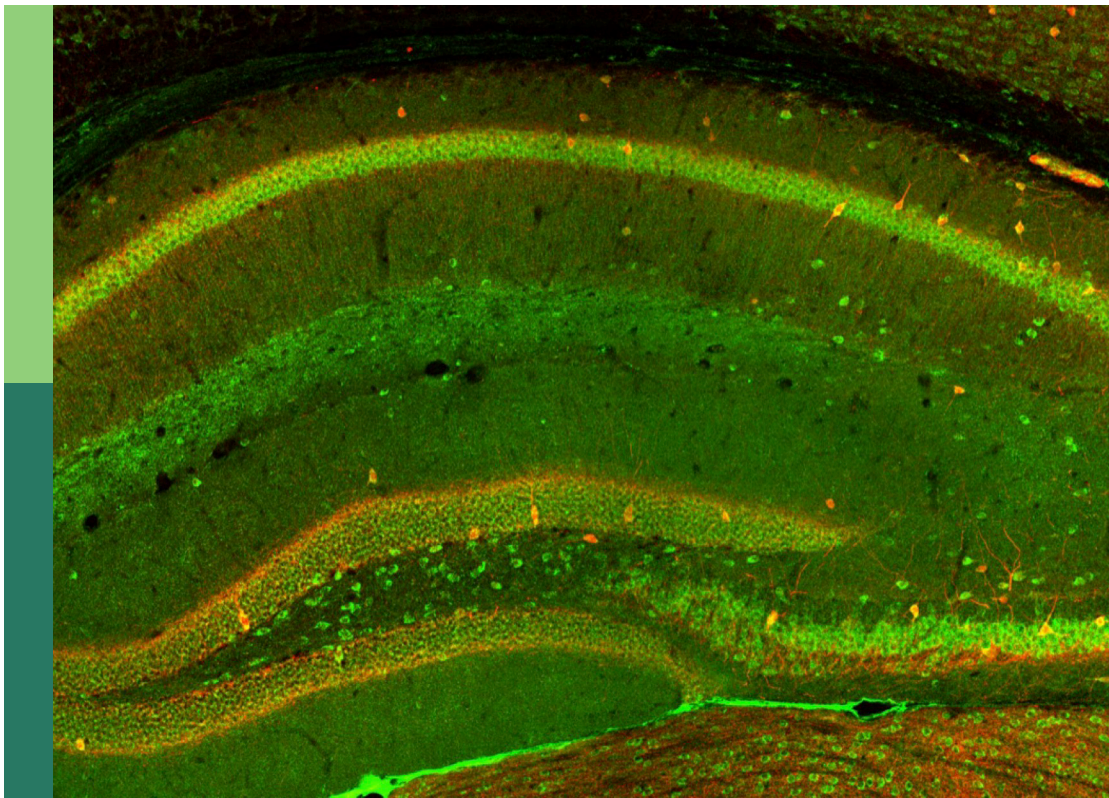

ISSN 1664-8714
ISBN 978-2-8325-3253-9
DOI 10.3389/978-2-8325-3253-9

About Frontiers

Frontiers is more than just an open access publisher of scholarly articles: it is a pioneering approach to the world of academia, radically improving the way scholarly research is managed. The grand vision of Frontiers is a world where all people have an equal opportunity to seek, share and generate knowledge. Frontiers provides immediate and permanent online open access to all its publications, but this alone is not enough to realize our grand goals.

Frontiers journal series

The Frontiers journal series is a multi-tier and interdisciplinary set of open-access, online journals, promising a paradigm shift from the current review, selection and dissemination processes in academic publishing. All Frontiers journals are driven by researchers for researchers; therefore, they constitute a service to the scholarly community. At the same time, the *Frontiers journal series* operates on a revolutionary invention, the tiered publishing system, initially addressing specific communities of scholars, and gradually climbing up to broader public understanding, thus serving the interests of the lay society, too.

Dedication to quality

Each Frontiers article is a landmark of the highest quality, thanks to genuinely collaborative interactions between authors and review editors, who include some of the world's best academicians. Research must be certified by peers before entering a stream of knowledge that may eventually reach the public - and shape society; therefore, Frontiers only applies the most rigorous and unbiased reviews. Frontiers revolutionizes research publishing by freely delivering the most outstanding research, evaluated with no bias from both the academic and social point of view. By applying the most advanced information technologies, Frontiers is catapulting scholarly publishing into a new generation.

What are Frontiers Research Topics?

Frontiers Research Topics are very popular trademarks of the *Frontiers journals series*: they are collections of at least ten articles, all centered on a particular subject. With their unique mix of varied contributions from Original Research to Review Articles, Frontiers Research Topics unify the most influential researchers, the latest key findings and historical advances in a hot research area.

Find out more on how to host your own Frontiers Research Topic or contribute to one as an author by contacting the Frontiers editorial office: frontiersin.org/about/contact

Therapeutic relevance and mechanisms of neuro-immune communication in brain injury

Topic editors

Yuchuan Ding — Wayne State University, United States
Feng Zhang — Third Hospital of Hebei Medical University, China
Zhang Pengyue — Yunnan University of Traditional Chinese Medicine, China
Xiangjian Zhang — Second Hospital of Hebei Medical University, China
Yunping Deng — University of Tennessee Health Science Center (UTHSC), United States
Yulong Bai — Fudan University, China

Citation

Ding, Y., Zhang, F., Pengyue, Z., Zhang, X., Deng, Y., Bai, Y., eds. (2023). *Therapeutic relevance and mechanisms of neuro-immune communication in brain injury*. Lausanne: Frontiers Media SA. doi: 10.3389/978-2-8325-3253-9

Table of contents

frontiers | Frontiers in Cellular Neuroscience

TYPE Editorial
PUBLISHED 01 August 2023
DOI 10.3389/fncel.2023.1209083

OPEN ACCESS

EDITED AND REVIEWED BY
Dirk M. Hermann,
University of Duisburg-Essen, Germany

*CORRESPONDENCE
Pengyue Zhang
✉ zpy19802000@163.com

RECEIVED 20 April 2023
ACCEPTED 20 July 2023
PUBLISHED 01 August 2023

CITATION
Zhang P, Bai Y, Zhang F, Zhang X, Deng Y and Ding Y (2023) Editorial: Therapeutic relevance and mechanisms of neuro-immune communication in brain injury.
Front. Cell. Neurosci. 17:1209083.
doi: 10.3389/fncel.2023.1209083

Editorial: Therapeutic relevance and mechanisms of neuro-immune communication in brain injury

Pengyue Zhang[1]*, Yulong Bai[2], Feng Zhang[3], Xiangjian Zhang[4], Yunping Deng[5] and Yuchuan Ding[6]

[1]Institute of Acupuncture, Tuina and Rehabilitation, The Second Clinical Medical School, Yunnan University of Traditional Chinese Medicine, Kunming, China, [2]Department of Rehabilitation Medicine, Huashan Hospital Affiliated to Fudan University, Shanghai, China, [3]Department of Rehabilitation Medicine, The Third Hospital of Hebei Medical University, Shijiazhuang, China, [4]Department of Neurology, Second Hospital of Hebei Medical University, Shijiazhuang, China, [5]Department of Anatomy and Neurobiology, University of Tennessee Health Science Center (UTHSC), Memphis, TN, United States, [6]Department of Neurosurgery, Wayne State University School of Medicine, Detroit, MI, United States

KEYWORDS

neuro-immune communication, inflammatory, brain injury, therapeutic strategy, neuroprotection

Editorial on the Research Topic
Therapeutic relevance and mechanisms of neuro-immune communication in brain injury

For many years, the central nervous system (CNS) was thought to be immune-privileged due to the presence of the blood-brain barrier (BBB) and the absence of lymphatic vasculature. However, recent studies have uncovered the intricate interactions between the CNS and the immune system. In particular, microglia–resident immune cells in the brain–share developmental origins and functions with monocytes in the immune system, playing crucial roles in monitoring and modulating neuronal activity (Vidal-Itriago et al., 2022).

Recent studies have revealed that the dura and meningeal compartments may serve as critical channels for communication between the CNS and the immune system. Numerous immune cells reside in the dura and meninges, and the cerebrospinal fluid (CSF) produced by the choroid plexus in the brain can enter the cervical lymph nodes and cranial bone marrow via the dura lymphatic system (Aspelund et al., 2015; Vera Quesada et al., 2023). This evidence suggests that the brain can regulate the immune system through molecules in the CSF (Kisler and Zlokovic, 2022; Mazzitelli et al., 2022; Pulous et al., 2022). Additionally, inflammatory factors released at injury sites can stimulate and regulate peripheral nerves through specific cytokines, such as pathogen-associated molecular patterns, TNF, and IL-1ß (Bourhy et al., 2022). Using optogenetics and chemogenetics, Poller and colleagues demonstrated that brain motor circuits can regulate neutrophil mobilization, distribution, and function during stress through skeletal-muscle-derived chemokines (Poller et al., 2022). At the same time, stress can mobilize bone marrow-derived monocytes to the brain via the hypothalamic-pituitary-adrenal (HPA) axis, exacerbating neuroinflammation and worsening anxiety-like behaviors (Niraula et al., 2018). These findings indicate that although the brain is immune-privileged, it still regulates and communicates with the immune system. Conversely, the immune system

also affects brain function. Dysregulation of the immune system is a critical cause and shared characteristic of neurological disorders, such as cerebral ischemia, intracerebral hemorrhage, brain trauma, and neurodegenerative diseases. In brain injury, microglia are activated and participate in neuroinflammatory responses, BBB permeability, the removal of dead cells and debris, and subsequent neurogenesis, synaptogenesis, and myelination through the release of soluble factors and phagocytic capacity (Paolicelli et al., 2022). Meanwhile, BBB destruction promotes mononuclear cell infiltration from the peripheral blood, facilitating crosstalk between the CNS and the immune system (Buckley and McGavern, 2022). As such, neuroimmune communication is not only an essential pathophysiological mechanism but also a potential therapeutic target for brain injury.

Although the neuroinflammatory response to brain injury has both favorable and unfavorable aspects, existing research suggests that nearly all current brain injury treatments can achieve neuroprotection by inhibiting the neuroinflammatory response.

Neuroprotection against synthetic drugs and natural extracts

Neuroinflammation can exacerbate both acute and secondary injury and lead to adverse long-term outcomes in brain injury. Based on the inflammatory signaling pathway, neuroscientists have found many drugs for the treatment of brain injury in animal studies, such as salvinorin A (a highly selective kappa opioid receptor agonist) (Misilimu et al., 2022), morphine (Rahimi et al., 2021), ACT001 (a sesquiterpene lactone derivative) (Cai et al., 2022), febuxostat (Wang et al., 2022), ethyl pyruvate (Shi et al., 2015), and amantadine (Leclerc et al., 2021). Traditional Chinese medicine formulas and natural extracts have been confirmed to be neuroprotective by regulating the neuroinflammatory response. These include Hu'po Anshen decoction (Shen et al., 2022), cordycepin (Wei et al., 2021), sinomenine (Hong et al., 2022), Rhodiola crenulate (Xie et al., 2022), parthenolide (Ding et al., 2022), and breviscapine (Pengyue et al., 2017). On this topic, Sun et al. found that casein kinase 2 can regulate NR2B phosphorylation, reduce neuroinflammation, and attenuate brain injury induced by intracerebral hemorrhage, and Cui et al. summarized the platelet-Tregs interaction in neuroinflammation after stroke: their works provide some new potential therapeutic targets for the regulation of neuroinflammation and treatment of brain injury. In addition, Wang et al. found that fo cused ultrasounds can improve the delivery of natural extracts into the brain. These studies will promote the development and application of drugs for the treatment of brain injury. Nevertheless, there is still a need for advancement and research in the clinical application of these synthetic drugs (Kakehi and Tompkins, 2021). Although Chinese traditional medicine has been widely used for the treatment of brain injury, it has been administered as an adjunctive treatment only, and its clinical effectiveness needs to be further verified.

Neuroprotection through rehabilitation

To date, rehabilitation is a widely used and effective treatment for brain injury in the clinic. Rehabilitation programs include stimulation with electricity, magnetism, light, and heat on the CNS and peripheral nervous system (PNS), along with physical therapy, virtual reality, motion imagination, and so on. Although the neuroprotective mechanism of rehabilitation involves multiple targets and multiple factors, inflammatory regulation is its pivotal process. Transcranial-direct-current-stimulation (TDCS) can decrease microglial activation and reduce the release of pro-inflammatory cytokines in experimental stroke models (Zhang et al., 2020; Kaviannejad et al., 2022a,b; Walter et al., 2022). Peripheral nerve electrical stimulation not only promotes nerve regeneration and ameliorates dysfunction but also regulates the neuroinflammatory response in the CNS and PNS (Chu et al., 2022). Exercise immediately after a stroke inhibits the activation of astrocytes and microglia cells and decreases the release of proinflammatory cytokines (Zhang et al., 2017). On this topic, Luo et al. observed that repetitive transcranial magnetic stimulation (TMS) inhibits inflammatory signaling pathways and promotes anti-inflammatory polarization of microglia in ischemic rats.

Neuroprotection through rehabilitation treatments using traditional Chinese medicine

Traditional Chinese medicine has been widely used in rehabilitation for the prevention and treatment of nervous system disorders. Examples include acupuncture and electric acupuncture, moxibustion, Tai Chi, Baduanjin, Yi Jin Jing, and five-fowl play (Zhang et al., 2017). The neuroprotective mechanisms of acupuncture for brain injury have been relatively well studied. In the traumatic brain injury model, researchers found that acupuncture inhibits M1 polarization of microglia by regulating RhoA/ROCK2 and TLR4/TRIF/MyD88 signaling pathways, thereby mitigating neuroinflammation in the acute, subacute, and chronic phases after TBI (Cavalli et al., 2018; Zhu et al., 2020; Cao et al., 2022). In stroke, electric acupuncture increases miR-223 and α7nAChR protein levels, inhibits NLRP3 inflammasome activation, and alleviates neuroinflammation (Jiang et al., 2019; Sha et al., 2019; Xin et al., 2022).

Neuroprotection through stem cell-based therapy

Brain injury leads to the loss of neural cells. Stem cells (such as neural stem cells and mesenchymal stem cells), which can proliferate, migrate, and differentiate into neural cells, can take part in nerve repair and neural plasticity by replacing the injured neural cells (Liu et al., 2022). Also, transplanted stem cells can suppress the neuroinflammatory response by sequestering the inflammatory/immune cells at the injury site and releasing

anti-inflammatory factors (Mashkouri et al., 2016; Borlongan and Rosi, 2022). In addition, recent evidence indicates that the stem cells modulate microglia M1/M2 phenotypes and suppress NLRP3 inflammasome-mediated inflammation by secreting an exosome rich in multiple miRNAs (Liu et al., 2021). It is worth noting that stem cell-derived exosomes can be genetically reconstructed and deliver functional bioactive molecules (Liu et al., 2021). Thus, stem cell-derived exosomes will promote the clinical application of stem cell-based therapy in the treatment of brain injury because they can cross the blood-brain barrier more easily, cannot block blood vessels, do not induce malignant transformation, and can be genetically reconstructed.

Overall, neuroimmune communication is correlated with the physiological functions of various tissues and organs and the internal environmental balance. Dysregulation of neuroimmune communication homeostasis is both the underlying pathological mechanism and the potential therapeutic target in brain injury. A thorough clarification of the cellular and molecular mechanisms of neuroimmune communication in brain injury is an essential and necessary endeavor in the search for new therapeutic targets for this type of disorder.

Author contributions

All authors listed have made a substantial, direct, and intellectual contribution to the work and approved it for publication.

Funding

This study was supported by the National Natural Science Foundation of China (81960731 and 81660384), the Joint Special Project of Traditional Chinese Medicine in Science and Technology Department of Yunnan Province [2019FF002(-008), 202001AZ070001-002, and 030], the Yunnan Province Biological Medicine Major Special Project (202102AA100016), the Yunnan Province University Innovation Team Projects (2019YGC04), and the Basic Research in Science and Technology Program of Yunnan Province (202101BA070001-116).

Conflict of interest

The authors declare that the research was conducted in the absence of any commercial or financial relationships that could be construed as a potential conflict of interest.

Publisher's note

References

Aspelund, A., Antila, S., Proulx, S. T., Karlsen, T. V., Karaman, S., Detmar, M., et al. (2015). A dural lymphatic vascular system that drains brain interstitial fluid and macromolecules. *J. Exp. Med.* 212, 991–999. doi: 10.1084/jem.20142290

Borlongan, M. C., and Rosi, S. (2022). Stem cell therapy for sequestration of traumatic brain injury-induced inflammation. *Int. J. Mol. Sci.* 23, 18, 10286. doi: 10.3390/ijms231810286

Bourhy, L., Mazeraud, A., Bozza, F. A., Turc, G., Lledo, P. M., and Sharshar, T. (2022). Neuro-inflammatory response and brain-peripheral crosstalk in sepsis and stroke. *Front. Immunol.* 13, 834649. doi: 10.3389/fimmu.2022.834649

Buckley, M. W., and McGavern, D. B. (2022). Immune dynamics in the CNS and its barriers during homeostasis and disease. *Immunol. Rev.* 306, 58–75. doi: 10.1111/imr.13066

Cai, L., Gong, Q., Qi, L., Xu, T., Suo, Q., and Li, X., Et al. (2022). ACT001 attenuates microglia-mediated neuroinflammation after traumatic brain injury via inhibiting AKT/NFkappaB/NLRP3 pathway. *Cell Commun. Signal.* 20, 56. doi: 10.1186/s12964-022-00862-y

Cao, L. X., Lin, S. J., Zhao, S. S., Wang, S. Q., Zeng, H., Chen, W. A., et al. (2022). Effects of acupuncture on microglial polarization and the TLR4/TRIF/MyD88 pathway in a rat model of traumatic brain injury. *Acupunct. Med.* 9645284221108214. doi: 10.1177/09645284221108214

Cavalli, L., Briscese, L., Cavalli, T., Andre, P., and Carboncini, M. C. (2018). Role of Acupuncture in the Management of Severe Acquired Brain Injuries (sABIs). *Evid. Based Complement. Alternat. Med.* 2018, 8107508. doi: 10.1155/2018/8107508

Chu, X. L., Song, X. Z., Li, Q., Li, Y. R., He, F., Gu, X. S., et al. (2022). Basic mechanisms of peripheral nerve injury and treatment via electrical stimulation. *Neural Regen Res.* 17, 2185–2193. doi: 10.4103/1673-5374.335823

Ding, W., Cai, C., Zhu, X., Wang, J., and Jiang, Q. (2022). Parthenolide ameliorates neurological deficits and neuroinflammation in mice with traumatic brain injury by suppressing STAT3/NF-kappaB and inflammasome activation. *Int. Immunopharmacol.* 108, 108913. doi: 10.1016/j.intimp.2022.108913

Hong, H., Lu, X., Lu, Q., Huang, C., and Cui, Z. (2022). Potential therapeutic effects and pharmacological evidence of sinomenine in central nervous system disorders. *Front. Pharmacol.* 13, 1015035. doi: 10.3389/fphar.2022.1015035

Jiang, T., Wu, M., Zhang, Z., Yan, C., Ma, Z., He, S., et al. (2019). Electroacupuncture attenuated cerebral ischemic injury and neuroinflammation through alpha7nAChR-mediated inhibition of NLRP3 inflammasome in stroke rats. *Mol. Med.* 25, 22. doi: 10.1186/s10020-019-0091-4

Kakehi, S., and Tompkins, D. M. (2021). A review of pharmacologic neurostimulant use during rehabilitation and recovery after brain injury. *Ann. Pharmacother.* 55, 1254–1266. doi: 10.1177/1060028020983607

Kaviannejad, R., Karimian, S. M., Riahi, E., and Ashabi, G. (2022a). A single immediate use of the cathodal transcranial direct current stimulation induces neuroprotection of hippocampal region against global cerebral ischemia. *J. Stroke Cerebrovasc. Dis.* 31, 106241. doi: 10.1016/j.jstrokecerebrovasdis.2021.106241

Kaviannejad, R., Karimian, S. M., Riahi, E., and Ashabi, G. (2022b). Using dual polarities of transcranial direct current stimulation in global cerebral ischemia and its following reperfusion period attenuates neuronal injury. *Metab. Brain Dis.* 37, 1503–1516. doi: 10.1007/s11011-022-00985-8

Kisler, K., and Zlokovic, B. V. (2022). How the brain regulates its own immune system. *Nat. Neurosci.* 25, 532–534. doi: 10.1038/s41593-022-01066-w

Leclerc, A. M., Riker, R. R., Brown, C. S., May, T., Nocella, K., Cote, J., et al. (2021). Amantadine and modafinil as neurostimulants following acute stroke: a retrospective study of intensive care unit patients. *Neurocrit. Care.* 34, 102–111. doi: 10.1007/s12028-020-00986-4

Liu, H., Wei, T., Huang, Q., Liu, W., Yang, Y., Jin, Y., et al. (2022). The roles, mechanism, and mobilization strategy of endogenous neural stem cells in brain injury. *Front. Aging Neurosci.* 14, 924262. doi: 10.3389/fnagi.2022.924262

Liu, X., Zhang, M., Liu, H., Zhu, R., He, H., Zhou, Y., et al.(2021). Bone marrow mesenchymal stem cell-derived exosomes attenuate cerebral ischemia-reperfusion injury-induced neuroinflammation and pyroptosis by modulating microglia M1/M2 phenotypes. *Exp. Neurol.* 341, 113700. doi: 10.1016/j.expneurol.2021.113700

Mashkouri, S., Crowley, M. G., Liska, M. G., Corey, S., and Borlongan, C. V. (2016). Utilizing pharmacotherapy and mesenchymal stem cell therapy to reduce inflammation following traumatic brain injury. *Neural Regen Res*. 11, 1379–1384. doi: 10.4103/1673-5374.191197

Mazzitelli, J. A., Smyth, L., Cross, K. A., Dykstra, T., Sun, J., Du, S., et al. (2022). Cerebrospinal fluid regulates skull bone marrow niches via direct access through dural channels. *Nat. Neurosci*. 25, 555–560. doi: 10.1038/s41593-022-01029-1

Misilimu, D., Li, W., Chen, D., Wei, P., Huang, Y., Li, S., et al. (2022). Intranasal salvinorin a improves long-term neurological function via immunomodulation in a mouse ischemic stroke model. *J. Neuroimmune Pharmacol*. 17, 350–366. doi: 10.1007/s11481-021-10025-4

Niraula, A., Wang, Y., Godbout, J. P., and Sheridan, J. F. (2018). Corticosterone production during repeated social defeat causes monocyte mobilization from the bone marrow, glucocorticoid resistance, and neurovascular adhesion molecule expression. *J. Neurosci*. 38, 2328–2340. doi: 10.1523/JNEUROSCI.2568-17.2018

Paolicelli, R. C., Sierra, A., Stevens, B., Tremblay, M. E., Aguzzi, A., and Ajami, B., et al. (2022). Microglia states and nomenclature: a field at its crossroads. *Neuron*. 110, 3458–3483. doi: 10.1016/j.neuron.2022.10.020

Pengyue, Z., Tao, G., Hongyun, H., Liqiang, Y., and Yihao, D. (2017). Breviscapine confers a neuroprotective efficacy against transient focal cerebral ischemia by attenuating neuronal and astrocytic autophagy in the penumbra. *Biomed. Pharmacother*. 90, 69–76. doi: 10.1016/j.biopha.2017.03.039

Poller, W. C., Downey, J., Mooslechner, A. A., Khan, N., Li, L., Chan, C. T., et al. (2022). Brain motor and fear circuits regulate leukocytes during acute stress. *Nature*. 607, 578–584.doi: 10.1038/s41586-022-04890-z

Pulous, F. E., Cruz-Hernandez, J. C., Yang, C., Kaya, Z., Paccalet, A., Wojtkiewicz, G., et al. (2022). Cerebrospinal fluid can exit into the skull bone marrow and instruct cranial hematopoiesis in mice with bacterial meningitis. *Nat. Neurosci*. 25, 567–576. doi: 10.1038/s41593-022-01060-2

Rahimi, S., Dadfar, B., Tavakolian, G., Asadi, R. A., Rashid, S. A., and Siahposht-Khachaki, A. (2021). Morphine attenuates neuroinflammation and blood-brain barrier disruption following traumatic brain injury through the opioidergic system. *Brain Res. Bull*. 176, 103–111. doi: 10.1016/j.brainresbull.2021.08.010

Sha, R., Zhang, B., Han, X., Peng, J., Zheng, C., Zhang, F., et al. (2019). Electroacupuncture alleviates ischemic brain injury by inhibiting the miR-223/NLRP3 pathway. *Med. Sci. Monit*. 25, 4723–4733. doi: 10.12659/MSM.917213

Shen, J., Li, Y. Z., Yao, S., Zhu, Z. W., Wang, X., Sun, H. H., et al. (2022). Hu'po anshen decoction accelerated fracture-healing in a rat model of traumatic brain injury through activation of PI3K/AKT pathway. *Front. Pharmacol*. 13, 952696. doi: 10.3389/fphar.2022.952696

Shi, H., Wang, H. L., Pu, H. J., Shi, Y. J., Zhang, J., Zhang, W. T., et al. (2015). Ethyl pyruvate protects against blood-brain barrier damage and improves long-term neurological outcomes in a rat model of traumatic brain injury. *CNS Neurosci. Ther*. 21, 374–384. doi: 10.1111/cns.12366

Vera Quesada, C. L., Rao, S. B., Torp, R., and Eide, P. K. (2023). Immunohistochemical visualization of lymphatic vessels in human dura mater: methodological perspectives. *Fluids Barriers CNS*. 20, 23. doi: 10.1186/s12987-023-00426-3

Vidal-Itriago, A., Radford, R., Aramideh, J. A., Maurel, C., Scherer, N. M., Don, E. K., et al. (2022). Microglia morphophysiological diversity and its implications for the CNS. *Front. Immunol*. 13, 997786. doi: 10.3389/fimmu.2022.997786

Walter, H. L., Pikhovych, A., Endepols, H., Rotthues, S., Barmann, J., Backes, H., et al. (2022). Transcranial-direct-current-stimulation accelerates motor recovery after cortical infarction in mice: the interplay of structural cellular responses and functional recovery. *Neurorehabil. Neural Repair*. 36, 701–714. doi: 10.1177/15459683221124116

Wang, X., Zhang, C., Li, Y., Xu, T., Xiang, J., Bai, Y., et al. (2022). High-throughput mrna sequencing reveals potential therapeutic targets of febuxostat in secondary injury after intracerebral hemorrhage. *Front. Pharmacol*. 13, 833805. doi: 10.3389/fphar.2022.833805

Wei, P., Wang, K., Luo, C., Huang, Y., Misilimu, D., Wen, H., et al. (2021). Cordycepin confers long-term neuroprotection via inhibiting neutrophil infiltration and neuroinflammation after traumatic brain injury. *J. Neuroinflammation*. 18, 137. doi: 10.1186/s12974-021-02188-x

Xie, N., Fan, F., Jiang, S., Hou, Y., Zhang, Y., Cairang, N., et al. (2022). Rhodiola crenulate alleviates hypobaric hypoxia-induced brain injury via adjusting NF-kappaB/NLRP3-mediated inflammation. *Phytomedicine*. 103, 154240. doi: 10.1016/j.phymed.2022.154240

Xin, Y. Y., Wang, J. X., and Xu, A. J. (2022). Electroacupuncture ameliorates neuroinflammation in animal models. *Acupunct. Med*. 40, 474–483. doi: 10.1177/09645284221076515

Zhang, K. Y., Rui, G., Zhang, J. P., Guo, L., An, G. Z., Lin, J. J., et al. (2020). Cathodal tDCS exerts neuroprotective effect in rat brain after acute ischemic stroke. *BMC Neurosci*. 21, 21. doi: 10.1186/s12868-020-00570-8

Zhang, Q., Zhang, J., Yan, Y., Zhang, P., Zhang, W., and Xia, R. (2017). Proinflammatory cytokines correlate with early exercise attenuating anxiety-like behavior after cerebral ischemia. *Brain Behav*. 7, e00854. doi: 10.1002/brb3.854

Zhu, M. M., Lin, J. H., Qing, P., Pu, L., Chen, S. L., Lin, S. J., et al. (2020). Manual acupuncture relieves microglia-mediated neuroinflammation in a rat model of traumatic brain injury by inhibiting the RhoA/ROCK2 pathway. *Acupunct. Med*. 38, 426–434. doi: 10.1177/0964528420912248

frontiers in Cellular Neuroscience

ORIGINAL RESEARCH
published: 16 November 2021
doi: 10.3389/fncel.2021.774569

Activation of Adenosine Monophosphate-Activated Protein Kinase Drives the Aerobic Glycolysis in Hippocampus for Delaying Cognitive Decline Following Electroacupuncture Treatment in APP/PS1 Mice

Jianhong Li[1†], Bingxue Zhang[1†], Weiwei Jia[1], Minguang Yang[2], Yuhao Zhang[1], Jiayong Zhang[1], Le Li[1], Tingting Jin[1], Zhifu Wang[3], Jing Tao[3], Lidian Chen[3], Shengxiang Liang[1] and Weilin Liu[2*]*

[1] TCM Rehabilitation Research Center of SATCM, Fujian University of Traditional Chinese Medicine, Fuzhou, China, [2] National-Local Joint Engineering Research Center of Rehabilitation Medicine Technology, Fujian University of Traditional Chinese Medicine, Fuzhou, China, [3] College of Rehabilitation Medicine, Fujian University of Traditional Chinese Medicine, Fuzhou, China

OPEN ACCESS

Edited by:
Feng Zhang,
Third Hospital of Hebei Medical University, China

Reviewed by:
Dongfeng Qu,
University of Oklahoma Health Sciences Center, United States
Luwen Zhu,
Heilongjiang University of Chinese Medicine, China

***Correspondence:**
Weilin Liu
liuweilin12@fjtcm.edu.cn
Shengxiang Liang
sxliang@fjtcm.edu.cn

[†] These authors have contributed equally to this work

Specialty section:
This article was submitted to Cellular Neuropathology, a section of the journal Frontiers in Cellular Neuroscience

Received: 12 September 2021
Accepted: 12 October 2021
Published: 16 November 2021

Citation:
Li J, Zhang B, Jia W, Yang M, Zhang Y, Zhang J, Li L, Jin T, Wang Z, Tao J, Chen L, Liang S and Liu W (2021) Activation of Adenosine Monophosphate-Activated Protein Kinase Drives the Aerobic Glycolysis in Hippocampus for Delaying Cognitive Decline Following Electroacupuncture Treatment in APP/PS1 Mice. Front. Cell. Neurosci. 15:774569. doi: 10.3389/fncel.2021.774569

Aerobic glycolysis (AG), an important pathway of glucose metabolism, is dramatically declined in Alzheimer's disease (AD). AMP-activated protein kinase (AMPK) is a key regulator to maintain the stability of energy metabolism by promoting the process of AG and regulating glucose metabolism. Interestingly, it has been previously reported that electroacupuncture (EA) treatment can improve cognitive function in AD through the enhancement of glucose metabolism. In this study, we generated AMPK-knockdown mice to confirm the EA effect on AMPK activation and further clarify the mechanism of EA in regulating energy metabolism and improving cognitive function in APP/PS1 mice. The behavioral results showed that EA treatment can improve the learning and memory abilities in APP/PS1 mice. At the same time, the glucose metabolism in the hippocampus was increased detected by MRI-chemical exchange saturation transfer (MRI-CEST). The expression of proteins associated with AG in the hippocampus was increased simultaneously, including hexokinase II (HK2), 6-phosphofructo-2-kinase/fructose-2,6-biphosphatase 3 (PFKFB3), and pyruvate kinase M2 (PKM2). Moreover, the knockdown of AMPK attenuated AG activated by EA treatment. In conclusion, this study proves that EA can activate AMPK to enhance the process of AG in the early stage of AD.

Keywords: electroacupuncture, Alzheimer's disease, aerobic glycolysis, learning and memory, adenosine monophosphate-activated protein kinase (AMPK)

INTRODUCTION

Alzheimer's disease (AD) is the most common neurodegenerative disease, which is clinically characterized by progressive cognitive impairment, accounting for 60–80% of all dementia cases. According to the AD report of 2018, approximately 50 million people worldwide are affected by dementia, with the number expected to reach 152 million by 2050 (Peprah and McCormack, 2019).

Glucose metabolism dysfunction is a serious manifestation of AD, which even emerges earlier than cognitive decline and dementia (Daulatzai, 2017; Kuehn, 2020). Fluorodeoxyglucose positron emission tomography (FDG-PET) could measure glucose metabolism within the brain, which has been used to aid dementia diagnosis (Arbizu et al., 2018; Wilson et al., 2019). Research in this area has shown that the glucose metabolism was impaired in several brain regions during AD progression, and this dysfunction usually starts in the memory-related brain regions, such as the entorhinal cortex, parietal lobe, posterior cingulate cortex, notably the hippocampus and associated temporal areas (Minoshima et al., 1997; Mosconi, 2005). Some researchers pointed out that many pathological changes that arise downstream of glucose metabolism dysfunction may be the cause of neuronal degenerative changes in AD (Chen and Zhong, 2013).

The glucose metabolism route consists of glycolysis and mitochondrial oxidative phosphorylation, and the latter is the main pathway for energy production in mitochondrion promoting the survival and function of neurons (Akram, 2014; Jin and Diano, 2018). In the past century, Otto Warburg first observed that aerobic glycolysis (AG) was utilized to support cancer cell proliferation (Riester et al., 2018). Since then, AG has been a major focus in the field of cancer metabolic research. In recent years, several studies have found that abnormal AG is associated with AD. As the review of the literature concluded that glucose metabolism dysfunction during AD progression, including decreased glucose uptake and glucose utilization, may be related to the impairment of AG, leading to permanent neurological impairments (An et al., 2018). In the initial stage of AD, amyloid-beta (Aβ) fragments could cause abnormal mitochondrial dynamics, resulting in mitochondrial dysfunction and neuronal damage, which makes AG an important energy supplement way (Manczak et al., 2016; Yin et al., 2020). Another study has found that the AG was increased in response to the inhibition of oxidative phosphorylation in cultured cortical neurons (Santangelo et al., 2021). Moreover, some scholars have found that the process of AG could attenuate neuronal death caused by Aβ oligomers (Newington et al., 2011). Further studies found that AG can improve the ability of neurons to attenuate Aβ-mediated neurotoxicity by increasing the expression of pyruvate dehydrogenase kinase 1 (PDK1) and lactate dehydrogenase A (LDHA) (Newington et al., 2012).

Interestingly, animal studies have found that electroacupuncture (EA) treatment could elevate glucose metabolism (Dong et al., 2015; Liu et al., 2017). A large number of studies have shown that EA is a proven means of therapeutic intervention to improve cognitive function and life quality of patients with AD (Zhou et al., 2015; Jia et al., 2017). In the past studies, we have found that EA at the DU20 and the DU24 acupoints could improve the cognitive performance of APP/PS1 mice through increasing glucose metabolism (Lin et al., 2016; Liu et al., 2017). However, the mechanism of EA treatment improving cognitive function in AD is needed for further exploration. Studies have demonstrated that the reduction of AMP-activated protein kinase (AMPK) could result in progressive loss of neuronal functions, suggesting that restoration of AMPK expression may serve as a potential therapeutic target for AD (Yang et al., 2015). AMPK is considered a key regulator of energy metabolism as it can control glucose metabolism and regulate glycolysis flux (Yan et al., 2018). Studies have indicated that AMPK could promote glucose metabolism by regulating proteins associated with AG, such as hexokinase II (HK2), 6-phosphofructo-2-kinase/fructose-2,6-biphosphatase 3 (PFKFB3), and pyruvate kinase M2 (PKM2) (Liu et al., 2019; Xu et al., 2019). Additionally, studies have also found that the expression levels of HK2, PFKFB3, and PKM2 were changed in AD, which may be associated with the impairment of memory and other cognitive function (Bigl et al., 1999; Cisternas et al., 2019). Taking into account these findings, we hypothesized that EA treatment might enhance AG through AMPK to improve the learning and memory abilities in APP/PS1 mice, and in this study, AMPK-knockdown mice were generated to confirm this hypothesis.

MATERIALS AND METHODS

Animals and Ethics

In this study, APP/PS1 double-transgenic mice were used as the AD animal model. APP/PS1 double-transgenic mice [B6C3-TG (APPswe, PSEN1dE9) 85Dbo/MmJNju], Camk2a-cre mice, and wild type (WT) mice were obtained from Nanjing University – Nanjing Biomedical Research Institute; AMPKa1(loxp/loxp) mice were purchased from Xiamen University (Stock No: 014141). The animals were fed in the SPF animal experimental center of Fujian University of Traditional Chinese Medicine, each cage for 4–5 animals, free to water and food. The SPF room was set up for a standard day and night system (12/12 h light/dark cycle), with the temperature at 22° and humidity at 50–70%. APP/PS1 mice applied in this experiment were obtained by crossing male APP/PS1 mice to female WT mice. To produce AMPK-knockdown APP/PS1 mice, AMPKa1(loxp/loxp) mice were interbred with APP/PS1 mice to obtain APP/PS1 + AMPKa1(loxp/loxp) mice, and these mice were mated to Camk2a-cre mice to obtain APP/PS1 + AMPKa1$^{(+/-)}$ mice. The genotypes of the offsprings were identified using the polymerase chain reaction. All experiments involving animals were approved by the Fujian University of Traditional Chinese Medicine Animal Experimentation Ethics Committee, and the experiments are operated and implemented in strict accordance with the provisions of the national animal protection laws and regulations.

Experimental Protocol

After gene identification, 4-month-old mice were divided into five groups as follows: WT group, AD group, AD + EA group, AD + AMPK$^{(+/-)}$ group, and AD + AMPK$^{(+/-)}$ + EA group, each group with 10 mice. The detailed experimental timeline is depicted in **Figure 1**. For EA treatment, the mice were fixed on a special device. Mice were sedated by lightly stroking the body. Stainless steel acupuncture steel (0.32 mm diameter; Huatuo, Suzhou Medical Appliance Factory, Suzhou, China) was inserted to a depth of 2–3 mm at DU20 and DU24 acupoints according to the acupuncture point map of experimental animals and the

acupuncture and moxibustion science. Then, the EA instrument (model: G6805; Suzhou Medical Appliance Factory, Suzhou, China) was used with a frequency of sparse and dense waves of 1/20 Hz, a voltage of 2 V, for 30 min, once a day, 5 times a week, for 4 weeks.

Novel Object Recognition Test

The novel object recognition test was used to assess recognition memory. It was performed according to the previously explained method (Bevins and Besheer, 2006). In brief, the apparatus includes a rectangular open-field box, object "A," object "a," and object "B," in which the object "A" is the same as object "a." One day before the formal experiment, the mice were put into the open-field box for 10 min for acclimation. In the training session, two identical objects "A" and "a" were placed on the two adjacent corners of the open-field box, and then the mice were put into the open-field box to explore for 10 min. Notably, 1 and 24 h after the training session, the mice were reintroduced to the same task, but one of the familiar objects applied during the training session was replaced by a novel object "B," and the mice were put into the open-field box to explore for 5 min. During the experiment, the trajectory and behavior including the time of each mouse contact with the objects were recorded using the camera of Super Maze. After each trial, the open-field box and objects were cleaned with 70% of ethanol to eliminate the presence of any olfactory cues. Evaluation index: the mice were considered to be exploring when the animal nose was toward the object within 2 cm. In this study, recognition index = {Time(B)/[Time(A) + Time(B)]}.

Morris Water Maze Test

Morris water maze test was used to evaluate the spatial learning and memory abilities of mice after EA intervention. A cylindrical tank with a radius of 60 cm surrounded by a wall of 50 cm high and filled with opaque water was used. The depth of the water is 30 cm, and the temperature is maintained at 25 ± 2°C. A transparent circular platform with a diameter of 6 cm was hidden below the water surface. Four spatial cues with different shapes and colors were pasted above the edge of the tank. The mice were allowed 16 sessions of a swim on the first 4 days, 4 sessions each day. In this stage, the mice were put into the water from four different quadrants, and the time spent to reach the escape platform was measured as escape latency. If the mice climbed to the escape platform within 90 s, record the time as escape latency, and if the mice did not reach the escape platform, record the escape latency as 90 s, and the mice were guided to the platform by the experimenter to learn for 15 s. On the 5th day, the escape platform in the Morris water maze was removed, and the mice were directly put into the opposite quadrant where the original platform was located to swim for 90 s. The swimming trajectory and behavior including the escape platform crossing times and the time spent in the target quadrant were tracked using the SuperMaze small animal behavior video analysis system.[1]

MRI-Chemical Exchange Saturation Transfer Imaging

The MRI-chemical exchange saturation transfer (MRI-CEST) scans in the 7.0 T magnetic resonance imaging small animal system (Bruker Biospec, Ettlingen, Germany) was applied to detect the levels of glucose metabolism, each group for four mice. One day before CEST imaging, food was removed, and the mice were fasted 12 h with free water access. Mice were anesthetized with 1.5% isoflurane. A volume coil with a radius of 3.6 cm was used as the transmitter and an orthogonal single-channel surface coil as the receiver during scanning. The T2WI image is scanned for reference prior to CEST imaging. The MAPSHIM program was utilized to calculate the first- and second-order parameters to optimize B0 field homogeneity.

The detailed acquisition parameters for T2WI were as follows: repetition time (TR) = 5,000 ms, echo time (TE) = 105.02 ms, field of view (FOV) = 16 mm × 16 mm, image matrix = 256 × 256, and slice thickness = 1 mm. CEST consisted of a continuous pulse for the 43 offset frequencies from −1,800 to 1,800 Hz with the interval of 90 Hz. The detailed acquisition parameters were as follows: TR = 5,000 ms, TE = 35.45 ms, B1 = 3.7 μT, FOV = 16 mm × 16 mm, image matrix = 45 × 45, and slice thickness = 1 mm.

Using the asymmetric magnetization transfer ratio (MTRasym), asymmetric equation: MTRasym (Δω) = [Ssat (−Δω)−Ssat (Δω)]/S0 (van Zijl and Yadav, 2011), and calculated CEST glucose metabolism image, including Δω, the exchange of content and free water frequency difference, the free water saturation before signal as S0, and free water for the Ssat signal after saturation were determined. The voxel counts were normalized by the mean intensity of the brain in the metabolism image of each mice. Then, ITK-snap[2] was also used to determine the left and right hippocampus regions of interest (ROI) manually and extract glucose metabolism values for each mouse.

Western Blotting

The hippocampus was extracted for Western blotting, four mice in each group. The RIPA lysis buffer and the BCA Kit were used to extract total protein and determine protein concentration, respectively. A total of 50 μg proteins were resolved by 10% sodium dodecyl-sulfate-polyacrylamide gel electrophoresis (SDS-PAGE) and then transferred to activated polyvinylidene fluoride (PVDF) membranes. The membranes were blocked with 5% skimmed milk for 2 h at room temperature, incubated with antibodies against AMPK (cat. No. ab131512, 1:1,000), PFKFB3 (cat. No. 13763-1-AP, 1:3,000), HK2 (cat. No. 22029-1-AP, 1:5,000), and PKM2 (cat. No. Ab137852, 1:1,000) at 4°C overnight, and subsequently incubated with horseradish peroxidase-conjugated (HRP-conjugated) secondary antibody (1:8,000) for 2 h. The protein bands were visualized with enhanced chemiluminescence and imaged with the Bio-Image Analysis system (Bio-Rad Laboratories, Inc.).

[1] http://www.softmaze.com

[2] http://www.itksnap.org/

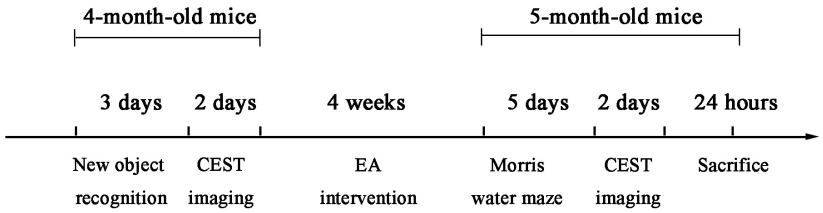

FIGURE 1 | The detailed timeline of the experiments, including the electroacupuncture (EA) treatment and time sequence.

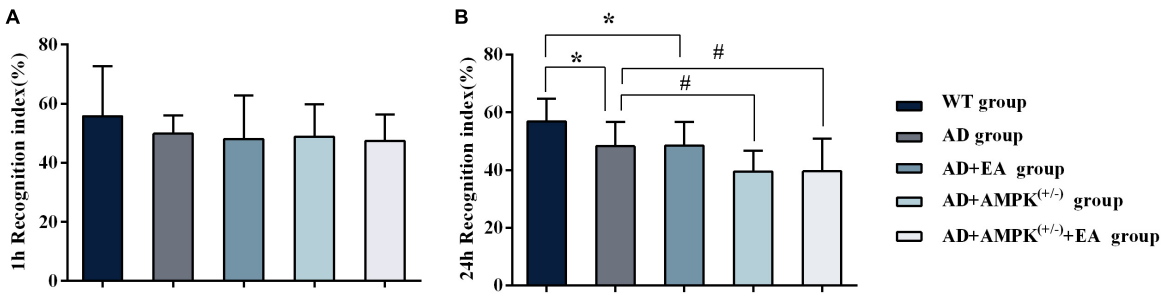

FIGURE 2 | Novel object recognition test showing decreased recognition index for the novel object in 4-month-old APP/PS1 mice. **(A)** The 1 h recognition index of five groups before EA intervention; **(B)** The 24 h recognition index of five groups before EA intervention. *$P < 0.05$ vs. the wild type (WT) group; #$P < 0.05$ vs. the Alzheimer's disease (AD) group.

Statistical Analysis

The statistical differences were evaluated using SPSS version 24.0 (Released 2016, IBM SPSS Statistics for Windows, IBM Corp., Armonk, NY). The values are expressed as means ± SEM. The escape latency of the Morris water maze was analyzed using the repeated measurement analysis method, other results were analyzed by one-way ANOVA, and multiple comparisons were performed using the Fisher's least significant difference (LSD) or Games-Howell test. The difference was considered to be significant when $P < 0.05$.

RESULTS

Electroacupuncture Treatment Alleviated Learning and Memory Impairment of APP/PS1 Mice

To observe the effects of EA treatment on the learning and memory abilities of APP/PS1 transgenic mice, the new object recognition test was applied before EA intervention in order to detect the recognition memory of each group, and the results were shown in **Figure 2**. The 24-h novel object recognition index of the AD group was decreased compared with the WT group ($P < 0.05$), and further analysis showed that the AD + AMPK$^{(+/-)}$ group was decreased compared with the AD group ($P < 0.05$) (**Figure 2B**). However, there was no significant difference in the 1-h novel object recognition index between individual groups (**Figure 2A**). After EA intervention, the learning and memory abilities of each group were detected using the Morris water maze, and the results were exhibited in **Figure 3**. Escape latency in the AD group was increased compared with the WT group. However, escape latency in the AD + EA group was decreased compared with the AD group, and the AD + AMPK$^{(+/-)}$ + EA group decreased compared with the AD + AMPK$^{(+/-)}$ group (**Figure 3A**). The escape platform crossing times and the 3rd quadrant time proportion in the AD group were decreased compared with the WT group ($P < 0.05$); the AD + EA group increased compared with the AD group ($P < 0.05$); the AD + AMPK$^{(+/-)}$ + EA group increased compared with the AD + AMPK$^{(+/-)}$ group ($P < 0.05$) (**Figures 3B,C**). The representative images of the Morris water maze in different groups were shown in **Figure 3D**. These results suggested that EA at DU20 and DU24 acupoints could improve the learning and memory abilities of APP/PS1 mice.

Electroacupuncture Treatment Increased Glucose Metabolism in Hippocampus of APP/PS1 Mice

To observe the effects of EA on hippocampus glucose metabolism of APP/PS1 transgenic mice, MRI-CEST imaging was conducted before and after the EA intervention. The results before the EA intervention were shown in **Figure 4A**. One-way ANOVA results showed that there were no significant differences in glucose metabolism on the hippocampus (both left and right) between individual groups ($P > 0.05$). After EA intervention, the results in **Figure 4B** showed that the glucose metabolism in the right hippocampus of the AD group was decreased compared with the WT group ($P < 0.05$); the glucose metabolism in the hippocampus (left and right) of the AD + AMPK$^{(+/-)}$ group were decreased compared with the WT group ($P < 0.05$ and $P < 0.01$). However, the glucose metabolism in the left hippocampus of the AD + EA group was increased compared

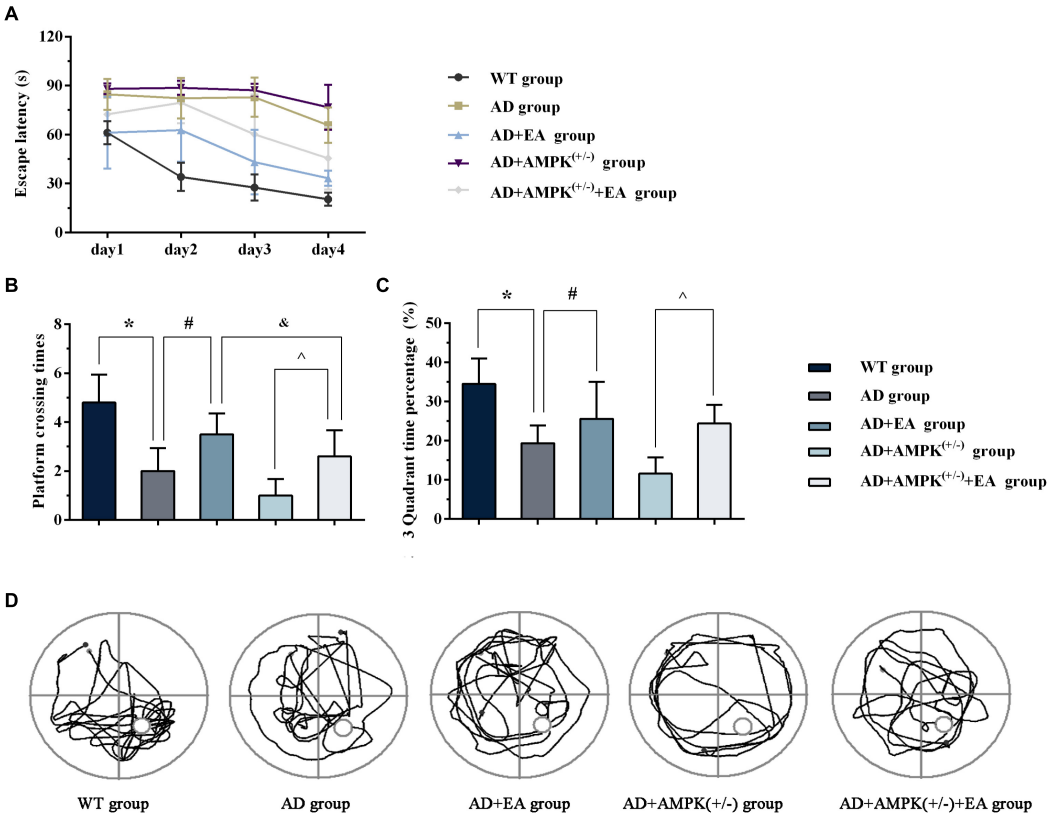

FIGURE 3 | Electroacupuncture intervention could improve the learning and memory abilities of APP/PS1 mice tested by Morris water maze. **(A)** The escape latency of five groups in Morris water maze after EA intervention; **(B)** The escape platform crossing times of five groups in Morris water maze after EA intervention; **(C)** The 3rd quadrant time percentage of five groups in Morris water maze after EA intervention; **(D)** Representative images of Morris water maze in different groups. $^{*}P < 0.05$ vs. the WT group; $^{\#}P < 0.05$ vs. the AD group; $^{\wedge}P < 0.05$ vs. the AD + AMP-activated protein kinase (AMPK)$^{(+/-)}$ group; $^{\&}P < 0.05$ vs. the AD + EA group.

with the AD group ($P < 0.05$). The glucose metabolism in the left hippocampus of the AD + AMPK$^{(+/-)}$ + EA group was decreased compared with the AD + EA group ($P < 0.05$). The typical CEST image was shown in **Figure 4C**. It suggested that EA at DU20 and DU24 acupoints could improve the hippocampus glucose metabolism of APP/PS1 mice.

Electroacupuncture Treatment Increased the Expression of Proteins Associated With Aerobic Glycolysis of APP/PS1 Mice

To observe the effects of EA on hippocampus AMPK and AG rate-limiting enzyme expression in APP/PS1 transgenic mice, Western blotting was performed and the results were shown in **Figure 5**. Compared with the WT group, the expression levels of AMPK, PFKFB3, HK2, and PKM2 were significantly decreased in the AD group ($P < 0.01$ or $P < 0.05$); compared with the AD group, the expression levels of AMPK, PFKFB3, HK2, and PKM2 were increased in the AD + EA group ($P < 0.05$); compared with the AD + AMPK$^{(+/-)}$ group, the expression levels of AMPK, PFKFB3, HK2, and PKM2 were increased in the AD + AMPK$^{(+/-)}$ + EA group ($P < 0.01$ or $P < 0.05$). Compared with the AD + EA group, the expression levels of AMPK, PFKFB3, HK2, and PKM2 were decreased in the AD + AMPK$^{(+/-)}$ + EA group ($P < 0.05$). The above results showed that the AMPK activity and the AG-related proteins were decreased in the hippocampus of APP/PS1 and APP/PS1 + AMPK$^{(+/-)}$ mice, while EA at DU20 and DU24 acupoints could activate AMPK to improve the expression levels of PFKFB3, HK2, and PKM2 in APP/PS1 transgenic mice.

DISCUSSION

Our previous studies have found that EA treatment could effectively elevate glucose metabolism to improve the learning and memory abilities in APP/PS1 mice (Liu et al., 2017). This study was designed to examine the underlying molecular mechanism *via* which EA treatment improved glucose metabolism in APP/PS1 mice. To elucidate this issue, the CRE-LOXP conditional knockout technology was used to generate APP/PS1 mice with AMPK knockdown. Combined with MRI-CEST imaging analysis, we confirmed that EA at the DU20 and DU24 acupoints could improve glucose metabolism in APP/PS1 mice to enhance learning and memory abilities. To gain further insight, we analyzed the proteins associated with AG in the hippocampus using the immunoblot analysis, and the results showed that the expression levels of AMPK, HK2,

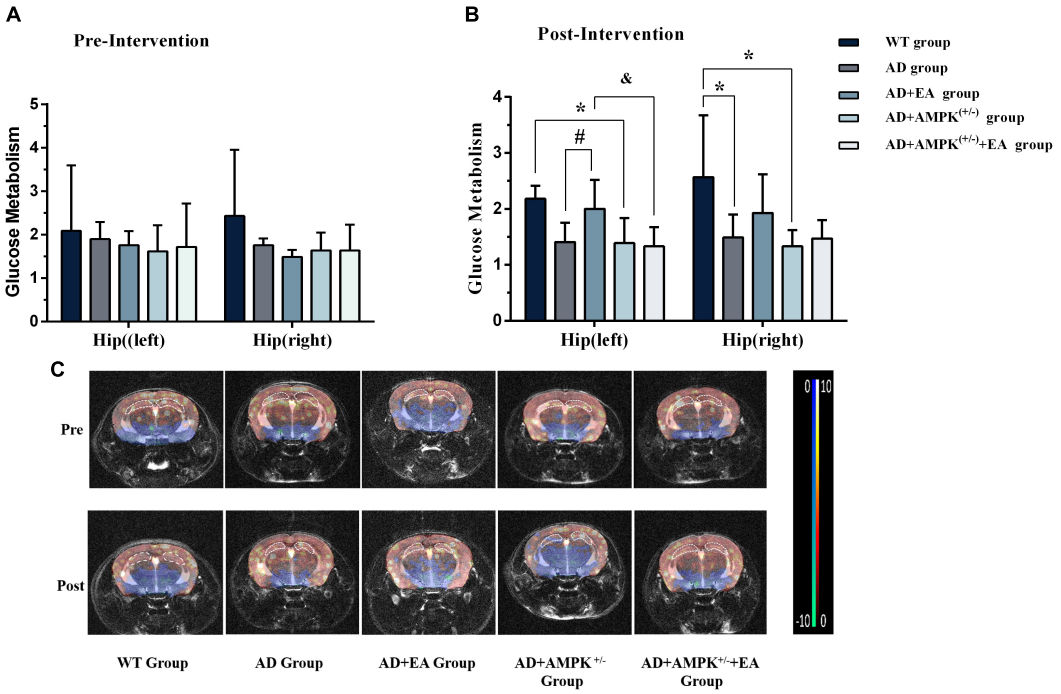

FIGURE 4 | Electroacupuncture intervention could increase glucose metabolism in the hippocampus of APP/PS1 mice. **(A)** The glucose metabolism in the hippocampus of five groups before EA intervention; **(B)** The glucose metabolism in the hippocampus of five groups after EA intervention; **(C)** The typical image of glucose metabolism in the hippocampus. $^{*}P < 0.05$ vs. the WT group; $^{\#}P < 0.05$ vs. the AD group; $^{\&}P < 0.05$ vs. the AD + EA group.

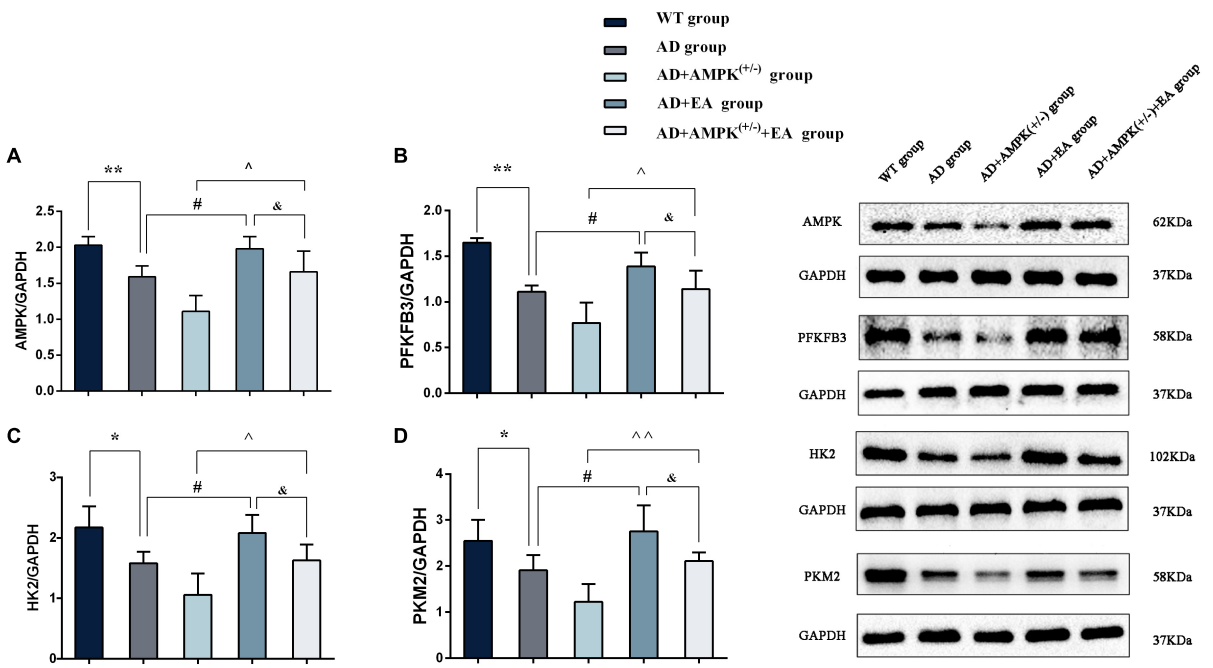

FIGURE 5 | Electroacupuncture intervention could promote the expression of aerobic glycolysis (AG)-related proteins. **(A–D)** The expression of AMPK, 2,6-fructose-biphosphatase 3 (PFKFB3), hexokinase II (HK2), and pyruvate kinase M2 (PKM2) in the hippocampus of five groups after EA intervention; (E) representative protein images of each AG-related protein in different groups. $^{*}P < 0.05$, $^{**}P < 0.01$ vs. the WT group; $^{\#}P < 0.05$ vs. the AD group; $^{\wedge}P < 0.05$; $^{\wedge\wedge}P < 0.01$ vs. the AD + AMPK$^{(+/-)}$ group; $^{\&}P < 0.05$ vs. the AD + EA group.

PFKFB3, and PKM2 were all increased after EA intervention. More interestingly, the effects of EA would be suppressed by AMPK knockdown suggesting that EA at the DU20 and DU24 acupoints could activate AMPK to regulate glucose metabolism improving the cognitive function of APP/PS1 mice.

The APP/PS1 double transgenic mice have been extensively employed in AD research. It was previously found that the learning and memory abilities of APP/PS1 mice were impaired at the 3rd month tested by Morris water (Edwards et al., 2014). Aβ plaque is a typical pathological manifestation of AD, and Aβ deposition could be detected in APP/PS1 mice aged 4 months (Malm et al., 2011; Ramos-Rodriguez et al., 2013). Abnormal glucose metabolism is one marker of AD. There was one study longitudinally examined glucose metabolism in APP/PS1 mice at the 2nd, 3.5th, 5th, and 8th month and found that the glucose metabolism was changed throughout the progression of the disease in many brain regions, such as the entorhinal cortex, hippocampus, and frontal cortex (Li et al., 2016). In this study, 4-month-old APP/PS1 transgenic mice were selected to conduct early EA treatment. The results of the new object recognition test showed that the recognition memory of APP/PS1 mice was impaired in the 4th month.

Mitochondria are important sites for glucose metabolism where ATP synthesis occurs. However, the mitochondrial architecture is disrupted in the early stage of AD, making AG a supplement source of brain energy (Butterfield and Halliwell, 2019; Lautenschager and Kaminski, 2019). It is regrettable that the AG itself is disrupted as the disease stage progresses. It was found that the spatial distribution of the AG is consistent with the Aβ-containing plaques in the brain of preclinical patients with AD (Vlassenko et al., 2010). Autopsy studies have found that the expression of glucose transporter genes (GLUT-3), the glycolysis flux, and its key rate-limiting enzyme activity was reduced in brain regions susceptible to AD (An et al., 2018). Additionally, one study found that PDK1 was also tended to be reduced in the cerebral cortex of patients with AD which is associated with brain AG declines (Newington et al., 2012). A higher rate of glycolytic often presented in the early stages of AD, which has been considered to be a compensatory mechanism for lower glucose metabolism. However, the process of AG was also impaired with disease progression, which eventually accelerated the deposition of senile plaques and caused irreversible neuronal loss and synaptic dysfunction leading to cognitive impairment (Poisnel et al., 2012; Verclytte et al., 2016). In this study, the glucose hypometabolism phenomenon was detected in APP/PS1 mice, but the difference was not statistically significance between two groups before EA intervention. We speculated that was an early stage when the mitochondrial dysfunction was developed in APP/PS1 mice, and at that time, AG could effectively compensate for the mitochondrial dysfunction.

A systematic review and meta-analysis revealed that EA treatment has potential advantages in improving the cognitive function and life quality of patients with AD (Shao et al., 2019). An animal study has shown that EA at Baihui (DU20) acupoint could improve the spatial learning and memory abilities of AD model mice through increasing the glucose metabolism in the hippocampus (Jia et al., 2017). Another study using 18F-FDG PET has found that the glucose metabolism levels in the hippocampus and frontotemporal cortex were increased after acupuncture intervention, accompanied by the improved learning and memory abilities tested using the Y-type maze (Lai et al., 2016). Our previous 18F-FDG study also found that EA at DU20 acupoint significantly increased glucose metabolism in the cerebral cortex and hippocampus of APP/PS1 transgenic mice (Liu et al., 2017). In this study, we found that the learning and memory abilities of APP/PS1 mice were improved after EA at the DU20 and DU24 acupoints for 4 weeks. Meanwhile, the results of CEST imaging showed that the level of glucose metabolism in APP/PS1 mice was significantly increased.

As a powerful metabolic regulator, activated AMPK and its downstream proteins are extensively involved in glucose metabolism, playing a critical role in the recovery of damaged neurons (Wang et al., 2012). For its great potential to delay the onset or progression of AD, AMPK has emerged as a key target for the treatment of AD in recent years. In this study, it was found that the glucose metabolism level of APP/PS1 transgenic mice was further reduced after AMPK knockdown. With deficient mitochondrial function in AD, the process of glucose oxidative phosphorylation is hindered, resulting in neurons using AG for glucose metabolism. It was found that AG is significantly reduced in AD, while upregulation of this process could attenuate Aβ-induced neurotoxicity (Bisri et al., 2016). In certain brain regions, the increase of AG is associated with an enrichment gene expression involved in synaptic plasticity, an important neural basis for learning and memory abilities (Magistretti, 2014).

Hexokinase is the most important rate-limiting enzyme of the AG, known for four subtypes, namely, HK-I, HK-II, HK-III, and HK-IV. Although HK-I and HK-II both contain the glucose kinase domain, only the glucose kinase domain of HK-II presents activity, which is not affected by the negative feedback of glucose-6- phosphate (Tan and Miyamoto, 2015). Studies have shown that HK2 expression levels were significantly decreased in AD (Cuadrado-Tejedor et al., 2011) while enhancing HK-II activity through Wnt Signaling is capable of stimulating glycolysis rate to increase glucose uptake in cortical neurons (Cisternas et al., 2016). Another study also demonstrated that activated AMPK could upregulate the HK-II level to improve glycolysis flux contributing to increased glucose metabolism under the condition of insufficient ATP supply (Hung et al., 2017). In addition, changes in HK-II expression might be associated with the pathological manifestation in specific brain regions of AD (Rosa and Cesar, 2016). PFKFB3 is the isotype 3 of the PFKFB family, with the highest kinase and phosphatase activity among all isotypes (Sakakibara et al., 1997), which could also promote the process of AG (Bando et al., 2005). Studies have found that activated AMPK could promote the activation of PFKFB3, increasing the process of AG when the production of glycolysis was decreased (Yi et al., 2019). The PKM2, one of the four types of pyruvate kinases, is also abundant in brain tissue (Ye et al., 2012). Studies have found that there is feedback regulation between AMPK and PKM2 to promote AG (Liu et al., 2019). Our study found that EA at the DU20 and DU24 acupoints could improve the expression of AMPK, HK, PFK, and

PKM2 in the hippocampus, and the beneficial effects are reversed by AMPK knockdown.

CONCLUSION

Through AMPK-knockdown in APP/PS1 mice, this study demonstrated that EA treatment could activate AMPK to enhance AG of glucose metabolism in the hippocampus to improve the learning and memory abilities in APP/PS1 mice.

DATA AVAILABILITY STATEMENT

The original data supporting the conclusions of this article are available on request to the corresponding authors.

ETHICS STATEMENT

The animal study was reviewed and approved by Fujian University of Traditional Chinese Medicine Laboratory Animal Center. Written informed consent was obtained from the owners for the participation of their animals in this study.

AUTHOR CONTRIBUTIONS

JT, LC, SL, and WL contributed to conception and design of the study. JL, BZ, WJ, and MY collected the data. YZ, JZ, LL, TJ, and ZW performed the statistical analysis. JL and BZ wrote the first draft of the manuscript. SL and WL revised the manuscript. All authors contributed to manuscript revision, read, and approved the submitted version.

FUNDING

This study was supported by the Project of the National Resource Center for Chinese Materia Medica (2060302-1902-04), the Youth Science Foundation of Fujian Provincial Health Commission (2019-1-65), and the Science and Technology Platform Construction Project of the Fujian Science and Technology Department (2018Y2002).

REFERENCES

Akram, M. (2014). Citric acid cycle and role of its intermediates in metabolism. *Cell Biochem. Biophys.* 68, 475–478. doi: 10.1007/s12013-013-9750-1

An, Y., Varma, V. R., Varma, S., Casanova, R., Dammer, E., Pletnikova, O., et al. (2018). Evidence for brain glucose dysregulation in Alzheimer's disease. *Alzheimers Dement.* 14, 318–329.

Arbizu, J., Festari, C., Altomare, D., Walker, Z., Bouwman, F., Rivolta, J., et al. (2018). Clinical utility of FDG-PET for the clinical diagnosis in MCI. *Eur. J. Nucl. Med. Mol. Imaging* 45, 1497–1508. doi: 10.1007/s00259-018-4039-7

Bando, H., Atsumi, T., Nishio, T., Niwa, H., Mishima, S., Shimizu, C., et al. (2005). Phosphorylation of the 6-phosphofructo-2-kinase/fructose 2,6-bisphosphatase/PFKFB3 family of glycolytic regulators in human cancer. *Clin. Cancer Res.* 11, 5784–5792. doi: 10.1158/1078-0432.ccr-05-0149

Bevins, R. A., and Besheer, J. (2006). Object recognition in rats and mice: a one-trial non-matching-to-sample learning task to study 'recognition memory'. *Nat. Protoc.* 1, 1306–1311. doi: 10.1038/nprot.2006.205

Bigl, M., Bruckner, M. K., Arendt, T., Bigl, V., and Eschrich, K. (1999). Activities of key glycolytic enzymes in the brains of patients with Alzheimer's disease. *J. Neural Transm. (Vienna)* 106, 499–511. doi: 10.1007/s007020050174

Bisri, T., Utomo, B. A., and Fuadi, I. (2016). Exogenous lactate infusion improved neurocognitive function of patients with mild traumatic brain injury. *Asian J. Neurosurg.* 11, 151–159. doi: 10.4103/1793-5482.145375

Butterfield, D. A., and Halliwell, B. (2019). Oxidative stress, dysfunctional glucose metabolism and Alzheimer disease. *Nat. Rev. Neurosci.* 20, 148–160.

Chen, Z., and Zhong, C. (2013). Decoding Alzheimer's disease from perturbed cerebral glucose metabolism: implications for diagnostic and therapeutic strategies. *Prog. Neurobiol.* 108, 21–43. doi: 10.1016/j.pneurobio.2013.06.004

Cisternas, P., Salazar, P., Silva-Alvarez, C., Barros, L. F., and Inestrosa, N. C. (2016). Activation of Wnt signaling in cortical neurons enhances glucose utilization through glycolysis. *J. Biol. Chem.* 291, 25950–25964. doi: 10.1074/jbc.m116.735373

Cisternas, P., Zolezzi, J. M., Martinez, M., Torres, V. I., Wong, G. W., and Inestrosa, N. C. (2019). Wnt-induced activation of glucose metabolism mediates the in vivo neuroprotective roles of Wnt signaling in Alzheimer disease. *J. Neurochem.* 149, 54–72. doi: 10.1111/jnc.14608

Cuadrado-Tejedor, M., Vilarino, M., Cabodevilla, F., Del, R. J., Frechilla, D., and Perez-Mediavilla, A. (2011). Enhanced expression of the voltage-dependent anion channel 1 (VDAC1) in Alzheimer's disease transgenic mice: an insight into the pathogenic effects of amyloid-beta. *J. Alzheimers Dis.* 23, 195–206. doi: 10.3233/JAD-2010-100966

Daulatzai, M. A. (2017). Cerebral hypoperfusion and glucose hypometabolism: key pathophysiological modulators promote neurodegeneration, cognitive impairment, and Alzheimer's disease. *J. Neurosci. Res.* 95, 943–972. doi: 10.1002/jnr.23777

Dong, W., Guo, W., Zheng, X., Wang, F., Chen, Y., Zhang, W., et al. (2015). Electroacupuncture improves cognitive deficits associated with AMPK activation in SAMP8 mice. *Metab. Brain Dis.* 30, 777–784.

Edwards, S. R., Hamlin, A. S., Marks, N., Coulson, E. J., and Smith, M. T. (2014). Comparative studies using the Morris water maze to assess spatial memory deficits in two transgenic mouse models of Alzheimer's disease. *Clin. Exp. Pharmacol. Physiol.* 41, 798–806. doi: 10.1111/1440-1681.12277

Hung, Y. P., Teragawa, C., Kosaisawe, N., Gillies, T. E., Pargett, M., Minguet, M., et al. (2017). Akt regulation of glycolysis mediates bioenergetic stability in epithelial cells. *Elife* 6:e27293.

Jia, Y., Zhang, X., Yu, J., Han, J., Yu, T., Shi, J., et al. (2017). Acupuncture for patients with mild to moderate Alzheimer's disease: a randomized controlled trial. *BMC Complement. Altern. Med.* 17:556. doi: 10.1186/s12906-017-2064-x

Jin, S., and Diano, S. (2018). Mitochondrial dynamics and hypothalamic regulation of metabolism. *Endocrinology* 159, 3596–3604. doi: 10.1210/en.2018-00667

Kuehn, B. M. (2020). In Alzheimer research, glucose metabolism moves to center stage. *JAMA* 323, 297–299.

Lai, X., Ren, J., Lu, Y., Cui, S., Chen, J., Huang, Y., et al. (2016). Effects of acupuncture at HT7 on glucose metabolism in a rat model of Alzheimer's disease: an 18F-FDG-PET study. *Acupunct. Med.* 34, 215–222. doi: 10.1136/acupmed-2015-010865

Lautenschager, J., and Kaminski, S. G. (2019). Mitochondrial degradation of amyloidogenic proteins–a new perspective for neurodegenerative diseases. *Prog. Neurobiol.* 181:101660. doi: 10.1016/j.pneurobio.2019.101660

Li, X. Y., Men, W. W., Zhu, H., Lei, J. F., Zuo, F. X., Wang, Z. J., et al. (2016). Age- and brain region-specific changes of glucose metabolic disorder, learning, and memory dysfunction in early Alzheimer's disease assessed in APP/PS1 transgenic mice using (18)F-FDG-PET. *Int. J. Mol. Sci.* 17:1707. doi: 10.3390/ijms17101707

Lin, R., Chen, J., Li, X., Mao, J., Wu, Y., Zhuo, P., et al. (2016). Electroacupuncture at the Baihui acupoint alleviates cognitive impairment and exerts neuroprotective effects by modulating the expression and processing of

brain-derived neurotrophic factor in APP/PS1 transgenic mice. *Mol. Med. Rep.* 13, 1611–1617. doi: 10.3892/mmr.2015.4751

Liu, M., Zhang, Z., Wang, H., Chen, X., and Jin, C. (2019). Activation of AMPK by metformin promotes renal cancer cell proliferation under glucose deprivation through its interaction with PKM2. *Int. J. Biol. Sci.* 15, 617–627. doi: 10.7150/ijbs.29689

Liu, W., Zhuo, P., Li, L., Jin, H., Lin, B., Zhang, Y., et al. (2017). Activation of brain glucose metabolism ameliorating cognitive impairment in APP/PS1 transgenic mice by electroacupuncture. *Free Radic. Biol. Med.* 112, 174–190. doi: 10.1016/j.freeradbiomed.2017.07.024

Magistretti, P. J. (2014). Synaptic plasticity and the Warburg effect. *Cell Metab.* 19, 4–5. doi: 10.1016/j.cmet.2013.12.012

Malm, T., Koistinaho, J., and Kanninen, K. (2011). Utilization of APPswe/PS1dE9 transgenic mice in research of Alzheimer's disease: focus on gene therapy and cell-based therapy applications. *Int. J. Alzheimers Dis.* 2011:517160. doi: 10.4061/2011/517160

Manczak, M., Kandimalla, R., Fry, D., Sesaki, H., and Reddy, P. H. (2016). Protective effects of reduced dynamin-related protein 1 against amyloid beta-induced mitochondrial dysfunction and synaptic damage in Alzheimer's disease. *Hum. Mol. Genet.* 25, 5148–5166.

Minoshima, S., Giordani, B., Berent, S., Frey, K. A., Foster, N. L., and Kuhl, D. E. (1997). Metabolic reduction in the posterior cingulate cortex in very early Alzheimer's disease. *Ann. Neurol.* 42, 85–94. doi: 10.1002/ana.410420114

Mosconi, L. (2005). Brain glucose metabolism in the early and specific diagnosis of Alzheimer's disease. FDG-PET studies in MCI and AD. *Eur. J. Nucl. Med. Mol. Imaging* 32, 486–510. doi: 10.1007/s00259-005-1762-7

Newington, J. T., Pitts, A., Chien, A., Arseneault, R., Schubert, D., and Cumming, R. C. (2011). Amyloid beta resistance in nerve cell lines is mediated by the Warburg effect. *PLoS One* 6:e19191. doi: 10.1371/journal.pone.0019191

Newington, J. T., Rappon, T., Albers, S., Wong, D. Y., Rylett, R. J., and Cumming, R. C. (2012). Overexpression of pyruvate dehydrogenase kinase 1 and lactate dehydrogenase A in nerve cells confers resistance to amyloid beta and other toxins by decreasing mitochondrial respiration and reactive oxygen species production. *J. Biol. Chem.* 287, 37245–37258. doi: 10.1074/jbc.M112.366195

Peprah, K., and McCormack, S. (2019). *Medical Cannabis for the Treatment of Dementia: A Review of Clinical Effectiveness and Guidelines*. Ottawa, ON: Canadian Agency for Drugs and Technologies in Health.

Poisnel, G., Herard, A. S., El, T. E. T. N., Bourrin, E., Volk, A., Kober, F., et al. (2012). Increased regional cerebral glucose uptake in an APP/PS1 model of Alzheimer's disease. *Neurobiol. Aging* 33, 1995–2005. doi: 10.1016/j.neurobiolaging.2011.09.026

Ramos-Rodriguez, J. J., Pacheco-Herrero, M., Thyssen, D., Murillo-Carretero, M. I., Berrocoso, E., Spires-Jones, T. L., et al. (2013). Rapid beta-amyloid deposition and cognitive impairment after cholinergic denervation in APP/PS1 mice. *J. Neuropathol. Exp. Neurol.* 72, 272–285. doi: 10.1097/NEN.0b013e318288a8dd

Riester, M., Xu, Q., Moreira, A., Zheng, J., Michor, F., and Downey, R. J. (2018). The Warburg effect: persistence of stem-cell metabolism in cancers as a failure of differentiation. *Ann. Oncol.* 29, 264–270. doi: 10.1093/annonc/mdx645

Rosa, J. C., and Cesar, M. C. (2016). Role of hexokinase and VDAC in neurological disorders. *Curr. Mol. Pharmacol.* 9, 320–331.

Sakakibara, R., Kato, M., Okamura, N., Nakagawa, T., Komada, Y., Tominaga, N., et al. (1997). Characterization of a human placental fructose-6-phosphate, 2-kinase/fructose-2,6-bisphosphatase. *J. Biochem.* 122, 122–128. doi: 10.1093/oxfordjournals.jbchem.a021719

Santangelo, R., Giuffrida, M. L., Satriano, C., Tomasello, M. F., Zimbone, S., and Copani, A. (2021). Beta-amyloid monomers drive up neuronal aerobic glycolysis in response to energy stressors. *Aging* 13, 18033–18050. doi: 10.18632/aging.203330

Shao, S., Tang, Y., Guo, Y., Tian, Z., Xiang, D., and Wu, J. (2019). Effects of acupuncture on patients with Alzheimer's disease: protocol for a systematic review and meta-analysis. *Medicine (Baltimore)* 98:e14242. doi: 10.1097/md.0000000000014242

Tan, V. P., and Miyamoto, S. (2015). HK2/hexokinase-II integrates glycolysis and autophagy to confer cellular protection. *Autophagy* 11, 963–964. doi: 10.1080/15548627.2015.1042195

van Zijl, P. C., and Yadav, N. N. (2011). Chemical exchange saturation transfer (CEST): what is in a name and what isn't? *Magn. Reson. Med.* 65, 927–948. doi: 10.1002/mrm.22761

Verclytte, S., Lopes, R., Lenfant, P., Rollin, A., Semah, F., Leclerc, X., et al. (2016). Cerebral hypoperfusion and hypometabolism detected by arterial spin labeling MRI and FDG-PET in early-onset Alzheimer's disease. *J. Neuroimaging* 26, 207–212.

Vlassenko, A. G., Vaishnavi, S. N., Couture, L., Sacco, D., Shannon, B. J., Mach, R. H., et al. (2010). Spatial correlation between brain aerobic glycolysis and amyloid-beta (Abeta) deposition. *Proc. Natl. Acad. Sci. U.S.A.* 107, 17763–17767.

Wang, S., Song, P., and Zou, M. H. (2012). AMP-activated protein kinase, stress responses and cardiovascular diseases. *Clin. Sci. (Lond.)* 122, 555–573.

Wilson, H., Pagano, G., and Politis, M. (2019). Dementia spectrum disorders: lessons learnt from decades with PET research. *J. Neural. Transm. (Vienna)* 126, 233–251. doi: 10.1007/s00702-019-01975-4

Xu, Z. P., Chang, H., Ni, Y. Y., Li, C., Chen, L., Hou, M., et al. (2019). Schistosoma japonicum infection causes a reprogramming of glycolipid metabolism in the liver. *Parasit. Vectors* 12:388. doi: 10.1186/s13071-019-3621-6

Yan, Y., Zhou, X. E., Xu, H. E., and Melcher, K. (2018). Structure and physiological regulation of AMPK. *Int. J. Mol. Sci.* 19:3534.

Yang, T. T., Shih, Y. S., Chen, Y. W., Kuo, Y. M., and Lee, C. W. (2015). Glucose regulates amyloid beta production via AMPK. *J. Neural. Transm. (Vienna)* 122, 1381–1390. doi: 10.1007/s00702-015-1413-5

Ye, J., Mancuso, A., Tong, X., Ward, P. S., Fan, J., Rabinowitz, J. D., et al. (2012). Pyruvate kinase M2 promotes de novo serine synthesis to sustain mTORC1 activity and cell proliferation. *Proc. Natl. Acad. Sci. U.S.A.* 109, 6904–6909. doi: 10.1073/pnas.1204176109

Yi, M., Ban, Y., Tan, Y., Xiong, W., Li, G., and Xiang, B. (2019). 6-Phosphofructo-2-kinase/fructose-2,6-biphosphatase 3 and 4: a pair of valves for fine-tuning of glucose metabolism in human cancer. *Mol. Metab.* 20, 1–13. doi: 10.1016/j.molmet.2018.11.013

Yin, J., Reiman, E. M., Beach, T. G., Serrano, G. E., Sabbagh, M. N., Nielsen, M., et al. (2020). Effect of ApoE isoforms on mitochondria in Alzheimer disease. *Neurology* 94, e2404–e2411.

Zhou, J., Peng, W., Xu, M., Li, W., and Liu, Z. (2015). The effectiveness and safety of acupuncture for patients with Alzheimer disease: a systematic review and meta-analysis of randomized controlled trials. *Medicine (Baltimore)* 94:e933. doi: 10.1097/md.0000000000000933

Conflict of Interest: The authors declare that the research was conducted in the absence of any commercial or financial relationships that could be construed as a potential conflict of interest.

Publisher's Note: All claims expressed in this article are solely those of the authors and do not necessarily represent those of their affiliated organizations, or those of the publisher, the editors and the reviewers. Any product that may be evaluated in this article, or claim that may be made by its manufacturer, is not guaranteed or endorsed by the publisher.

frontiers in Cellular Neuroscience

ORIGINAL RESEARCH
published: 21 March 2022
doi: 10.3389/fncel.2022.848967

Enhanced Medial Prefrontal Cortex and Hippocampal Activity Improves Memory Generalization in APP/PS1 Mice: A Multimodal Animal MRI Study

Weilin Liu[1†], Jianhong Li[2†], Le Li[2†], Yuhao Zhang[2], Minguang Yang[1], Shengxiang Liang[2], Long Li[2], Yaling Dai[2], Lewen Chen[2], Weiwei Jia[2], Xiaojun He[2], Huawei Lin[2] and Jing Tao[3]*

[1] National-Local Joint Engineering Research Center of Rehabilitation Medicine Technology, Fujian University of Traditional Chinese Medicine, Fuzhou, China, [2] TCM Rehabilitation Research Center of SATCM, Fujian University of Traditional Chinese Medicine, Fuzhou, China, [3] College of Rehabilitation Medicine, Fujian University of Traditional Chinese Medicine, Fuzhou, China

OPEN ACCESS

Edited by:
Zhang Pengyue,
Yunnan University of Traditional Chinese Medicine, China

Reviewed by:
Juan Li,
Chengdu University of Traditional Chinese Medicine, China
Junzhe Huang,
The Chinese University of Hong Kong, Hong Kong SAR, China

***Correspondence:**
Jing Tao
taojing01@fjtcm.edu.cn

[†] These authors have contributed equally to this work

Specialty section:
This article was submitted to Cellular Neuropathology, a section of the journal Frontiers in Cellular Neuroscience

Received: 05 January 2022
Accepted: 08 February 2022
Published: 21 March 2022

Citation:
Liu W, Li J, Li L, Zhang Y, Yang M, Liang S, Li L, Dai Y, Chen L, Jia W, He X, Lin H and Tao J (2022) Enhanced Medial Prefrontal Cortex and Hippocampal Activity Improves Memory Generalization in APP/PS1 Mice: A Multimodal Animal MRI Study. Front. Cell. Neurosci. 16:848967. doi: 10.3389/fncel.2022.848967

Memory generalization allows individuals to extend previously learned movement patterns to similar environments, contributing to cognitive flexibility. In Alzheimer's disease (AD), the disturbance of generalization is responsible for the deficits of episodic memory, causing patients with AD to forget or misplace things, even lose track of the way home. Cognitive training can effectively improve the cognition of patients with AD through changing thinking mode and memory flexibility. In this study, a T-shaped maze was utilized to simulate cognitive training in APP/PS1 mice to elucidate the potential mechanisms of beneficial effects after cognitive training. We found that cognitive training conducted by a T-shaped maze for 4 weeks can improve the memory generalization ability of APP/PS1 mice. The results of functional magnetic resonance imaging (fMRI) showed that the functional activity of the medial prefrontal cortex (mPFC) and hippocampus was enhanced after cognitive training, and the results of magnetic resonance spectroscopy (MRS) showed that the neurochemical metabolism of N-acetyl aspartate (NAA) and glutamic acid (Glu) in mPFC, hippocampus and reuniens (Re) thalamic nucleus were escalated. Furthermore, the functional activity of mPFC and hippocampus was negatively correlated with the escape latency in memory generalization test. Therefore, these results suggested that cognitive training might improve memory generalization through enhancing the functional activity of mPFC and hippocampus and increasing the metabolism of NAA and Glu in the brain regions of mPFC, hippocampus and Re nucleus.

Keywords: Alzheimer's disease, cognitive training, generalization, functional activity, neurochemical metabolism

INTRODUCTION

Memory generalization allows individuals to extend previously learned movement patterns to similar environments, which contributes to the maintenance of normal life activities. Studies in recent years have indicated that the disturbance of generalization is linked to multiple neurological and psychiatric diseases, such as posttraumatic stress disorder (PTSD) (Pedraza et al., 2019;

Wang et al., 2021). Even though overgeneralization of fear memories is linked to pathological states, generalization plays an essential role in the processes of learning and memory. People with Alzheimer's disease (AD) typically experience deficits in memory, executive function, language, and attention. Of these dysfunctions, episodic memory impairment has been widely recognized as the most noticeable and earliest symptoms, and the impairment of episodic memory causes patients with AD to forget or misplace things, experience difficulty in recalling the details of recent events, and lose track of the way home, disrupting the quality of normal life (Winocur et al., 2001). The improvement of generalization ability may help in the maintenance of normal episodic memory.

Based upon previous literature, the cognition of patients with AD can be improved after many forms of cognitive training, and the beneficial effects from cognitive training are associated with changed thinking mode and improved memory flexibility (Markovic et al., 2020). Previous studies have showed that computer-assisted cognitive training can effectively improve the learning memory ability in patients with mild cognitive impairment or Alzheimer's disease (Herrera et al., 2012; Vermeij et al., 2016; Cavallo and Angilletta, 2017). A clinical randomized controlled trial study demonstrated that memory training can enhance memory performance in older adults (Ball et al., 2002). A recent study also indicated that people with mild to moderate AD can learn and recall new episodic information well through memory training (Small and Cochrane, 2020). Since generalization ability is highly important for normal memory function, we can guess that cognitive training might improve memory capacity through memory generalization ability. In this study, we utilized a T-shaped maze to train memory flexibility in APP/PS1 mice to explore the mechanism for improved generalization ability after cognition training.

In the central nervous system (CNS), the hippocampus is a critical brain region that regulates memory and learning ability, especially episodic memories (Hainmueller and Bartos, 2020). The medial prefrontal cortex (mPFC) plays an important regulatory role in executive functions, strategy switching, and behavioral flexibility (Ragozzino et al., 2003; Ghods-Sharifi et al., 2008). The bidirectional synaptic connections among reuniens (Re) nucleus, mPFC and hippocampus have been confirmed with the application of virus tracing technology in recent years (Xu and Sudhof, 2013; Varela et al., 2014). In the process of learning and memory, the neural circuit of mPFC-Re-hippocampus coordinates the information between mPFC and hippocampus regulating memory generalization (Xu and Sudhof, 2013; Ito et al., 2018). In addition, the memory integration mechanism between mPFC and hippocampus supports not only the generalization of episodic memory but also conceptual learning. Studies pointed out that memory impairment in the early stage of patients with AD positively correlated with the atrophy of the prefrontal cortex and hippocampus (Carter et al., 2014). The neural activity of the Re nucleus can be influenced by tetanus toxin (TetTox) and lentiviral technology. Using these technologies, studies found that inhibited neural signal transmission in the Re nucleus would reduce the expression of c-fos in the CA1 regions of the hippocampus and mPFC, restraining memory generalization (Varela et al., 2014; Ito et al., 2015, 2018).

The destruction of the functional connection of the mPFC-Re-hippocampus neural circuit in patients with AD is associated with the decline of memory generalization ability. Previous studies showed that cognitive training could improve cognitive function through enhancing the functional connections between the frontal cortex, thalamus, and hippocampus (Li et al., 2016). Based on this, in this study, we utilized a T-shaped maze to simulate cognitive training to enhance the memory flexibility of APP/PS1 mice. Then, fMRI and MRS technologies were combined to elucidate the potential mechanisms of beneficial effects after cognitive training.

MATERIALS AND METHODS

Animals and Ethics

Male APP/PS1 double-transgenic mice [C57BL/6 × C3H] were purchased from the Nanjing Biomedical Research Institute of the Nanjing University as AD model mice. The mice required for the experiment were obtained by crossing male APP/PS1 double-transgenic mice with female wild-type mice [C57BL/6]. The animals were raised in SPF-level animal experiment center of the Fujian University of Traditional Chinese Medicine (FJTCM). Each cage contains 4 mice, and all animals were permitted to food and water. The environment of the SPF room is kept constant, with a standard day and night system (12 h light + 12 h dark), the room temperature at about 22°C, and the humidity of 50–70%. The experiments were operated and implemented in strict accordance with the provisions of the national animal protection laws and regulations, and all the ethics of experiments have been endorsed by the Animal Management Committee of the Fujian University of Traditional Chinese Medicine (FJTCMIACUC 2019031).

Experimental Protocol

The PCR technology was applied to identify the genotype of each mouse. According to previous studies, APP/PS1 mice present significant memory generalization decline at 6 months. Thus, this experiment selected 5-month-old APP/PS1 mice conducting cognitive training for 4 weeks. According to the random digital table method, the APP/PS1 double-transgenic mice were randomly divided into the model group (AD group) and the cognitive training group (Cog-group), with 8 mice in each group, and another 8 wild-type mice were selected into the wild-type group (WT group). The Morris water maze experiment was utilized to observe the generalization and learning memory ability of each group. MRI was used to detect the functional activity and neurochemical metabolism of brain regions related to memory generalization, including mPFC, hippocampus, and Re nucleus. The experimental operation was shown in **Figure 1A**.

Cognitive Training

The cognitive training method was modified based on a previous study (Talboom et al., 2014). A water T-maze was implemented to conduct cognitive training on APP/PS1 mice. A T-shaped

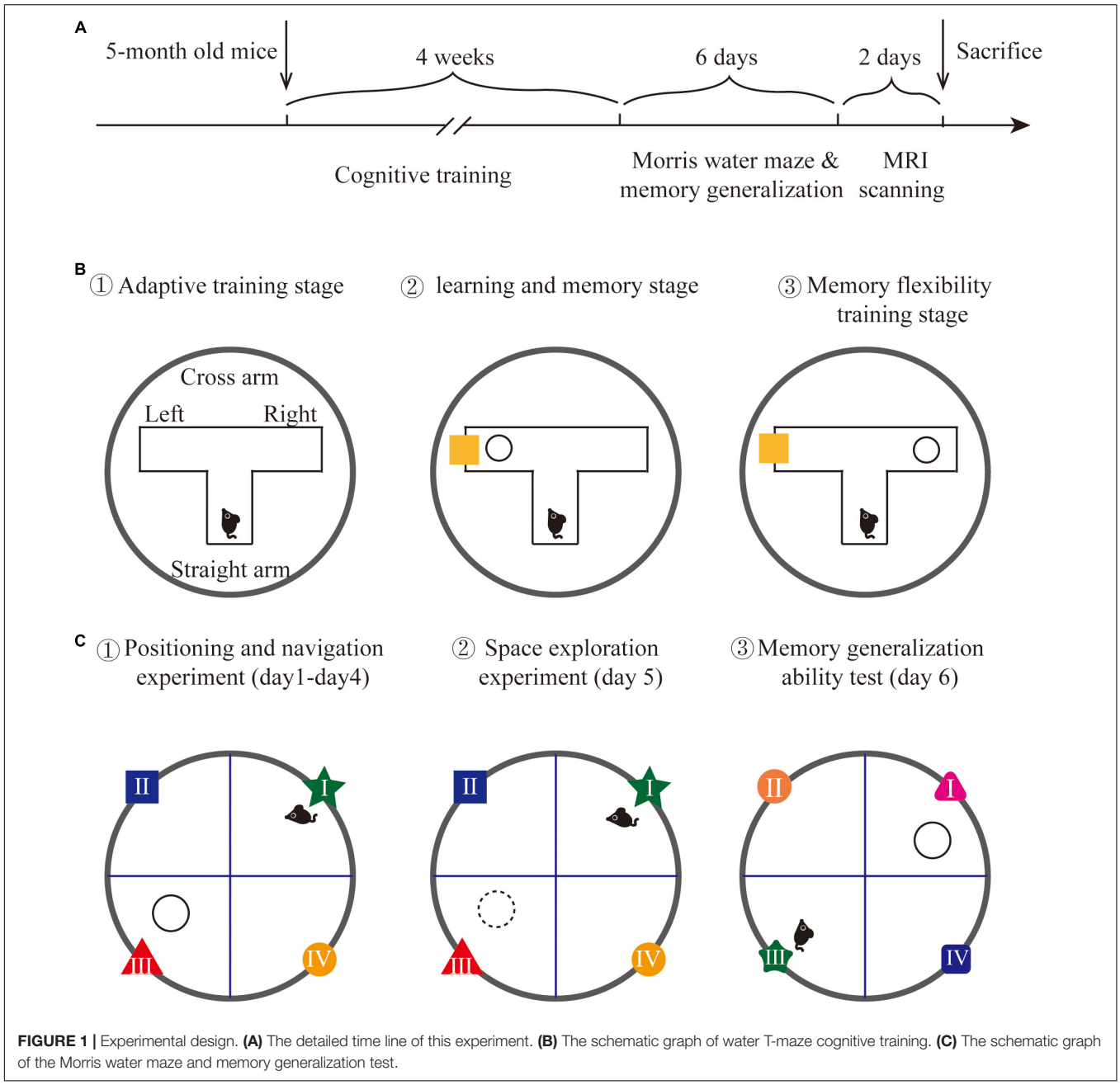

FIGURE 1 | Experimental design. **(A)** The detailed time line of this experiment. **(B)** The schematic graph of water T-maze cognitive training. **(C)** The schematic graph of the Morris water maze and memory generalization test.

maze was placed in a circular pool to form a water T-maze, with each arm length at 40 cm and width at 15 cm, and the water temperature at 23 ± 1°C. A circular escape platform with a diameter at 6 cm was placed 1 cm under the water surface. The reference object was placed on the inside of the cross arm. The position of the escape platform and the reference object can be freely changed in two different cross arms. The training on water T-maze includes three stages:

(1) *Adaptive training stage*: One day before training, each mouse was placed in the water T-maze from the end of the straight arm, freely explored for 3 min to familiar with the environment (no reference objects were placed).

(2) *Learning and memory stage*: The escape platform was randomly placed at the end of one cross arm, with a reference object in the same cross arm to guide the position of the escape platform. Each mouse was trained to find the escape platform correctly 8 times a day, training 6 days/week, lasting 2 weeks. The training is perfect if the mouse directly swims to and land on the escape platform after entering the water T-maze. If the mouse did not find the escape platform, it will be guided to the escape platform to learn for 15 s; each training interval was 10 min.

(3) *Memory flexibility training stage*: After the learning and memory stage, the escape platform was randomly placed at the end of one cross arm, with a reference object in the opposite cross

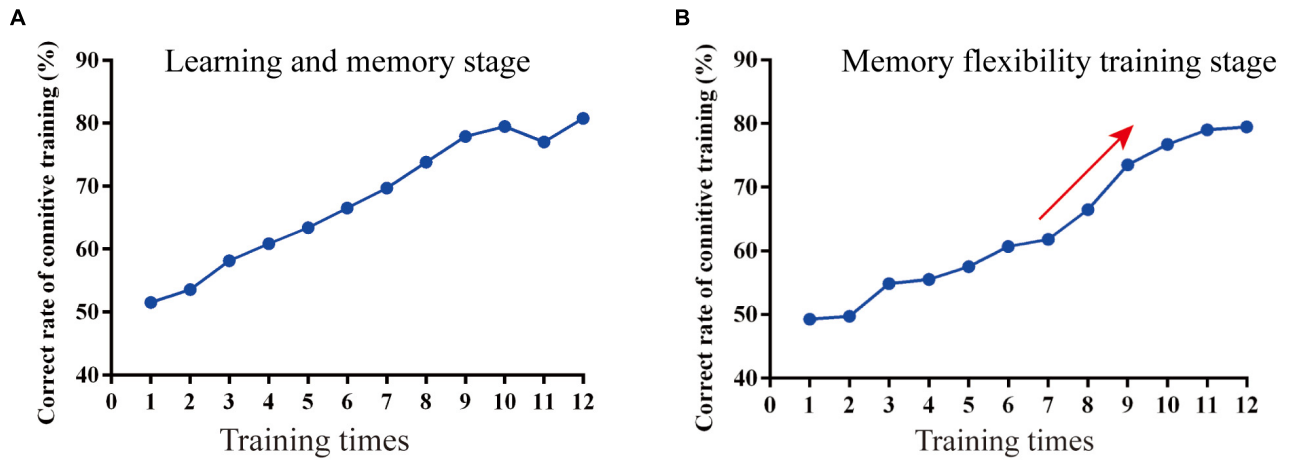

FIGURE 2 | The course of the memory flexibility training in APP/PS1 mice. **(A)** The correct rate in the learning and memory stage. **(B)** The correct rate in the memory flexibility training stage.

arm to train memory flexibility. The training period and method are the same as the learning and memory stage. The training method is shown in **Figure 1B**.

Memory Generalization Test

Memory generalization allows individuals to extend previously learned movement patterns to similar environments. According to this, we examined the memory generalization ability of mice by slightly changing the color and shape of the reference objects in the Morris water maze. The Morris water maze was a circular pool with 120 cm diameter, 50 cm height, and 30 cm water depth. The water temperature was constant at 23 ± 1°C. The circular pool was divided into four quadrants (recorded as the first quadrant, the second quadrant, the third quadrant, and the fourth quadrant) and an escape platform with a diameter of 6 cm was placed 2 cm under the water surface in the third quadrant. The water maze was surrounded by blue curtains, and the background was stable. The only reference objects were located on the inner wall of the water maze. A camera was mounted above the water maze to record the trajectory of each mouse. The Morris water maze experiment included 3 stages:

(1) *Positioning and navigation experiment*: At this stage, each mouse was put into the water from different quadrants. The time when each mouse entered the escape platform was recorded. If the mouse found the platform within 90 s and stayed more than 3 s, the time was recorded as the escape latency; if the mouse did not find the escape platform within 90 s, the escape latency was recorded as 90 s and the mouse was guided to the escape platform to learn for 15 s. This stage lasted for 4 days and 4 times a day.

(2) *Space exploration experiment*: On the 5th day of the experiment, the escape platform was removed. Then, each mouse was put into the water from the first quadrant, and the trajectory of each mouse within 90 s was recorded.

(3) *Memory generalization ability test*: The memory generalization ability test was performed on the 6th day of the experiment. The escape platform was placed in the first quadrant, and the shape and color of reference objects in the first quadrant and adjacent quadrants were changed. Then, each mouse was put into the water from the third quadrant, and the time that each mouse finds the escape platform was recorded as escape latency. The detection method is shown in **Figure 1C**.

Magnetic Resonance Imaging

The MRI analysis system (MiniMR-60 MRI System 7.0 T) was utilized to conduct the imaging scan. At the first, the mice were induced to anesthetize with 3% isoflurane. During the imaging scan, the head of each mouse was fixed under the surface coil, and 1.5% isoflurane was used to maintain anesthesia. The body temperature of each mouse was maintained at around 37°C by a hot water circulation system, and the breathing and heart rate were monitored to ensure the life state. The MRI scan included 2 parts: functional magnetic resonance imaging (fMRI) and magnetic resonance spectroscopy (MRS).

(1) *Functional magnetic resonance imaging*: After fixing the head of the mouse, location imaging was scanned, and the position of each mouse was adjusted to ensure the head was at the center of the image. Then, the T2-weighted imaging (T2WI) technique was carried out. The scanning parameters were mentioned as: TR/TE = 4,200/35 ms, FOV = 20 × 20 mm, averages = 4, image size = 256 × 256, slices = 35, and slice thickness = 0.5 mm. After the T2-weighted imaging, the supply of isoflurane was stopped, and the fMRI was conducted when the heart rate of each mouse returned to 80 beats/min. The scanning parameters were mentioned as: Echo time = 10,279 ms, repetition time = 2,000 ms, repetitions = 200, FOV = 20 × 20 mm, averages = 4, image size = 64 × 64, slices = 30, and slice thickness = 0.5 mm. After data collection, the Statistical Parametric Mapping (SPM) and Data Processing Assistant for Resting-State fMRI (DPARSF) software packages were used for data analysis.

(2) *Magnetic resonance spectroscopy*: T2WI images were used to determine the area of interest (volumes of interest, VOI).

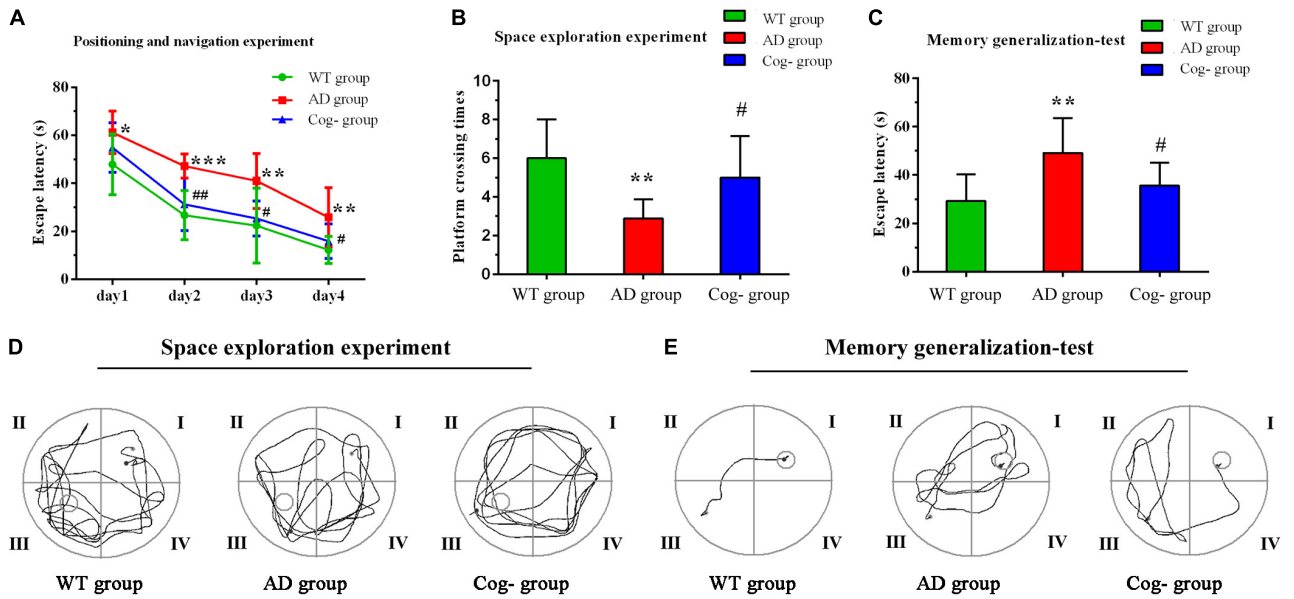

FIGURE 3 | Cognition performance after cognitive training in APP/PS1 mice. **(A–E)** Learning memory and memory generalization ability after cognitive training. **(A)** The escape latency of each group in the Morris water maze. **(B)** The escape platform crossing times of each group in the Morris water maze. **(C)** The escape latency of each group in the memory generalization test. **(D)** Representative diagram of each group in the space exploration experiment. **(E)** Representative diagram of each group in the memory generalization test. $^{*}P < 0.05$ compared with the WT group, $^{**}P < 0.01$ compared with the WT group, $^{***}P < 0.001$ compared with the WT group, $^{\#}P < 0.05$ compared with the AD group, $^{\#\#}P < 0.01$ compared with the AD group.

The mPFC, hippocampus and Re nucleus were selected as the VOI for scanning, and the scanning parameters were mentioned as: TR = 1,500 ms and TE = 144 ms. The position of these neurochemicals was shown as: NAA 2.02 parts per million (ppm), Glu 2.2 ppm, and Cr 3.05 ppm. After data collection, the software package TOPSPIN (v3.1, Bruker Biospin, Germany) was used to process spectral data. A quantum estimation (QUEST) method was used to calculate the ratio of the area under the peak of NAA and Cr (NAA/Cr), which represents the neurochemical metabolism level of NAA. The neurochemical metabolism level of Glu (Glu/Cr) was calculated using the same method.

Statistical Analysis

All data were expressed as means ± S.E.M and processed by SPSS25.0. The method of repeated measurement analysis was used in the escape latency in the Morris water maze. The data of platform crossing times, escape latency in memory generalization test and the data of MRS were analyzed by One-way ANOVA. The LSD method was used when the variance was homogeneous, and the Dunnett's T3 test was used when the variance was uneven. $P < 0.05$ was considered statistically significant. The regional homogeneity (ReHo) value of fMRI was analyzed by the one-way ANOVA and was considered statistically significant when more than 10 clusters existed differences ($P < 0.001$). Bivariate correlation analysis was utilized to analyze the correlation between the ReHo value of mPFC, hippocampus, and memory generalization ability. Pearson coefficient was used as the correlation coefficient, and $P < 0.05$ was regarded as statistically significant.

RESULTS

The Correct Rate Increased Over the Course of Cognitive Training in Alzheimer's Disease Mice

In the learning and memory stage (phase 1), the correct rate of the mice in the Cog-group finding the escape platform was increased over time, and the correct rate was close to 80% in the last 4 days of training (**Figure 2A**). In the memory flexibility training stage (phase 2), the correct rate of the mice in the Cog-group finding the escape platform was increased over time. There was a rapid ascending period on the 7th day of phase 2, and the correct rate was close to 80% in the last 4 days of phase 2 (**Figure 2B**).

Cognitive Training Improved the Memory Generalization Ability of Alzheimer's Disease Mice

The learning memory and generalization ability of each group were assessed after cognitive training. The results of Morris Water Maze showed that the escape latency of the AD group was increased compared with the WT group, while the Cog-group was decreased compared with the AD group; the escape platform crossing times of the AD group was decreased compared with the WT group, while the Cog-group was increased compared with the AD group ($P < 0.05$) (**Figures 3A,B,D**). After the test of Morris Water Maze, the background of the apparatus was changed to test the memory generalization ability of each group. The results showed that the escape latency of the AD group

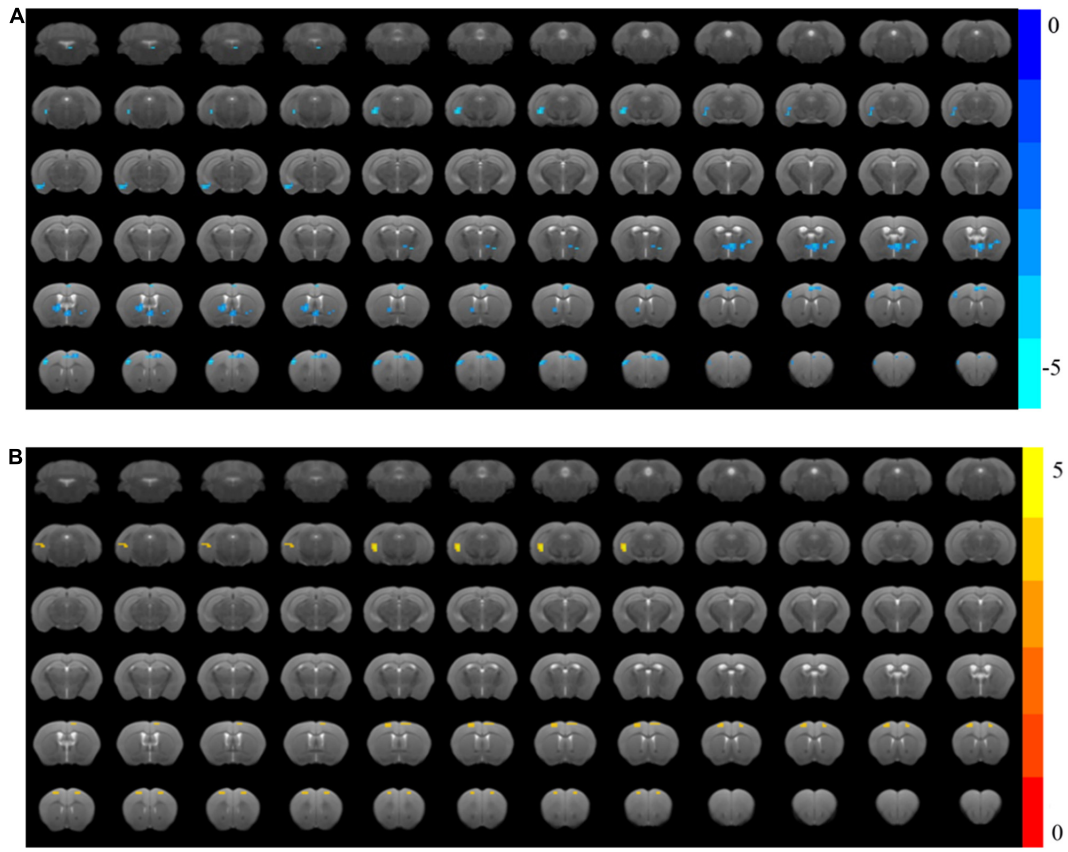

FIGURE 4 | Changes in brain functional activity after cognitive training in APP/PS1 mice. **(A)** The ReHo value of the AD group decreased significantly compared with the WT group. **(B)** The ReHo value of the Cog-group increased compared with the AD group.

was increased compared with the WT group, while the Cog-group was decreased compared with the AD group ($P < 0.05$) (**Figures 3C,E**). All these results suggested that cognitive training might effectively enhance the learning memory ability of AD mice through improving the generalization ability.

Cognitive Training Enhanced the Functional Activity of the Hippocampus and mPFC in Alzheimer's Disease Mice

One mouse in the Cog-group was excluded for the head movements during MRI. MRI was completed for all 23 mice and included in the analysis of whole-brain functional activity. The results showed that compared with the WT group, the functional activity of the brain in the AD group was decreased, which included the brain regions of the hippocampus (right), mPFC, motor cortex, somatosensory cortex (right), and cingulate gyrus (right) (**Figure 4A** and **Table 1**). However, the functional activity was increased after cognitive training. As the results presented that compared with the AD group, the functional activity of the brain in Cog-group was increased, which included the brain regions of the hippocampus (right), mPFC, and motor cortex (**Figure 4B** and **Table 1**). Furthermore, the results of the Pearson's and Spearman's correlation analyses showed that the functional activity of the mPFC and hippocampus was all negatively correlated with the escape latency in the memory generalization test ($r = -0.411$ and -0.455, $P < 0.05$) (**Figures 5A,B**). These results pointed out that recovering the functional activity of the brain might be a crucial mechanism to the improvement of the memory generalization ability on AD mice.

Cognitive Training Improved the Neurochemical Metabolism of the Hippocampus, mPFC, and Re Nucleus in Alzheimer's Disease Mice

In addition to functional activity analysis, MRS was performed to assess the neurochemical metabolism levels of memory generalization-related regions, including the hippocampus, mPFC and Re nucleus. In the left mPFC, the concentration of Glu and NAA in the AD group was decreased compared with the WT group ($P < 0.001$); however, the concentration of Glu and NAA in the Cog-group was increased compared with the AD group after cognitive training ($P < 0.01$) (**Figure 6A**). In the right mPFC, the concentration of Glu and NAA in the AD group was decreased compared with the WT group ($P < 0.001$); however, the concentration of Glu and NAA in the Cog-group was increased compared with the AD group ($P < 0.01$ or $P < 0.001$)

TABLE 1 | Regions showing significant changes in functional activity.

Brain region	AD group < WT Group		Cog-group > AD Group	
	Clusters	*t*-value	Clusters	*t*-value
Hippocampus right	15	−5.7016	13	5.2612
Medial prefrontal lobe	35	−4.5132	16	4.3032
Motor cortex left	34	−4.6837	16	4.3748
Motor cortex right	17	−4.8809	16	4.3032
Somatosensory cortex right	13	−4.8809	-	-
Cingulate gyrus right	10	−4.5209	-	-

(**Figure 6B**). In the left hippocampus, the concentration of Glu and NAA in the AD group was decreased compared with the WT group ($P < 0.001$ or $P < 0.01$); however, the concentration of Glu in the Cog-group was increased compared with the AD group ($P < 0.001$) (**Figure 6C**). In the right hippocampus, the concentration of Glu and NAA in the AD group was decreased compared with the WT group ($P < 0.001$ or $P < 0.01$); however, the concentration of Glu and NAA in the Cog-group was increased compared with the AD group ($P < 0.001$ or $P < 0.01$) (**Figure 6D**). In the Re nucleus, the concentration of Glu and NAA in the AD group was decreased compared with the WT group ($P < 0.01$); however, the concentration of Glu and NAA in the Cog-group was increased compared with the AD group ($P < 0.01$ or $P < 0.05$) (**Figure 6E**). The location of volumes of interest (VOI) and typical image of MRS are displayed in **Figure 6F**. All these results presented that the concentration of Glu and NAA was decreased in these brain regions related to memory generalization. Moreover, cognitive training could recover the neurochemical metabolism of AD mice.

DISCUSSION

Many forms of cognitive training could effectively improve cognitive function in patients with AD through changing thinking mode and memory flexibility. In this study, a T-shaped maze was carried out to conduct cognitive training on APP/PS1 mice. The results of behavior experiments presented that learning memory ability was impaired in APP/PS1 mice at 6 months of age. In contrast, cognitive training for 4 weeks could enhance the learning memory and generalization ability of APP/PS1 mice. The results of fMRI exhibited that the functional activity of mPFC and hippocampus was depressed in 6-month-old APP/PS1 mice, while cognitive training enhanced the functional activity of these two brain regions. Furthermore, the functional activity of mPFC and hippocampus was negatively correlated with the escape latency tested in the memory generalization test. At the same time, the results of MRS revealed that cognitive training was able to restore the neurochemical metabolism of Glu and NAA in mPFC, hippocampus, and Re nucleus. This study concluded that cognitive training can improve memory generalization by enhancing brain functional activity and restoring the levels of neurochemical metabolism.

The dysfunction of generalization is associated with memory deficiency in early AD. A study showed that non-dementia subjects with *ABCA7* mutation (an AD-related risk gene) are manifested as the decline of memory generalization (Sinha et al., 2019). A follow-up study indicated that subjects with poor memory generalization tests were the most likely to progress to mild cognitive impairment and Alzheimer's disease (Myers et al., 2008). Encouragingly, clinical research has highlighted the fact that cognitive training could recover the capacity of learning memory and generalization ability in patients with cognitive decline and impairment (Chan et al., 2016; Vermeij et al., 2016). Geographical Exercise for Cognitive Optimization task training enables patients with cognition impairment to complete similar tasks effortlessly besides routine tasks (Cavallo and Angilletta, 2017). Studies in animals have also shown that cognitive training could simultaneously alleviate the impairment of memory function (Talboom et al., 2014). In this study, we performed cognitive training in APP/PS1 mice through a T-shaped water maze and trained the memory flexibility of APP/PS1 mice by changing the relative positions between the escape platform and the reference object. We found that cognition training could improve the memory generalization ability in APP/PS1 mice. The results of this study proved that the T-shaped water maze training is an effective cognitive training method to train memory flexibility. However, a

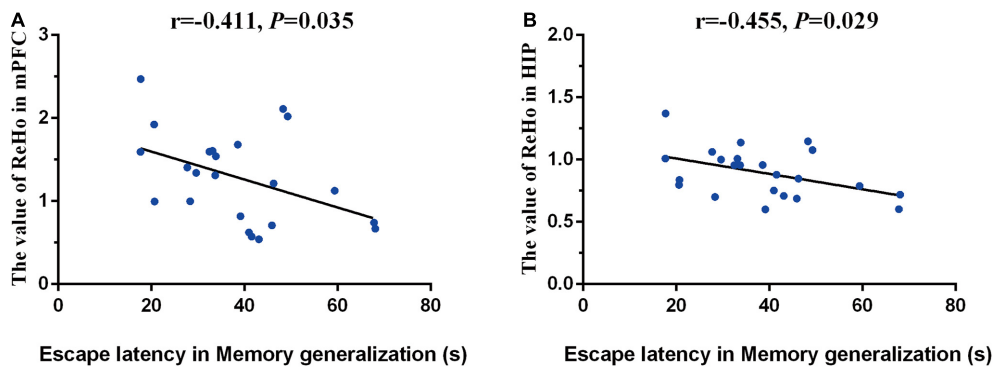

FIGURE 5 | Correlations between functional activity and memory generalization ability. **(A)** Correlation between the functional activity of mPFC and memory generalization ability. **(B)** Correlation between the functional activity of hippocampus and memory generalization ability.

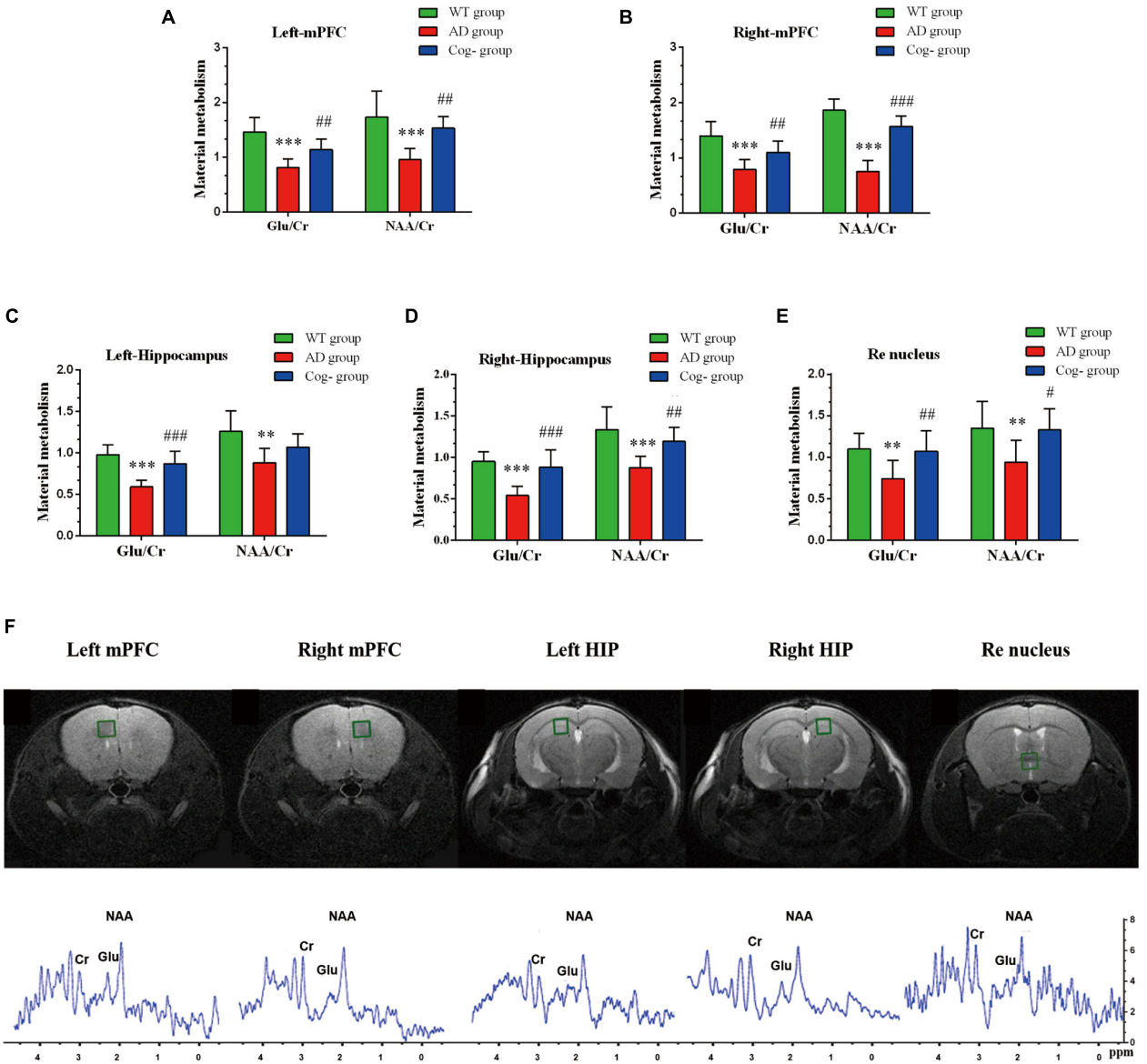

FIGURE 6 | Changes in neurochemical metabolism after cognitive training in APP/PS1 mice. **(A–E)** The neurochemical metabolism of Glu and NAA of each group in mPFC (left), mPFC (right), hippocampus (left), hippocampus (right), and Re nucleus. **(F)** The location and the representative graph in mPFC (left), mPFC (right), hippocampus (left), hippocampus (right), and Re nucleus. $^{*}P < 0.05$ compared with the WT group, $^{**}P < 0.01$ compared with the WT group, $^{***}P < 0.001$ compared with the WT group, $^{\#}P < 0.05$ compared with the AD group, $^{\#\#}P < 0.01$ compared with the AD group, $^{\#\#\#}P < 0.001$ compared with the AD group.

recent study showed that early cognitive training could rescue the recall of remote spatial memory but reduce cognitive flexibility in AD mice (Rai et al., 2020). Such a contradiction can be attributed to the difference in the cognitive training pattern. In clinical trials, the forms of cognitive training are also multitudinous, such as television-based cognitive training, computerized cognitive training, and mathematical training (Guo et al., 2020). Effects often vary between different forms of cognitive training.

The functional connections between default networks are considered to be the neural mechanism of cognitive decline (Greicius et al., 2004; Buckner et al., 2008). Functional connections between the hippocampus and the default network are also reduced in the initial stage of AD (Dillen et al., 2017). In contrast, cognitive training could ease the symptoms of AD through enhancing the brain functional connectivity and the functional activity (Engvig et al., 2014; Lin et al., 2014). Studies have found that computer-assisted cognitive training could strengthen the functional connectivity of the hippocampus and cerebral cortex (Lin et al., 2014). A randomized controlled study also found that the blood oxygen level-dependent signals in the hippocampus and cerebral cortex

were enhanced in patients with mild cognitive impairment after cognitive training (Hampstead et al., 2012). The neural circuit of mPFC-Re-hippocampus coordinates the memory information between mPFC and hippocampus, affecting memory generalization (Xu and Sudhof, 2013; Ito et al., 2018). In this study, three generalization-related brain regions were selected to conduct MRI scanning to evaluate the changes in functional activity. Our results showed that cognitive training can enhance the functional activity of mPFC and hippocampus. Furthermore, correlation analysis exhibited that the functional activity of the mPFC and hippocampus was negatively correlated with the escape latency in the memory generalization test. These results indicated that cognitive training may improve generalization ability by enhancing the functional activity of the mPFC and hippocampus. Animal studies also displayed that cognitive training could improve the cognitive function of AD model mice through enhancing hippocampus synaptic plasticity and promoting hippocampus neurogenesis (Jiang et al., 2015; Zeng et al., 2016). Similarly, cognitive training also promoted dopamine D1 receptor-mediated neuron activity in the mPFC of mice (Wass et al., 2013). Memory encoding and retrieval is closely related to the functional connection between the mPFC and hippocampus (Preston and Eichenbaum, 2013; Sekeres et al., 2018). The Re nucleus is anatomically connected with the mPFC and hippocampus to become an important neural network that regulates memory generalization (Cassel et al., 2013; Xu and Sudhof, 2013). The analysis results of this study showed that cognitive training can enhance the functional activity of the Re nucleus, but the voxel points extracted by the Re nucleus are less than 10, and the results need to be further improved (data not shown). In addition to the changes in the above-mentioned brain regions, the functional activity in the motor cortex of the Cog-group was also significantly enhanced. The method of cognitive training itself requiring mice swimming in the water T-maze might explain this phenomenon. Considering the influence of the exercise itself, it would be better to add a group to the experiment that only swimming without cognitive training.

As a non-invasive magnetic imaging technology, MRS has been extensively adopted for the detection of neurochemical metabolism in the brain of patients with neurodegenerative diseases (Gao and Barker, 2014; Sheikh-Bahaei et al., 2018). A particular study conducted whole-brain MRI scan on subjects with Alzheimer's disease or healthy control, and the results manifested that the contents of most neurochemicals, including NAA/Cr, Cho/Cr, and mI/Cr, are significantly reduced in the brains of patients with AD, from posterior cingulate gyrus and thalamus to frontotemporal area and basal ganglia (Su et al., 2016). Abnormal brain neurochemical metabolism may be a considerable cause of cognitive impairment in Alzheimer's disease, and scientists have pointed out that restoring neurochemical metabolism is of major significance to support cognitive function. Studies have presented that repetitive transcranial magnetic stimulation (rTMS) combined with cognitive training is potential to boost the NAA/Cr ratio in the prefrontal cortex of patients with Alzheimer's disease, while the increase in NAA/Cr ratio was negatively correlated with the decline of Alzheimer's Disease Assessment Scale (ADAS-cog) (Zhang et al., 2019). In addition, another study also revealed that memory enhancement training can reduce the choline compounds in the hippocampus of the elderly with mild cognitive impairment (Yang et al., 2016). At the same time, the increase in NAA/Cr is also a symbol of cognitive improvement of Alzheimer's disease after treatment with donepezil and other drugs (Moon et al., 2016). The compound of NAA is a crucial indicator to reflect the functional state of neurons, while Glu is the most bountiful excitatory neurotransmitter in the central nervous system (Griffith et al., 2008; Chen et al., 2012; Shen et al., 2018). Clinical studies have demonstrated that patients with amnestic mild cognitive impairment have their concentration of glutamate in the cingulate gyrus decreased (Zeydan et al., 2017). Animal research also revealed that compared with the wild-type mice, the neurochemical metabolism of NAA and Glu in the cerebral cortex and hippocampus of APP/PS1 model mice was declined (Patel et al., 2018). Thus, the potential of cognitive training to improve learning memory and generalization capacity on APP/PS1 mice could be related to the increase of NAA and Glu concentration. The Re nucleus in the thalamus contains a large number of glutamatergic neurons, and studies have shown that the mPFC is capable of exciting the hippocampus indirectly through the excitatory glutamatergic relay in the Re nucleus (Hur and Zaborszky, 2005; Vertes et al., 2007). In recent years, studies have disclosed that cognitive training can not only strengthen the functional connections of the brain but also restore the extent of brain neurochemical metabolism (Yang et al., 2016; Zhang et al., 2019). In this study, we selected NAA/Cr as an indicator to reflect the functions of neurons and Glu/Cr as an indicator to reflect the activity of glutamatergic neurons. The results of this experiment displayed that the concentrations of NAA and Glu in the mPFC, hippocampus and Re nucleus of 6-month-old APP/PS1 model mice were all declined, while cognitive training for 4 weeks was capable of improving the metabolism of NAA and Glu. Apart from MRS, high-performance liquid chromatography (HPLC) is an advanced analytical technique that can quantitatively detect the distribution and content of neurochemicals. Thus, the change in neurochemical metabolism detected by MRS would be worthy of further quantitative validation.

CONCLUSION

Cognitive training could improve the generalization ability that might be linked to enhance the functional activity of mPFC and hippocampus and improve the metabolism of NAA and Glu in APP/PS1 mice.

DATA AVAILABILITY STATEMENT

The original contributions presented in the study are included in the article/supplementary material, further inquiries can be directed to the corresponding author/s.

ETHICS STATEMENT

The animal study was reviewed and approved by the Animal Management Committee of Fujian University of Traditional Chinese Medicine.

AUTHOR CONTRIBUTIONS

JT and WL contributed to the conception and design of the study and revised the manuscript. JL, LeL, YZ, YD, LC, WJ, and MY collected the data. SL, XH, LoL, and HL performed the statistical analysis. JL and LeL wrote the first draft of the manuscript. All authors contributed to manuscript revision, and read and approved the submitted version.

FUNDING

This study was supported by the project of the National Natural Science Foundation of China (81873353).

REFERENCES

Ball, K., Berch, D. B., Helmers, K. F., Jobe, J. B., Leveck, M. D., Marsiske, M., et al. (2002). Effects of cognitive training interventions with older adults: a randomized controlled trial. *JAMA* 288, 2271–2281.

Buckner, R. L., Andrews-Hanna, J. R., and Schacter, D. L. (2008). The brain's default network: anatomy, function, and relevance to disease. *Ann. N. Y. Acad. Sci.* 1124, 1–38. doi: 10.1196/annals.1440.011

Carter, S. F., Embleton, K. V., Anton-Rodriguez, J. M., Burns, A., Ralph, M. A., and Herholz, K. (2014). Regional neuronal network failure and cognition in late-onset sporadic Alzheimer disease. *AJNR Am. J. Neuroradiol.* 35, S18–S30. doi: 10.3174/ajnr.A3895

Cassel, J. C., Pereira, D. V. A., Loureiro, M., Cholvin, T., Dalrymple-Alford, J. C., and Vertes, R. P. (2013). The reuniens and rhomboid nuclei: neuroanatomy, electrophysiological characteristics and behavioral implications. *Prog. Neurobiol.* 111, 34–52. doi: 10.1016/j.pneurobio.2013.08.006

Cavallo, M., and Angilletta, C. (2017). Similarity among tasks is the key to show generalization of cognitive training effects in Alzheimer's disease: a case study. *Neuropsychol. Dev. Cogn. B Aging. Neuropsychol. Cogn.* 24, 247–255. doi: 10.1080/13825585.2016.1184611

Chan, S. C., Lam, T. L., Fong, K. N., Pang, M. Y., and Chan, C. C. (2016). Generalization of context-specific training in individuals with mild cognitive impairment: an event-related potential study. *Dement Geriatr. Cogn. Dis. Extra* 6, 568–579. doi: 10.1159/000453546

Chen, S. Q., Cai, Q., Shen, Y. Y., Wang, P. J., Teng, G. J., Li, M. H., et al. (2012). (1)H-MRS evaluation of therapeutic effect of neural stem cell transplantation on Alzheimer's disease in AbetaPP/PS1 double transgenic mice. *J. Alzheimers Dis.* 28, 71–80. doi: 10.3233/JAD-2010-110893

Dillen, K., Jacobs, H., Kukolja, J., Richter, N., von Reutern, B., Onur, O. A., et al. (2017). Functional disintegration of the default mode network in prodromal Alzheimer's disease. *J. Alzheimers Dis.* 59, 169–187. doi: 10.3233/JAD-161120

Engvig, A., Fjell, A. M., Westlye, L. T., Skaane, N. V., Dale, A. M., Holland, D., et al. (2014). Effects of cognitive training on gray matter volumes in memory clinic patients with subjective memory impairment. *J. Alzheimers Dis.* 41, 779–791. doi: 10.3233/JAD-131889

Gao, F., and Barker, P. B. (2014). Various MRS application tools for Alzheimer disease and mild cognitive impairment. *AJNR Am. J. Neuroradiol.* 35, S4–S11. doi: 10.3174/ajnr.A3944

Ghods-Sharifi, S., Haluk, D. M., and Floresco, S. B. (2008). Differential effects of inactivation of the orbitofrontal cortex on strategy set-shifting and reversal learning. *Neurobiol. Learn. Mem.* 89, 567–573. doi: 10.1016/j.nlm.2007.10.007

Greicius, M. D., Srivastava, G., Reiss, A. L., and Menon, V. (2004). Default-mode network activity distinguishes Alzheimer's disease from healthy aging: evidence from functional MRI. *Proc. Natl. Acad. Sci. U.S.A.* 101, 4637–4642. doi: 10.1073/pnas.0308627101

Griffith, H. R., den Hollander, J. A., Okonkwo, O. C., O'Brien, T., Watts, R. L., and Marson, D. C. (2008). Brain metabolism differs in Alzheimer's disease and Parkinson's disease dementia. *Alzheimers Dement* 4, 421–427. doi: 10.1016/j.jalz.2008.04.008

Guo, W., Zang, M., Klich, S., Kawczynski, A., Smoter, M., and Wang, B. (2020). Effect of combined physical and cognitive interventions on executive functions in older adults: a meta-analysis of outcomes. *Int. J. Environ. Res. Public Health* 17:6166. doi: 10.3390/ijerph17176166

Hainmueller, T., and Bartos, M. (2020). Dentate gyrus circuits for encoding, retrieval and discrimination of episodic memories. *Nat. Rev. Neurosci.* 21, 153–168. doi: 10.1038/s41583-019-0260-z

Hampstead, B. M., Stringer, A. Y., Stilla, R. F., Giddens, M., and Sathian, K. (2012). Mnemonic strategy training partially restores hippocampal activity in patients with mild cognitive impairment. *Hippocampus* 22, 1652–1658. doi: 10.1002/hipo.22006

Herrera, C., Chambon, C., Michel, B. F., Paban, V., and Alescio-Lautier, B. (2012). Positive effects of computer-based cognitive training in adults with mild cognitive impairment. *Neuropsychologia* 50, 1871–1881. doi: 10.1016/j.neuropsychologia.2012.04.012

Hur, E. E., and Zaborszky, L. (2005). Vglut2 afferents to the medial prefrontal and primary somatosensory cortices: a combined retrograde tracing in situ hybridization study [corrected]. *J. Comp. Neurol.* 483, 351–373. doi: 10.1002/cne.20444

Ito, H. T., Moser, E. I., and Moser, M. B. (2018). Supramammillary nucleus modulates spike-time coordination in the prefrontal-thalamo-hippocampal circuit during navigation. *Neuron* 99, 576.e5–587.e5. doi: 10.1016/j.neuron.2018.07.021

Ito, H. T., Zhang, S. J., Witter, M. P., Moser, E. I., and Moser, M. B. (2015). A prefrontal-thalamo-hippocampal circuit for goal-directed spatial navigation. *Nature* 522, 50–55. doi: 10.1038/nature14396

Jiang, X., Chai, G. S., Wang, Z. H., Hu, Y., Li, X. G., Ma, Z. W., et al. (2015). Spatial training preserves associative memory capacity with augmentation of dendrite ramification and spine generation in Tg2576 mice. *Sci. Rep.* 5:9488. doi: 10.1038/srep09488

Li, T., Yao, Y., Cheng, Y., Xu, B., Cao, X., Waxman, D., et al. (2016). Cognitive training can reduce the rate of cognitive aging: a neuroimaging cohort study. *BMC Geriatr.* 16:12. doi: 10.1186/s12877-016-0194-5

Lin, Z. C., Tao, J., Gao, Y. L., Yin, D. Z., Chen, A. Z., and Chen, L. D. (2014). Analysis of central mechanism of cognitive training on cognitive impairment after stroke: resting-state functional magnetic resonance imaging study. *J. Int. Med. Res.* 42, 659–668. doi: 10.1177/0300060513505809

Markovic, G., Bartfai, A., Ekholm, J., Nilsson, C., Schult, M. L., and Lofgren, M. (2020). Daily management of attention dysfunction two-four years after brain injury and early cognitive rehabilitation with attention process training: a qualitative study. *Neuropsychol. Rehabil.* 30, 523–544. doi: 10.1080/09602011.2018.1482770

Moon, C. M., Kim, B. C., and Jeong, G. W. (2016). Effects of donepezil on brain morphometric and metabolic changes in patients with Alzheimer's disease: a DARTEL-based VBM and (1)H-MRS. *Magn. Reson. Imaging* 34, 1008–1016. doi: 10.1016/j.mri.2016.04.025

Myers, C. E., Kluger, A., Golomb, J., Gluck, M. A., and Ferris, S. (2008). Learning and generalization tasks predict short-term cognitive outcome in nondemented elderly. *J. Geriatr. Psychiatry Neurol.* 21, 93–103. doi: 10.1177/0891988708316858

Patel, A. B., Tiwari, V., Veeraiah, P., and Saba, K. (2018). Increased astroglial activity and reduced neuronal function across brain in AbetaPP-PS1 mouse model of Alzheimer's disease. *J. Cereb. Blood Flow Metab.* 38, 1213–1226. doi: 10.1177/0271678X17709463

Pedraza, L. K., Sierra, R. O., Giachero, M., Nunes-Souza, W., Lotz, F. N., and de Oliveira, A. L. (2019). Chronic fluoxetine prevents fear memory generalization and enhances subsequent extinction by remodeling hippocampal dendritic spines and slowing down systems consolidation. *Transl. Psychiatry* 9:53. doi: 10.1038/s41398-019-0371-3

Preston, A. R., and Eichenbaum, H. (2013). Interplay of hippocampus and prefrontal cortex in memory. *Curr. Biol.* 23, R764–R773.

Ragozzino, M. E., Kim, J., Hassert, D., Minniti, N., and Kiang, C. (2003). The contribution of the rat prelimbic-infralimbic areas to different forms of task switching. *Behav. Neurosci.* 117, 1054–1065. doi: 10.1037/0735-7044.117.5.1054

Rai, S. P., Krohn, M., and Pahnke, J. (2020). Early cognitive training rescues remote spatial memory but reduces cognitive flexibility in Alzheimer's disease mice. *J. Alzheimers Dis.* 75, 1301–1317. doi: 10.3233/JAD-200161

Sekeres, M. J., Winocur, G., and Moscovitch, M. (2018). The hippocampus and related neocortical structures in memory transformation. *Neurosci. Lett.* 680, 39–53. doi: 10.1016/j.neulet.2018.05.006

Sheikh-Bahaei, N., Sajjadi, S. A., Manavaki, R., McLean, M., O'Brien, J. T., and Gillard, J. H. (2018). Positron emission tomography-guided magnetic resonance spectroscopy in Alzheimer disease. *Ann. Neurol.* 83, 771–778. doi: 10.1002/ana.25202

Shen, Z., Lei, J., Li, X., Wang, Z., Bao, X., and Wang, R. (2018). Multifaceted assessment of the APP/PS1 mouse model for Alzheimer's disease: applying MRS, DTI, and ASL. *Brain Res.* 1698, 114–120. doi: 10.1016/j.brainres.2018.08.001

Sinha, N., Reagh, Z. M., Tustison, N. J., Berg, C. N., Shaw, A., Myers, C. E., et al. (2019). ABCA7 risk variant in healthy older African Americans is associated with a functionally isolated entorhinal cortex mediating deficient generalization of prior discrimination training. *Hippocampus* 29, 527–538. doi: 10.1002/hipo.23042

Small, J. A., and Cochrane, D. (2020). Spaced retrieval and episodic memory training in Alzheimer's disease. *Clin. Interv. Aging* 15, 519–536. doi: 10.2147/CIA.S242113

Su, L., Blamire, A. M., Watson, R., He, J., Hayes, L., and O'Brien, J. T. (2016). Whole-brain patterns of (1)H-magnetic resonance spectroscopy imaging in Alzheimer's disease and dementia with Lewy bodies. *Transl. Psychiatry* 6:e877. doi: 10.1038/tp.2016.140

Talboom, J. S., West, S. G., Engler-Chiurazzi, E. B., Enders, C. K., Crain, I., and Bimonte-Nelson, H. A. (2014). Learning to remember: cognitive training-induced attenuation of age-related memory decline depends on sex and cognitive demand, and can transfer to untrained cognitive domains. *Neurobiol. Aging* 35, 2791–2802. doi: 10.1016/j.neurobiolaging.2014.06.008

Varela, C., Kumar, S., Yang, J. Y., and Wilson, M. A. (2014). Anatomical substrates for direct interactions between hippocampus, medial prefrontal cortex, and the thalamic nucleus reuniens. *Brain Struct. Funct.* 219, 911–929. doi: 10.1007/s00429-013-0543-5

Vermeij, A., Claassen, J. A., Dautzenberg, P. L., and Kessels, R. P. (2016). Transfer and maintenance effects of online working-memory training in normal ageing and mild cognitive impairment. *Neuropsychol. Rehabil.* 26, 783–809. doi: 10.1080/09602011.2015.1048694

Vertes, R. P., Hoover, W. B., Szigeti-Buck, K., and Leranth, C. (2007). Nucleus reuniens of the midline thalamus: link between the medial prefrontal cortex and the hippocampus. *Brain Res. Bull.* 71, 601–609. doi: 10.1016/j.brainresbull.2006.12.002

Wang, J., Sun, X., Lu, J., Dou, H., and Lei, Y. (2021). Generalization gradients for fear and disgust in human associative learning. *Sci. Rep.* 11:14210. doi: 10.1038/s41598-021-93544-7

Wass, C., Pizzo, A., Sauce, B., Kawasumi, Y., Sturzoiu, T., Ree, F., et al. (2013). Dopamine D1 sensitivity in the prefrontal cortex predicts general cognitive abilities and is modulated by working memory training. *Learn. Mem.* 20, 617–627. doi: 10.1101/lm.031971.113

Winocur, G., McDonald, R. M., and Moscovitch, M. (2001). Anterograde and retrograde amnesia in rats with large hippocampal lesions. *Hippocampus* 11, 18–26. doi: 10.1002/1098-1063(2001)11:1<18::AID-HIPO1016>3.0.CO;2-5

Xu, W., and Sudhof, T. C. (2013). A neural circuit for memory specificity and generalization. *Science* 339, 1290–1295. doi: 10.1126/science.1229534

Yang, H., Leaver, A. M., Siddarth, P., Paholpak, P., Ercoli, L., St, C. N., et al. (2016). Neurochemical and neuroanatomical plasticity following memory training and yoga interventions in older adults with mild cognitive impairment. *Front. Aging Neurosci.* 8:277. doi: 10.3389/fnagi.2016.00277

Zeng, J., Jiang, X., Hu, X. F., Ma, R. H., Chai, G. S., Sun, D. S., et al. (2016). Spatial training promotes short-term survival and neuron-like differentiation of newborn cells in Abeta1-42-injected rats. *Neurobiol. Aging* 45, 64–75. doi: 10.1016/j.neurobiolaging.2016.05.005

Zeydan, B., Deelchand, D. K., Tosakulwong, N., Lesnick, T. G., Kantarci, O. H., Machulda, M. M., et al. (2017). Decreased glutamate levels in patients with amnestic mild cognitive impairment: an sLASER Proton MR spectroscopy and PiB-PET study. *J. Neuroimaging* 27, 630–636. doi: 10.1111/jon.12454

Zhang, F., Qin, Y., Xie, L., Zheng, C., Huang, X., and Zhang, M. (2019). High-frequency repetitive transcranial magnetic stimulation combined with cognitive training improves cognitive function and cortical metabolic ratios in Alzheimer's disease. *J. Neural. Transm. (Vienna)* 126, 1081–1094. doi: 10.1007/s00702-019-02022-y

Conflict of Interest: The authors declare that the research was conducted in the absence of any commercial or financial relationships that could be construed as a potential conflict of interest.

Publisher's Note: All claims expressed in this article are solely those of the authors and do not necessarily represent those of their affiliated organizations, or those of the publisher, the editors and the reviewers. Any product that may be evaluated in this article, or claim that may be made by its manufacturer, is not guaranteed or endorsed by the publisher.

frontiers | Frontiers in Cellular Neuroscience

ORIGINAL RESEARCH
published: 12 April 2022
doi: 10.3389/fncel.2022.878345

Repetitive Transcranial Magnetic Stimulation Improves Neurological Function and Promotes the Anti-inflammatory Polarization of Microglia in Ischemic Rats

Jing Luo[1†], Yuan Feng[2†], Mingyue Li[1†], Mingyu Yin[1], Feng Qin[3] and Xiquan Hu[1*]*

[1] Department of Rehabilitation Medicine, The Third Affiliated Hospital, Sun Yat-sen University, Guangzhou, China, [2] Department of Hepatobiliary Surgery, The Third Affiliated Hospital, Sun Yat-sen University, Guangzhou, China, [3] Department of Neurosurgery, Lingnan Hospital, The Third Affiliated Hospital, Sun Yat-sen University, Guangzhou, China

OPEN ACCESS

Edited by:
Zhang Pengyue,
Yunnan University of Traditional Chinese Medicine, China

Reviewed by:
Yue Lan,
Guangzhou First People's Hospital, China
Marco Cambiaghi,
University of Verona, Italy
Hua Yuan,
Fourth Military Medical University, China

***Correspondence:**
Feng Qin
qinfeng2@mail.sysu.edu.cn
Xiquan Hu
huxiquan@mail.sysu.edu.cn

[†] These authors have contributed equally to this work

Specialty section:
This article was submitted to Cellular Neuropathology, a section of the journal Frontiers in Cellular Neuroscience

Received: 17 February 2022
Accepted: 15 March 2022
Published: 12 April 2022

Citation:
Luo J, Feng Y, Li M, Yin M, Qin F and Hu X (2022) Repetitive Transcranial Magnetic Stimulation Improves Neurological Function and Promotes the Anti-inflammatory Polarization of Microglia in Ischemic Rats.
Front. Cell. Neurosci. 16:878345.
doi: 10.3389/fncel.2022.878345

Ischemic stroke (IS) is a severe neurological disease that is difficult to recovery. Previous studies have shown that repetitive transcranial magnetic stimulation (rTMS) is a promising therapeutic approach, while the exact therapy mechanisms of rTMS in improving neural functional recovery remain unclear. Furthermore, the inflammatory environment may influence the rehabilitation efficacy. Our study shows that long-term rTMS stimulation will significantly promote neurogenesis, inhibit apoptosis, and control inflammation. rTMS inhibits the activation of transcription factors nuclear factor kappa b (NF-κB) and signal transducer and activator of transcription 6 (STAT6) and promotes the anti-inflammatory polarization of microglia. Obvious promotion of anti-inflammatory cytokines production is observed both *in vitro* and *in vivo* through rTMS stimulation on microglia. In addition, neural stem cells (NSCs) cultured in conditioned medium (CM) from microglia treated with rTMS showed downregulation of apoptosis and upregulation of neuronal differentiation. Overall, our results illustrate that rTMS can modulate microglia with anti-inflammatory polarization variation, promote neurogenesis, and improve neural function recovery.

Keywords: rehabilitation, repetitive transcranial magnetic stimulation, ischemic stroke, inflammation, microglia

INTRODUCTION

Ischemic stroke (IS) acts as a leading cause of death and disability (Benjamin et al., 2019; Kelmanson et al., 2021). Due to the limitation of the treatment time window and medical conditions, about 70–80% of the surviving patients with cerebral infarction still have varying degrees of dysfunction (Girotra et al., 2020). Apoptosis and necrosis are the two main cell death modes in the acute phase of cerebral infarction (Lipton, 1999), and neurogenesis is an important basis for the recovery of nerve function (Koh and Park, 2017). Therefore, how to inhibit nerve apoptosis and promote neurogenesis is a momentous research direction for the recovery of nerve function after cerebral infarction.

The rapid development of rehabilitation medicine makes it possible to restore the neurological function of stroke patients well and greatly improves the quality of life. Repetitive transcranial

magnetic stimulation (rTMS), a non-invasive brain stimulation technology based on the principle of Faraday electromagnetic induction (Vidal-Dourado et al., 2014), can effectively promote the recovery of neurological function. Based on the induction of repetitive current pulses in the brain, rTMS is obtained by applying an electromagnetic coil to generate a magnetic field near the scalp. For the advantages in terms of non-invasiveness and safety, with minimal or no side effects (Peruzzotti-Jametti et al., 2013), rTMS has been widely used in clinical rehabilitation treatment of patients with cerebral infarction (Luber and Lisanby, 2014; Koch et al., 2019; Liu et al., 2020; Wang et al., 2020; Yin et al., 2020). Relative studies believe that rTMS acts on neurorehabilitation and may relate to the following factors: mutual inhibition between the bilateral hemispheres of the brain (Carson, 2020), regulating the excitability of the brain (Hallett, 2000; Tan et al., 2013), improving brain metabolism and cerebral blood flow (Paillere et al., 2011; Shinba et al., 2018), and rebuilding brain function networks and regulating the transmission of a variety of neurotransmitters (Yin et al., 2020; Natale et al., 2021). Previous reports by us and others confirmed that rTMS could improve the neurological function after cerebral infarction and promote neurogenesis (Guo et al., 2017; Luo et al., 2017; Cui et al., 2019). It can be seen that rTMS has a very wide range of functions, and its internal mechanism is also quite complicated which needs to be further elucidated.

Many strategies have been trialed to find the mechanism for obtaining the best effect of rTMS treatment. For such purposes, many studies focus on the mechanism of rTMS acting on the neural stem cells (NSCs) and neural precursor cells (NPCs), which are related to neurogenesis, and astrocytes or microglia connected with neuroinflammation (Hong et al., 2020). For instance, rTMS has therapeutic effects on depression because it can reverse the decrease of NSCs and enhance neurogenesis, and rTMS could regulate the balance between proliferation and apoptosis of NSCs (Zhao et al., 2019). For neuroprotective effect, it has been reported that rTMS could improve functional recovery by inhibiting neurotoxic polarization of astrocytes in ischemic rats, which means rTMS may regulate inflammation through the action of neural glial cells (Sasso et al., 2016; Cullen et al., 2019; Clarke et al., 2021).

Microglia, one of the macrophages residing in the central nervous system, plays a key role during neural damage (Nayak et al., 2014; Prinz et al., 2019). Traditionally, microglia activation has been thought to play a detrimental role in IS, for its inhibition can reduce brain damage caused by ischemia stroke (Ma et al., 2017). However, a growing number of evidences indicate it is essential for promoting nerve recovery after stroke, and the differential polarization of microglia may explain the biphasic effect (Xiong et al., 2016; Kanazawa et al., 2017; Ma et al., 2017). Many studies show that rTMS can reduce the release of proinflammatory cytokines and inhibit the activation of microglia (Kim et al., 2013; Yang et al., 2020; Zong et al., 2020), whereas contradictory research indicates that rTMS could induce the microglia to inflammatory phenotype, while reducing neurogenesis (Muri et al., 2020).

At present, the function of rTMS on microglia of IS is still unclear. The aim of this study was to explore the changes in the phenotype and function of microglia after rTMS treatment. At the same time, we also observed the effects of rTMS-stimulated microglia supernatant on the proliferation and apoptosis of NSCs.

MATERIALS AND METHODS

Rats

A total of 80 male spontaneously hypertensive rats (SHRs) weighing 200–240 g were purchased from the Beijing Vital River Laboratory Animal Technology Co. Ltd., China. SHRs were allocated to each group randomly. Rats were housed in the same animal care facility during a 12 h light/dark cycle throughout the protocol with free access to food and water. All animal protocols were approved and reviewed by the Sun Yat-sen University Institutional Animal Care and Use Committee.

Transient Middle Cerebral Artery Occlusion

Middle cerebral artery occlusion (MCAO) surgery was performed on SHR under anesthesia as our prior studies described (Luo et al., 2017). In brief, SHRs were anesthetized by intraperitoneal injection of 3.5% chloral hydrate (350 mg/kg). A filament (nylon suture with a rounded tip) was inserted into the left internal carotid artery to block the left middle cerebral artery. After 90 min of MCAO, the filament was pulled back to restore blood flow (reperfusion). Criteria for successful model preparation were that after the rat was awake from anesthesia, the left limb was paralyzed, and the modified neurological severity score (mNSS) score met the inclusion. Rats with moderately neurological dysfunction with a mNSS of 7–12 were included in the group. Exclusion criterion included rats that were found to have subarachnoid hemorrhage or no paralysis, or died before the sampling time, mild (mNSS of 1–6) or severely damaged (mNSS of 13–18). For the proliferation assay, daily injections of bromodeoxyuridine (BrdU, 50 mg/kg; B5002, Sigma-Aldrich, United States) were given intraperitoneally for every group at 1 day after the MCAO, to label dividing cells until 7 days after MCAO.

Isolation and Culture of Rat Microglia

Microglia were isolated from cultures of newborn Wistar rat brain and tissue dissociated by trituration with trypsin (Gibco, United States) as described previously (Giulian and Baker, 1986). In brief, isolated cerebral cortices from newborn Wistar rats were taken off the meninges, minced in Roswell Park Memorial Institute (RPMI) 1640 basal medium (Gibco, United States), a complete medium and 10% fetal bovine serum (FBS, Gibco, United States) before being dissociated by trituration in 0.25% trypsin. Cells were plated in 75 cm^2 plastic culture flasks containing 10 ml complete medium with 10% FBS at a density of 1×10^6 cells/ml. Culture flasks were vigorously agitated on a rotary shaker for 12 h (37°C, 180 rpm) after 7 days of culture. Then, GFAP (+) astroglia remained adherent to the flasks, and the resulting cell suspension, rich in microglia, was placed in new plastic flasks (10^5 cells/ml) and allowed to adhere at 37°C.

Isolation and Culture of Rat Neural Stem Cells

Neural stem cells were isolated from fetal rats at embryonic day 14.5 (E14.5) as previously reported (Azari et al., 2011). Briefly, brains from embryos were isolated and dissociated by accutase (Gibco, United States). Then, cell suspension was filtered with a 70 μm cell strainer. Ammonium chloride lysis was used to remove red blood cells, and the rest cells were added to culture flasks in NSCs culture medium. NSCs culture medium contained low glucose-Dulbecco's Modified Eagle's Medium (L-DMEM) with 2% (v/v) B27 (Gibco, United States), epidermal growth factor (EGF, 20 ng/mL, PeproTech) and mitogens basic fibroblast growth factor (bFGF, 20 ng/mL, PeproTech).

Experimental Grouping and Repetitive Transcranial Magnetic Stimulation

In vitro, microglia were randomly divided into tms (+) group and TMS (−) group. In TMS (−) group, 1 μg/ml lipopolysaccharide (LPS) was added in microglia culture medium to activate microglia for 18 h. Then, the medium was replaced with fresh medium and continued to culture for 72 h before subsequent testing. In TMS (+) group, microglia were activated by LPS as TMS (−) group did. Then, microglia in fresh culture medium were treated with rTMS one time a day for 2 days. Microglia in the TMS (+) group were applied at 10 Hz, 30% maximum output intensity of the machine, with 20 pulses per train, 10 s intertrain interval, and a of total 60 trains (1,200 pulses) for 11 min 44 s. Microglia were used for subsequent testing after 72 h culture (rTMS were treated two times). Microglial-derived conditioned medium (CM) from above two groups were collected, centrifuged, and stored at −80°C for subsequent experiments.

In vivo, SHRs were randomly divided into three groups, namely, SHAM group ($n = 24$), TMS (−) group ($n = 24$), and TMS (+) group ($n = 24$). All groups were divided into two subgroups on the 7th and 28th days after rTMS ($n = 12$). Rats in the TMS (+) group received 10 Hz rTMS with a total of 60 trains, 20 pulses per train (1,200 pulses), 10 s intertrain interval, for 11 min 44 s. Rats in the TMS (−) group experienced the same experimental manipulations by placing an inactive coil on the rats' head. SHR receiving rTMS were stimulated for 7 days (short-term observation point) and 28 days (long-term observation point) during a 2-day period a week, beginning at 2 days after MCAO. The SHAM group were housed in standard cages supplied with adequate food and water but received no stimulation.

TMS treatment was conducted with a MagPro X100 magnetic stimulators (The MagVenture Company, Denmark). The magnetic stimulation coil is an ultra-small figure-of-eight coil (MC-B35, Dantec, Denmark) specially designed for animals, with 24 mm inner diameter and 47 mm outer diameter, an output frequency of 1–100 Hz, and a maximum output magnetic field strength of 4.2 T. Motor-evoked potentials (MEPs) were measured at the right hind limbs, quadriceps femoris muscle, using electromyography (MedelecSynergy; Oxford Instruments, Surrey, United Kingdom), as previously described (Luo et al., 2017).

Primary Microglia Proliferation Assay

Carboxyfluorescein succinimidyl ester (CFSE, Invitrogen, United States) staining (2 μmol/L) was used to assess primary microglia (PM) proliferation. The cells were incubated for 10 min at 37°C. Then, the original staining volume of culture medium were added five times to the cells and incubated for 5 min. The cells were pelleted by centrifugation and then suspended and distributed to 6-well plates. After 3 days of culture, microglia were collected and analyzed by flow cytometry.

Neural Stem Cells Assay

Neural stem cells were dissociated and cultured in matrigel-coated (Corning, United States) 6-wells culture plates at a density of 2×10^5/well. Cells were cultured with NSCs culture medium for 48 h. Then, the culture medium was replaced by CM collected from microglia to promote differentiation. Culture medium were changed every 3 days.

For the proliferation assay, NSCs were tested at day 3 after cultured with microglia CM. NSCs were incubated with 10 mM BrdU at 37°C for 6 h. Then, cells were fixed with paraformaldehyde (PFA) and incubated in 2 mol/L HCl and washed in 1 M borate solution two times. Later, cells were blocked with 5% normal goat serum for 1 h at room temperature. Then, cells were incubated with BrdU (ab207175, Abcam, United States) and NESTIN (ab81462, Abcam, United States) antibodies overnight at 4°C. Finally, cells were incubated with secondary antibody and Hoechst stain before examined with the fluorescence microscope.

For TUNEL staining, NSCs were tested at day 3 after cultured with microglia CM. NSCs were stained with the TUNEL technique using an apoptosis detection kit (MA0223, Meilunbio, China) according to the manufacturer's protocols. In brief, cells were fixed with fix solution (MA0192, Meilunbio, China) for 30 min. Proteinase K (20 μg/ml) was added to each sample so that the solution covers the entire sample area and incubated for 5 min at room temperature. Furthermore, 50 μl TUNEL detection solution was added dropwise to the sample and incubated in the dark for 60 min at 37°C. After all, the slices were washed 2–3 times with PBS and examined under an EVOS M5000 imaging system.

For differentiation assay, cells were collected at day 9, and RNA was isolated by RNA Quick Purification kit (ESscience, China). qPCR was used to test the expression levels of specific markers.

Enzyme-Linked Immunosorbent Assay

Tumor necrosis factor (TNF)-α, interleukin (IL)-1β, IL-4, and IL-10 production was measured using enzyme-linked immunosorbent assay (ELISA) quantitation kits (all from MEIMIAN, China) as per the manufacturer's protocols.

RNA Isolation and qPCR

RNA was isolated from the brain tissue by RNA Quick Purification kit (ESscience, China). cDNA was prepared using a Revert Aid First Strand cDNA Synthesis Kit (Thermo Scientific, United States). The cDNA obtained was subjected to qPCR

with the SYBR Green reagent (Thermo Scientific, United States) using the rat primers listed in **Supplementary Table 1**. Expression levels were normalized to those of glyceraldehyde-3-phosphate dehydrogenase (GAPDH). The primers are listed in **Supplementary Table 1**.

Western Blotting Analysis

Cells and brain tissues were extracted, and the protein concentration was measured using a bicinchoninic acid (BCA) protein assay kit (Beyotime, China). Proteins were separated using 8 or 12% sulfate-polyacrylamide gel electrophoresis and then transferred to a polyvinylidene fluoride (PVDF) membrane. Then, the membrane was blocked with Tris-buffered saline (TBS)/T containing 5% non-fat dry milk and analyzed for the target proteins. The specific antibodies used recognized cleaved-caspase3, p-nuclear factor of kappa light polypeptide gene enhancer in B-cell inhibitor, alpha (IκBα) (AP0707, ABclonal, China), p-NFκB (AP0123, ABclonal, China), and p-STAT6 (#56554, CST, United States).

Immunofluorescent Staining

For cells assay, microglia were washed with PBS and fixed with 15 min treatment of 4% cold PFA. Fixed cells were washed three times before being treated with permeabilization buffer. Furthermore, cells were treated with primary antibodies incubated in PBS overnight at 4°C. All cells were washed three times and treated with secondary antibodies for 1 h at room temperature in the next morning. Cells were then washed three times before being mounted using Fluoroshield with DAPI and glass coverslips. Cells were imaged using an EVOS M5000 imaging system (Thermo Fisher Scientific, United States).

Brain sections were incubated in 2 N HCl at 37°C for 30 min for BrdU immunostaining and washed in 0.1 M borate solution two times for 10 min, incubated in 3% H_2O_2 for 30 min, and blocked with 5% normal goat serum for 1 h at room temperature. BrdU (AB207175, Abcam, United States) and DCX (AB2253, Millipore, United States), the double-immunofluorescence staining, was performed to observe neurogenesis, and sections were incubated with primary antibodies overnight at 4°C. After rinsing three times in PBS for 5 min each, sections were incubated for 1 h at 37°C with a secondary antibody. Fluorescence signals were examined under an EVOS M5000 imaging system.

For TUNEL assay, frozen slices were stained with the TUNEL technique using an apoptosis detection kit (MA0223, Meilunbio, China) according to the manufacturer's protocols. In brief, slices were fixed with 30 min treatment of 4% PFA at room temperature. The liquid was gently aspirated, and the slices were immersed in PBS and incubated at room temperature for 10 min. Furthermore, 100 μl of proteinase K (20 μg/ml) was added to each sample so that the solution covers the entire sample area and incubated for 10 min at room temperature. Then, 50 μl TUNEL detection solution was added dropwise to the sample and incubated in the dark for 60 min at 37°C. After all, the slices were washed 2–3 times with PBS and examined under an EVOS M5000 imaging system.

Infarct Volume Measurement and MRI

Rats were anesthetized with 1.5–2.5% isoflurane. MR scans were performed 7 and 28 days after rTMS using a 7 Tesla system with Bruker console (Bruker Biospin, PharmaScan 70/16, United States). For T2-weighted imaging, a 35 mm^2 × 35 mm^2 field of view (FOV) and a 128 × 128 image matrix were used to obtain the initial RARE anatomical scan, where all six echoes were at equal echo time intervals and under the same readout gradient polarity in T2 × WI. The total time for each sequence was about 5–10 min. Finally, the area of interest of each animal was measured to quantify the ischemic volume.

Neurobehavioral Evaluation

Modified Neurological Severity Score

The neurobehavioral motor outcome was evaluated using the mNSS, performed at 7 and 28 days after rTMS. mNSS includes four tests, namely, motor, sensory, balance, and reflex tests. Scores from all the tests were summed to give the mNSS a score of 0–18. Rats with moderate neurological dysfunction (scores of 7–12) at 2 days after rTMS were selected for use in the subsequent experimental procedures.

Novel Object Recognition Tests and Morris Water Maze Test

The novel object recognition (NOR) test and the Morris water maze (MWM) are used to evaluate neurobehavioral cognitive function of each group at 28 days after rTMS as previously described (Luo et al., 2017).

In brief, the NOR test values were expressed as a percentage of the discrimination ratio calculated according to the following formula: Discrimination ratio (%) = (N − F) / (N + F) × 100%, where *N* represents the time spent in exploring the new object and F represents the time spent in exploring the same object.

The rats first received place navigation test for 5 days for MWM. Rats were gently put into the water maze and released facing the wall from one of four quadrants in a random order. They were allowed to find the escape platform for 60 s. The escape latency was measured and analyzed. A 60-s spatial probe test was conducted with the platform removed at the day after the place navigation test. The dwelling time in the target quadrant where the platform was located before and the time of crossing the platform area were recorded during the training.

Statistical Analysis

All results are expressed as mean ± SEM. Statistical comparisons were made using a Student's *t*-test (between two groups) or a one-way ANOVA (for multigroup comparisons). $P < 0.05$ was considered to represent a significant difference. Analysis and graphing were performed using the Prism 7.0 software package. **Figure 8** was obtained using BioRender.com.

RESULTS

Neurological Function Assay

As shown in **Figure 1A**, rats were treated with rTMS at 3 days after cerebral ischemia. To investigate the best course of

treatment, rTMS were applied to the ischemic rats, and short-term treatment observation point (at day 7) and long-term treatment observation point (at day 28) were used to evaluate the treatment effect (**Figure 1B**). At 28 days after rTMS, as indicated by the results of NOR and MWM tests, the TMS (+) group shows a significant improvement in neurocognitive behavioral function. The rats were trained on the cued water maze, and escape latency decreased after rTMS treatment (**Figure 2A**). Compared with TMS (−) group, rats subjected to rTMS exhibited a higher discrimination ratio (**Figure 2B**). In the spatial probe test, rats subjected to rTMS showed greater numbers of platform crossings (**Figure 2C**) and longer time spent in the target quadrant (**Figure 2D**).

To investigate the effects of different course of rTMS treatment on neurological function in ischemic rats, the mNSS scale was applied to assess the neurological function. Compared with TMS (−) group, TMS (+) group exhibited a lower mNSS values at day 7, and the mNSS values became even lower at day 28 (**Figure 2E**). Besides, the relative infarct volume showed no difference in the TMS (+) group compared to TMS (−) group at 7 days after rTMS, and the TMS (+) group exhibited a reduced infarct volume at day 28 (**Figure 2F**). The above data proved that

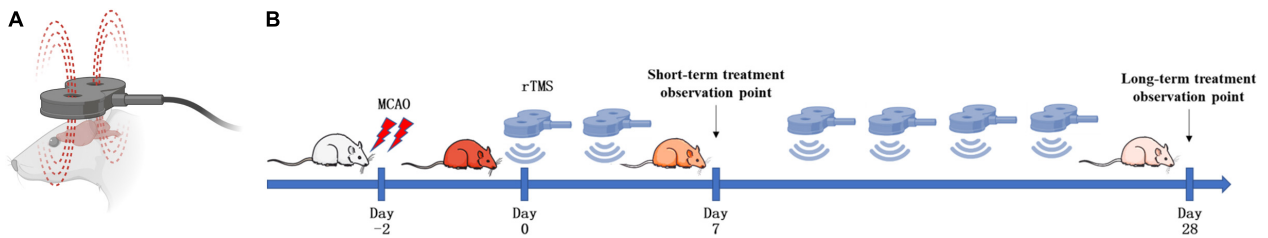

FIGURE 1 | Schematic diagram of the strategy to stimulate ischemic rats. **(A)** Stimulation coil and method. A magnetic stimulator with a figure-of-eight coil was used to stimulate conscious rats. **(B)** Experimental schedule. Rats were treated with repetitive transcranial magnetic stimulation (rTMS) at day 3 after cerebral ischemia.

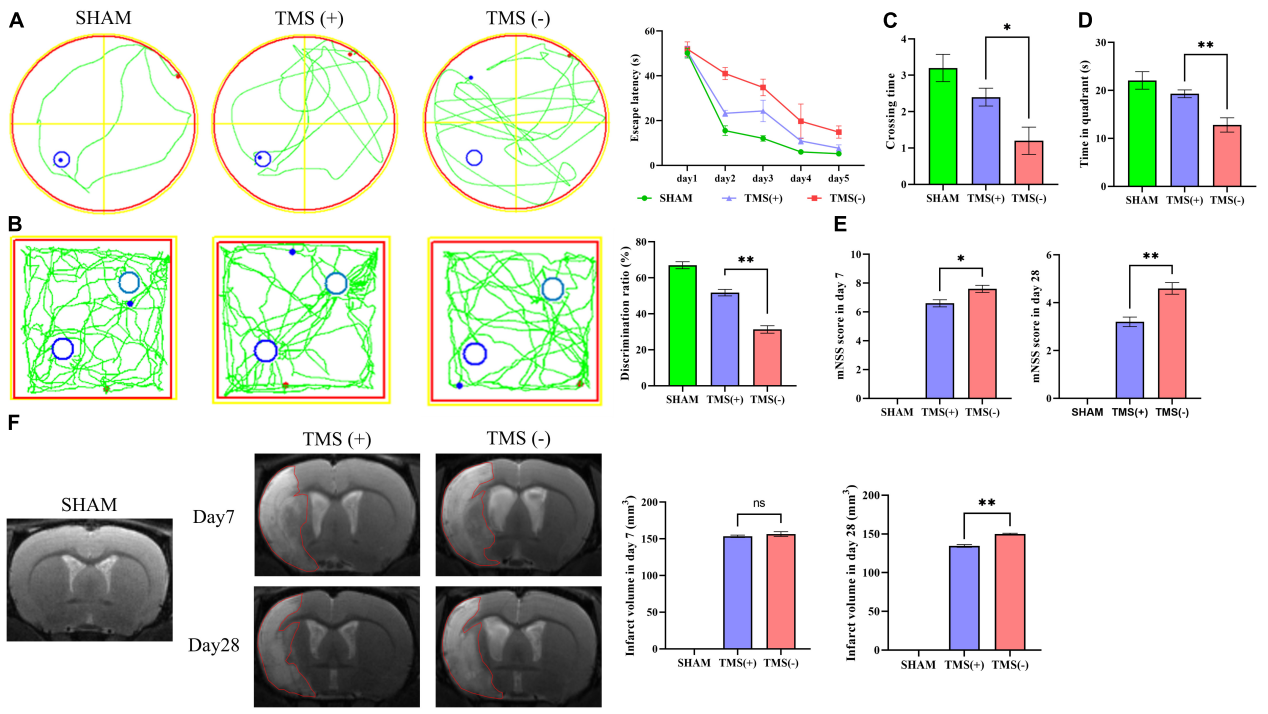

FIGURE 2 | Analysis of neural function recovery of experimental ischemic rats. **(A)** Representative swimming path of each group in the Morris water maze test and analysis of the escape latency to the platform during the training days of the Morris water maze test (n = 5 per group). **(B)** Exploration patterns were recorded in the novel object recognition (NOR) test; green lines are exploring patterns of rats; blue circles represent two different objects. Discrimination ratios were measured (n = 5 per group). **(C)** Comparisons of the times crossing the target area and **(D)** time spent in the target quadrant during the probe trial (n = 5 per group). **(E)** Comparison of modified neurological severity scores (mNSS) in each group (n = 5 per group). **(F)** Cerebral infarct volume reflected by MRI and comparison of infarct volume in each group (n = 3 per group). Data are shown as mean ± SEM. Statistical significance was determined with the unpaired Student's t-test. $^{*}P < 0.05$ and $^{**}P < 0.01$, and ns means no significant.

rTMS could improve the recovery of neurological function, and long-term treatment presented a better therapeutic effect.

Neural Regeneration and Tissue Apoptosis

To verify whether rTMS contributes to the neural regeneration, the effect of short-term (7 days) and long-term (28 days) rTMS on $BrdU^+$ and DCX^+ NPCs was analyzed. As shown in **Figure 3A**, compared with TMS (−) group, the level of NPC population in TMS (+) group was close in day 7, whereas the level in TMS (+) group was higher for the population analysis in day 28. The results suggested that rTMS play an important role in the neural regeneration, and long-term rTMS could better support neurogenesis.

Additionally, we analyzed the potential role of rTMS in apoptosis (**Figure 3B**). We found rTMS also partially restored the apoptosis of the cerebral cortex in short-term and long-term treatment. Simultaneously, the expression of cleaved-caspase3, a critical executioner of apoptosis, was significantly downregulated in the TMS (+) group of both short-term and long-term treatment (**Figure 3C**). All the above data suggest that short-term and long-term treatments of rTMS play an important role in reducing cerebral cortex apoptosis.

Neurotoxic Effects Assay

Cerebral ischemia rats are known to suffer neurotoxic effects caused by the secretion of proinflammatory cytokines. TNF-α and IL-1β are classical inflammatory cytokines after cerebral ischemia, while IL-4 and IL-10 are anti-inflammatory cytokines. As shown in **Figure 4A**, compared with the TMS (−) group, the mRNA levels of TNF-α and IL-1β were not obviously affected by rTMS at day 7 but was inhibited by rTMS at day 28. Similar phenomena were also observed through ELISA. As shown in **Figure 4B**, long-term treatment of rTMS showed a significant inhibition of TNF-α and IL-1β. However, qPCR and ELISA both showed that IL-4 and IL-10 mRNA expression and protein secretion were increased in the rTMS treatment group at day 7, and IL-10 maintained high expression and secretion in the rTMS treatment group at day 28 (**Figures 4A,B**).

Nuclear factor kappa b (NF-κB) and signal transducer and activator of transcription 6 (STAT6) are transcription factors previously reported to be involved in the secretion of proinflammatory cytokines. Many studies believe that neuroinflammatory damage caused by cerebral ischemia is highly related to their activation. Therefore, we explored whether these factors are involved in the rTMS-mediated regulation of inflammatory factors. After rTMS treatment, the protein levels of p-IκBα, p-NF-κB, and p-STAT6 were significantly downregulated (**Figure 4C**). These findings indicated that rTMS could inhibit the activation of the NF-κB and STAT6.

Polarization of Microglia in Ischemic Rats

Microglia include an amount of principal immune cells in the brain that respond to the pathophysiological changes induced by IS. As shown in **Figure 5A**, short-term and long-term treatment of rTMS did not change the percentage of the proliferation rate of microglia. Furthermore, we analyzed the polarization phenotype of microglia and found that rTMS could effectively reduce the inflammatory polarization of $Iba\text{-}1^+$ and $CD86^+$ microglia in long-term rTMS treatment, while there was no obvious change in short-term rTMS treatment group (**Figure 5B**). When comparing

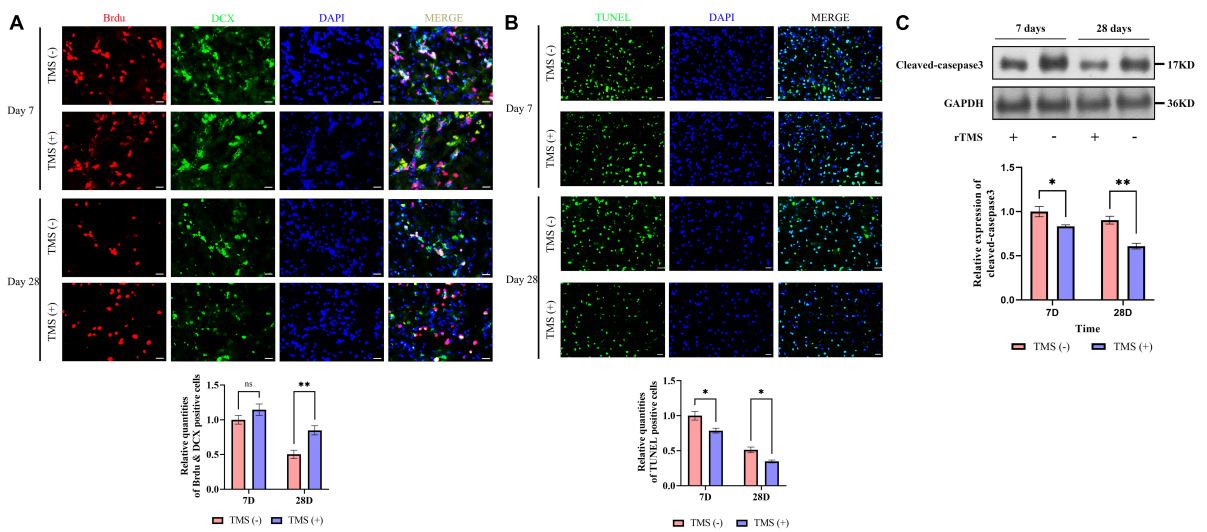

FIGURE 3 | Effects of rTMS on neural regeneration and apoptosis. **(A)** Quantitative analysis of $BrdU^+$ and DCX^+ newborn neural precursor cells (NPCs) in TMS (–) and TMS (+) groups ($n = 5$). Quantity of NPCs in TMS (–) group of day 7 was normalized as control. **(B)** Quantitative analysis of TUNEL-positive apoptotic cells in transcranial magnetic stimulation (TMS) (–) and TMS (+) groups ($n = 3$). Quantity of TUNEL-positive cells in TMS (–) group of day 7 was normalized as control. **(C)** Western blotting analysis of cleaved-caspase3 in TMS (–) and TMS (+) groups ($n = 4$). Expression levels of cleaved-caspase3 in TMS (–) group of day 7 were normalized as control. Data are shown as mean ± SEM. Statistical significance was determined with the unpaired Student's *t*-test. Scale bar, 10 μm, $^*P < 0.05$ and $^{**}P < 0.01$, and ns means no significant.

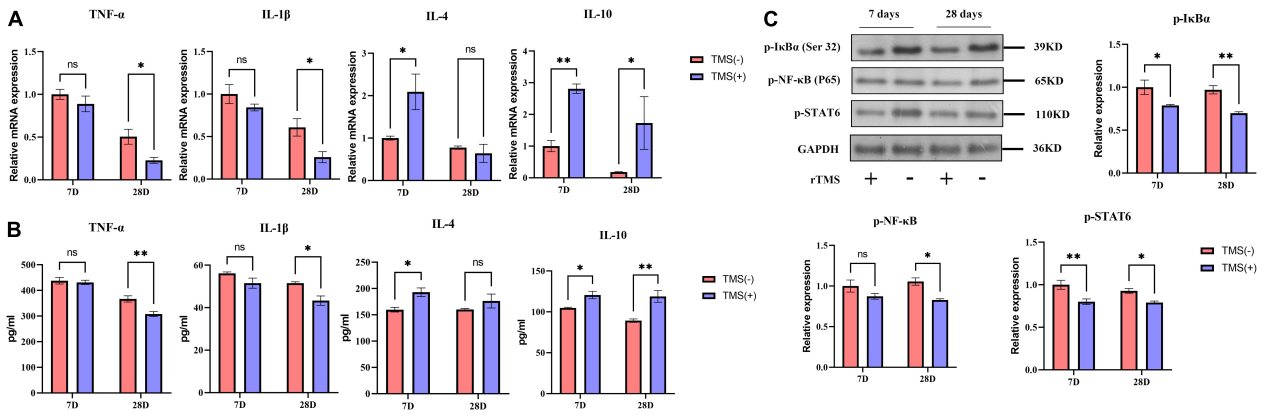

FIGURE 4 | Effects of rTMS on inflammation regulation in experimental ischemic rats. mRNA expression levels **(A)** and secretion **(B)** of inflammatory and anti-inflammatory cytokines in TMS (–) and TMS (+) groups (n = 3). **(C)** Normalized expression of phosphorylation of nuclear factor of kappa light polypeptide gene enhancer in B-cells inhibitor, alpha (IκBα), nuclear factor kappa B (NF-κB), and signal transducer and activator of transcription 6 (STAT6) in TMS (–) and TMS (+) groups (n = 3). Data are shown as mean ± SEM. Statistical significance was determined with the unpaired Student's t-test. $^{*}P < 0.05$ and $^{**}P < 0.01$, and ns means no significant.

anti-inflammatory polarization of Iba-1^{+} and CD206^{+} microglia in TMS (−) and TMS (+) group, the Iba-1^{+} and CD206^{+} microglia in short-term and long-term rTMS treatment group were both increased (**Figure 5C**). The above data indicated that rTMS might promote anti-inflammatory transformation of microglia in ischemic rats.

Lipopolysaccharide has been reported to induce the proinflammatory transition of microglia. Hence, to further verify whether rTMS could contribute to the polarization transition of microglia, PM were extracted, and rTMS were applied to PM activated by LPS *in vitro* (**Figure 6A**). As shown in **Figure 6B**, PM exhibited low proliferative activity *in vitro* with or without rTMS treatment, for there was nearly no obvious change in the population of proliferation cell. Then, the effects of rTMS on microglia polarization were further verified. With rTMS treatment, PM showed no obvious change tendency of CD86^{+} phenotype but an obvious increase in CD206^{+} cell proportion (**Figures 6C,D**).

To further confirm the rTMS effects reverse neurotoxic microglia into neuroprotective phenotype *in vitro*, we then analyzed the secretion of proinflammatory cytokines (TNF-α and IL-1β) and anti-inflammatory cytokines (IL-4 and IL-10) in PM. In comparison with the TMS (−) group, there was no obvious difference in the secretion of proinflammatory cytokines TNF-α and IL-1β (**Figure 6E**), whereas the secretion of anti-inflammatory cytokines IL-4 and IL-10 was upregulated in the TMS (+) group (**Figure 6E**). Overall, these results indicated that rTMS could promote the anti-inflammatory polarization and anti-inflammatory cytokine secretion of microglia.

Neural Stem Cells Treated With Conditioned Medium From Microglia

Neural stem cells were isolated and highly expressed NESTIN and SOX2. To investigate the effect of different microglial CM on NSCs characteristics, NSCs were cultured in CM collected from non-rTMS-stimulated microglia [TMS (−)-CM] or rTMS-stimulated microglia [TMS (+)-CM]. NSCs cultured in TMS (−)-CM or TMS (+)-CM had a lower quantities of BrdU incorporation cells, whereas TMS (+)-CM group showed no obvious difference from TMS (−)-CM group (**Figure 7A**). Moreover, when we looked at the effect of apoptosis by CM culture, TMS (−)-CM and TMS (+)-CM both increase the apoptosis rate of NSCs. However, the TUNEL incorporation of TMS (+)-CM was relative less than TMS (−)-CM group (**Figure 7B**), and the expression of cleaved-caspase3 was lower (**Figure 7C**).

Additionally, we further tested whether CM could regulate the NSCs fate. The results indicated that both TMS (−)-CM and TMS (+)-CM could promote NSCs differentiation for the expression of stem cell marker SOX2 was obviously downregulated (**Figure 7D**). In addition, TMS (−)-CM and TMS (+)-CM both displayed an obvious stimulation effect to upregulate the expression of astrocytes marker GFAP, whereas TMS (+)-CM showed a stronger effect to upregulate the expression of neuronal precursor cell marker TUBB3 (**Figure 7D**). The results indicate that rTMS can promote neuronal differentiation through affecting microglia polarization.

DISCUSSION

In the past few years, the general safety and efficacy of rTMS for the functional recovery after IS have been demonstrated in numerous basic research and clinical trials (Luber and Lisanby, 2014; Liu et al., 2020; Wang et al., 2020; Yin et al., 2020; Hong et al., 2021; Natale et al., 2021). This study confirms that the function of rTMS in relieving nerve inflammation damage and promotes nerve tissue regeneration are related to promoting the anti-inflammatory polarization of microglia. rTMS could improve functional recovery, which is associated with the reduction of apoptosis and enhancement of neurogenesis. Results

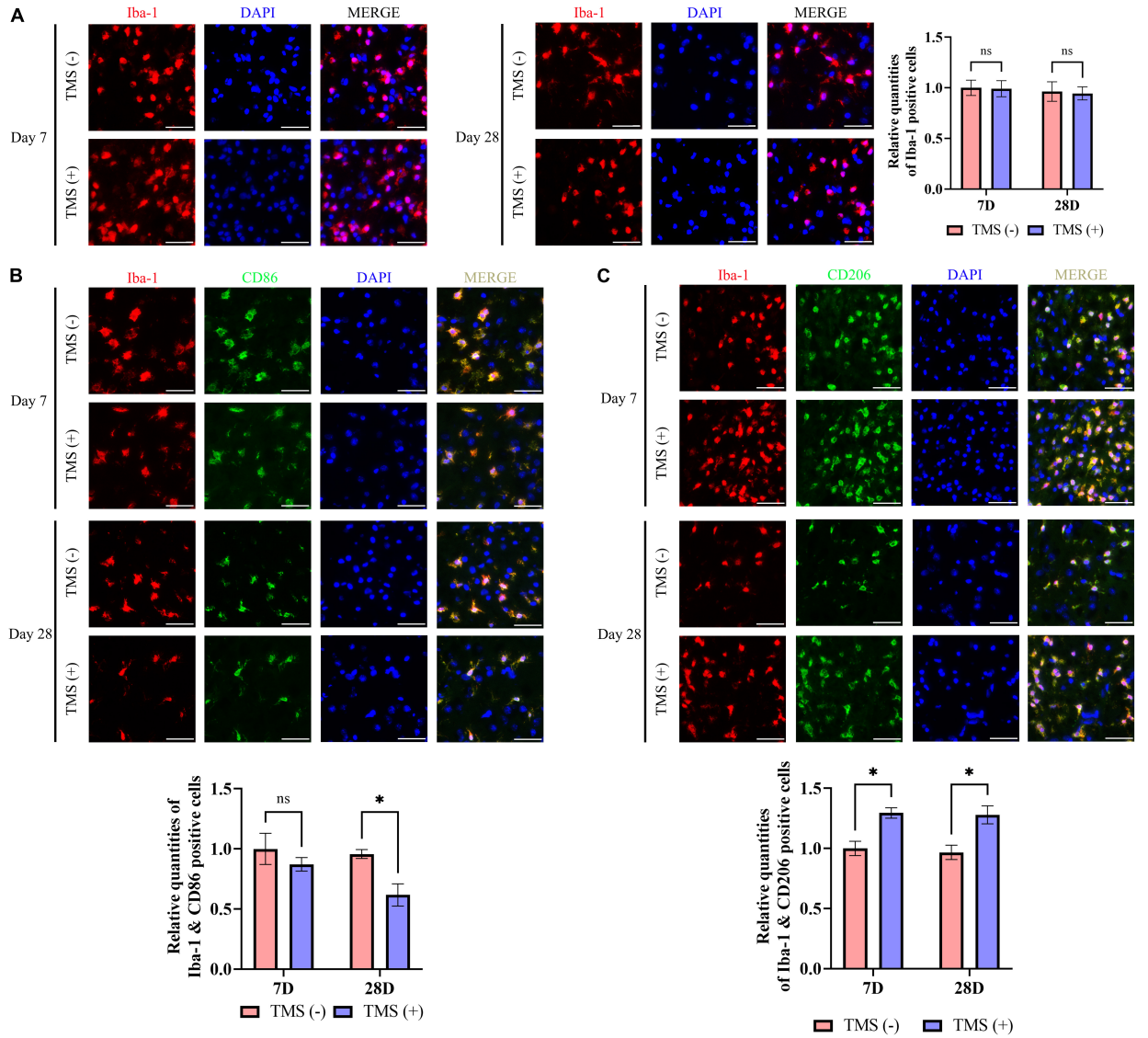

FIGURE 5 | Neuroprotective transformation of microglia in ischemic cerebral cortex. **(A)** Quantitative analysis of Iba-1 positive microglia in TMS (–) and TMS (+) groups (n = 3). Quantity of Iba-1 positive cells in TMS (–) group was normalized as control. Iba-1$^+$ and CD86$^+$ neurotoxic **(B)** and Iba-1$^+$ and CD206$^+$ neuroprotective **(C)** microglia in TMS (–) and TMS (+) groups (n = 3). Quantity of Iba-1$^+$ and CD86$^+$ or Iba-1$^+$ and CD206$^+$ cells in TMS (–) group was normalized as control. Data are shown as mean ± SEM. Statistical significance was determined with the unpaired Student's t-test. Scale bar, 20 μm, $^*P < 0.05$, and ns means no significant.

in vivo and *in vitro* analysis indicated that rTMS could promote the anti-inflammatory polarization of microglia in an independent way. Collectively, these characteristics revealed that the anti-inflammatory polarization of microglia could secrete more neuroprotective anti-inflammatory cytokines for the healing of inflammatory injury. Further testing in comparison between short-term and long-term treatment of rTMS confirmed that long-term rTMS could obtain better nerve repair and inflammation control effect. We concluded that rTMS shows a significant transition of anti-inflammatory polarization of microglia for treating IS.

Inflammation is initiated during the acute phase of stroke and is likely to become the predominant injury mechanism lasting for several days. Generally speaking, proinflammatory intracellular signaling cascades lead to the release of proinflammatory cytokines, such as IL-1β and TNF-α, to initiate a local immune response. This process results in local and systemic immune system activation, that exacerbates neuronal injury. However, it is also reported that inflammatory may contribute to neuroprotection and later tissue repair (Jayaraj et al., 2019; Lambertsen et al., 2019). Therefore, it is a tricky choice to not only relieve stroke but also reduce inflammation. From the perspective of safety and effectiveness, the goal of recent experiments seems to have shifted from regulating of proinflammatory mechanisms to promoting a more protective cell phenotype, with the goal of promoting neural recovery.

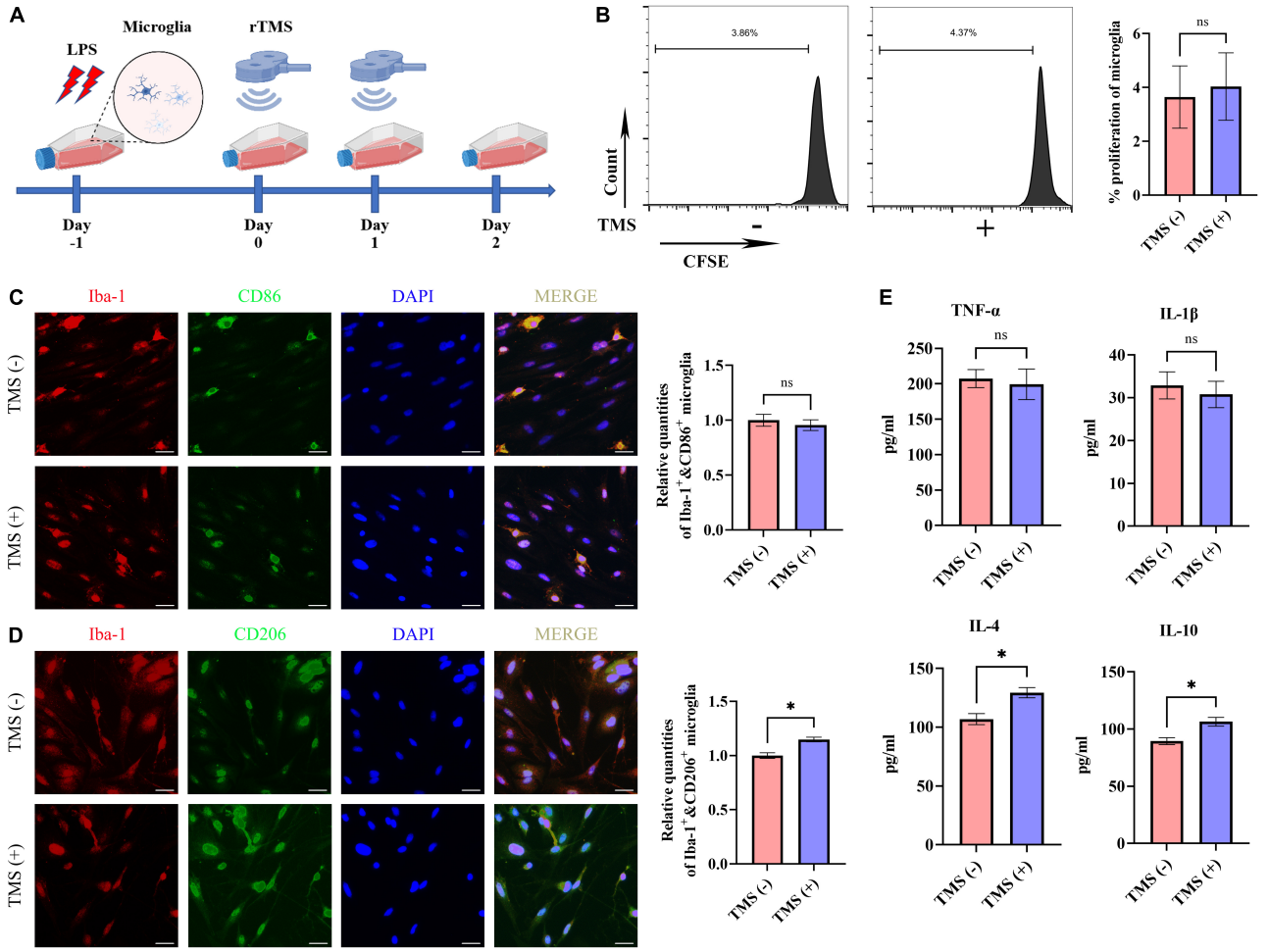

FIGURE 6 | Neuroprotective polarization of microglia activated by lipopolysaccharide (LPS). **(A)** The experiment timelines of rTMS stimulation for microglia activated by LPS. Microglia were treated with rTMS at 1 day after LPS stimulation. **(B)** Carboxyfluorescein succinimidyl ester (CFSE) analysis of cell proliferation. Quantitative analysis of Iba-1$^+$ and CD86$^+$ neurotoxic microglia **(C)** and Iba-1$^+$ and CD206$^+$ neuroprotective microglia **(D)** in TMS (–) and TMS (+) groups (n = 3). Quantity of Iba-1$^+$ and CD86$^+$ or Iba-1$^+$ and CD206$^+$ cells in TMS (–) group was normalized as control. **(E)** The secretion of inflammatory and anti-inflammatory cytokines in TMS (–) and TMS (+) groups (n = 3). Data are shown as mean ± SEM. Scale bar, 10 μm, $^*P < 0.05$ and $^{**}P < 0.01$, and ns means no significant.

In fact, our data indicated that rTMS did not seem to be a way to quickly eliminate inflammation, for IL-1β and TNF-α were not reduced in a short time. However, IL-4 and IL-10 were quickly upregulated and rTMS maintained their high-expression for a long time. It not only ensures the long-term control of inflammation but also facilitates the repair of nerves under inflammation.

Microglia are important players of the innate immune system and the first responders to the ischemic tissue. It has been well established that the effect of microglia is considered with neuroprotective and neurotoxic aspects. Activated neurotoxic microglia could secrete proinflammatory cytokines (e.g., IL-1β and TNF-α) and further enlarge the infarct. Conversely, neuroprotective microglia could secrete anti-inflammatory cytokines (e.g., IL-4 and IL-10) and protect neurons against ischemic damage. Previous studies have revealed that rTMS could induce a shift in microglia phenotype activation *in vivo* and reduce proinflammatory cytokines (Hong et al., 2020; Zong et al., 2020). Our data are partially similar to the above research conclusions, for rTMS could promote the anti-inflammatory polarization of microglia. In our study, we also found that rTMS would not change the total number or proportion of microglia *in vivo* or *in vitro* treatment. In addition, we did not find rTMS could downregulate the proportion of proinflammatory CD86$^+$ microglia *in vitro*, and same phenomenon existed *in vivo*. Although long-term rTMS treatment showed the ability to reduce the expression of CD86, it might be caused by promoting other functional cells such as astrocytes to secrete anti-inflammatory factors to act on the neurotoxic microglia. Therefore, our data are more inclined to believe that rTMS can promote the polarization of anti-inflammatory microglia to exert long-term neuroprotective functions, rather than directly change proinflammatory polarization of microglia.

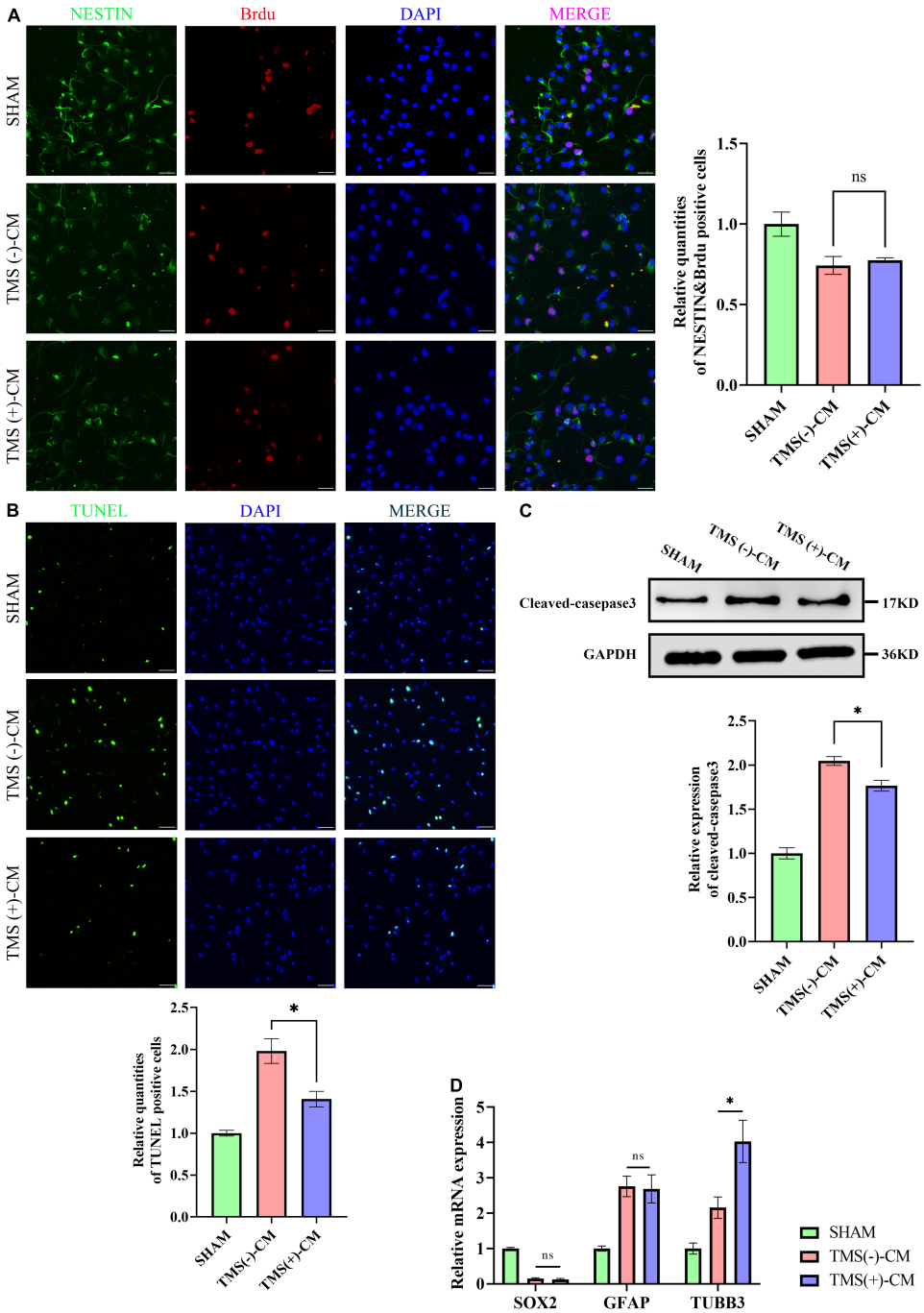

FIGURE 7 | Effect of microglia-derived conditioned medium (CM) on neural stem cells (NSCs). **(A)** Quantitative analysis of BrdU$^+$ and NESTIN$^+$ NSCs in NSCs treated with or without microglia-derived CMs (n = 3), scale bar, 10 μm. Quantity of NESTIN$^+$ and BrdU$^+$ cells in TMS (–) group was normalized as control. **(B)** Quantitative analysis of TUNEL-positive apoptotic cells in NSCs treated with or without microglia-derived CMs (n = 3), Scale bar, 25 μm. Quantity of TUNEL-positive cells in TMS (–) group was normalized as control. **(C)** Western blotting analysis of cleaved-caspase3 in NSCs treated with or without microglia-derived CMs (n = 3). **(D)** Relative mRNA expression of SOX2, GFAP, and TUBB3 (n = 3). Data are shown as mean ± SEM. Statistical significance was determined with the unpaired Student's t-test. *$P < 0.05$, and ns means no significant.

Microglia are believed to affect the NSCs fate. Enhanced astrocytogenesis and neurogenesis were observed, while NSCs were treated with CM from microglia stimulated with LPS (Nakanishi et al., 2007; Shigemoto-Mogami et al., 2014). Our results showed that both TMS (−)-CM and TMS (+)-CM could promote NSCs differentiation. Compared with TMS (−)-CM, TMS (+)-CM exhibited a higher tendency to differentiate into neurons, whereas TMS (−)-CM were more likely to induce NSCs

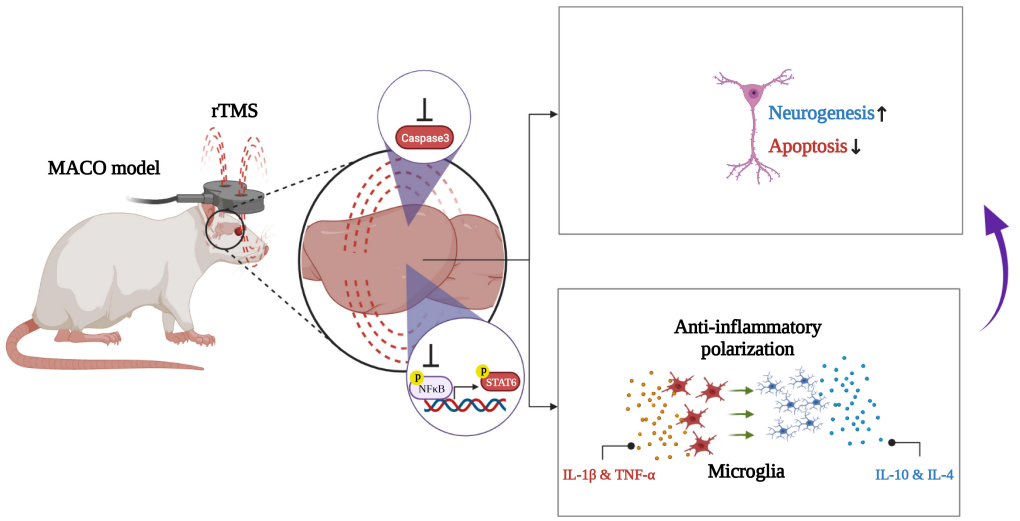

FIGURE 8 | Schematic illustration of rTMS-mediated anti-inflammatory polarization of microglia and neural recovery.

into astrocytes. Differences in soluble cytokine types of CMs may explain the differences in NSCs fate. For example, IL-1β is believed to reduce NSC or NPC proliferation, and neuronal differentiation (Crampton et al., 2012; Zunszain et al., 2012; Chen et al., 2013), but enhance astrogliogenesis (Ling et al., 1998). Kynurenine pathway and signal transducer and activator of transcription 3 (STAT3) pathway are believed to be activated by IL-1β and contribute to the above effect (Zunszain et al., 2012; Chen et al., 2013); TNF-α decreases neurogenesis and upregulates the expression of HES-1, previously believed as an antineurogenic transcription (Nakamura et al., 2000; Johansson et al., 2008); IL-4 and IL-10 both have antiapoptotic effect. IL-4 can reduce the proliferation rate but promote neuronal and glial differentiation, while IL-10 promotes the proliferation but its effect on differentiation is not obvious (Kiyota et al., 2012; Lim et al., 2013). The soluble cytokines from microglia have both positive and negative role on neurogenesis or neuroapoptosis, while some researchers have recently explained the effects of rTMS on brain from other perspective of regulating the neurogenesis and dendritic complexity in the hippocampus or primary motor cortex (Cambiaghi et al., 2021, 2020). High-frequency rTMS can affect the type and quantity of the cytokines by regulating the polarization of microglia, which partly explains the role of rTMS in promoting neurogenesis and inhibiting neuroapoptosis *in vivo* and *in vitro*.

CONCLUSION

In conclusion, our work demonstrates that rTMS helps neurorehabilitation by promoting the anti-inflammatory polarization of microglia (**Figure 8**). These data preliminarily confirm that rTMS can independently induce the neuroprotective phenotype of microglia. Based on our findings, we suggested that rTMS can further explore the optimization of treatment parameters in response to changes in microglial phenotype.

DATA AVAILABILITY STATEMENT

The original contributions presented in the study are included in the article/**Supplementary Material**, further inquiries can be directed to the corresponding authors.

ETHICS STATEMENT

The animal study was reviewed and approved by the Sun Yat-sen University Institutional Animal Care and Use Committee.

AUTHOR CONTRIBUTIONS

XH and FQ were responsible for the study design and manuscript drafting. JL, YF, and ML carried out most of the experimental work, such as MCAO model and immunostaining assay, cell extraction and culturing, Western blot, RNA purification, and real-time-PCR. MY conducted TMS stimulation and data analysis. All authors read and approved the manuscript.

FUNDING

This research was financially supported by the National Natural Science Foundation of China (81702232, 82172546, 81972151, and 82100560), Medical Scientific Research Foundation of Guangdong Province (A2021110), and China Postdoctoral Science Foundation (2021M703704).

SUPPLEMENTARY MATERIAL

The Supplementary Material for this article can be found online at: https://www.frontiersin.org/articles/10.3389/fncel.2022.878345/full#supplementary-material

REFERENCES

Azari, H., Sharififar, S., Rahman, M., Ansari, S., and Reynolds, B. A. (2011). Establishing embryonic mouse neural stem cell culture using the neurosphere assay. *J. Vis. Exp.* 47:2457. doi: 10.3791/2457

Benjamin, E. J., Muntner, P., Alonso, A., Bittencourt, M. S., Callaway, C. W., Carson, A. P., et al. (2019). Heart disease and stroke statistics-2019 update: a report from the american heart association. *Circulation* 139, e56–e528. doi: 10.1161/CIR.0000000000000659

Cambiaghi, M., Cherchi, L., Masin, L., Infortuna, C., Briski, N., Caviasco, C., et al. (2021). High-frequency repetitive transcranial magnetic stimulation enhances layer II/III morphological dendritic plasticity in mouse primary motor cortex. *Behav. Brain Res.* 410:113352. doi: 10.1016/j.bbr.2021.113352

Cambiaghi, M., Crupi, R., Bautista, E. L., Elsamadisi, A., Malik, W., Pozdniakova, H., et al. (2020). The effects of 1-Hz rTMS on emotional behavior and dendritic complexity of mature and newly generated dentate gyrus neurons in male mice. *Int. J. Environ. Res. Public Health* 17:4047. doi: 10.3390/ijerph17114074

Carson, R. G. (2020). Inter-hemispheric inhibition sculpts the output of neural circuits by co-opting the two cerebral hemispheres. *J. Physiol.* 598, 4781–4802. doi: 10.1113/JP279793

Chen, E., Xu, D., Lan, X., Jia, B., Sun, L., Zheng, J. C., et al. (2013). A novel role of the STAT3 pathway in brain inflammation-induced human neural progenitor cell differentiation. *Curr. Mol. Med.* 13, 1474–1484. doi: 10.2174/15665240113139990076

Clarke, D., Beros, J., Bates, K. A., Harvey, A. R., Tang, A. D., Rodger, J., et al. (2021). Low intensity repetitive magnetic stimulation reduces expression of genes related to inflammation and calcium signalling in cultured mouse cortical astrocytes. *Brain Stimul.* 14, 183–191. doi: 10.1016/j.brs.2020.12.007

Crampton, S. J., Collins, L. M., Toulouse, A., Nolan, Y. M., and O'Keeffe, G. W. (2012). Exposure of foetal neural progenitor cells to IL-1beta impairs their proliferation and alters their differentiation - a role for maternal inflammation? *J. Neurochem.* 120, 964–973. doi: 10.1111/j.1471-4159.2011.07634.x

Cui, M., Ge, H., Zeng, H., Yan, H., Zhang, L., Feng, H., et al. (2019). Repetitive transcranial magnetic stimulation promotes neural stem cell proliferation and differentiation after intracerebral hemorrhage in mice. *Cell Transplant.* 28, 568–584. doi: 10.1177/0963689719834870

Cullen, C. L., Senesi, M., Tang, A. D., Clutterbuck, M. T., Auderset, L., O'Rourke, M. E., et al. (2019). Low-intensity transcranial magnetic stimulation promotes the survival and maturation of newborn oligodendrocytes in the adult mouse brain. *Glia* 67, 1462–1477. doi: 10.1002/glia.23620

Girotra, T., Lekoubou, A., Bishu, K. G., and Ovbiagele, B. (2020). A contemporary and comprehensive analysis of the costs of stroke in the United States. *J. Neurol. Sci.* 410:116643. doi: 10.1016/j.jns.2019.116643

Giulian, D., and Baker, T. J. (1986). Characterization of ameboid microglia isolated from developing mammalian brain. *J. Neurosci.* 6, 2163–2178. doi: 10.1523/JNEUROSCI.06-08-02163.1986

Guo, F., Lou, J., Han, X., Deng, Y., and Huang, X. (2017). Repetitive transcranial magnetic stimulation ameliorates cognitive impairment by enhancing neurogenesis and suppressing apoptosis in the hippocampus in rats with ischemic stroke. *Front. Physiol.* 8:559. doi: 10.3389/fphys.2017.00559

Hallett, M. (2000). Transcranial magnetic stimulation and the human brain. *Nature* 406, 147–150. doi: 10.1038/35018000

Hong, Y., Liu, Q., Peng, M., Bai, M., Li, J., Sun, R., et al. (2020). High-frequency repetitive transcranial magnetic stimulation improves functional recovery by inhibiting neurotoxic polarization of astrocytes in ischemic rats. *J. Neuroinflammation* 17:150. doi: 10.1186/s12974-020-01747-y

Hong, Z., Zheng, H., Luo, J., Yin, M., Ai, Y., Deng, B., et al. (2021). Effects of Low-Frequency repetitive transcranial magnetic stimulation on language recovery in poststroke survivors with aphasia: an updated meta-analysis. *Neurorehabil. Neural Repair* 35, 680–691. doi: 10.1177/15459683211011230

Jayaraj, R. L., Azimullah, S., Beiram, R., Jalal, F. Y., and Rosenberg, G. A. (2019). Neuroinflammation: friend and foe for ischemic stroke. *J. Neuroinflammation* 16:142. doi: 10.1186/s12974-019-1516-2

Johansson, S., Price, J., and Modo, M. (2008). Effect of inflammatory cytokines on major histocompatibility complex expression and differentiation of human neural stem/progenitor cells. *Stem Cells* 26, 2444–2454. doi: 10.1634/stemcells.2008-0116

Kanazawa, M., Ninomiya, I., Hatakeyama, M., Takahashi, T., and Shimohata, T. (2017). Microglia and monocytes/macrophages polarization reveal novel therapeutic mechanism against stroke. *Int. J. Mol. Sci* 18:2135. doi: 10.3390/ijms18102135

Kelmanson, I. V., Shokhina, A. G., Kotova, D. A., Pochechuev, M. S., Ivanova, A. D., Kostyuk, A. I., et al. (2021). In vivo dynamics of acidosis and oxidative stress in the acute phase of an ischemic stroke in a rodent model. *Redox Biol.* 48:102178. doi: 10.1016/j.redox.2021.102178

Kim, J. Y., Choi, G. S., Cho, Y. W., Cho, H., Hwang, S. J., and Ahn, S. H. (2013). Attenuation of spinal cord injury-induced astroglial and microglial activation by repetitive transcranial magnetic stimulation in rats. *J. Korean Med. Sci.* 28, 295–299. doi: 10.3346/jkms.2013.28.2.295

Kiyota, T., Ingraham, K. L., Swan, R. J., Jacobsen, M. T., Andrews, S. J., and Ikezu, T. (2012). AAV serotype 2/1-mediated gene delivery of anti-inflammatory interleukin-10 enhances neurogenesis and cognitive function in APP+PS1 mice. *Gene Ther.* 19, 724–733. doi: 10.1038/gt.2011.126

Koch, G., Bonni, S., Casula, E. P., Iosa, M., Paolucci, S., Pellicciari, M. C., et al. (2019). Effect of cerebellar stimulation on gait and balance recovery in patients with hemiparetic stroke: a randomized clinical trial. *JAMA Neurol.* 76, 170–178. doi: 10.1001/jamaneurol.2018.3639

Koh, S. H., and Park, H. H. (2017). Neurogenesis in stroke recovery. *Transl. Stroke Res.* 8, 3–13. doi: 10.1007/s12975-016-0460-z

Lambertsen, K. L., Finsen, B., and Clausen, B. H. (2019). Post-stroke inflammation-target or tool for therapy? *Acta Neuropathol.* 137, 693–714. doi: 10.1007/s00401-018-1930-z

Lim, S. H., Park, E., You, B., Jung, Y., Park, A. R., Park, S. G., et al. (2013). Neuronal synapse formation induced by microglia and interleukin 10. *PLoS One* 8:e81218. doi: 10.1371/journal.pone.0081218

Ling, Z. D., Potter, E. D., Lipton, J. W., and Carvey, P. M. (1998). Differentiation of mesencephalic progenitor cells into dopaminergic neurons by cytokines. *Exp. Neurol.* 149, 411–423. doi: 10.1006/exnr.1998.6715

Lipton, P. (1999). Ischemic cell death in brain neurons. *Physiol. Rev.* 79, 1431–1568. doi: 10.1152/physrev.1999.79.4.1431

Liu, Y., Yin, M., Luo, J., Huang, L., Zhang, S., Pan, C., et al. (2020). Effects of transcranial magnetic stimulation on the performance of the activities of daily living and attention function after stroke: a randomized controlled trial. *Clin. Rehabil.* 34, 1465–1473. doi: 10.1177/0269215520946386

Luber, B., and Lisanby, S. H. (2014). Enhancement of human cognitive performance using transcranial magnetic stimulation (TMS). *Neuroimage* 85(Pt 3), 961–970. doi: 10.1016/j.neuroimage.2013.06.007

Luo, J., Zheng, H., Zhang, L., Zhang, Q., Li, L., Pei, Z., et al. (2017). High-Frequency repetitive transcranial magnetic stimulation (rTMS) improves functional recovery by enhancing neurogenesis and activating BDNF/TrkB signaling in ischemic rats. *Int. J. Mol. Sci* 18:455. doi: 10.3390/ijms18020455

Ma, Y., Wang, J., Wang, Y., and Yang, G. Y. (2017). The biphasic function of microglia in ischemic stroke. *Prog. Neurobiol.* 157, 247–272. doi: 10.1016/j.pneurobio.2016.01.005

Muri, L., Oberhansli, S., Buri, M., Le, N. D., Grandgirard, D., Bruggmann, R., et al. (2020). Repetitive transcranial magnetic stimulation activates glial cells and inhibits neurogenesis after pneumococcal meningitis. *PLoS One* 15:e232863. doi: 10.1371/journal.pone.0232863

Nakamura, Y., Sakakibara, S., Miyata, T., Ogawa, M., Shimazaki, T., Weiss, S., et al. (2000). The bHLH gene hes1 as a repressor of the neuronal commitment of CNS stem cells. *J. Neurosci.* 20, 283–293. doi: 10.1523/JNEUROSCI.20-01-00283.2000

Nakanishi, M., Niidome, T., Matsuda, S., Akaike, A., Kihara, T., and Sugimoto, H. (2007). Microglia-derived interleukin-6 and leukaemia inhibitory factor promote astrocytic differentiation of neural stem/progenitor cells. *Eur. J. Neurosci.* 25, 649–658. doi: 10.1111/j.1460-9568.2007.05309.x

Natale, G., Pignataro, A., Marino, G., Campanelli, F., Calabrese, V., Cardinale, A., et al. (2021). Transcranial magnetic stimulation exerts "rejuvenation". Effects on corticostriatal synapses after partial dopamine depletion. *Mov. Disord.* 36, 2254–2263. doi: 10.1002/mds.28671

Nayak, D., Roth, T. L., and McGavern, D. B. (2014). Microglia development and function. *Annu. Rev. Immunol.* 32, 367–402. doi: 10.1146/annurev-immunol-032713-120240

Paillere, M. M., Martinot, J. L., Ringuenet, D., Galinowski, A., Gallarda, T., Bellivier, F., et al. (2011). Baseline brain metabolism in resistant depression and response

to transcranial magnetic stimulation. *Neuropsychopharmacology* 36, 2710–2719. doi: 10.1038/npp.2011.161

Peruzzotti-Jametti, L., Bacigaluppi, M., Sandrone, S., and Cambiaghi, M. (2013). Emerging subspecialties in neurology: transcranial stimulation. *Neurology* 80, e33–e35. doi: 10.1212/WNL.0b013e3182833d74

Prinz, M., Jung, S., and Priller, J. (2019). Microglia biology: one century of evolving concepts. *Cell* 179, 292–311. doi: 10.1016/j.cell.2019.08.053

Sasso, V., Bisicchia, E., Latini, L., Ghiglieri, V., Cacace, F., Carola, V., et al. (2016). Repetitive transcranial magnetic stimulation reduces remote apoptotic cell death and inflammation after focal brain injury. *J. Neuroinflammation* 13:150. doi: 10.1186/s12974-016-0616-5

Shigemoto-Mogami, Y., Hoshikawa, K., Goldman, J. E., Sekino, Y., and Sato, K. (2014). Microglia enhance neurogenesis and oligodendrogenesis in the early postnatal subventricular zone. *J. Neurosci.* 34, 2231–2243. doi: 10.1523/JNEUROSCI.1619-13.2014

Shinba, T., Kariya, N., Matsuda, S., Matsuda, H., and Obara, Y. (2018). Increase of frontal cerebral blood volume during transcranial magnetic stimulation in depression is related to treatment effectiveness: a pilot study with near-infrared spectroscopy. *Psychiatry Clin. Neurosci.* 72, 602–610. doi: 10.1111/pcn.12680

Tan, T., Xie, J., Tong, Z., Liu, T., Chen, X., and Tian, X. (2013). Repetitive transcranial magnetic stimulation increases excitability of hippocampal CA1 pyramidal neurons. *Brain Res.* 1520, 23–35. doi: 10.1016/j.brainres.2013.04.053

Vidal-Dourado, M., Conforto, A. B., Caboclo, L. O., Scaff, M., Guilhoto, L. M., and Yacubian, E. M. (2014). Magnetic fields in noninvasive brain stimulation. *Neuroscientist* 20, 112–121. doi: 10.1177/1073858413491145

Wang, Q., Zhang, D., Zhao, Y. Y., Hai, H., and Ma, Y. W. (2020). Effects of high-frequency repetitive transcranial magnetic stimulation over the contralesional motor cortex on motor recovery in severe hemiplegic stroke: a randomized clinical trial. *Brain Stimul.* 13, 979–986. doi: 10.1016/j.brs.2020.03.020

Xiong, X. Y., Liu, L., and Yang, Q. W. (2016). Functions and mechanisms of microglia/macrophages in neuroinflammation and neurogenesis after stroke. *Prog. Neurobiol.* 142, 23–44. doi: 10.1016/j.pneurobio.2016.05.001

Yang, L., Su, Y., Guo, F., Zhang, H., Zhao, Y., Huang, Q., et al. (2020). Deep rTMS mitigates behavioral and neuropathologic anomalies in Cuprizone-Exposed mice through reducing microglial proinflammatory cytokines. *Front. Integr. Neurosci.* 14:556839. doi: 10.3389/fnint.2020.556839

Yin, M., Liu, Y., Zhang, L., Zheng, H., Peng, L., Ai, Y., et al. (2020). Effects of rTMS treatment on cognitive impairment and Resting-State brain activity in stroke patients: a randomized clinical trial. *Front. Neural Circuits* 14:563777. doi: 10.3389/fncir.2020.563777

Zhao, C. G., Qin, J., Sun, W., Ju, F., Zhao, Y. L., Wang, R., et al. (2019). RTMS regulates the balance between proliferation and apoptosis of spinal cord derived neural Stem/Progenitor cells. *Front. Cell. Neurosci.* 13:584. doi: 10.3389/fncel.2019.00584

Zong, X., Dong, Y., Li, Y., Yang, L., Li, Y., Yang, B., et al. (2020). Beneficial effects of theta-burst transcranial magnetic stimulation on stroke injury via improving neuronal microenvironment and mitochondrial integrity. *Transl. Stroke Res.* 11, 450–467. doi: 10.1007/s12975-019-00731-w

Zunszain, P. A., Anacker, C., Cattaneo, A., Choudhury, S., Musaelyan, K., Myint, A. M., et al. (2012). Interleukin-1beta: a new regulator of the kynurenine pathway affecting human hippocampal neurogenesis. *Neuropsychopharmacology* 37, 939–949. doi: 10.1038/npp.2011.277

Conflict of Interest: The authors declare that the research was conducted in the absence of any commercial or financial relationships that could be construed as a potential conflict of interest.

Publisher's Note: All claims expressed in this article are solely those of the authors and do not necessarily represent those of their affiliated organizations, or those of the publisher, the editors and the reviewers. Any product that may be evaluated in this article, or claim that may be made by its manufacturer, is not guaranteed or endorsed by the publisher.

frontiers | Frontiers in Cellular Neuroscience

ORIGINAL RESEARCH
published: 12 May 2022
doi: 10.3389/fncel.2022.882127

Low-Intensity Focused Ultrasound Alleviates Spasticity and Increases Expression of the Neuronal K-Cl Cotransporter in the L4–L5 Sections of Rats Following Spinal Cord Injury

Ye-Hui Liao[1,2], *Mo-Xian Chen*[1], *Shao-Chun Chen*[1], *Kai-Xuan Luo*[1], *Bing Wang*[1], *Li-Juan Ao*[1]* and *Yao Liu*[1]*

[1] School of Rehabilitation, Kunming Medical University, Kunming, China, [2] Department of Orthopaedics, Affiliated Hospital of Southwest Medical University, Luzhou, China

OPEN ACCESS

Edited by:
Feng Zhang,
Third Hospital of Hebei Medical University, China

Reviewed by:
Xu-Yun Hua,
Shanghai University of Traditional Chinese Medicine, China
Jaekwang Lee,
Korea Food Research Institute (KFRI), South Korea

***Correspondence:**
Li-Juan Ao
aolijuan@kmmu.edu.cn
Yao Liu
175381219@qq.com

Specialty section:
This article was submitted to Cellular Neuropathology, a section of the journal Frontiers in Cellular Neuroscience

Received: 23 February 2022
Accepted: 19 April 2022
Published: 12 May 2022

Citation:
Liao Y-H, Chen M-X, Chen S-C, Luo K-X, Wang B, Ao L-J and Liu Y (2022) Low-Intensity Focused Ultrasound Alleviates Spasticity and Increases Expression of the Neuronal K-Cl Cotransporter in the L4–L5 Sections of Rats Following Spinal Cord Injury. Front. Cell. Neurosci. 16:882127. doi: 10.3389/fncel.2022.882127

Low-intensity focused ultrasound (LIFU) has been shown to provide effective activation of the spinal cord neurocircuits. The aim of this study was to investigate the effects of LIFU in order to alleviate spasticity following spinal cord injury (SCI) by activating the spinal neurocircuits and increasing the expression of the neuronal K-Cl cotransporter KCC_2. Adult male Sprague Dawley (SD) rats (220–300 g) were randomly divided into a sham control group, a $LIFU^-$ group, and a $LIFU^+$ group. The mechanical threshold hold (g) was used to evaluate the behavioral characteristics of spasm. Electromyography (EMG) was used to assess activation of the spinal cord neurocircuits and muscle spontaneous contraction. Spasticity was assessed by frequency-dependent depression (FDD). The expression of KCC_2 of the lumbar spinal cord was determined via western blot (WB) and immunofluorescence (IF) staining. The spinal cord neurocircuits were activated by LIFU simulation, which significantly reduced the mechanical threshold (g), FDD, and EMG recordings (s) after 4 weeks of treatment. WB and IF staining both demonstrated that the expression of KCC_2 was reduced in the $LIFU^-$ group ($P < 0.05$). After 4 weeks of LIFU stimulation, expression of KCC_2 had significantly increased ($P < 0.05$) in the $LIFU^+$ group compared with the $LIFU^-$ group. Thus, we hypothesized that LIFU treatment can alleviate spasticity effectively and upregulate the expression of KCC_2 in the L4–L5 section of SCI rats.

Keywords: low-intensity focused ultrasound, neurocircuits, spasticity, spinal cord injury, KCC_2

INTRODUCTION

Spasticity (involuntary contractions of paralyzed muscles) is an important complication of patients suffering from spinal cord injury (SCI) or stroke, and seriously affects their quality of life (Holtz et al., 2017; Pan et al., 2022). Studies have shown that 65% of SCI patients suffer muscle hypertonia, hyperreflexia, and spasticity (Sköld et al., 1999; Holtz et al., 2017). The pathogenesis of spasticity following SCI is complex, while increasing excitability of the motor neurons below the spinal damage lever play important roles (Sheean, 2002). In a normal spinal cord, the balance of excitation and inhibition plays an important role in physiological motor responses. Following SCI, descending

input, such as serotoninergic descending tracts from upper motor neurons, become damaged, which contributes to disruption of the excitation/inhibition balance (Brocard et al., 2016). Loss of the serotoninergic descending tracts, the inhibitory interneurons, such as Renshaw cells connected to the motor neurons, and suppressing excitation of the motor neurons, can reduce feedback from GABAergic neurons (Carr et al., 1999; Wootz et al., 2013). With a reduction in efficient inhibition by the interneurons, the motor units below the SCI show a prolonged depolarization, and even with a brief sensory stimulation (<20 ms) (Lin et al., 2007). All of the above-mentioned factors were found to lead to spasticity following SCI (Boulenguez and Vinay, 2009; Boulenguez et al., 2010). Thus, increasing activation of the spinal cord neurocircuits above the SCI section would be a feasible method for reducing the excitability of the spinal cord below the SCI, thus alleviating spasticity (Kupcova Skalnikova et al., 2013).

Therefore, as one of the serious complications of upper motor neuron syndrome (Sheean, 2002), spasticity has a complex pathogenesis. However, there is still no effective treatment. Drugs, surgery, and rehabilitation therapy are often used to improve the symptoms of spasmodic patients. Moreover, there are still some deficiencies in the above treatment methods for such spasmodic symptoms, including, skin lesions caused by medical treatments (Lannin et al., 2007), muscle weakness and infection at the injection site induced by botulinum toxin injection (Elbasiouny et al., 2010), and muscle weakness caused by baclofen (Kirshblum, 1999), etc.

KCC_2 is an important K^+-Cl^- transporter on the cell membrane of mature motor neurons, which can remove intracellular Cl^- to the extracellular zone, thus maintaining a low concentration of chloride ions ($[Cl^-]_i$) in motor neurons (Nilius and Droogmans, 2003). Lower $[Cl^-]_i$ plays an important role in maintaining gamma-aminobutyric acid (GABA) and glycine inhibition for motor neurons (Viemari et al., 2011; Mazzone et al., 2021). It has been reported that the expression of KCC_2 was significantly downregulated on the motor neurons of the spinal cord below the injury level of the spinal cord (Boulenguez et al., 2010). The downregulation of KCC_2 in the cell membranes of motor neurons leads to increased intracellular $[Cl^-]_i$, weakening the inhibitory effect of GABA and glycine to motor neurons, increasing the excitability of motor neurons, and finally leading to limb spasticity (Mazzone et al., 2021).

As a potential non-invasive neuromodulatory technology, the therapeutic effect of low-intensity focused ultrasound (LIFU) on central nervous system diseases has been a focus of research in recent years (Legon et al., 2018; Lipsman et al., 2018; Darrow, 2019). According to animal experiments, eye movements, pupil dilation, and animal paw and/or tail movements were observed when the central nervous system was stimulated by LIFU, and changes in electromyography (EMG) signals were also detected (Darrow, 2019). A recent study confirmed that LIFU exerted effective action on the deep brain region and increased the expression of C-fos positive cells (Hou et al., 2021). It has been reported that LIFU irradiation of specific areas of the cerebral cortex in primates and humans can significantly reduce the amplitude of cortical-evoked potential and enhance the ability of tactile discrimination (Legon et al., 2018). Both cellular and animal experiments have confirmed that LIFU not only affects the activation and depolarization of Ca^{2+} and Na^+ ion channels on the cell membrane (Kubanek et al., 2016) but also upregulates the expression of brain-derived neurotrophic factor (BDNF) following central nerve injury (Yang et al., 2015; Ni et al., 2017; Blackmore et al., 2019). In a previous study, our team also confirmed that LIFU stimulation can activate the spinal cord neurocircuits (Liao et al., 2021a) and increase the expression of KCC_2 of the spinal cords of neuropathic pain rats effectively (Liao et al., 2021b). However, whether LIFU can activate the spinal cord neurocircuits, upregulate the expression of KCC_2, and then alleviate spasticity post-SCI spasm is still not completely clear. In this study, we used LIFU to stimulate the lumbar spinal cords of SCI rats, electrophysiology tests and behavior assessment to evaluate its therapeutic effects, and western blotting (WB) and immunofluorescence (IF) staining to examine the expression of KCC_2 in the lumbar spinal cord in order to explore the possible mechanism of LIFU treatment.

MATERIALS AND METHODS

Animals and Experimental Drugs

Adult male Sprague Dawley (SD) rats (200–280 g) were purchased from the Animal Experiment Center of Kunming Medical University, Yunnan Province, China. The animals were housed in a temperature-controlled facility with a day–night cycle of 12/12 h and free access to food and water. The study design is shown in **Figure 1**. A total of 30 animals were randomly divided into three groups: (i) a sham operation group ($n = 10$), in which the rats received all the surgical procedures except for SCI at T10; (ii) a $LIFU^-$ group ($n = 10$), in which the rats received spinal cord injury (SCI) and LIFU treatment but with the ultrasonic amplifier always turned off; and (iii) a $LIFU^+$ group ($n = 10$), where all the rats received SCI and LIFU treatment, as shown in **Figure 1A**. Neuromotor functional and behaviors assessment was performed at pre-SCI, 1 d pre-LIFU, and 1, 2, 3, 4 weeks post-LIFU; an EMG test for activation of the spinal cord neurocircuits was performed 1 d pre-LIFU; and EMG tests for spasm, H-reflex tests, WB, and IF staining were performed 4 weeks post-LIFU, as shown in **Figure 1B**.

Surgical Procedures in Rats

The SCI surgical procedures were performed as described in previous reports (Brocard et al., 2016), and the spinal cord was transected at the T10 level. Briefly, rats were anesthetized with 2% isoflurane and fixed in the prone position. The hair on the back was shaved off and the skin at the T9–T11 vertebra was incised. The paravertebral muscles were dissected bluntly from T9 to T11. T10 laminectomy was performed carefully in order to expose the epidural and spinal cord, which were then cut transversally with sharp blades, followed by suturing of the paravertebral muscles and skin, layer by layer. The incision was disinfected once again, 0.9% NaCl was injected intraperitoneally to prevent dehydration, and the animals were placed in a 37°C incubator until awakening from anesthesia. Penicillin (160,000 units, qd) was postoperatively injected intraperitoneally for 3 d. Manually

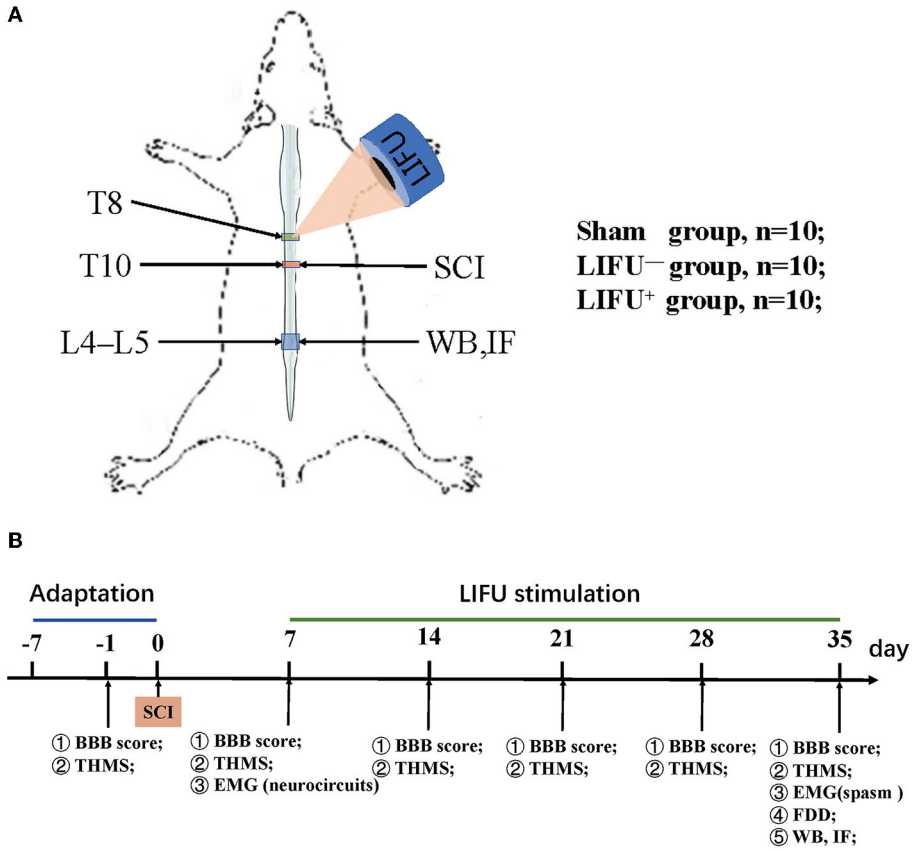

FIGURE 1 | Experimental design of the study. **(A)** Modeling and ultrasound therapy. **(B)** Experimental design. The Basso, Beattie, and Bresnahan (BBB) score and threshold hold (g) of mechanical stimulation (THMS) were tested 1 d before the spinal cord injury (SCI) and weekly starting from 7 d post-injury (dpi); electromyography (EMG) of the neurocircuits and spasm were tested before/after low-intensity focused ultrasound (LIFU) treatment separately; frequency-dependent depression (FDD), western blot (WB), and immunofluorescence (IF) staining were tested following the end of LIFU treatment.

assisted urination was performed daily until the autonomous reflex of urination was restored.

LIFU Treatment Program

LIFU stimulation of the spinal cord was performed as described previously (Liao et al., 2021a,b). Briefly, before LIFU treatment, the hair around the ultrasonic irradiation site on the back of each rat was shaved off. The ultrasonic probe was fixed with a clapper in order to ensure that the ultrasound focus was located at the spinal cord. An ultrasonic coupling agent was applied between the transducer and the spinal skin in order to ensure that there was no bubble in the space. The LIFU parameters were as follows: sine pulse, frequency = 4 MHz, pulse repetition rate (PRF) = 0.8 kHz, radiation intensity (RI) = 0.65 MPa, and duty cycle (DC) = 50%. The ultrasound system included a signal generator (DG4202, RIGOL, China), a power amplifier (Dahan Radio Studio, China), and an ultrasonic probe (DOBO, China). LIFU treatment was started 1 week after SCI, once a day, 20 min each time, for a total of 4 weeks. Calibrated hydrophones (2010, Precision Acoustics Ltd, Dorchester, UK) were used to measure the acoustic field distribution and the acoustic intensity parameters.

Behaviors Assessment of Spasticity

The threshold hold (g) of mechanical stimulation (THMS) of the tail to induce spasm spasticity, such as a muscle spasm or hyperreflexia (Corleto et al., 2015), was recorded as described in the literature (Plantier et al., 2019). Generally, after the rats familiarized themselves with the test environment for 15 min, a microsensor that could detect pressure was installed between the fingers and the tail of the rat. When muscle spasm was observed in the hind limb, as shown in **Supplementary Video 1**, the pressure on the tail was recorded. If no muscle twitch or spasm was observed when the pressure was ≥3,000 g, the pressure was recorded as 3,000 g. The measurements were repeated three times, with an interval of 5 min, and the mean value of the three measurements was calculated.

Neuromotor Functional Assessment

The Basso, Beattie, and Bresnahan (BBB) locomotor scale (Basso et al., 1995) was used to evaluate neuromotor function before and after LIFU treatment. The BBB scores ranged from 0 to 21 points, which included joint movement, gait coordination, and paw placement. Slight paralysis (score of 14–21) shows sustained hind leg coordination, moderate paralysis (score of 8–13) shows

the ability to land on the palm without bearing weight, and severe paralysis (score of 0–7) shows no movement or slight movement of one or two joints (Yu et al., 2021).

Electrophysiological Tests and Analysis

Electrophysiological assessment of spasticity included H-reflex and EMG, which have been described in the literature (Corleto et al., 2015; Beverungen et al., 2020). The EMG test was performed as previously described (Liao et al., 2021a). Briefly, the EMG signal was recorded using a concentric circular electrode, which was inserted into the soleus (Sol) muscle. The reference electrode was inserted percutaneously into the tail. The EMG signal was amplified by an A-M system, filtered over the range 200 Hz−5 kHz, and analyzed by a computer running Signal 5 software (Signal, Cambridge Electronics Design Ltd., Cambridge, UK). For the activation of the spinal cord neurocircuits test, the EMG was recorded when the spinal cord was receiving LIFU stimulation. The EMG test for hind limb spasm was evoked by a mechanical stimulation of the tail (1,500 g for 1 s stimuli, repeated three times at 10 s intervals).

For the H-reflex test, the rats were mildly anesthetized. A pair of stimulating electrodes, which were used for evoking the H-reflex, were inserted percutaneously around the tibial nerve, and a pair of recording electrodes, which were used for recording the H- and M-waves, were inserted percutaneously into the interosseous muscle at the fifth phalange. The reference electrode was inserted percutaneously into the tail. The H-reflex was induced by an independent pulse (100 μs) produced by the A-M system. The stimulus intensity that caused the maximum H-reflex was used to evoke frequency-dependent depression (FDD). A successive stimulus (20 times) was performed, and the H/M ratio was calculated by taking the average of the final 15 stimuli. The changes in H-reflex at 0.5, 1, 5, and 10 Hz were calculated as a percentage of the response obtained at 0.2 Hz. FDD data were presented as the mean ± standard error on the mean (SEM). After the last electrophysiological test, the rats were sacrifice for WB and IF staining.

Western Blot

WB was used to examine the protein expression of KCC_2 in L4–L5 spinal cord. After the final electrophysiological examination, the rats were given an intraperitoneal injection of an overdose of anesthetics perfused with ice saline (0.9% NaCl). The L4–L5 spinal cord was extracted and stored at −80°C immediately before the protein test. The spinal tissues (0.1 g) were lysed with radioimmunoprecipitation assay (RIPA) buffer (1 ml, Solarbio Life Sciences, Beijing, China) and phenylmethylsulfonyl fluoride (PMSF) (10 μl, Solarbio). The protein concentration was determined using a BCA protein assay kit (Beyotime Biotechnology, Shanghai, China) after centrifugation at 12,000 rpm at 4°C for 15 min. Following electrophoresis and transfer to nitrocellulose, the membrane was blocked with 5% skim (fat-free) milk for 2 h, washed with a mixture of tris-buffered saline and Polysorbate 20 (TBST) three times for 15 min each time, following incubation with primary antibody (KCC_2, 1:1,000, Cell Signaling, Danvers, MA, USA; β-Actin, 1:4,000, Santa Cruz Biotechnology, Dallas, TX, USA) at 4°C overnight. After washing with TBST three times, the membranes were incubated with a second antibody (peroxidase-conjugated AffiniPure goat anti-mouse/rabbit, 1:2,000, ZSGB-BIO, Beijing, China) at room temperature for 2 h. ImageJ software (https://imagej.nih.gov/ij) was used to quantify the optical density of the protein bands.

Immunofluorescence Staining

Following an overdose of anesthetics, the rats were perfused with phosphate-buffered saline (PBS) and 4% paraformaldehyde. The L4–L5 spinal cord was extracted and fixed with 4% paraformaldehyde overnight at room temperature. The fixed tissue was dehydrated with 10, 20, and 30% sucrose, step by step, following embedding in Tissue-Tek OCT medium and slicing into 6-μm-thick sections. After blocking with 3% bovine serum and 0.3% Triton X-100 in PBS, the sections were incubated with primary antibodies overnight at 4°C, followed by incubation with secondary antibodies for 2 h at room temperature. The primary antibodies used were rabbit antibody to KCC_2 (1:100) and NeuN (1:100) (all Cell Signaling, USA). The secondary antibodies,

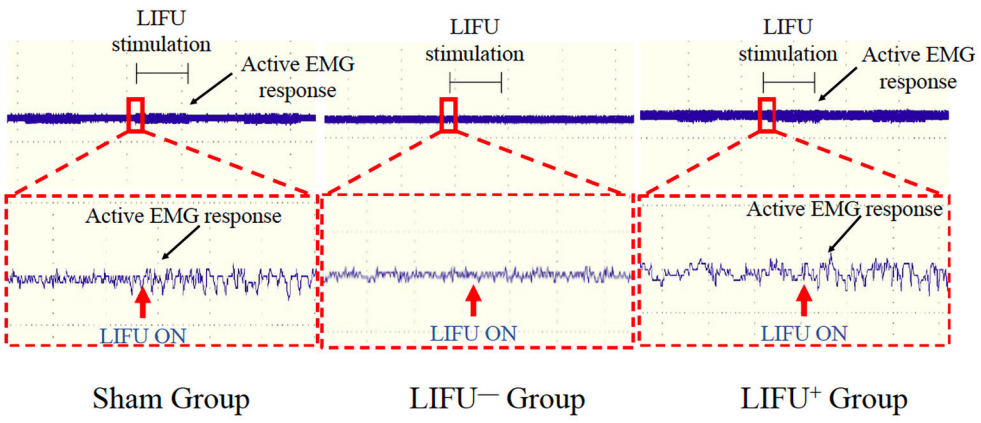

FIGURE 2 | Activation of the spinal cord neurocircuits by low-intensity focused ultrasound (LIFU) stimulation. The red arrow shows the LIFU turning on point; the black arrow shows the active EMG response.

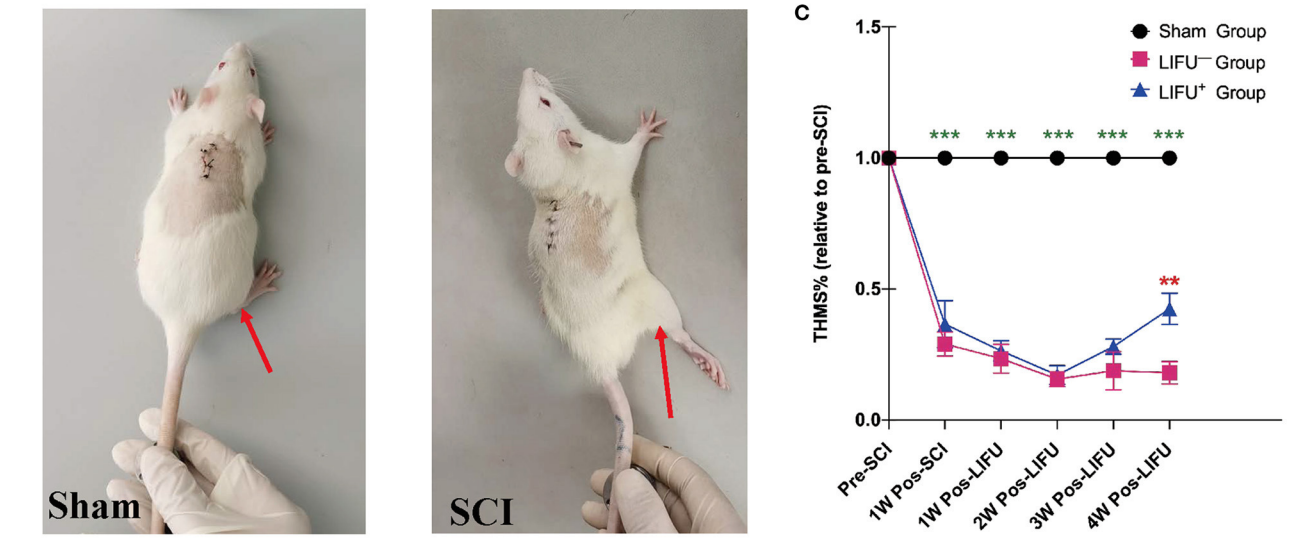

FIGURE 3 | Threshold hold (g) of mechanical stimulation (THMS) test for the spasm. **(A)** A normal hind limb motor response to tail pinching was shown by the sham operation rats. **(B)** A typical hind limb motor response to tail pinching was shown by the spinal cord injury (SCI) rats. **(C)** This shows the THMS responses to tail pinching. ***$P < 0.001$, compared with the sham group; **$P < 0.01$, compared with the LIFU$^-$ group; one-way analysis of variance (ANOVA) with a least significant difference (LSD) test; $n = 10$; mean ± standard error on the mean (SEM).

anti-rabbit IgG (H + L), F(ab′)2 fragment (Alexa Fluor® 488 Conjugate), and anti-mouse IgG (H + L), F(ab′)2 fragment (Alexa Fluor® 594 Conjugate) were used for fluorescence staining. A fluorescence microscope (Olympus Corporation, Tokyo, Japan) was used to obtain the fluorescence images. ImageJ software was used to quantify the fluorescence intensity.

Statistical Analysis

All of the data are presented as the mean ± SEM. One-way analysis of variance (ANOVA) and least significant difference (LSD) were used for comparing the different groups. When the results showed a difference, Fisher's protected LSD tests were used for pairwise comparisons. SPSS 20.0 software (IBM, New York, NY, USA) and Prism 8 (GraphPad Software Inc., San Diego, CA, USA) were used for statistical analysis and histogram making. Two-tailed P-values < 0.05 were considered statistically significant.

RESULTS

Activation of Spinal Cord Neurocircuits by LIFU Stimulation

Activation of the spinal cord neurocircuits can lead to recruitment of the hind leg muscles and can be recorded by EMG. In this study, LIFU stimulation induced a significant recruitment of soleus muscle and was recorded by EMG, as shown in **Figure 2**. In the LIFU$^+$ stimulation group, we could also clearly hear the EMG sound produced by the muscle recruitment with stimulation by LIFU, and without the EMG sound in the LIFU$^-$ stimulation group, as shown in **Supplementary Video 2**.

TABLE 1 | BBB scores in sham, LIFU$^-$ and LIFU$^+$ group at different time pre- and pos- spinal cord injury(SCI) and low intensity focus ultrasound (LIFU) treatment.

	Sham	LIFU$^-$	LIFU$^+$
Pre-SCI	20.7 ± 0.15	20.5 ± 0.22	20.4 ± 0.26
1w-pos SCI	20.4 ± 0.27	0.8 ± 0.33***	1.1 ± 0.35***
1w-pos LIFU	20.2 ± 0.25	0.8 ± 0.32***	1.0 ± 0.33***
2w-pos LIFU	20.6 ± 0.22	1.0 ± 0.30***	1.3 ± 0.34***
3w-pos LIFU	20.4 ± 0.37	0.9 ± 0.25***	1.4 ± 0.34***
4w-pos LIFU	20.6 ± 0.22	1.3 ± 0.30***	2.8 ± 0.47***##

****$P < 0.001$, indicated significant difference when compared with Sham group; ##$P < 0.01$, indicated significant difference when compared with LIFU$^-$ group. $n = 10$, one-way ANOVA and LSD test.*

Effect of LIFU on Reducing Spasticity

One week into the operation, the rats in the sham operation group showed no muscle twitch or hind limb spasm, as shown in **Figure 3A**, **Supplementary Video 1**; while in the SCI group, the rats showed significant muscle twitch and hind limb spasm following mechanical stimulation of the tail, as shown in **Figure 3B**, **Supplementary Video 1**. One week after SCI, the threshold of mechanical stimulation was significantly reduced in the LIFU$^-$ and LIFU$^+$ groups ($P < 0.05$) when compared with the sham group, but there was no difference between the LIFU$^-$ and LIFU$^+$ groups ($P > 0.05$). In the LIFU$^+$ group, the mechanical stimulation threshold increased ($P < 0.05$) after 4 weeks of LIFU treatment when compared with the LIFU$^-$ group, as shown in **Figure 3C**.

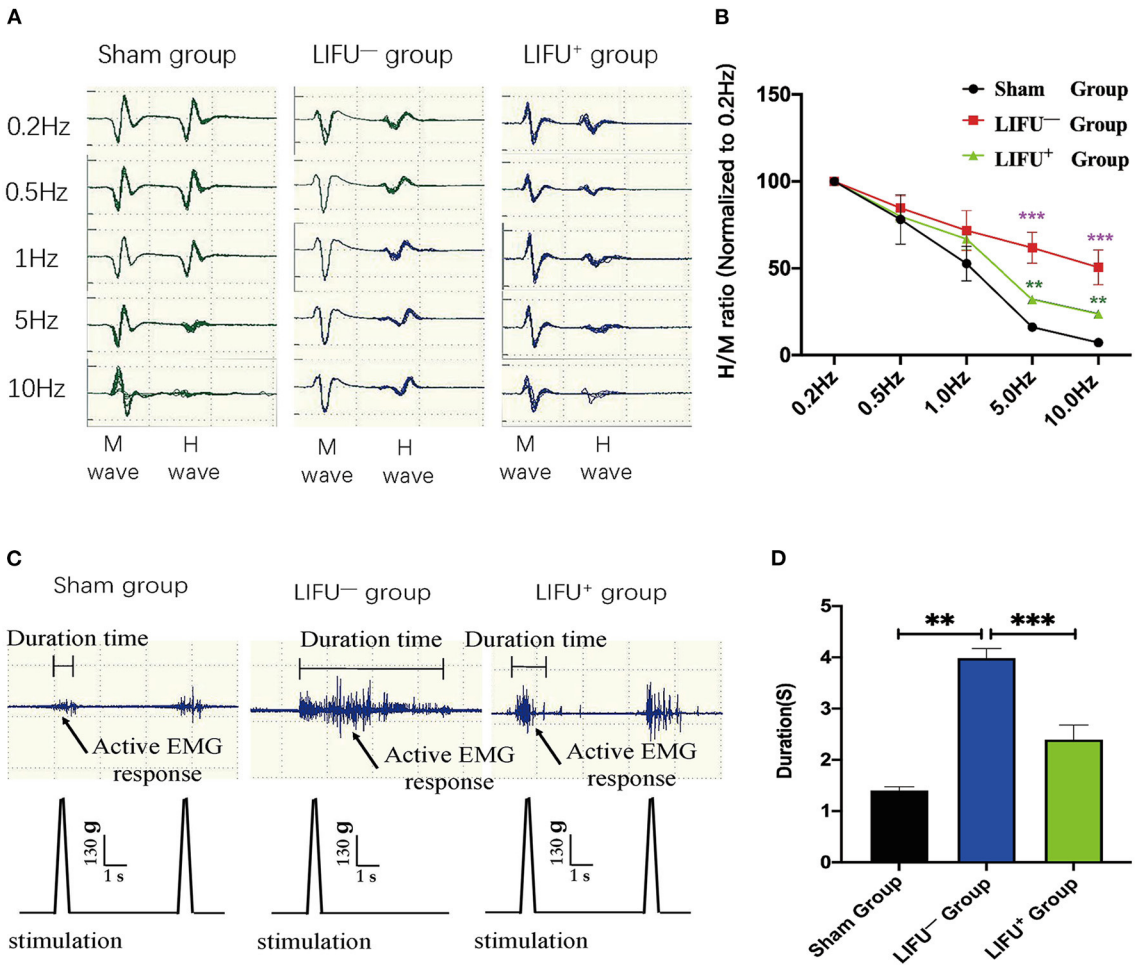

FIGURE 4 | Change in frequency-dependent depression (FDD) and electromyograph (EMG) after 4 weeks of LIFU stimulation. **(A)** A typical H_{max}/M_{max} recording over a series of 20 stimulations at 0.2, 0.5, 1, 5, and 10 Hz. The amplitude of the H-reflex decreased with increasing stimulus frequency. **(B)** FDD was normalized to intact (0.2 Hz) and showed significant differences among the different groups at 5 and 10 Hz stimuli; $^{***}P < 0.001$, compared with the sham group; $^{**}P < 0.05$, compared with the LIFU$^-$ group; one-way ANOVA with LSD test; $n = 10$, mean ± SEM. **(C)** a typical EMG recording; the black arrow shows the active EMG response following LIFU stimulation. **(D)** after 4 weeks of LIFU treatment; the durations of the EMGs were significantly different among the three groups; $^{**}P < 0.01$ in the LIFU$^-$ group compared with the sham group; $^{***}P < 0.001$ in the LIFU$^+$ group compared with the LIFU$^-$ group; one-way ANOVA with LSD test; $n = 10$, mean ± SEM.

Effect of LIFU on Increasing Neuromotor Function

Comparison of the BBB scores showed no significant differences ($P > 0.05$) among the three groups at the pre-SCI points. One week after SCI, the BBB score of the SCI group (LIFU$^-$ and LIFU$^+$) had reduced significantly ($P < 0.05$), but there was no significant difference between the LIFU$^-$ and the LIFU$^+$ group. After 4 weeks of LIFU stimulation, the BBB scores of the LIFU$^+$ group increased compared with those of the LIFU$^-$ group ($P < 0.05$), while still being below those of the sham group ($P < 0.05$), as listed in **Table 1**.

LIFU Alleviated FDD and EMG

FDD was shown to depress spasticity, as shown in **Figure 4A**. After 4 weeks of LIFU treatment, FDD showed no significant differences among the three groups at 0.5 and 1 Hz stimulation. After 5 and 10 Hz stimulation, however, the FDD of the LIFU$^-$ group was significantly higher than that of the sham group ($P < 0.05$). Following LIFU stimulation, the FDD decreased, and that of the LIFU$^+$ group was lower than that of the LIFU$^-$ group ($P < 0.05$), as shown in **Figure 4B**. The EMG showed the response time of soleus muscle after stimulation of the tail, as shown in **Figure 4C**. The response time of the LIFU$^-$ group was significantly longer than that of the sham group. Following LIFU stimulation, the response time of the LIFU$^+$ group was shortened compared with that of the LIFU$^-$ group, as shown in **Figure 4D**.

Effects of LIFU on the Expression of Protein

Following SCI, the expression level of KCC_2 was reduced (Boulenguez et al., 2010). Downregulation of KCC_2 expression had been reported to be one of the important molecular

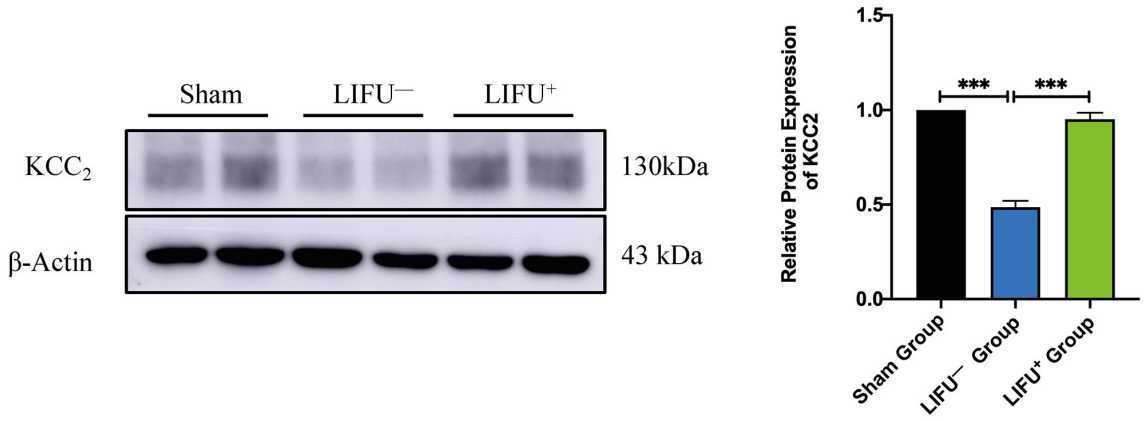

FIGURE 5 | Protein expression of KCC_2 in the sham group, $LIFU^-$ group, and $LIFU^+$ group after 4 weeks of LIFU treatment. Western blot (WB) showing the expression of KCC_2; histogram showing the intensity of protein expression for the different groups. These result show that the intensity of KCC_2 expression significantly decreased following SCI (***$P < 0.001$, compared with the sham group; one-way ANOVA with LSD test; $n = 5$, mean ± SEM); following LIFU treatment, the intensity of KCC_2 expression significantly increased (***$P < 0.001$, compared with the $LIFU^-$ group; one-way ANOVA with LSD test; $n = 5$, mean ± SEM).

mechanisms of limb spasm following SCI (Boulenguez et al., 2010). In this study, the expression levels of KCC_2 in the lumbar L4–L5 spinal cord of the $LIFU^-$ group were significantly downregulated compared with the sham group at 5 weeks following SCI. In the $LIFU^+$ group, the expression of KCC_2 was significantly upregulated ($P < 0.05$) compared with the $LIFU^-$ group after 4 weeks of LIFU treatment ($P < 0.05$), as shown in **Figure 5**.

Immunofluorescence

Immunofluorescence was used to observe the effect of LIFU on the changes in KCC expression in lumbar spinal cord. The results showed that KCC_2 had co-expression with the neurons, as shown in **Figure 6A**. The ImageJ software analysis showed that expression of KCC_2 was reduced in the $LIFU^-$ group compared with the sham group ($P < 0.05$), while expression of KCC_2 increased in the $LIFU^+$ group compared with those in the $LIFU^-$ group ($P < 0.05$), as shown in **Figure 6B**.

DISCUSSION

Most studies have reported that neuromodulation techniques have been extensively studied and proved to be effetely in many diseases' treatment (Pan et al., 2022; Wang, 2022), such as repetitive functional magnetic stimulation (rFMS) alleviated the urinary retention for the patients after spinal cord injury (Zhang et al., 2022), promote the rehabilitation after brain tumor surgery (Dadario et al., 2022); Electrical nerve stimulation, which has been used for treating neuropathic pain, has been shown to be an effective treatment for reducing spasticity (Fernández-Tenorio et al., 2019; Tapia Pérez, 2019). The reduction in spasticity by functional electrical stimulation (FES) has also been confirmed by clinical studies, including a significant reduction in quadriceps tone in incomplete spinal cord patients and an increase in voluntary muscle strength after receiving FES (Granat et al., 1993). A randomized trial of different modalities of electrical stimulation demonstrated that FES significantly improved spasticity following SCI (Sivaramakrishnan et al., 2018). Physical rehabilitation training has also been used for treating spasticity. After receiving bike training, the spasticity of SCI rats was significantly reduced (Beverungen et al., 2020). A prospective clinical trial showed that passive rhythmic leg exercise significantly reduced spasticity in SCI veterans (Rayegani et al., 2011). Another study also confirmed that combined FES and passive leg movements successfully reduced spastic muscle tone in SCI patients (Krause et al., 2008). In this study, we first used ultrasound to stimulate the spinal cord in order to treat spasticity and found that LIFU stimulation significantly reduced spasticity in SCI rats.

LIFU stimulation has been regarded as a potential neuromodulatory method for treating many neurological disorders, and studies of LIFU stimulation for neuromodulation have moved from rodents to non-human primates to humans (King et al., 2013; Ai et al., 2018). King et al. (2013) applied LIFU to stimulate the brain and successfully induced a motor response. A recent study has also confirmed that LIFU with a higher duty cycle (DC = 70%) produced excitatory neuromodulatory effects, while a lower duty cycle (DC = 5%) produced suppressive neuromodulatory effects (Lee et al., 2016; Yoon et al., 2019; Kim et al., 2021). In a clinical study, transcranial ultrasound stimulation significantly upregulated the memory network of Alzheimer's patients (Beisteiner et al., 2020). In the present study, spasticity in rats following SCI was evaluated using the methods reported in the literature (Plantier et al., 2019), and our results confirmed that spasticity of the hind limbs in rats with SCI was significantly alleviated (**Figure 3**) and motor function significantly improved (**Table 1**) following LIFU (DC = 50%) stimulation of the spinal cord. Electrophysiological tests (FDD and EMG) also confirmed that LIFU stimulation successfully alleviated spasticity (**Figure 4**). The results suggest that LIFU

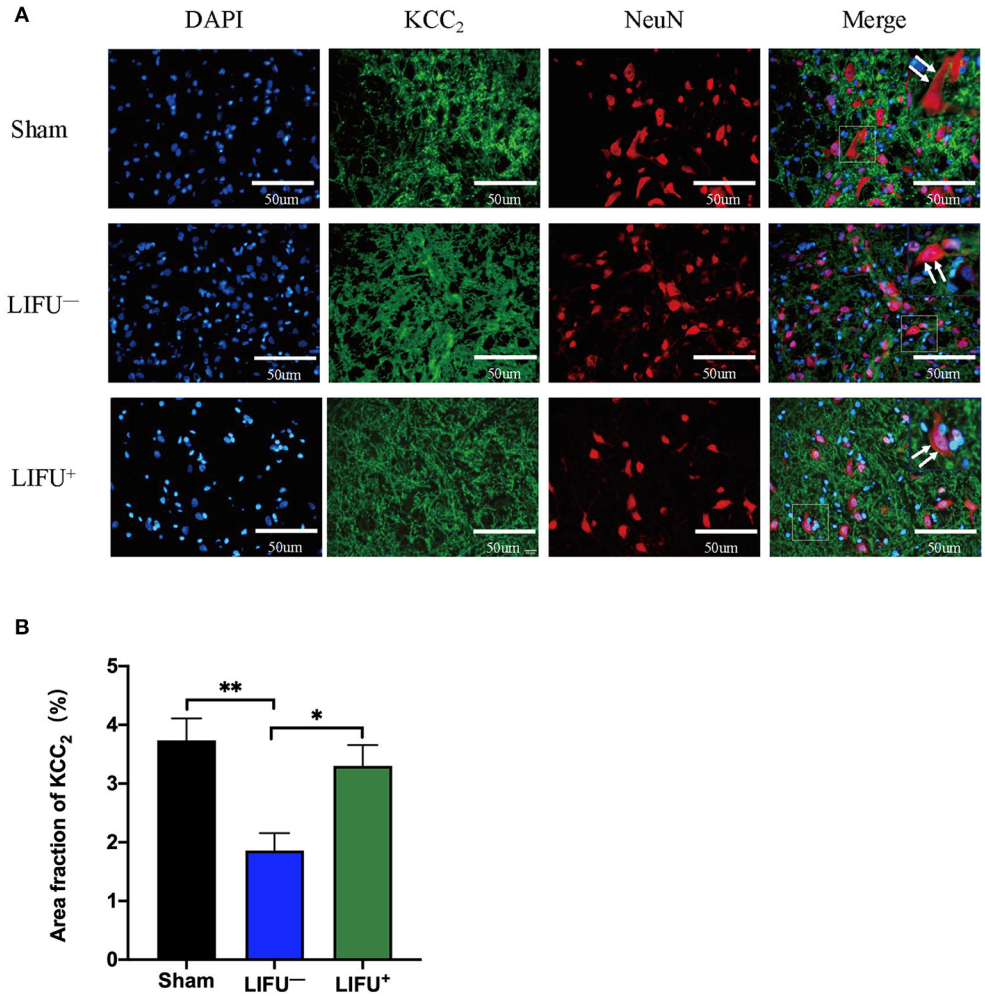

FIGURE 6 | Immunofluorescence (IF) staining showing the expression of KCC. **(A)** Positive expressions of KCC_2 are stained green and neurons are stained red; the expression of KCC_2 was merged on the membranes of neurons (white arrow). **(B)** Histogram showing expression of the KCC_2 protein for the different groups. The results show that the intensity of KCC_2 expression was significantly reduced (**$P < 0.01$, compared with the sham group; one-way ANOVA with LSD test; $n = 5$, mean ± SEM); following LIFU treatment, the intensity of KCC_2 expression significantly increased (*$P < 0.05$, compared with the LIFU$^-$ group; one-way ANOVA with LSD test; $n = 5$, mean ± SEM). Scale bar = 50 μm.

stimulation of the spinal cord has a potentially important value in the treatment of spasticity following SCI.

A previous study showed that SCI leads to damage of the reticulo-spinal pathways, which reduces activation of Renshaw cells (Mazzocchio and Rossi, 1989, 1997). From previous studies, FES and exercise training were found to activate mainly the Renshaw cells in the spinal cord by stimulating the peripheral nerves, thus increasing negative feedback by the Renshaw cells to the α motor neurons and reducing spasticity (Aydin et al., 2005; Sivaramakrishnan et al., 2018). A study by Ahmed and Wieraszko (2012) showed that activation of the sensorimotor cortex by weak electrical signals significantly increased the expression of GABAergic spinal interneurons and GABAergic terminals, and also showed that stimulation of the spinal cord by electrical currents also increased the release of D-2,3-^{3}H-aspartic acid, which restored motor control for SCI patients (Ahmed and Wieraszko, 2012). In animal experiments, it has been found that LIFU can cause behavioral and electrophysiological changes when the animals received central nervous system regulation (Tufail et al., 2010; Cheng et al., 2014). In previous studies, we confirmed that LIFU can activate the neurocircuits of the spinal cord effectively (Liao et al., 2021a). Li et al. (2020) applied ultrasound-driven piezoelectric current to successfully activate the spinal cord neurocircuits of SCI rats. A clinical study confirmed that epidural electrical stimulation can modulate the spinal network of complete SCI patients and help recovery of the motor function of paraplegic patients (Gill et al., 2018; Ridler, 2018). Thus, damaged spinal cords can also be activated and modulated. The present study also successfully activated the spinal cord neurocircuits with LIFU stimulation, recorded by EMG in the sham and SCI groups (**Figure 2**). Thus, we speculated that LIFU activation of spinal cord nerve

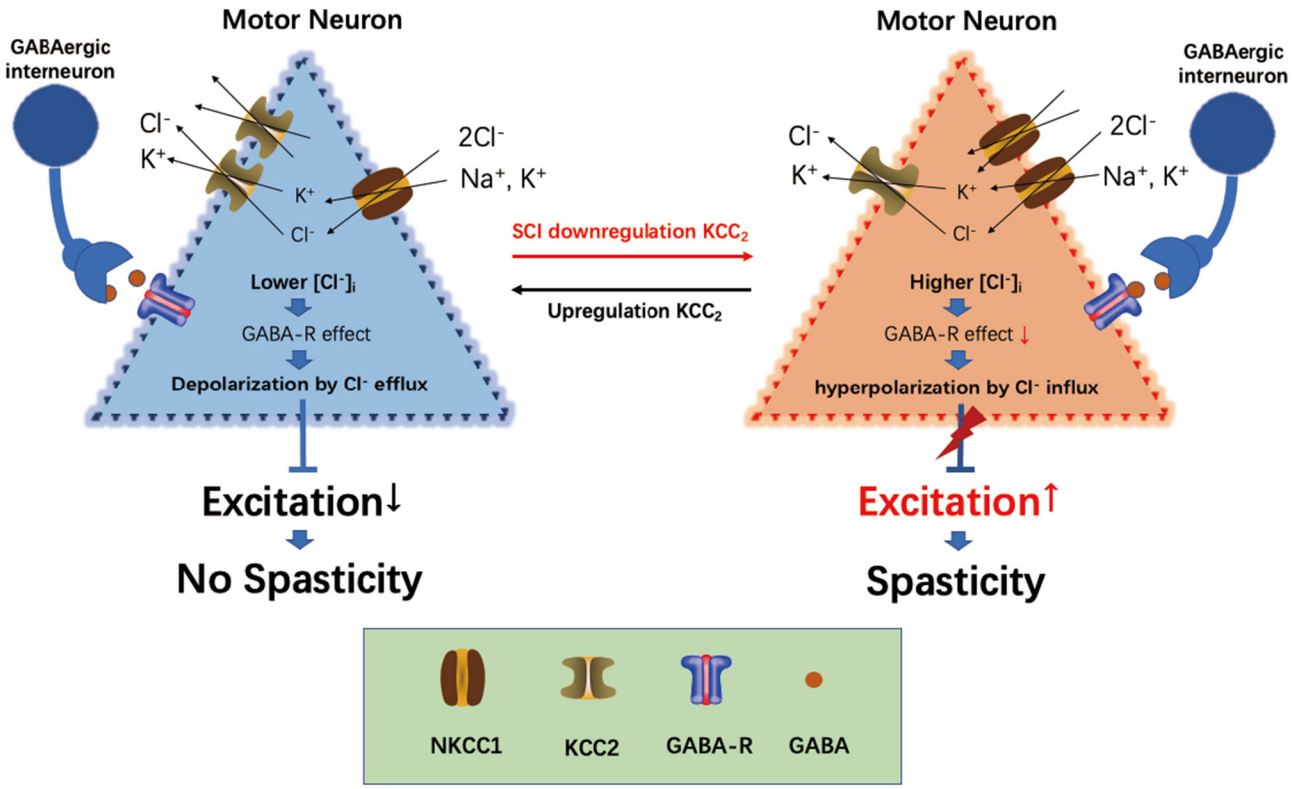

FIGURE 7 | Overview of current views on the role of KCC_2, NKCC1, and GABA in spasticity induction following spinal cord injury (SCI).

circulation may increase the inhibitory effect of spinal cord interneurons, and thus reduce spasticity following SCI.

GABA is the main inhibitory neurotransmitter present in the central nervous system, and its inhibitory effect depends on its achieving a lower gradient of $[Cl^-]_i$ in cells (Kahle et al., 2008; Ben-Ari et al., 2012). The intracellular $[Cl^-]_i$ concentration gradient in neurons is established and maintained by the cation-chloride cotransporter (Slc12a) family on the neural membrane (Delpire and Mount, 2002; Payne et al., 2003). KCC_2 (Slc12a5) is the only Cl^--extruding protein present in neuron cells, which extrude intracellular Cl^- to the extracellular environment to maintain a lower Cl^- concentration in neuron cells, thus maintaining the inhibitory effect of GABA (Boulenguez et al., 2010). The Na^+-K^+-$2Cl^-$ cotransporter NKCC1 (Slc12a2) is the Cl^--importing protein, which transports extracellular Cl^- into cells, thus maintaining a higher intracellular $[Cl^-]_i$ concentration in neurons and reducing the inhibitory effect of GABA on neurons. The interaction between KCC_2 and NKCC1 maintains Cl^- homeostasis in neurons and regulates the inhibitory effect of GABA (Plotkin et al., 1997; Delpire and Staley, 2014). Following SCI, the expressions of KCC_2 and NKCC1 were mutually regulated through the with-no-lysine [K] (WNK) kinase pathway, and the protein level between downregulation of KCC_2 and upregulation of NKCC1 showed a significant negative correlation (Côté et al., 2014; Kahle and Delpire, 2016). The downregulation of KCC_2 and upregulation of NKCC1 in the lumbar spinal cord led to an increased intracellular concentration of $[Cl^-]_i$ in the neurons and destroyed homeostasis (Côté et al., 2014). The breaking of $[Cl^-]_i$ homeostasis also reduced the inhibitory effect of GABA and increased the sensitivity of the motor neurons (Viemari et al., 2011), which resulted in spasticity (Kahle et al., 2008; Côté et al., 2014) (**Figure 7**).

Following upregulation of KCC_2 expression and downregulation of NKCC1 expression in the lumbar spinal cord by drugs or exercise treatment, hind limb spasticity was significantly reduced (Côté et al., 2014; Beverungen et al., 2020). In this study, we used IF staining to test the expression of KCC_2, and the results showed that KCC_2 was co-expressed on the neuron membrane and LIFU treatment significantly improved the expression of KCC_2 (**Figures 6A,B**). WB also showed that the expression of KCC_2 in the lumbar spinal cord of rats in the $LIFU^-$ group was significantly downregulated compared to that in the sham group. In the LIFU treatment group, the expression of KCC_2 in the lumbar spinal cord was upregulated (**Figure 5**), and hind limb spasticity was also reduced (**Figure 3C**). Based on these results, we speculated that LIFU stimulation also enhances the effectiveness of GABA by upregulating KCC_2 expression, which then reduces spasticity.

Spasticity is a common complication of SCI, which seriously reduces patients' quality of life (Maynard et al., 1990; Westgren and Levi, 1998; Holtz et al., 2017). Clinically, the treatment of spasticity following SCI includes the use of oral baclofen, baclofen pump (Dykstra et al., 2007; de Sousa et al., 2022), botulinum toxin injection (Picelli et al., 2019), and motor nerve blocking

(Demir et al., 2018; Zhang et al., 2021). These treatments have various side effects or require surgery. Therefore, it is important to find a specific physical rehabilitation method with limited side effects and overall positive outcomes. Previous studies have confirmed that LIFU can activate spinal cord neurocircuits effectively and not result in SCI. In this study, we also demonstrated that LIFU can activate spinal neurocircuits and decrease spasticity following SCI in rats. These results provide a theoretical basis for the clinical application of LIFU in the treatment of spasticity and a new and effective rehabilitation procedure for spasm patients following SCI.

CONCLUSION

The results of our study suggest that low-intensity focused ultrasound (LIFU) stimulation can activate the spinal cord neurocircuits successfully and alleviate spasticity in rats effectively following spinal cord injury (SCI). Effective treatment may be related to up-expression of KCC_2 in the cell membranes of neurons by LIFU stimulation.

DATA AVAILABILITY STATEMENT

The original contributions presented in the study are included in the article/**Supplementary Material**, further inquiries can be directed to the corresponding author/s.

ETHICS STATEMENT

The animal study was reviewed and approved by Animal Ethics Committee of Kunming Medical University.

AUTHOR CONTRIBUTIONS

YL and L-JA contributed to the design of the study. Y-HL, K-XL, M-XC, and BW contributed to the acquisition of data. Y-HL, YL, and S-CC contributed to the statistical analysis. Y-HL and YL drafted the manuscript. YL, S-CC, and L-JA revised the manuscript. All authors contributed to the article and approved the submitted version.

FUNDING

This work was supported by the National Natural Science Foundation of China (Grant Nos. 81960421 and 82060421), the Science and Technology Innovative Team Grant of Kunming Medical University (No. CXTD201905), and the Basic Research Program of Yunnan Science and Technology Department (No. 202101AT070255).

ACKNOWLEDGMENTS

We would like to thank Professor Eng-Ang of the National University of Singapore for his kind academic and linguistic assistance. We also thank Charlesworth Author Services (https://www.cwauthors.com.cn) for their language editing during the preparation of this manuscript.

SUPPLEMENTARY MATERIAL

The Supplementary Material for this article can be found online at: https://www.frontiersin.org/articles/10.3389/fncel.2022.882127/full#supplementary-material

Supplementary Video 1 | This shows a normal hind limb motor movement response to tail pinching in the sham operation rats (related to **Figure 3A**) and spinal cord injury (SCI) rats (related to **Figure 3B**).

Supplementary Video 2 | Electromyograph (EMG) showing a typical activation of the spinal cord neurocircuits by $LIFU^+$ stimulation for the sham operation rats (related to the **Figure 2** sham group), $LIFU^-$ stimulation for the sham operation rats (related to the **Figure 2** $LIFU^-$ group), and $LIFU^+$ stimulation in the spinal cord injury (SCI) rats (related to the **Figure 2** $LIFU^+$ group).

REFERENCES

Ahmed, Z., and Wieraszko, A. (2012). Trans-spinal direct current enhances corticospinal output and stimulation-evoked release of glutamate analog, D-2,3-^{3}H-aspartic acid. *J. Appl. Physiol. (1985)* 112, 1576–1592. doi: 10.1152/japplphysiol.00967.2011

Ai, L., Bansal, P., Mueller, J. K., and Legon, W. (2018). Effects of transcranial focused ultrasound on human primary motor cortex using 7T fMRI: a pilot study. *BMC Neurosci.* 19, 56. doi: 10.1186/s12868-018-0456-6

Aydin, G., Tomruk, S., Keleş, I., Demir, S. O., and Orkun, S. (2005). Transcutaneous electrical nerve stimulation versus baclofen in spasticity: clinical and electrophysiologic comparison. *Am. J. Phys. Med. Rehabil.* 84, 584–592. doi: 10.1097/01.phm.0000171173.86312.69

Basso, D. M., Beattie, M. S., and Bresnahan, J. C. (1995). A sensitive and reliable locomotor rating scale for open field testing in rats. *J. Neurotrauma* 12, 1–21. doi: 10.1089/neu.1995.12.1

Beisteiner, R., Matt, E., Fan, C., Baldysiak, H., Schönfeld, M., Philippi Novak, T., et al. (2020). Transcranial pulse stimulation with ultrasound in Alzheimer's disease-a new navigated focal brain therapy. *Adv. Sci.* 7, 1902583. doi: 10.1002/advs.201902583

Ben-Ari, Y., Khalilov, I., Kahle, K. T., and Cherubini, E. (2012). The GABA excitatory/inhibitory shift in brain maturation and neurological disorders. *Neuroscientist* 18, 467–486. doi: 10.1177/1073858412438697

Beverungen, H., Klaszky, S. C., Klaszky, M., and Cote, M. P. (2020). Rehabilitation decreases spasticity by restoring chloride homeostasis through the brain-derived neurotrophic factor-KCC2 pathway after spinal cord injury. *J. Neurotrauma* 37, 846–859. doi: 10.1089/neu.2019.6526

Blackmore, J., Shrivastava, S., Sallet, J., Butler, C. R., and Cleveland, R. O. (2019). Ultrasound neuromodulation: a review of results, mechanisms and safety. *Ultrasound Med. Biol.* 45, 1509–1536. doi: 10.1016/j.ultrasmedbio.2018.12.015

Boulenguez, P., Liabeuf, S., Bos, R., Bras, H., Jean-Xavier, C., Brocard, C., et al. (2010). Down-regulation of the potassium-chloride cotransporter KCC2 contributes to spasticity after spinal cord injury. *Nat. Med.* 16, 302–307. doi: 10.1038/nm.2107

Boulenguez, P., and Vinay, L. (2009). Strategies to restore motor functions after spinal cord injury. *Curr. Opin. Neurobiol.* 19, 587–600. doi: 10.1016/j.conb.2009.10.005

Brocard, C., Plantier, V., Boulenguez, P., Liabeuf, S., Bouhadfane, M., Viallat-Lieutaud, A., et al. (2016). Cleavage of Na(+) channels by calpain increases persistent Na(+) current and promotes spasticity after spinal cord injury. *Nat. Med.* 22, 404–411. doi: 10.1038/nm.4061

Carr, P. A., Pearson, J. C., and Fyffe, R. E. (1999). Distribution of 5-hydroxytryptamine-immunoreactive boutons on immunohistochemically-identified Renshaw cells in cat and rat lumbar spinal cord. *Brain Res.* 823, 198–201. doi: 10.1016/S0006-8993(98)01210-4

Cheng, K., Xia, P., Lin, Q., Shen, S., Gao, M., Ren, S., et al. (2014). Effects of low-intensity pulsed ultrasound on integrin-FAK-PI3K/Akt mechanochemical transduction in rabbit osteoarthritis chondrocytes. *Ultrasound Med. Biol.* 40, 1609–1618. doi: 10.1016/j.ultrasmedbio.2014.03.002

Corleto, J. A., Bravo-Hernandez, M., Kamizato, K., Kakinohana, O., Santucci, C., Navarro, M. R., et al. (2015). Thoracic 9 spinal transection-induced model of muscle spasticity in the rat: a systematic electrophysiological and histopathological characterization. *PLoS ONE* 10, e0144642. doi: 10.1371/journal.pone.0144642

Côté, M. P., Gandhi, S., Zambrotta, M., and Houlé, J. D. (2014). Exercise modulates chloride homeostasis after spinal cord injury. *J. Neurosci.* 34, 8976–8987. doi: 10.1523/JNEUROSCI.0678-14.2014

Dadario, N., Young, I., Zhang, X., Teo, C., Doyen, S., and Sughrue, M. (2022). Prehabilitation and rehabilitation using data-driven, parcel-guided transcranial magnetic stimulation treatment for brain tumor surgery: proof of concept case report. *Brain Netw. Modul.* 1, 48–56. doi: 10.4103/2773-2398.340144

Darrow, D. P. (2019). Focused ultrasound for neuromodulation. *Neurotherapeutics* 16, 88–99. doi: 10.1007/s13311-018-00691-3

de Sousa, N., Santos, D., Monteiro, S., Silva, N., Barreiro-Iglesias, A., and Salgado, A. J. (2022). Role of baclofen in modulating spasticity and neuroprotection in spinal cord injury. *J. Neurotrauma* 39, 249–258. doi: 10.1089/neu.2020.7591

Delpire, E., and Mount, D. B. (2002). Human and murine phenotypes associated with defects in cation-chloride cotransport. *Annu. Rev. Physiol.* 64, 803–843. doi: 10.1146/annurev.physiol.64.081501.155847

Delpire, E., and Staley, K. J. (2014). Novel determinants of the neuronal Cl(-) concentration. *J. Physiol.* 592, 4099–4114. doi: 10.1113/jphysiol.2014.275529

Demir, Y., San, A. U., Kesikburun, S., Yaşar, E., and Yilmaz, B. (2018). The short-term effect of ultrasound and peripheral nerve stimulator-guided femoral nerve block with phenol on the outcomes of patients with traumatic spinal cord injury. *Spinal Cord* 56, 907–912. doi: 10.1038/s41393-018-0142-7

Dykstra, D., Stuckey, M., DesLauriers, L., Chappuis, D., and Krach, L. (2007). Intrathecal baclofen in the treatment of spasticity. *Acta Neurochir. Suppl.* 97, 163–171. doi: 10.1007/978-3-211-33079-1_22

Elbasiouny, S. M., Moroz, D., Bakr, M. M., and Mushahwar, V. K. (2010). Management of spasticity after spinal cord injury: current techniques and future directions. *Neurorehabil. Neural Repair* 24, 23–33. doi: 10.1177/1545968309343213

Fernández-Tenorio, E., Serrano-Muñoz, D., Avendaño-Coy, J., and Gómez-Soriano, J. (2019). Transcutaneous electrical nerve stimulation for spasticity: a systematic review. *Neurologia* 34, 451–460. doi: 10.1016/j.nrl.2016.06.009

Gill, M. L., Grahn, P. J., Calvert, J. S., Linde, M. B., Lavrov, I. A., Strommen, J. A., et al. (2018). Neuromodulation of lumbosacral spinal networks enables independent stepping after complete paraplegia. *Nat. Med.* 24, 1677–1682. doi: 10.1038/s41591-018-0175-7

Granat, M. H., Ferguson, A. C., Andrews, B. J., and Delargy, M. (1993). The role of functional electrical stimulation in the rehabilitation of patients with incomplete spinal cord injury–observed benefits during gait studies. *Paraplegia* 31, 207–215. doi: 10.1038/sc.1993.39

Holtz, K. A., Lipson, R., Noonan, V. K., Kwon, B. K., and Mills, P. B. (2017). Prevalence and effect of problematic spasticity after traumatic spinal cord injury. *Arch. Phys. Med. Rehabil.* 98, 1132–1138. doi: 10.1016/j.apmr.2016.09.124

Hou, X., Qiu, Z., Xian, Q., Kala, S., Jing, J., Wong, K. F., et al. (2021). Precise ultrasound neuromodulation in a deep brain region using nano gas vesicles as actuators. *Adv. Sci.* 8, e2101934. doi: 10.1002/advs.202101934

Kahle, K. T., and Delpire, E. (2016). Kinase-KCC2 coupling: Cl- rheostasis, disease susceptibility, therapeutic target. *J. Neurophysiol.* 115, 8–18. doi: 10.1152/jn.00865.2015

Kahle, K. T., Staley, K. J., Nahed, B. V., Gamba, G., Hebert, S. C., Lifton, R. P., et al. (2008). Roles of the cation-chloride cotransporters in neurological disease. *Nat. Clin. Pract. Neurol.* 4, 490–503. doi: 10.1038/ncpneuro0883

Kim, H. C., Lee, W., Kunes, J., Yoon, K., Lee, J. E., Foley, L., et al. (2021). Transcranial focused ultrasound modulates cortical and thalamic motor activity in awake sheep. *Sci. Rep.* 11, 19274. doi: 10.1038/s41598-021-98920-x

King, R. L., Brown, J. R., Newsome, W. T., and Pauly, K. B. (2013). Effective parameters for ultrasound-induced in vivo neurostimulation. *Ultrasound Med. Biol.* 39, 312–331. doi: 10.1016/j.ultrasmedbio.2012.09.009

Kirshblum, S. (1999). Treatment alternatives for spinal cord injury related spasticity. *J. Spinal Cord Med.* 22, 199–217. doi: 10.1080/10790268.1999.11719570

Krause, P., Szecsi, J., and Straube, A. (2008). Changes in spastic muscle tone increase in patients with spinal cord injury using functional electrical stimulation and passive leg movements. *Clin. Rehabil.* 22, 627–634. doi: 10.1177/0269215507084648

Kubanek, J., Shi, J., Marsh, J., Chen, D., Deng, C., and Cui, J. (2016). Ultrasound modulates ion channel currents. *Sci. Rep.* 6, 24170. doi: 10.1038/srep24170

Kupcova Skalnikova, H., Navarro, R., Marsala, S., Hrabakova, R., Vodicka, P., Gadher, S. J., et al. (2013). Signaling proteins in spinal parenchyma and dorsal root ganglion in rat with spinal injury-induced spasticity. *J. Proteom.* 91, 41–57. doi: 10.1016/j.jprot.2013.06.028

Lannin, N. A., Novak, I., and Cusick, A. (2007). A systematic review of upper extremity casting for children and adults with central nervous system motor disorders. *Clin. Rehabil.* 21, 963–976. doi: 10.1177/0269215507079141

Lee, W., Lee, S. D., Park, M. Y., Foley, L., Purcell-Estabrook, E., Kim, H., et al. (2016). Image-guided focused ultrasound-mediated regional brain stimulation in sheep. *Ultrasound Med. Biol.* 42, 459–470. doi: 10.1016/j.ultrasmedbio.2015.10.001

Legon, W., Bansal, P., Tyshynsky, R., Ai, L., and Mueller, J. K. (2018). Transcranial focused ultrasound neuromodulation of the human primary motor cortex. *Sci. Rep.* 8, 10007. doi: 10.1038/s41598-018-28320-1

Li, S., Alam, M., Ahmed, R. U., Zhong, H., Wang, X. Y., Ng, S., et al. (2020). Ultrasound-driven piezoelectric current activates spinal cord neurocircuits and restores locomotion in rats with spinal cord injury. *Bioelectron. Med.* 6, 13. doi: 10.1186/s42234-020-00048-2

Liao, Y. H., Chen, M. X., Chen, S. C., Luo, K. X., Wang, B., Liu, Y., et al. (2021a). Effects of noninvasive low-intensity focus ultrasound neuromodulation on spinal cord neurocircuits *in vivo*. *Evid. Based Comp. Altern. Med.* 2021, 8534466. doi: 10.1155/2021/8534466

Liao, Y. H., Wang, B., Chen, M. X., Liu, Y., and Ao, L. J. (2021b). LIFU alleviates neuropathic pain by improving the KCC(2) expression and inhibiting the CaMKIV-KCC(2) pathway in the L4-L5 section of the spinal cord. *Neural Plast.* 2021, 6659668. doi: 10.1155/2021/6659668

Lin, C. S., Macefield, V. G., Elam, M., Wallin, B. G., Engel, S., and Kiernan, M. C. (2007). Axonal changes in spinal cord injured patients distal to the site of injury. *Brain* 130, 985–994. doi: 10.1093/brain/awl339

Lipsman, N., Meng, Y., Bethune, A. J., Huang, Y., Lam, B., Masellis, M., et al. (2018). Blood-brain barrier opening in Alzheimer's disease using MR-guided focused ultrasound. *Nat. Commun.* 9, 2336. doi: 10.1038/s41467-018-04529-6

Maynard, F. M., Karunas, R. S., and Waring, W. P. III. (1990). Epidemiology of spasticity following traumatic spinal cord injury. *Arch. Phys. Med. Rehabil.* 71, 566–569.

Mazzocchio, R., and Rossi, A. (1989). Recurrent inhibition in human spinal spasticity. *Ital. J. Neurol. Sci.* 10, 337–347. doi: 10.1007/BF02333781

Mazzocchio, R., and Rossi, A. (1997). Involvement of spinal recurrent inhibition in spasticity. further insight into the regulation of Renshaw cell activity. *Brain* 120 (Pt 6), 991–1003. doi: 10.1093/brain/120.6.991

Mazzone, G. L., Mohammadshirazi, A., Aquino, J. B., Nistri, A., and Taccola, G. (2021). GABAergic mechanisms can redress the tilted balance between excitation and inhibition in damaged spinal networks. *Mol. Neurobiol.* 58, 3769–3786. doi: 10.1007/s12035-021-02370-5

Ni, X. J., Wang, X. D., Zhao, Y. H., Sun, H. L., Hu, Y. M., Yao, J., et al. (2017). The effect of low-intensity ultrasound on brain-derived neurotropic factor expression in a rat sciatic nerve crushed injury model. *Ultrasound Med. Biol.* 43, 461–468. doi: 10.1016/j.ultrasmedbio.2016.09.017

Nilius, B., and Droogmans, G. (2003). Amazing chloride channels: an overview. *Acta Physiol. Scand.* 177, 119–147. doi: 10.1046/j.1365-201X.2003.01060.x

Pan, J.-X., Jia, Y.-B., and Liu, H. (2022). Application of repetitive peripheral magnetic stimulation for recovery of motor function after stroke based on neuromodulation: a narrative review. *Brain Netw. Modul.* 1, 13–19. doi: 10.4103/2773-2398.340140

Payne, J. A., Rivera, C., Voipio, J., and Kaila, K. (2003). Cation-chloride co-transporters in neuronal communication, development and trauma. *Trends Neurosci.* 26, 199–206. doi: 10.1016/S0166-2236(03)00068-7

Picelli, A., Santamato, A., Chemello, E., Cinone, N., Cisari, C., Gandolfi, M., et al. (2019). Adjuvant treatments associated with botulinum toxin injection for managing spasticity: an overview of the literature. *Ann. Phys. Rehabil. Med.* 62, 291–296. doi: 10.1016/j.rehab.2018.08.004

Plantier, V., Sanchez-Brualla, I., Dingu, N., Brocard, C., Liabeuf, S., Gackière, F., et al. (2019). Calpain fosters the hyperexcitability of motoneurons after spinal cord injury and leads to spasticity. *Elife* 8:e51404. doi: 10.7554/eLife.51404.sa2

Plotkin, M. D., Snyder, E. Y., Hebert, S. C., and Delpire, E. (1997). Expression of the Na-K-2Cl cotransporter is developmentally regulated in postnatal rat brains: a possible mechanism underlying GABA's excitatory role in immature brain. *J. Neurobiol.* 33, 781–795. doi: 10.1002/(SICI)1097-4695(19971120)33:6<781::AID-NEU6>3.0.CO;2-5

Rayegani, S. M., Shojaee, H., Sedighipour, L., Soroush, M. R., Baghbani, M., and Amirani, O. B. (2011). The effect of electrical passive cycling on spasticity in war veterans with spinal cord injury. *Front. Neurol.* 2, 39. doi: 10.3389/fneur.2011.00039

Ridler, C. (2018). Spinal stimulation and physical therapy helps paraplegic patients to walk again. *Nat. Rev. Neurol.* 14, 631. doi: 10.1038/s41582-018-0092-x

Sheean, G. (2002). The pathophysiology of spasticity. *Eur. J. Neurol.* 9(Suppl. 1), 3–9; dicussion 53–61. doi: 10.1046/j.1468-1331.2002.0090s1003.x

Sivaramakrishnan, A., Solomon, J. M., and Manikandan, N. (2018). Comparison of transcutaneous electrical nerve stimulation (TENS) and functional electrical stimulation (FES) for spasticity in spinal cord injury - A pilot randomized cross-over trial. *J. Spinal Cord Med.* 41, 397–406. doi: 10.1080/10790268.2017.1390930

Sköld, C., Levi, R., and Seiger, A. (1999). Spasticity after traumatic spinal cord injury: nature, severity, and location. *Arch. Phys. Med. Rehabil.* 80, 1548–1557. doi: 10.1016/S0003-9993(99)90329-5

Tapia Pérez, J. H. (2019). Spinal cord stimulation: beyond pain management. *Neurologia*. doi: 10.1016/j.nrl.2019.05.009. [Epub ahead of print].

Tufail, Y., Matyushov, A., Baldwin, N., Tauchmann, M. L., Georges, J., Yoshihiro, A., et al. (2010). Transcranial pulsed ultrasound stimulates intact brain circuits. *Neuron* 66, 681–694. doi: 10.1016/j.neuron.2010.05.008

Viemari, J. C., Bos, R., Boulenguez, P., Brocard, C., Brocard, F., Bras, H., et al. (2011). Chapter 1–importance of chloride homeostasis in the operation of rhythmic motor networks. *Prog. Brain Res.* 188, 3–14. doi: 10.1016/B978-0-444-53825-3.00006-1

Wang, C. (2022). The role of neuromodulation to drive neural plasticity in stroke recovery: a narrative review. *Brain Netw. Modul.* 1, 2–8. doi: 10.4103/2773-2398.339171

Westgren, N., and Levi, R. (1998). Quality of life and traumatic spinal cord injury. *Arch. Phys. Med. Rehabil.* 79, 1433–1439. doi: 10.1016/S0003-9993(98)90240-4

Wootz, H., Fitzsimons-Kantamneni, E., Larhammar, M., Rotterman, T. M., Enjin, A., Patra, K., et al. (2013). Alterations in the motor neuron-renshaw cell circuit in the Sod1(G93A) mouse model. *J. Comp. Neurol.* 521, 1449–1469. doi: 10.1002/cne.23266

Yang, F. Y., Lu, W. W., Lin, W. T., Chang, C. W., and Huang, S. L. (2015). Enhancement of neurotrophic factors in astrocyte for neuroprotective effects in brain disorders using low-intensity pulsed ultrasound stimulation. *Brain Stimul.* 8, 465–473. doi: 10.1016/j.brs.2014.11.017

Yoon, K., Lee, W., Lee, J. E., Xu, L., Croce, P., Foley, L., et al. (2019). Effects of sonication parameters on transcranial focused ultrasound brain stimulation in an ovine model. *PLoS ONE* 14, e0224311. doi: 10.1371/journal.pone.0224311

Yu, Z., Cheng, X., Chen, J., Huang, Z., He, S., Hu, H., et al. (2021). Spinal cord parenchyma vascular redistribution underlies hemodynamic and neurophysiological changes at dynamic neck positions in cervical spondylotic myelopathy. *Front. Neuroanat.* 15, 729482. doi: 10.3389/fnana.2021.729482

Zhang, J., Mao, G., Feng, Y., Zhang, B., Liu, B., Lu, X., et al. (2021). Inhibiting spasticity by blocking nerve signal conduction in rats with spinal cord transection. *IEEE Trans. Neural Syst. Rehabil. Eng.* 29, 2355–2364. doi: 10.1109/TNSRE.2021.3124530

Zhang, J.-J., Chen, Y., Wu, L.-L., Gao, F., Li, Y., and An, B.-C. (2022). Clinical effect of repetitive functional magnetic stimulation of sacral nerve roots on urinary retention after spinal cord injury: a case-control study. *Brain Netw. Modul.* 1, 31–38. doi: 10.4103/2773-2398.340142

Conflict of Interest: The authors declare that the research was conducted in the absence of any commercial or financial relationships that could be construed as a potential conflict of interest.

Publisher's Note: All claims expressed in this article are solely those of the authors and do not necessarily represent those of their affiliated organizations, or those of the publisher, the editors and the reviewers. Any product that may be evaluated in this article, or claim that may be made by its manufacturer, is not guaranteed or endorsed by the publisher.

frontiers | Frontiers in Cellular Neuroscience

ORIGINAL RESEARCH
published: 17 May 2022
doi: 10.3389/fncel.2022.884788

Focused Ultrasound Promotes the Delivery of Gastrodin and Enhances the Protective Effect on Dopaminergic Neurons in a Mouse Model of Parkinson's Disease

Yuhong Wang[1†], Kaixuan Luo[1†], Junrui Li[1], Yehui Liao[1], Chengde Liao[2], Wen-Shiang Chen[3], Moxian Chen[1] and Lijuan Ao[1*]*

[1] School of Rehabilitation, Kunming Medical University, Kunming, China, [2] Yunnan Cancer Center, Department of Radiology, Yunnan Cancer Hospital, The Third Affiliated Hospital of Kunming Medical University, Kunming, China, [3] Department of Physical Medicine and Rehabilitation, National Taiwan University Hospital, National Taiwan University College of Medicine, Taipei City, Taiwan

OPEN ACCESS

Edited by:
Feng Zhang,
Third Hospital of Hebei Medical University, China

Reviewed by:
Zengbing Lu,
The Chinese University of Hong Kong, Hong Kong SAR, China
Sheng Zhang,
Zhejiang Provincial People's Hospital, China

***Correspondence:**
Moxian Chen
chenmoxian@kmmu.edu.cn
Lijuan Ao
13508710081@qq.com

[†] These authors have contributed equally to this work

Specialty section:
This article was submitted to Cellular Neuropathology, a section of the journal Frontiers in Cellular Neuroscience

Received: 27 February 2022
Accepted: 19 April 2022
Published: 17 May 2022

Citation:
Wang Y, Luo K, Li J, Liao Y, Liao C, Chen W-S, Chen M and Ao L (2022) Focused Ultrasound Promotes the Delivery of Gastrodin and Enhances the Protective Effect on Dopaminergic Neurons in a Mouse Model of Parkinson's Disease. Front. Cell. Neurosci. 16:884788. doi: 10.3389/fncel.2022.884788

Parkinson's disease (PD) is the second most common chronic neurodegenerative disease globally; however, it lacks effective treatment at present. Focused ultrasound (FUS) combined with microbubbles could increase the efficacy of drug delivery to specific brain regions and is becoming a promising technology for the treatment of central nervous system diseases. In this study, we explored the therapeutic potential of FUS-mediated blood–brain barrier (BBB) opening of the left striatum to deliver gastrodin (GAS) in a subacute PD mouse model induced by 1-methyl-4-phenyl-1,2,3,6-tetrahydropyridine (MPTP). The concentration of GAS in the left hemisphere was detected by ultra-high performance liquid chromatography electrospray Q-Orbitrap mass spectrometry (UHPLC/ESI Q-Orbitrap) and the distribution of tyrosine hydroxylase (TH) neurons was detected by immunohistochemical staining. The expression of TH, Dopamine transporter (DAT), cleaved-caspase-3, B-cell lymphoma 2 (Bcl-2), brain-derived neurotrophic factor (BDNF), postsynaptic density protein 95 (PSD-95), and synaptophysin (SYN) protein were detected by western blotting. Analysis showed that the concentration of GAS in the left hemisphere of PD mice increased by approximately 1.8-fold after the BBB was opened. FUS-mediated GAS delivery provided optimal neuroprotective effects and was superior to the GAS or FUS control group. In addition, FUS enhanced GAS delivery significantly increased the expression of Bcl-2, BDNF, PSD-95, and SYN protein in the left striatum ($P < 0.05$) and reduced the levels of cleaved-caspase-3 remarkably ($P = 0.001$). In conclusion, the enhanced delivery by FUS effectively strengthened the protective effect of GAS on dopaminergic neurons which may be related to the reinforcement of the anti-apoptotic activity and the expression of synaptic-related proteins in the striatum. Data suggests that FUS-enhanced GAS delivery may represent a new strategy for PD treatment.

Keywords: focused ultrasound, blood–brain barrier, gastrodin, Parkinson's disease, drug delivery

INTRODUCTION

Parkinson's disease (PD) is characterized with resting tremor, bradykinesia, rigidity, and postural balance disorders, which is accompanied by non-motor symptoms such as anxiety and depression, and seriously damages patients' quality of life (Armstrong and Okun, 2020). In 2016, approximately 6.1 million people were diagnosed with PD worldwide, which was about 2.4-fold higher than the number in 1990 (GBD, 2018). Drugs such as carbidopa-levodopa and dopamine agonists can alleviate the dyskinesia caused by early PD; however, their efficacy fluctuates with long-term use, leading to adverse reactions such as dyskinesia and on-off phenomena, thus making it difficult to control the patient's condition (Armstrong and Okun, 2020).

The blood–brain barrier (BBB) blocks the entry of certain therapeutic drugs into the brain and represents a key obstacle in terms of treating PD. Under physiological conditions, 98% of drugs with a molecular weight of fewer than 400 Daltons and almost 100% of drugs with a molecular weight of more than 500 Daltons cannot pass through the tight junctions of BBB (Pardridge, 2005). Focused ultrasound (FUS) is a new method that could open the BBB and is highly penetrative, non-invasive with good localization and reversibility. In animal and clinical trials, researchers have demonstrated that the combination of FUS and microbubbles can safely as well as reversibly induce the opening of the BBB under specific parameters (Rezai et al., 2020; Wu et al., 2020; Pouliopoulos et al., 2021; Yang et al., 2021). Recently, our team found that the delivery of gastrodin (GAS) *via* FUS-induced BBB opening could improve memory impairment and neuropathology in a mouse model of Alzheimer's disease (Luo et al., 2022). Moreover, studies have shown that the FUS-mediated delivery of neurotrophic factors and genes can effectively inhibit the rapid progression of neurodegeneration in a mouse model of PD and improve neurological function (Mead et al., 2017; Ji et al., 2019).

Gastrodin, the main active component of *Gastrodia elata,* exerts neuroprotective effects in various neurological diseases. Many studies have confirmed the efficacy of GAS in treating PD (Yan et al., 2019; He et al., 2021). The mechanism of action may involve the anti-oxidation effect (Wang et al., 2014), anti-inflammation effect (Li et al., 2012) and the inhibition of apoptosis (Chen et al., 2017) by GAS. However, only a tiny amount of GAS can enter and disperse throughout the brain in terms of intravenous or oral administration (Lin et al., 2008). Kumar et al. (2013) found that increasing the dose of orally administered GAS could enhance the therapeutic effect of GAS in PD. In another study, Haddadi et al. (2018) attempted to inject GAS into the substantia nigra of rats directly by microinjection; although the concentration of drug increased in specific brain region, the invasive nature of the method was challenging from a clinical point of view. Therefore, it is necessary to identify a non-invasive method to increase the concentration of GAS in specific brain regions without increasing the drug dose as this may represent an effective method to improve the treatment efficiency of PD.

We hypothesize that FUS mediated BBB opening can safely and effectively increase the concentration of GAS in the brain (including the striatum), thus enhancing the protective effect of GAS on dopaminergic neurons (**Figure 1A**). After confirming that FUS can safely and effectively open the BBB of the left striatum, we established a subacute PD mouse model by injecting 1-methyl-4-phenyl-1,2,3,6-tetrahydropyridine (MPTP). ultra-high performance liquid chromatography electrospray Q-Orbitrap mass spectrometry (UHPLC/ESI Q-Orbitrap) was then used to detect the concentration of GAS in the left hemisphere of the PD mice. Finally, the therapeutic effect of GAS delivered by FUS on PD mice was evaluated by immunohistochemical staining and western blotting.

MATERIALS AND METHODS

Animals

The protocol of this experiment was approved by the Animal Ethics Committee of Kunming Medical University (KMMU2019076). All the experimental procedures followed the guidelines for the care of laboratory animals. All male C57BL/6J mice (8 weeks old, 20–22 g) were purchased from the Experimental Animal Center of Kunming Medical University and housed at 25°C ± 2°C with a fixed 12 h light/dark cycle. All mice had free access to food and water.

Study Design

In order to test the safety of the BBB opening induced by FUS, healthy C57BL/6J mice were randomly divided into Sham group and FUS output voltage groups of 100, 150, and 200 mV. The opening of the BBB was visualized by Evans blue (EB, Millipore Sigma, Burlington, MA, United States) that exudated from the blood stream, and the safety was verified by hematoxylin-eosin (H&E) as well as Nissl staining. By considering the EB-stained area of the brain section and the results of pathological staining, the optimal FUS parameters to open the BBB were determined. Next, we investigated the efficacy of FUS-induced BBB opening to delivery GAS in PD mice. After adaptation for 2 weeks, 48 male C57BL/6J mice were randomly divided into five subgroups: a Sham group (n = 8), an MPTP group (n = 8), an MPTP + GAS group (n = 12), an MPTP + FUS group (n = 8) and an MPTP + FUS + GAS group (n = 12). To establish a subacute model of PD on C57BL/6J mice, MPTP (Sigma-Aldrich, St. Louis, MO, United States) was dissolved in saline and subcutaneously injected 30 mg/kg for 5 consecutive days. The Sham group was injected with an equal volume of saline instead. Next, the MPTP + GAS group and the MPTP + FUS + GAS group were intraperitoneally injected with GAS (100 mg/kg/d) for 19 consecutive days; the other groups were injected with saline. FUS sonication was carried out once every 3 days with a total of 6 times. The Sham group, the MPTP group, and the MPTP + GAS group received placebo FUS sonications. Mice in the MPTP + FUS + GAS group were intraperitoneally injected with GAS immediately after the opening of the BBB to facilitate its delivery into the brain. We employed UHPLC/ESI Q-Orbitrap to assess the concentration of GAS in the left hemisphere. Behavioral tests were performed on the 1st, 7th, 13th, and 19th days after MPTP injection to evaluate the motor function of mice.

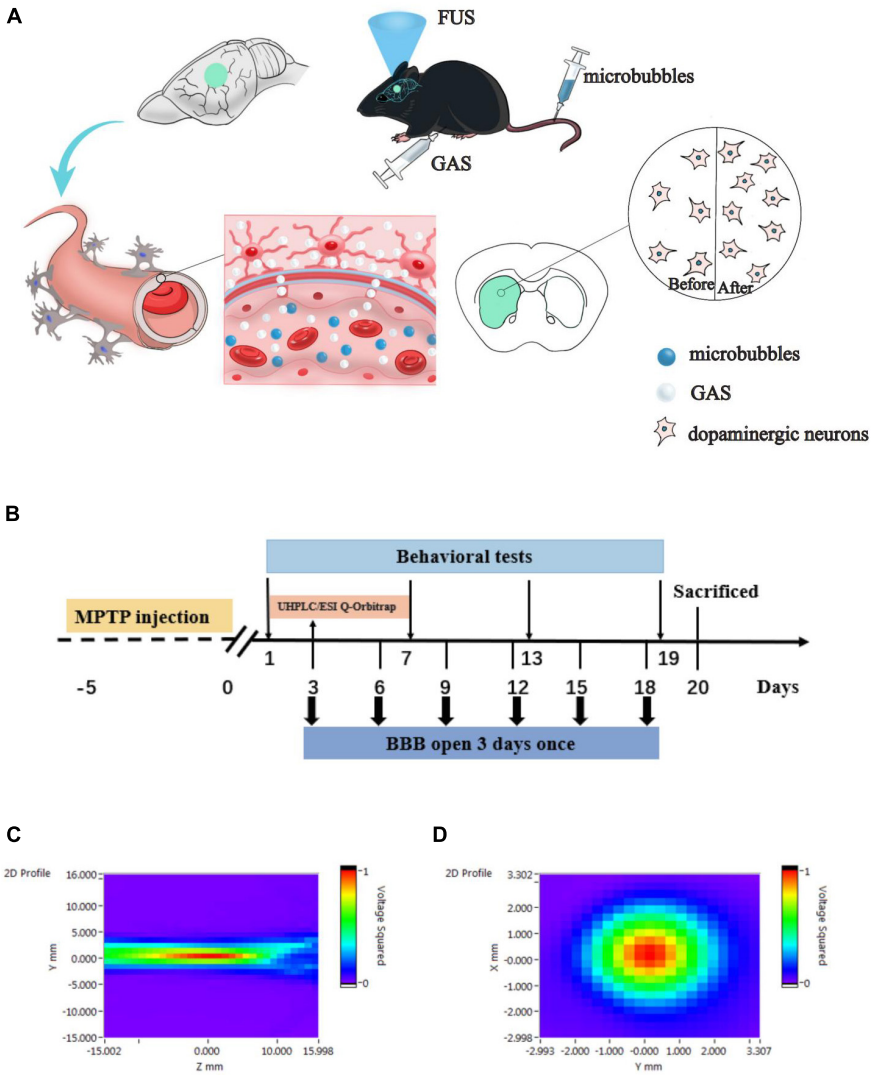

FIGURE 1 | (A) Hypothesis of the delivery of gastrodin (GAS) by focused ultrasound (FUS)-induced blood–brain barrier (BBB) opening. FUS induced BBB opening increased the delivery of GAS to specific brain regions in Parkinson's disease (PD) mice, thereby enhanced neuroprotective effect on dopaminergic neurons. **(B)** Details relating to experimental timing including behavioral testing and FUS operation. MPTP, 1-methyl-4-phenyl-1,2,3,6-tetrahydropyridine; UHPLC/ESI Q-Orbitrap, ultra-high performance liquid chromatography electrospray Q-Orbitrap mass spectrometry. **(C,D)** Acoustic pressure distribution of the lateral and axial direction.

The body weight of the mice was monitored every 3 days once. The mice were sacrificed on the 20th day for relevant biochemical tests (**Figure 1B**).

Blood–Brain Barrier Opening Induced by Focused Ultrasound

The FUS sonication system consisted of a waveform generator (RIGOL DG4202, Suzhou, China), a power amplifier (Mini-circuits LZY-22+, New York, United States), and a focused ultrasonic transducer (fundamental frequency: 1 MHz, focal length: 4 cm, diameter: 15 mm). Two-dimensional sound field distributions were measured using a calibrated needle hydrophone (2010, Precision Acoustics, Dorchester, United Kingdom). The lateral and axial sound pressure distributions are shown in **Figures 1C,D**, which indicates that the ultrasound transducer was well focused. The mice were anesthetized with isoflurane in the animal chamber and then the heads were fixed with prone position. The anesthesia was maintained continuously by inhaled isoflurane with a concentration of 1% through an anesthesia machine (RWD R500, Shenzhen, Guangdong, China). Next, we shaved the fur on the top of the mouse's head off and removed any remaining fur with hair removal cream. The ultrasonic transducer was placed in an adapter designed for directional FUS delivery and fixed to the left striatum region (0.5 mm front Bregma, 2 mm left). Then, we filled the gap between the mouse scalp and the ultrasound adapter with ultrasound couplant. SonoVue (Bracco Imaging BV,

Milan, Italy) microbubbles (1.25 μl/g) were injected into the tail vein. Ten seconds later, the mice were sonicated with FUS. The pulse repetition frequency of FUS was 1 Hz, with a pulse width of 10 ms, and an exposure time of 60 s, output voltage of 100, 150, and 200 mV were used.

Assessment of Blood–Brain Barrier Disruption and Safety

Twenty-four male C57BL/6J mice were randomly divided into a Sham group (n = 6) and the FUS group. The FUS group was further divided into 100, 150, and 200 mV groups (n = 6 for each group) to determine the optimal output voltage for FUS-induced BBB opening when other parameters were fixed. Immediately after FUS sonication, 2% of EB dye (6.25 μl/g) was injected through the tail vein. We injected microbubbles and EB dye in the Sham group with placebo FUS sonication. The mice were euthanized after 4 h of EB circulation and then the brain was fixed in paraformaldehyde solution for 24 h (n = 3 for each group). Next, we prepared coronal brain slices which covered the center of the ultrasound-sonicated region. The BBB opened area was visualized by EB penetration.

Brain tissues from mice in the Sham and FUS group were collected at 4 h after FUS sonication (n = 3 for each group) to test the safety of FUS-induced BBB opening. After dehydration and fixation, tissues were embedded in paraffin and then cut into coronal sections with the thickness of 4 μm. Paraffin sections of the center of sonicated brain region were dewaxed in xylene and anhydrous ethanol and then stained with H&E (Service G1003, Wuhan, Hubei, China). For Nissl staining, the paraffin sections were dewaxed and stained with toluidine blue, differentiated with glacial acetic acid, cleared with xylene, and then sealed with neutral gum. After the optical parameters were determined on normal C57BL/6J mice, we carried out BBB opening of left striatum by FUS for six times with the optimal parameters on PD mice and reassessed the safety by H&E and Nissl staining. Images of the left cortex and striatum in the brain sections were acquired using a dissecting microscope (Olympus, Japan).

Assessment of Motor Function

Pole Test

As previously described, we performed the pole test to assess motor function of mice. A 50-cm–long pole was wrapped with gauze to prevent mice from slipping and a wooden ball was placed on the top (Zhang et al., 2017). The bottom was covered with bedding to protect the mice from fall injury. Mice were trained three times in advance to ensure that all mice could bow their heads down when placed on the ball. Each mouse was placed on the wooden ball and the total time that mouse taken to climb from the top of the pole to the bottom was recorded.

Paw Grip Endurance Test

The Paw grip endurance test can evaluate comprehensive motor function, such as muscle strength, muscle tone, and ataxia (Hutter-Saunders et al., 2012). We chose a 45 cm × 30 cm rectangular stainless steel screen, the built-in mesh is 1 cm^2, and the screen is 25 cm high from the pad. During the test, we placed the mice horizontally on the grid and then quickly flipped the grid 180°, and recorded the time that mice fell off the grid. The upper limit was up to 90 s.

Detection of Gastrodin Concentration by UHPLC/ESI Q-Orbitrap

We examined GAS concentration in the left hemisphere of mouse after the first time of BBB opening by FUS. Mice in the MPTP + GAS and MPTP + FUS + GAS groups (n = 4 for each group) were randomly selected and sacrificed 30 min after the injection of GAS. The tissue of the left hemisphere was separated and placed in a cryotube at −80°C. A standard sample of GAS (G299059-5 g, 62499-27-8, ≥98%, Aladdin, Shanghai, China) was weighed and mixed with pure methanol to prepare a 5.0 mg/ml reserve solution which was then diluted into 1000, 500, 200, 100, and 50 ng/mL standard solutions for analysis and to create a GAS standard curve. The tissue samples were weighed, mixed with methanol, grinded and then centrifuged; the supernatant was taken for testing subsequently. Levels of GAS in the left hemisphere were then quantified with a UltiMate 3000 RS chromatograph (Thermo Fisher Scientific, Waltham, MA, United States) and Q-Exactive high-resolution mass spectrometer (Thermo Fisher Scientific, Waltham, MA, United States). We used a positive electrospray ionization source (ESI); the electrospray voltage was 3.2 kV, the capillary temperature was 300°C, high purity argon was used as the impact gas, the sheath gas was 40 Arb, and the auxiliary gas was 15 Arb. The system was equipped with a Waters T3 150 × 2.1 mm, 3-μm column with an automatic injection volume of 5 μl and a flow rate of 0.30 ml/min. Chromatogram acquisition and the integration of analytes were processed by Xcalibur 4.1 software (Thermo Fisher Scientific, Waltham, MA, United States). Linear regression was performed with a weighting factor of 1/X.

Immunohistochemistry Staining

In order to evaluate the effects of MPTP administration and different treatments on dopaminergic neurons in the nigrostriatal pathway, we performed tyrosine hydroxylase (TH) immunohistochemical staining to the striatum and substantia nigra brain tissue of each group. Paraffin sections of brain tissue (4-μm-thick) were prepared from each mouse. Following antigen repair and sealing, the sections were incubated with TH antibody (Cat. No. ab137869, dilution 1:500, Abcam, Cambridge, United Kingdom) at 4°C. A biotinylated goat anti-rabbit secondary antibody (Service GB23303, dilution 1:200, Wuhan, China) was added the next day and TH staining was observed under a microscope after 50 min incubation at room temperature.

Western Blotting

Fresh left striatum and substantia nigra were collected and stored at −80°C for use. The total proteins were extracted by adding radioimmunoprecipitation assay (RIPA) buffer and phenylmethanesulfonyl fluoride (PMSF) protease inhibitor. A bicinchoninic acid (BCA) protein concentration determination kit (Beyotime, China) was used to measure the protein concentration of each sample. Supernatants were dissolved in sample buffer at a protein concentration of 20 μg and

separated by 10% sodium dodecyl sulfate-polyacrylamide gel electrophoresis (SDS-PAGE). Separated proteins were then transferred to a polyvinylidene fluoride (PVDF) membrane (Millipore Sigma, Burlington, MA, United States). After blocking with 5% skimmed milk for 2 h, the PVDF membrane was incubated with primary antibodies and placed overnight in a refrigerator at 4°C. The primary antibodies included TH (Cat. No. ab137869, dilution 1:5000, Abcam, Cambridge, United Kingdom), Dopamine transporter (DAT, Cat. No. 22524-1-AP, dilution 1:2000, Proteintech, Rosemont, IL, United States), B-cell lymphoma 2 (Bcl-2, Cat. No. 26593-1-AP, dilution 1:2000, Proteintech, Rosemont, IL, United States), caspase-3 (Cat. No. 19677-1-AP, dilution 1:2000, Proteintech, Rosemont, IL, United States), postsynaptic density protein 95 (PSD-95, Cat. No. 20665-1-Ig, dilution 1:2000, Proteintech, Rosemont, IL, United States), synaptophysin (SYN, Cat. No. 60191-1-Ig, dilution 1:2000, Proteintech, Rosemont, IL, United States), brain-derived neurotrophic factor (BDNF, Cat. No. 66292-1-Ig, dilution 1:2000, Proteintech, Rosemont, IL, United States), GAPDH (Cat. No. 60004-1-Ig, dilution 1:2000, Proteintech, Rosemont, IL, United States), β-Actin (Cat. No. sc-47778, dilution 1:2000, Santa Cruz Biotechnology, Dallas, TX, United States), and α-Tubulin (cat. No. 66031-1-Ig, dilution 1:2000, Proteintech, Rosemont, IL, United States). Following incubation with primary antibodies, the membranes were incubated with anti-rabbit/anti-mouse immunoglobulin G (IgG) enzyme-linked antibody labeled with secondary anti-horseradish peroxidase (HRR-) for 90 min at room temperature. Finally, after washing with TBST, the membranes were developed on a gel developer and the gray values of different protein bands were quantified.

Statistical Analysis

All data are expressed as mean ± standard error of the mean (SEM). We used SPSS version 25.0 (IBM, Armonk, NY, United States) for statistical analysis. The independent sample *t*-test was used to compare the mean difference between the two groups. One-way ANOVA was used to compare differences in means among the five subgroups. When analysis of variance showed significant differences, pairwise comparisons between means were performed with the least significant difference (LSD) test for *post hoc* analysis. Statistical graphs were generated using GraphPad Prism software version 8.0 (GraphPad Software, Inc., San Diego, CA, United States). Differences were considered to be significant when $P < 0.05$ (bilateral).

RESULTS

Efficacy and Safety of Focused Ultrasound-Induced Blood–Brain Barrier Opening

First, we investigated the efficacy of FUS-induced BBB opening by evaluating the EB penetration. As shown in **Figure 2A**, all FUS groups were stained by EB, indicating that FUS increased the permeability of the BBB and facilitated EB entry into the brain. However, in the 100 mV group, the penetration depth was shallow and limited to the cortex. There was prominent EB infiltration in the left striatum of the 150 and 200 mV groups, and the EB infiltration area was larger in the 200 mV group. However, H&E staining showed that the sonicated cortex and striatum in the 200 mV group had obvious erythrocyte exudation. In contrast, there was no bleeding in other groups, the cells were evenly arranged, and the nucleoli were normal (**Figure 2B**). For Nissl staining, the neurons of mice in 100 mV, 150 mV, and Sham group were in good shape and obvious abnormality was absent (**Figure 2C**). Therefore, 150 mV was selected as the optimal output voltage. After six times' opening of BBB in PD mice, we again performed histological analysis. Likewise, H&E staining showed no hemorrhage in the ultrasound-sonicated brain area (**Figure 2D**). The distribution and size of Nissl bodies in the MPTP group and MPTP + FUS group were homogeneous (**Figure 2E**). The body weight changes of the mice during the experiment are shown in **Figure 2F**. During the treatment period, there was no statistical difference of body weight between the MPTP + FUS, MPTP + FUS + GAS and the MPTP groups ($P > 0.05$). These data show that it is safe and feasible to use FUS to repeatedly induce the opening of the BBB.

Focused Ultrasound-Induced Blood–Brain Barrier Opening Increased the Uptake of Gastrodin in the Left Hemisphere of Parkinson's Disease Mice

The concentration of GAS in the left hemisphere was 0.3679 ng/mg in the MPTP + GAS group, After FUS-induced BBB opening, the concentration of GAS increased significantly ($P = 0.03$), reaching to 0.6619 ng/mg, approximately 1.8-fold higher than the MPTP + GAS group (**Figure 3**).

Movement Defect Were Induced by 1-Methyl-4-Phenyl-1,2,3,6-Tetrahydropyridine but Recovered 7 Days Later

The climbing time of the pole test in each group was statistically longer than that of the Sham group ($P < 0.05$), while the grid grasping time in the paw grip endurance test was significantly shorter when compared to the Sham group on day 1 ($P < 0.05$). These data suggest that MPTP induced dyskinesia and the PD model was established successfully. The climbing time of the pole test as well as the grid grasping time in the paw grip endurance test between all groups at day 7, 13, and 19 lacked statistical significance ($P > 0.05$), indicating an auto recovery of movement defect (**Supplementary Figures 1A,B**).

FUS + GAS Increased the Expression of Tyrosine Hydroxylase and Dopamine Transporter in the Left Nigrostriatal Pathway

To investigate the effect of FUS + GAS treatment on dopaminergic neurons in the nigrostriatal pathway of PD mice, we used immunohistochemistry assay to stain TH, and the results are shown in **Figures 4A–C**. Compared with the MPTP group,

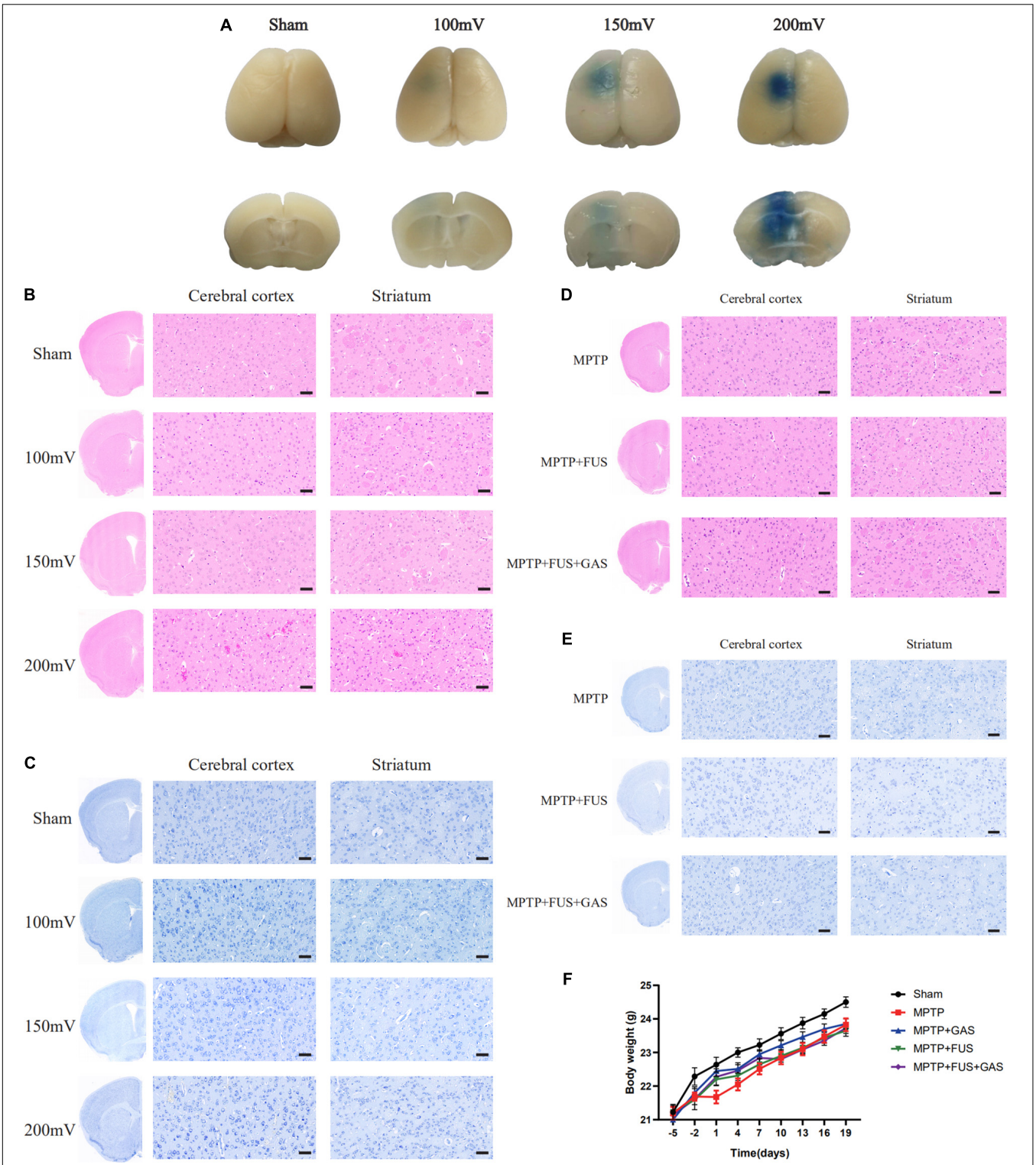

FIGURE 2 | Efficacy and safety of focused ultrasound (FUS)-induced blood–brain barrier (BBB) opening. **(A)** Penetration of Evans blue in the brains of mice in different groups 4 h after FUS-induced BBB opening, $n = 3$. **(B)** H&E staining results of sonicated cerebral cortex and striatum in different groups 4 h after FUS-induced BBB opening, $n = 3$, scale bar = 50 μm. **(C)** Nissl staining results of sonicated cerebral cortex and striatum in different groups 4 h after FUS-induced BBB opening, $n = 3$, scale bar = 50 μm. **(D)** H&E staining results of sonicated cerebral cortex and striatum in Parkinson's disease (PD) mice after a total of six times' BBB opening induced by FUS, $n = 3$. Scale bar = 50 μm. **(E)** Nissl staining results of sonicated cerebral cortex and striatum in PD mice after a total of six times' BBB opening induced by FUS, $n = 3$. Scale bar = 50 μm. **(F)** The body weight change curve of mice in each group.

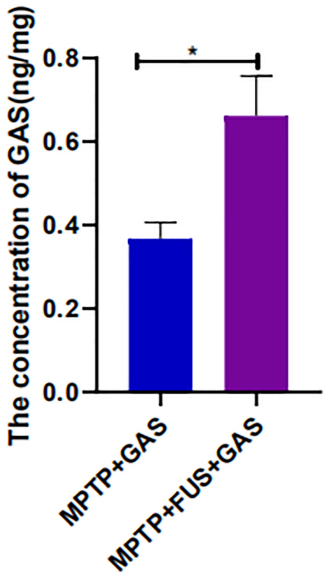

FIGURE 3 | Changes of GAS concentration in the mice's left hemisphere of the MPTP + GAS group and the MPTP + FUS + GAS group. Compared to the MPTP + GAS group, $^{*}P < 0.05$; *T*-test, $n = 4$, mean ± SEM.

the density of TH- positive fibers and the number of TH-positive cells in the nigrostriatal pathway of the MPTP + FUS + GAS group recovered significantly ($P = 0.016$). Further qualitative analysis of the protein expression levels of TH and DAT in the left striatum and substantia nigra showed that the protein expression levels of TH and DAT in the MPTP group were lower than the levels of the Sham group ($P < 0.05$). When dealt with FUS + GAS treatment, the protein levels of TH as well as DAT in the left striatum and substantia nigra increased and were significantly higher than those of the MPTP group ($P < 0.05$), while there was no significance ($P > 0.05$) between the Sham group and the FUS + GAS group (**Figures 4D–I**). Compared with the MPTP group, the number of TH neurons in the left nigrostriatal pathway and the protein expression levels of TH and DAT were increased with varying degrees after FUS or GAS treatment, although there was no statistical significance ($P > 0.05$). Collectively, these results suggest that FUS-induced BBB opening allows the entry of GAS, thus promoting dopamine synthesis and effectively ameliorated MPTP-induced dopaminergic neuron death.

The Focused Ultrasound Mediated Gastrodin Delivery Enhanced Anti-apoptotic Effects

We found that the level of cleaved-caspase-3 protein in the left striatum after MPTP injection was significantly higher than that of the Sham group ($P = 0.014$) and the level of Bcl-2 significantly decreased ($P < 0.001$), suggesting that the administration of MPTP led to remarkable apoptosis. When dealt with FUS + GAS treatment, the expression level of cleaved-caspase-3 in the left striatum were significantly lower than that of the MPTP group

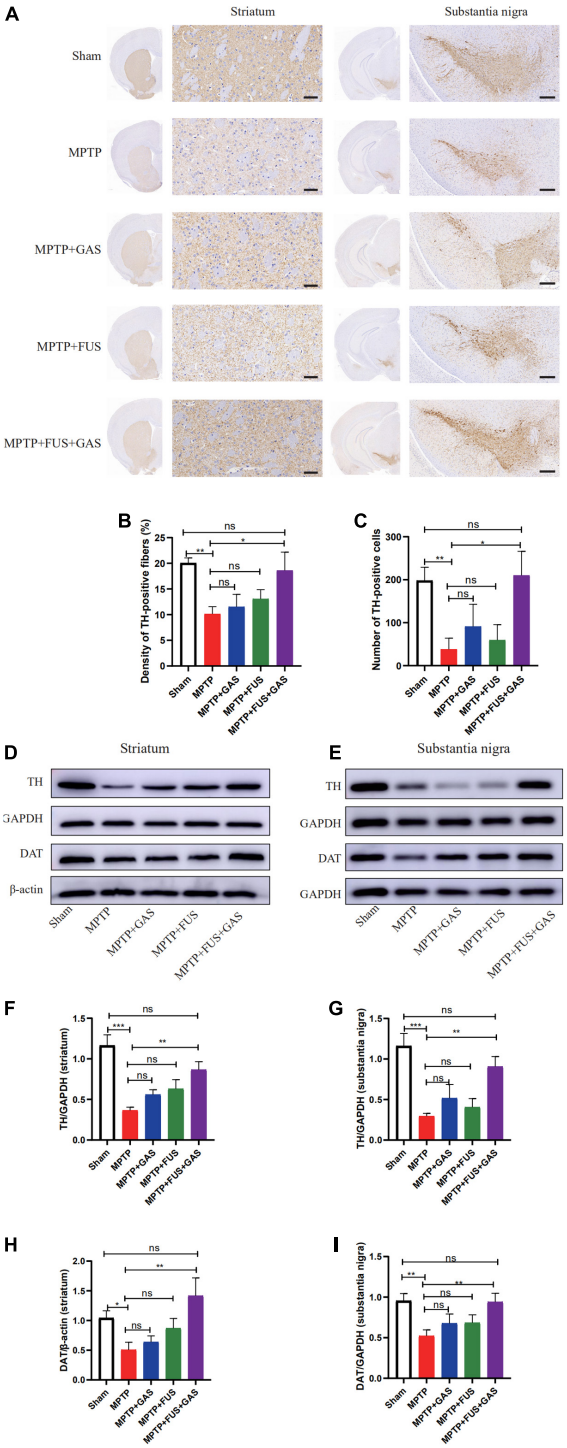

FIGURE 4 | (A) Comparison of the immunohistochemical staining of tyrosine hydroxylase (TH)-positive nerve fibers in the left striatum and substantia nigra of mice in each group, $n = 3$. Scale bars = 50 μm for images in stratum; 200 μm for images in substantia nigra. **(B)** Changes of TH-positive nerve fibers in the left striatum of mice in each group. **(C)** Number changes of TH-positive cells in the left substantia nigra of mice in each group. **(D,E)** Representative images of the protein levels of TH and Dopamine transporter (DAT) in the left striatum and substantia nigra of mice in each group.

(Continued)

FIGURE 4 | (F–I) The left striatum and substantia nigra of mice in each group and changes in the protein expression of TH and DAT. Compared to MPTP group, *$P < 0.05$; **$P < 0.01$; ***$P < 0.001$, no significance (ns), $P > 0.05$. One-way ANOVA with LSD test; $n = 5$, mean ± SEM.

($P = 0.001$). Furthermore, the expression levels of Bcl-2 were significantly up-regulated by FUS + GAS treatment compared with the MPTP group ($P = 0.001$); the anti-apoptotic effect of FUS + GAS was stronger than GAS treatment alone ($P < 0.05$) (**Figures 5A,B**).

Focused Ultrasound Mediated Gastrodin Delivery Upregulated the Expressions of Brain-Derived Neurotrophic Factor, Synaptophysin, and Postsynaptic Density Protein 95

Next, we performed western blotting to investigate the effect of FUS + GAS treatment on the expressions of BDNF, SYN, and PSD-95 in the left striatum of PD mice (**Figure 6**). We found that the protein expression levels of BDNF, SYN, and PSD-95 decreased after the injection of MPTP ($P < 0.05$) while increased after FUS or GAS treatment. The protein levels of BDNF ($P < 0.001$), SYN ($P < 0.001$) and PSD-95 ($P = 0.003$) in the FUS + GAS group were also significantly higher than those of the MPTP group (**Figures 6A–C**). The BDNF level was higher in FUS + GAS group in comparison of FUS and GAS group ($P < 0.01$). For the expression levels of SYN and PSD-95, the mean values of the FUS + GAS group were higher than that of FUS as well as GAS group, but there was no statistical difference ($P > 0.05$). These results suggest that the delivery of GAS by FUS increased the expression of BDNF, SYN, and PSD-95 in the left striatum of MPTP mice.

DISCUSSION

In this study, we demonstrated that (1) FUS combined with microbubbles can repeatedly, effectively and non-invasively open the BBB in the striatum of rodents without causing tissue damage. This method also increased the concentration of GAS in the left hemisphere by approximately 1.8-fold; (2) When delivered by FUS, GAS effectively increased the number of dopaminergic neurons in the nigrostriatal pathway; (3) When delivered by FUS, GAS effectively enhanced the anti-apoptotic ability in the striatum and promoted the expression of BDNF and synaptic-related proteins. This study innovatively identified that FUS-induced BBB opening can promote the intraperitoneally injected GAS into the brain and significantly enhances the neuroprotective effect of GAS on dopaminergic neurons in the nigrostriatal pathway.

There are several methods facilitating the delivery of drugs into the brain including intra-arterial infusion of hypertonic solution (Kiviniemi et al., 2017), electroacupuncture stimulation (Zhang et al., 2020), electroporation (Lorenzo et al., 2019), intracranial injection (Liu Y. X. et al., 2018), and intranasal administration (Su et al., 2020), but these methods have obvious limitations. Hypertonic solution and electroacupuncture stimulation open the BBB extensively rather than locally, resulting in the high risk of pathogens and toxic substances to enter the brain. Electroporation and intracranial injection are invasive treatments and face big challenge to repeated operations. Enzymes quickly degrade drugs administered intranasally, and the clearing function of nasal cilia reduces the time that drug get contact with the nasal epithelial cells, which decreases drug absorption. Under appropriate parameters, FUS combined with microbubbles can open the BBB non-invasively, locally, and reversibly thus enhances the delivery of antibodies (Jordão et al., 2010), neurotrophic factors (Lin et al., 2016; Karakatsani et al., 2019), nanoparticles (Ohta et al., 2020) and macromolecular drugs (Park et al., 2017; Wei et al., 2021) to specific brain regions. Due to the drug's short half-life, it is necessary to open the BBB to deliver the drug repeatedly. Several previous studies reported that when the BBB was continuously opened 8 times in non-human primates at a frequency of every 15 days once, there were no pathological changes in the EEG and somatosensory evoked potentials (Horodyckid et al., 2017). Another research group opened the BBB every 2 days once in rodents and found that repeated BBB opening by FUS at low sound pressure with appropriate microbubbles dose did not cause tissue damage or behavior change. Nevertheless, there were slight and transient behavioral changes when the pressure was significantly higher than required or with excessive microbubbles dose (Tsai et al., 2018). We opened the BBB every 3 days once for a total of 6 times in this experiment. During the experiment, there was no significant difference in mice's body weight between the FUS group and the MPTP group. At the same time, the pathological sections of the striatum and cortex in the sonicated site showed no abnormality, indicating that the ultrasonic parameters used in this experiment are safe and feasible, exerting great potential to repeated delivery of drugs by FUS.

It was hypothesized that the degeneration of substantia nigra neurons in PD originate from the distal axon (Cheng et al., 2010). It is reported that approximately 30% of the dopamine neurons in the substantia nigra can be damaged while in the striatum it can be as severe as 50–70% in PD (Ma et al., 1997; Cheng et al., 2010). On this basis, the striatum may be an ideal target for PD treatment. MPTP induces PD-related symptoms by damaging dopaminergic neurons and decreasing the density of axons as well as dendrites in the nigrostriatal pathway. Therefore, we selected the MPTP-induced subacute PD model to simulate the symptoms of PD and took striatum as the treatment target. We found that FUS-induced opening of the BBB followed by intraperitoneal injection of GAS significantly increased the number of TH-positive nerve fibers and the expression of TH as well as DAT in the left striatum of PD mice. The concentration of GAS in the left hemisphere increased after FUS-induced BBB opening; the increased concentration enables more GAS to act directly on the damaged dopaminergic neurons. In the study of Ji et al. (2019) FUS was used to open the BBB of the striatum and substantia nigra. The curative effect of the FUS + BDNF group was stronger than that of the FUS group and the BDNF intranasal

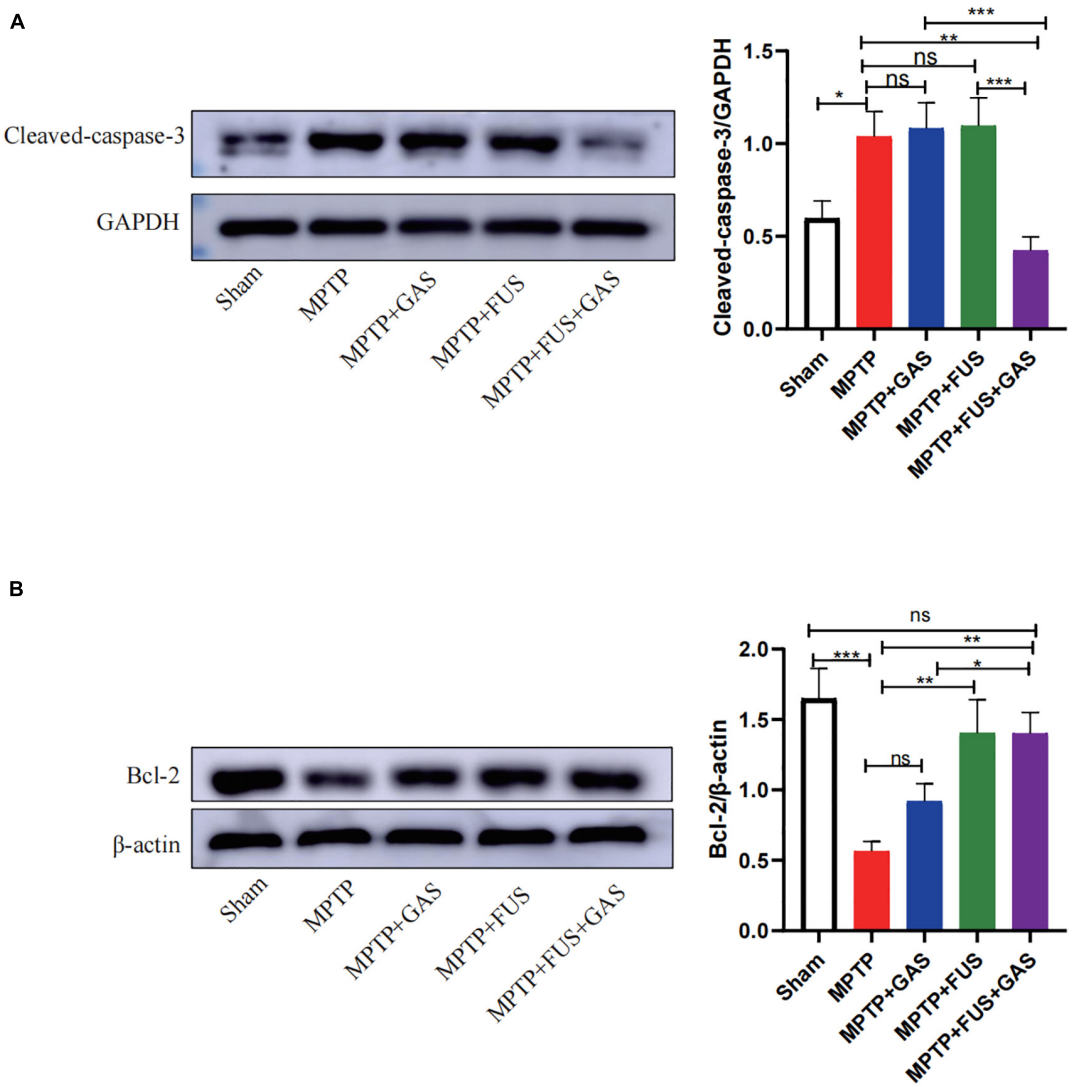

FIGURE 5 | (A) Changes in the expression of cleaved-caspase-3 in the left striatum of mice in each group. **(B)** Changes in the expression of B-cell lymphoma 2 (Bcl-2) protein in the left striatum of mice in each group. Compared to MPTP group, $^{*}P < 0.05$; $^{**}P < 0.01$; $^{***}P < 0.001$, no significance (ns), $P > 0.05$. One-way ANOVA with LSD test; $n = 5$; mean ± SEM.

administration group. Therefore, increasing the release of drugs in the nigrostriatal pathway may be an effective way to improve drug efficacy for the treatment of PD.

Many studies have found that the therapeutic efficacy of GAS is closely related to the therapeutic dose. In terms of AD treatment, 200 mg/kg of GAS was shown to restore the learning and memory ability of AD mice and reduced the deposition of Aβ plaques in the brain; the efficacy of this dose was much higher than that of 100 and 50 mg/kg (Zhou et al., 2016). In another study, Doo et al. (2014) compared the therapeutic effects of GAS at doses of 200, 400, and 800 mg/kg in rats with PD. The improvement of motor function of the 800 mg/kg group was greater than other groups; furthermore, the 800 mg/kg group showed a therapeutic effect earlier than the low-dose group. Although increasing the dose can improve the drug's efficacy, GAS has a short half-life and is poorly permeable to BBB, which limits its therapeutic effect (Liu Y. et al., 2018). Opening the BBB is a good way to increase the GAS concentration in the brain and to prolong the half-life. It was shown that during the 24 h of BBB opening, GAS in CSF maintained at a high concentration (Kung et al., 2021). In this study, we used FUS to non-invasively as well as effectively enhance the transport of GAS into the left hemisphere, which increased the concentration of GAS in the hemisphere of mice by approximately 1.8 times, effectively improved the therapeutic efficacy of GAS. Compared with the single intraperitoneal injection therapy, FUS induced BBB opening and transferred greater amount of GAS into the brain parenchyma and should reduce the drug consumption by plasma proteins and enzymes. Wang et al. (2009) found that GAS was concentrated in the cortex and cerebellum when

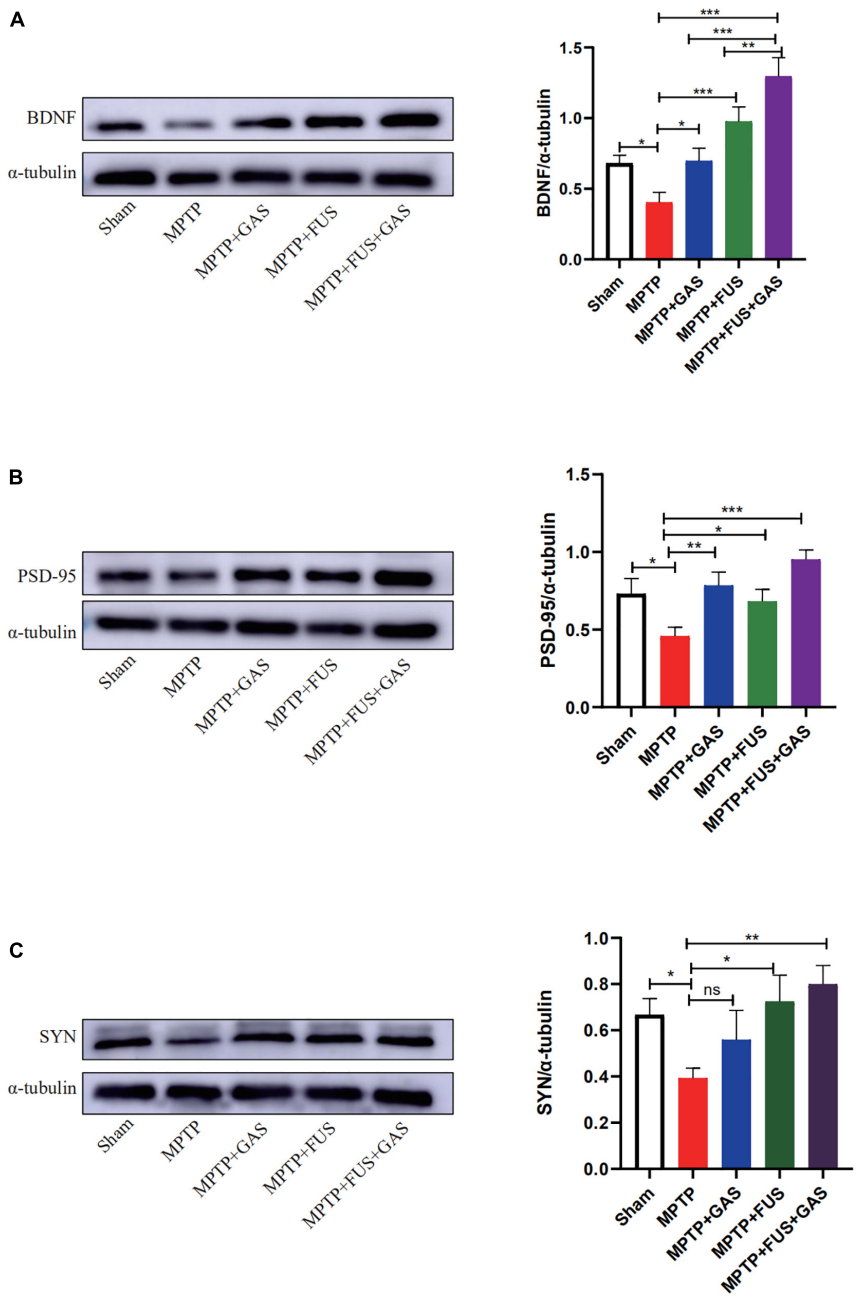

FIGURE 6 | (A–C) Changes in the protein expression of brain-derived neurotrophic factor (BDNF), postsynaptic density protein 95 (PSD-95), and synaptophysin (SYN) in the left striatum of mice in each group. Compared to MPTP group, $^{*}P < 0.05$ compared to MPTP group; $^{**}P < 0.01$; $^{***}P < 0.001$, no significance (ns), $P > 0.05$. One-way ANOVA with LSD test; $n = 5$, mean ± SEM.

entered the brain, and only 4.2% of the drugs could enter the striatum. We used FUS to open the BBB in the striatal region so that the drug can be concentrated in a specific brain region to give play to its effect. Therefore, non-invasive and local BBB opening by FUS may be an effective way to enhance GAS delivery and to reduce the injection dose or frequency of administration to a certain extent and exerts broad prospects for clinical application.

Apoptosis is one of the main causes of dopaminergic neuron death in PD mice. The inhibition of apoptosis has been considered as a potential therapeutic strategy for PD. In the present study, we found that MPTP increased the expression of cleaved-caspase-3 protein in the striatum and decreased the expression of Bcl-2 protein, that is MPTP promoted apoptosis. However, the apoptosis was reversed by FUS + GAS treatment. Therefore, we speculate that the protective effect of FUS + GAS

on dopaminergic neurons is partly due to the enhanced anti-apoptotic effect in the striatum. A previous study also found that GAS increased the expression of Bcl-2 and inhibited MPTP-induced caspase-3 activation and protected dopaminergic neurons, in which the anti-apoptotic effect increased as the dosage of GAS increased (Kumar et al., 2013). In the present study, the anti-apoptotic effect of the FUS + GAS group was significantly higher than the GAS group; this may also be related to the increase of GAS concentration after the opening of the BBB.

The reduction of dopamine in the striatum of PD may be related to fiber degeneration or loss and the synaptic reduction in the nigrostriatal pathway, while the effective transport of dopamine is closely related to the integrity of the nigrostriatal pathway (Villalba and Smith, 2018). After injury to the nervous system, the levels of SYN reflect the degree of synaptic remodeling; furthermore, the accumulation of PSD-95 in synapses can promote synaptic maturation as well as excitatory synapse enhancement (Kim et al., 2007). It has been found that MPTP reduces the density of dendritic spines in the striatum of mice and increases the expression of SYN while PSD-95 can restore the density of dendritic spines and relieve the symptoms of PD, at least to some extent (Toy et al., 2014). In addition, the increased expression of SYN and GAP43 can promote axonal regeneration and synaptic remodeling, thereby repairs the damaged dopamine transport pathway and increases dopamine release (Wang et al., 2008). BDNF can promote the maturation and genesis of synapses, and the increased expression of BDNF is essential to the increase of synaptic activity (Lipsky and Marini, 2007; Sen et al., 2016). In the present study, we found that FUS + GAS treatment could increase the expression of BDNF significantly and improve the reduced PSD-95 and SYN level in the PD model induced by MPTP. That is, FUS + GAS may increase the number of terminal synaptic vesicles and the striatal synaptic density of dopaminergic neurons by increasing the expression of BDNF, which favors the enhancement of synaptic transmission, and promotes the release of dopamine. In addition, BDNF is also closely related to the growth and development of dopaminergic neurons (Palasz et al., 2020); therefore, an increase of BDNF may also improve the neuroprotective effect of FUS + GAS.

The pole and paw grip endurance tests are the most used behavioral methods to test MPTP-induced dopamine damage in the substantia nigra and striatum. Previous studies described dyskinesia of subacute PD mice induced by the injection of MPTP (Koppula et al., 2021; Qi et al., 2021). However, some studies have found that dyskinesia is not always apparent in this model, it may even present hyperactivity (Rousselet et al., 2003; Zhang et al., 2017). In the present study, the immunohistochemical staining of mice at the 20 days showed the dopaminergic neurons in the nigrostriatal pathway were severely damaged; however, the impairment of motor function in the experimental mice was not consistent with the pathological manifestations. This may be related to the compensatory ability of the dopaminergic system. It has been found that when the dopamine neurons in the nigra striatum were damaged, the striatum itself has a special compensatory mechanism, that is, the remaining dopaminergic neurons may release more dopamine and result in a significant increase in the proportion of dopamine metabolites in the striatum (Luchtman et al., 2009; Zhang et al., 2017), thus improve the dyskinesia. What's more, Rousselet et al. (2003) suggested that dopamine in the prefrontal cortex may be transferred to the nigrostriatal system to play a compensatory role. The recovery of activity in MPTP mice may also be related to the increase of norepinephrine content. One study found a significant norepinephrine increase in the striatum of MPTP-induced subacute PD mice, which may lead to overactivity (Rousselet et al., 2003).

There are some limitations in the present study. First of all, the GAS concentration in the hemisphere was detected quantitatively by UHPLC/ESI Q-Orbitrap. However, the distribution and metabolism of GAS in the brain are not clear, which demands further research. Secondly, the dose of GAS (100 mg/kg) that was intraperitoneal injected in this study originates from the past experimental reports in rodents (60–800 mg/kg) (Doo et al., 2014; Wang et al., 2014; Liu Y. et al., 2018). In the view that opening of BBB will increase GAS concentration in the hemisphere of mice, it is necessary to explore the optimal dose of GAS under the appearance of FUS-induced BBB opening in terms of treating PD. Furthermore, the effective maintaining time of GAS in the brain which is delivered by FUS-induced BBB opening need to be further clarified to determine the best frequency of BBB opening induced by FUS.

CONCLUSION

In this study, FUS was employed to induce the BBB opening of striatal repetitively and safely in a mouse model of PD, which significantly increased the concentration of GAS in the sonicated hemisphere and effectively promoted the protective effect of GAS on dopaminergic neurons, representing an exciting option for the treatment of PD. The enhanced delivery of GAS by FUS induced BBB opening may provide a promising alternative for the treatment of chronic neurodegenerative diseases.

DATA AVAILABILITY STATEMENT

The raw data supporting the conclusions of this article will be made available by the authors, without undue reservation.

ETHICS STATEMENT

The animal study was reviewed and approved by the Animal Ethics Committee of Kunming Medical University.

AUTHOR CONTRIBUTIONS

LA and MC contributed to the design of the study. YW, KL, and JL carried out the experiment. YW, CL, and W-SC analyzed

the data. YW and KL composed the manuscript. All authors contributed to the article and approved the submitted version.

FUNDING

This work was supported by the National Natural Science Foundation of China (Grant No. 81960421) and National Key R&D Program of China (Grant No. 2018YFC2001600).

ACKNOWLEDGMENTS

We wish to acknowledge the illustration support of Qi Sun and Prof. Hailong Yang, who has supported in the study design. We owe our thanks to LetPub (https://www.letpub.com) for its linguistic assistance in preparing this manuscript.

SUPPLEMENTARY MATERIAL

The Supplementary Material for this article can be found online at: https://www.frontiersin.org/articles/10.3389/fncel.2022.884788/full#supplementary-material

Supplementary Figure 1 | Behavioral changes of mice in each group at different time points. **(A,B)** The pole climbing time and grip time of mice in each group were compared at different time points after injection of 1-methyl-4-phenyl-1,2,3,6-tetrahydropyridine (MPTP). Compared to the Sham group. $^{*}P < 0.05$; $^{**}P < 0.01$; $^{***}P < 0.001$. One-way ANOVA with LSD test; $n = 8$, mean ± SEM.

REFERENCES

Armstrong, M. J., and Okun, M. S. (2020). Diagnosis and Treatment of Parkinson Disease: A Review. *JAMA* 323, 548–560. doi: 10.1001/jama.2019.22360

Chen, L., Liu, X., Wang, H., and Qu, M. (2017). Gastrodin Attenuates Pentylenetetrazole-Induced Seizures by Modulating the Mitogen-Activated Protein Kinase-Associated Inflammatory Responses in Mice. *Neurosci. Bull.* 33, 264–272. doi: 10.1007/s12264-016-0084-z

Cheng, H. C., Ulane, C. M., and Burke, R. E. (2010). Clinical progression in Parkinson disease and the neurobiology of axons. *Ann. Neurol.* 67, 715–725. doi: 10.1002/ana.21995

Doo, A. R., Kim, S. N., Hahm, D. H., Yoo, H. H., Park, J. Y., Lee, H., et al. (2014). Gastrodia elata Blume alleviates L-DOPA-induced dyskinesia by normalizing FosB and ERK activation in a 6-OHDA-lesioned Parkinson's disease mouse model. *BMC Complement. Altern. Med.* 14:107. doi: 10.1186/1472-6882-14-107

GBD (2018). Global, regional, and national burden of Parkinson's disease, 1990-2016: a systematic analysis for the Global Burden of Disease Study 2016. *Lancet Neurol.* 17, 939–953. doi: 10.1016/S1474-4422(18)30295-3

Haddadi, R., Poursina, M., Zeraati, F., and Nadi, F. (2018). Gastrodin microinjection suppresses 6-OHDA-induced motor impairments in parkinsonian rats: insights into oxidative balance and microglial activation in SNc. *Inflammopharmacology* 26, 1305–1316. doi: 10.1007/s10787-018-0470-4

He, J., Li, X., Yang, S., Li, Y., Lin, X., Xiu, M., et al. (2021). Gastrodin extends the lifespan and protects against neurodegeneration in the Drosophila PINK1 model of Parkinson's disease. *Food Funct.* 12, 7816–7824. doi: 10.1039/d1fo00847a

Horodyckid, C., Canney, M., Vignot, A., Boisgard, R., Drier, A., Huberfeld, G., et al. (2017). Safe long-term repeated disruption of the blood-brain barrier using an implantable ultrasound device: a multiparametric study in a primate model. *J. Neurosurg.* 126, 1351–1361. doi: 10.3171/2016.3.JNS151635

Hutter-Saunders, J. A., Gendelman, H. E., and Mosley, R. L. (2012). Murine motor and behavior functional evaluations for acute 1-methyl-4-phenyl-1,2,3,6-tetrahydropyridine (MPTP) intoxication. *J. Neuroimmune Pharmacol.* 7, 279–288. doi: 10.1007/s11481-011-9269-4

Ji, R., Smith, M., Niimi, Y., Karakatsani, M. E., Murillo, M. F., Jackson-Lewis, V., et al. (2019). Focused ultrasound enhanced intranasal delivery of brain derived neurotrophic factor produces neurorestorative effects in a Parkinson's disease mouse model. *Sci. Rep.* 9:19402. doi: 10.1038/s41598-019-55294-5

Jordão, J. F., Ayala-Grosso, C. A., Markham, K., Huang, Y., Chopra, R., Mclaurin, J., et al. (2010). Antibodies targeted to the brain with image-guided focused ultrasound reduces amyloid-beta plaque load in the TgCRND8 mouse model of Alzheimer's disease. *PLoS One* 5:e10549. doi: 10.1371/journal.pone.0010549

Karakatsani, M. E., Wang, S., Samiotaki, G., Kugelman, T., Olumolade, O. O., Acosta, C., et al. (2019). Amelioration of the nigrostriatal pathway facilitated by ultrasound-mediated neurotrophic delivery in early Parkinson's disease. *J. Control. Release* 303, 289–301. doi: 10.1016/j.jconrel.2019.03.030

Kim, M. J., Futai, K., Jo, J., Hayashi, Y., Cho, K., and Sheng, M. (2007). Synaptic accumulation of PSD-95 and synaptic function regulated by phosphorylation of serine-295 of PSD-95. *Neuron* 56, 488–502. doi: 10.1016/j.neuron.2007.09.007

Kiviniemi, V., Korhonen, V., Kortelainen, J., Rytky, S., Keinänen, T., and Tuovinen, T. (2017). Real-time monitoring of human blood-brain barrier disruption. *PLoS One* 12:e0174072. eCollection 2017 doi: 10.1371/journal.pone.0174072

Koppula, S., Alluri, R., and Kopalli, S. R. (2021). Coriandrum sativum attenuates microglia mediated neuroinflammation and MPTP-induced behavioral and oxidative changes in Parkinson's disease mouse model. *Excli. J.* 20, 835–850. doi: 10.17179/excli2021-3668

Kumar, H., Kim, I. S., More, S. V., Kim, B. W., Bahk, Y. Y., and Choi, D. K. (2013). Gastrodin protects apoptotic dopaminergic neurons in a toxin-induced Parkinson's disease model. *Evid. Based Complement Altern. Med.* 2013:514095. doi: 10.1155/2013/514095

Kung, Y., Hsiao, M. Y., Yang, S. M., Wen, T. Y., Chen, M., Liao, W. H., et al. (2021). A single low-energy shockwave pulse opens blood-cerebrospinal fluid barriers and facilitates gastrodin delivery to alleviate epilepsy. *Ultrason. Sonochem.* 78:105730. doi: 10.1016/j.ultsonch.2021.105730

Li, C., Chen, X., Zhang, N., Song, Y., and Mu, Y. (2012). Gastrodin inhibits neuroinflammation in rotenone-induced Parkinson's disease model rats. *Neural. Regen. Res.* 7, 325–331. doi: 10.3969/j.issn.1673-5374.2012.05.001

Lin, C. Y., Hsieh, H. Y., Chen, C. M., Wu, S. R., Tsai, C. H., Huang, C. Y., et al. (2016). Non-invasive, neuron-specific gene therapy by focused ultrasound-induced blood-brain barrier opening in Parkinson's disease mouse model. *J. Control Rel.* 235, 72–81. doi: 10.1016/j.jconrel.2016.05.052

Lin, L. C., Chen, Y. F., Lee, W. C., Wu, Y. T., and Tsai, T. H. (2008). Pharmacokinetics of gastrodin and its metabolite p-hydroxybenzyl alcohol in rat blood, brain and bile by microdialysis coupled to LC-MS/MS. *J. Pharm. Biomed. Anal.* 48, 909–917. doi: 10.1016/j.jpba.2008.07.013

Lipsky, R. H., and Marini, A. M. (2007). Brain-derived neurotrophic factor in neuronal survival and behavior-related plasticity. *Ann. N. Y. Acad. Sci.* 1122, 130–143. doi: 10.1196/annals.1403.009

Liu, Y., Gao, J., Peng, M., Meng, H., Ma, H., Cai, P., et al. (2018). A Review on Central Nervous System Effects of Gastrodin. *Front. Pharmacol.* 9:24. doi: 10.3389/fphar.2018.00024

Liu, Y. X., Liu, W. J., Zhang, H. R., and Zhang, Z. W. (2018). Delivery of bevacizumab by intracranial injection: assessment in glioma model. *Onco Targets Ther.* 11, 2673–2683. doi: 10.2147/OTT.S159913

Lorenzo, M. F., Thomas, S. C., Kani, Y., Hinckley, J., Lee, M., Adler, J., et al. (2019). Temporal Characterization of Blood-Brain Barrier Disruption with High-Frequency Electroporation. *Cancers (Basel)* 11:E1850. doi: 10.3390/cancers11121850

Luchtman, D. W., Shao, D., and Song, C. (2009). Behavior, neurotransmitters and inflammation in three regimens of the MPTP mouse model of Parkinson's disease. *Physiol. Behav.* 98, 130–138. doi: 10.1016/j.physbeh.2009.04.021

Luo, K., Wang, Y., Chen, W. S., Feng, X., Liao, Y., Chen, S., et al. (2022). Treatment Combining Focused Ultrasound with Gastrodin Alleviates Memory Deficit and

Neuropathology in an Alzheimer's Disease-Like Experimental Mouse Model. *Neural. Plast.* 2022:5241449. doi: 10.1155/2022/5241449

Ma, S. Y., Röyttä, M., Rinne, J. O., Collan, Y., and Rinne, U. K. (1997). Correlation between neuromorphometry in the substantia nigra and clinical features in Parkinson's disease using disector counts. *J. Neurol. Sci.* 151, 83–87. doi: 10.1016/s0022-510x(97)00100-7

Mead, B. P., Kim, N., Miller, G. W., Hodges, D., Mastorakos, P., Klibanov, A. L., et al. (2017). Novel Focused Ultrasound Gene Therapy Approach Noninvasively Restores Dopaminergic Neuron Function in a Rat Parkinson's Disease Model. *Nano. Lett.* 17, 3533–3542. doi: 10.1021/acs.nanolett.7b00616

Ohta, S., Kikuchi, E., Ishijima, A., Azuma, T., Sakuma, I., and Ito, T. (2020). Investigating the optimum size of nanoparticles for their delivery into the brain assisted by focused ultrasound-induced blood-brain barrier opening. *Sci. Rep.* 10, 18220. doi: 10.1038/s41598-020-75253-9

Palasz, E., Wysocka, A., Gasiorowska, A., Chalimoniuk, M., Niewiadomski, W., and Niewiadomska, G. (2020). BDNF as a Promising Therapeutic Agent in Parkinson's Disease. *Int. J. Mol. Sci.* 21:1170. doi: 10.3390/ijms21031170

Pardridge, W. M. (2005). The blood-brain barrier: bottleneck in brain drug development. *NeuroRx* 2, 3–14. doi: 10.1602/neurorx.2.1.3

Park, J., Aryal, M., Vykhodtseva, N., Zhang, Y. Z., and Mcdannold, N. (2017). Evaluation of permeability, doxorubicin delivery, and drug retention in a rat brain tumor model after ultrasound-induced blood-tumor barrier disruption. *J. Control Rel.* 250, 77–85. doi: 10.1016/j.jconrel.2016.10.011

Pouliopoulos, A. N., Kwon, N., Jensen, G., Meaney, A., Niimi, Y., Burgess, M. T., et al. (2021). Safety evaluation of a clinical focused ultrasound system for neuronavigation guided blood-brain barrier opening in non-human primates. *Sci. Rep.* 11:15043. doi: 10.1038/s41598-021-94188-3

Qi, H., Shen, D., Jiang, C., Wang, H., and Chang, M. (2021). Ursodeoxycholic acid protects dopaminergic neurons from oxidative stress *via* regulating mitochondrial function, autophagy, and apoptosis in MPTP/MPP(+)-induced Parkinson's disease. *Neurosci. Lett.* 741, 135493. doi: 10.1016/j.neulet.2020.135493

Rezai, A. R., Ranjan, M., D'haese, P. F., Haut, M. W., Carpenter, J., Najib, U., et al. (2020). Noninvasive hippocampal blood-brain barrier opening in Alzheimer's disease with focused ultrasound. *Proc. Natl. Acad. Sci. U S A* 117, 9180–9182. doi: 10.1073/pnas.2002571117

Rousselet, E., Joubert, C., Callebert, J., Parain, K., Tremblay, L., Orieux, G., et al. (2003). Behavioral changes are not directly related to striatal monoamine levels, number of nigral neurons, or dose of parkinsonian toxin MPTP in mice. *Neurobiol. Dis.* 14, 218–228. doi: 10.1016/s0969-9961(03)00108-6

Sen, A., Hongpaisan, J., Wang, D., Nelson, T. J., and Alkon, D. L. (2016). Protein Kinase Cϵ (PKCϵ) Promotes Synaptogenesis through Membrane Accumulation of the Postsynaptic Density Protein PSD-95. *J. Biol. Chem.* 291, 16462–16476. doi: 10.1074/jbc.M116.730440

Su, Y., Sun, B., Gao, X., Dong, X., Fu, L., Zhang, Y., et al. (2020). Intranasal Delivery of Targeted Nanoparticles Loaded With miR-132 to Brain for the Treatment of Neurodegenerative Diseases. *Front. Pharmacol.* 11:1165. doi: 10.3389/fphar.2020.01165

Toy, W. A., Petzinger, G. M., Leyshon, B. J., Akopian, G. K., Walsh, J. P., Hoffman, M. V., et al. (2014). Treadmill exercise reverses dendritic spine loss in direct and indirect striatal medium spiny neurons in the 1-methyl-4-phenyl-1,2,3,6-tetrahydropyridine (MPTP) mouse model of Parkinson's disease. *Neurobiol. Dis.* 63, 201–209. doi: 10.1016/j.nbd.2013.11.017

Tsai, H. C., Tsai, C. H., Chen, W. S., Inserra, C., Wei, K. C., and Liu, H. L. (2018). Safety evaluation of frequent application of microbubble-enhanced focused ultrasound blood-brain-barrier opening. *Sci. Rep.* 8, 17720. doi: 10.1038/s41598-018-35677-w

Villalba, R. M., and Smith, Y. (2018). Loss and remodeling of striatal dendritic spines in Parkinson's disease: from homeostasis to maladaptive plasticity? *J. Neural. Transm. (Vienna)* 125, 431–447. doi: 10.1007/s00702-017-1735-6

Wang, Q., Chen, G., and Zeng, S. J. (2009). Study on the Metabolism of Gastrodin in Rat Brain, Liver, Kidney and Different Brain Regions Homogenate. *Chin. J. Mod. Appl. Pharm.* 26, 614–619.

Wang, Q. D., Gu, P., and Dong, Q. Y. (2008). The effect of repetitive transcranial magnetic stimulation on the expressions of growth associated protein-43 and synaptophysin in striatum of Parkinson's disease model mice. *Chin. J. Gerontol.* 19, 1885–1888.

Wang, X. L., Xing, G. H., Hong, B., Li, X. M., Zou, Y., Zhang, X. J., et al. (2014). Gastrodin prevents motor deficits and oxidative stress in the MPTP mouse model of Parkinson's disease: involvement of ERK1/2-Nrf2 signaling pathway. *Life Sci.* 114, 77–85. doi: 10.1016/j.lfs.2014.08.004

Wei, H. J., Upadhyayula, P. S., Pouliopoulos, A. N., Englander, Z. K., Zhang, X., Jan, C. I., et al. (2021). Focused Ultrasound-Mediated Blood-Brain Barrier Opening Increases Delivery and Efficacy of Etoposide for Glioblastoma Treatment. *Int. J. Radiat. Oncol. Biol. Phys.* 110, 539–550. doi: 10.1016/j.ijrobp.2020.12.019

Wu, S. K., Tsai, C. L., Huang, Y., and Hynynen, K. (2020). Focused Ultrasound and Microbubbles-Mediated Drug Delivery to Brain Tumor. *Pharmaceutics* 13.:15. doi: 10.3390/pharmaceutics13010015

Yan, J., Yang, Z., Zhao, N., Li, Z., and Cao, X. (2019). Gastrodin protects dopaminergic neurons *via* insulin-like pathway in a Parkinson's disease model. *BMC Neurosci.* 20:31. doi: 10.1186/s12868-019-0512-x

Yang, Q., Zhou, Y., Chen, J., Huang, N., Wang, Z., and Cheng, Y. (2021). Gene Therapy for Drug-Resistant Glioblastoma *via* Lipid-Polymer Hybrid Nanoparticles Combined with Focused Ultrasound. *Int. J. Nanomedicine.* 16, 185–199. doi: 10.2147/IJN.S286221

Zhang, Q. S., Heng, Y., Mou, Z., Huang, J. Y., Yuan, Y. H., and Chen, N. H. (2017). Reassessment of subacute MPTP-treated mice as animal model of Parkinson's disease. *Acta. Pharmacol. Sin.* 38, 1317–1328. doi: 10.1038/aps.2017.49

Zhang, S., Gong, P., Zhang, J., Mao, X., Zhao, Y., Wang, H., et al. (2020). Specific Frequency Electroacupuncture Stimulation Transiently Enhances the Permeability of the Blood-Brain Barrier and Induces Tight Junction Changes. *Front. Neurosci.* 14:582324. doi: 10.3389/fnins.2020.582324

Zhou, N. N., Zhu, R., Zhao, X. M., Zhang, J. M., and Liang, P. (2016). [Effect and mechanism of gastrodin inhibiting β-amyloid plaques in brain of mice]. *Yao. Xue. Xue. Bao.* 51, 588–594.

Conflict of Interest: The authors declare that the research was conducted in the absence of any commercial or financial relationships that could be construed as a potential conflict of interest.

Publisher's Note: All claims expressed in this article are solely those of the authors and do not necessarily represent those of their affiliated organizations, or those of the publisher, the editors and the reviewers. Any product that may be evaluated in this article, or claim that may be made by its manufacturer, is not guaranteed or endorsed by the publisher.

frontiers | Frontiers in Cellular Neuroscience

MINI REVIEW
published: 29 June 2022
doi: 10.3389/fncel.2022.955385

Thrombo-Inflammation and Immunological Response in Ischemic Stroke: Focusing on Platelet-Tregs Interaction

Jieqiong Cui[1,2†], Huayan Li[2†], Zongning Chen[3†], Ting Dong[4], Xiying He[2], Yuanyuan Wei[1], Zhengkun Li[2], Jinfeng Duan[5], Ting Cao[2], Qian Chen[2], Dongmei Ma[2], Yang Zhou[2], Bo Wang[2], Mingqin Shi[1], Qin Zhang[4], Lei Xiong[1]* and Dongdong Qin[1]**

[1] School of Basic Medical Sciences, Yunnan University of Chinese Medicine, Kunming, China, [2] The First School of Clinical Medicine, Yunnan University of Chinese Medicine, Kunming, China, [3] Department of General Medicine, Lijiang People's Hospital, Lijiang, China, [4] Department of Laboratory Medicine, The First People's Hospital of Yunnan Province, Kunming, China, [5] School of Chinese Medicine, Yunnan University of Chinese Medicine, Kunming, China

OPEN ACCESS

Edited by:
Feng Zhang,
Third Hospital of Hebei Medical University, China

Reviewed by:
Yaoyi Wang,
Fudan University, China
Zizhang Sheng,
Columbia University Irving Medical Center, United States

***Correspondence:**
Qin Zhang
zhangqinkm@126.com
Lei Xiong
xlluck@sina.com
Dongdong Qin
qindong108@163.com

† These authors have contributed equally to this work

Specialty section:
This article was submitted to Cellular Neuropathology, a section of the journal Frontiers in Cellular Neuroscience

Received: 28 May 2022
Accepted: 13 June 2022
Published: 29 June 2022

Citation:
Cui J, Li H, Chen Z, Dong T, He X, Wei Y, Li Z, Duan J, Cao T, Chen Q, Ma D, Zhou Y, Wang B, Shi M, Zhang Q, Xiong L and Qin D (2022) Thrombo-Inflammation and Immunological Response in Ischemic Stroke: Focusing on Platelet-Tregs Interaction. Front. Cell. Neurosci. 16:955385. doi: 10.3389/fncel.2022.955385

Strokes are mainly caused by thromboembolic obstruction of a major cerebral artery. Major clinical manifestations include paralysis hemiplegia, aphasia, memory, and learning disorders. In the case of ischemic stroke (IS), hyperactive platelets contribute to advancing an acute thrombotic event progression. Therefore, the principal goal of treatment is to recanalize the occluded vessel and restore cerebral blood flow by thrombolysis or mechanical thrombectomy. However, antiplatelets or thrombolytic therapy may increase the risk of bleeding. Beyond the involvement in thrombosis, platelets also contribute to the inflammatory process induced by cerebral ischemia. Platelet-mediated thrombosis and inflammation in IS lie primarily in the interaction of platelet receptors with endothelial cells and immune cells, including T-cells, monocytes/macrophages, and neutrophils. Following revascularization, intervention with conventional antiplatelet medicines such as aspirin or clopidogrel does not substantially diminish infarct development, most likely due to the limited effects on the thrombo-inflammation process. Emerging evidence has shown that T cells, especially regulatory T cells (Tregs), maintain immune homeostasis and suppress immune responses, playing a critical immunomodulatory role in ischemia-reperfusion injury. Hence, considering the deleterious effects of inflammatory and immune responses, there is an urgent need for more targeted agents to limit the thrombotic-inflammatory activity of platelets and minimize the risk of a cerebral hemorrhage. This review highlights the involvement of platelets in neuroinflammation and the evolving role of Tregs and platelets in IS. In response to all issues, preclinical and clinical strategies should generate more viable therapeutics for preventing and managing IS with immunotherapy targeting platelets and Tregs.

Keywords: ischemic stroke, platelets, thromboinflammation, regulatory T cells, immunomodulation

INTRODUCTION

According to the Global Burden of Disease Study, the number of deaths from stroke has increased significantly over the last decade, and remained the second-leading cause of death worldwide (GBD 2019 Stroke Collaborators, 2021). Stroke is a heterogeneous disease with acute central nervous system (CNS) focal injury caused by vascular causes, including ischemic stroke (IS), intracerebral hemorrhage (ICH) and pathogenic subtypes (Sacco et al., 2013). The Global Stroke Fact Sheet 2022 states that over 62% of incident strokes are IS (Feigin et al., 2022). Generally, most IS are due to intracranial atherosclerosis and/or *in situ* thrombosis. Furthermore, vascular embolism of atherosclerotic plaques from the aortic arch, carotid artery, or heart also cause IS (Kim et al., 2018; Campbell et al., 2019). Currently, treatments of IS mainly include thrombolysis, antiplatelet, anticoagulation, antithrombosis, and rapid recanalization through mechanical thrombectomy (Crunkhorn, 2018). Mainstay drugs are alteplase, aspirin, clopidogrel hydrogen sulfate, and dual antiplatelet agents (Johnston et al., 2018; Powers, 2020). However, the overall efficacy is limited by the narrow treatment time window, thrombo-inflammation, and ischemia-reperfusion injury. Therefore, it is necessary to combine antiplatelet, anti-inflammatory, and neuroprotective treatments (Stanzione et al., 2020).

In the past decade, molecular and immunological studies have elaborated the additional functions of platelets in the vascular system. Platelets not only play a role in vascular integrity and remodeling, but also they are associated with thrombosis and inflammation, regulating innate or adaptive immunity (Koupenova et al., 2018; Morrell et al., 2019; Hubbard et al., 2021). Platelets support immune responses and maintain immune cell homeostasis to produce and release many immune molecules, directly influencing the development of vascular inflammatory diseases (Morrell et al., 2019). Regulatory T cells are a subset of T cells that control autoimmune responsiveness *in vivo* and are divided into natural regulatory T cells (nTregs) and adaptive regulatory T cells (iTregs). They play a vital role in balancing immune responses by actively suppressing pathogenic immune activation and maintaining immune tolerance (Ferreira et al., 2019). Recent research reports that Tregs infiltrating the brain are critical for behavioral recovery and neural repair (Shi et al., 2021). Therefore, the platelet-immune interface is crucial to understand the pathogenesis of IS and develop optimal treatments. This review briefly summarizes the function of platelet activation and the pathological mechanism of thrombo-inflammation in IS. We also focus on the interaction of platelets with circulating immune cells, especially Tregs, and outline the complex functions of platelets. Furthermore, interventions of IS through targeting platelet-Tregs are also reviewed. In conclusion, the role of platelets in IS and the potential of Tregs as targets for IS intervention require further in-depth investigation (**Figure 1**). In the future, we hope that more definitive personalized platelets and Tregs-targeted immunotherapy will be able to intervene IS, as well as provide nerve repair and regeneration.

PLATELET ACTIVATION AND THROMBO-INFLAMMATION IN ISCHEMIC STROKE

Platelets are derived from megakaryocyte precursors (Ghoshal and Bhattacharyya, 2014), and δ-granules contain ADP, 5-hydroxytryptamine, polyphosphates, calcium, histamine, and glutamate, which are necessary for hemostasis (Koupenova et al., 2017). Platelet activation processes include intracellular calcium flux, negative translocation of phospholipids, α-granule release, and shape change (Furie and Furie, 2008; Rubenstein and Yin, 2018). The platelet hemostatic program is highly dependent on the glycoprotein receptor complexes GPIb-V-IX and GPVI-FcgR (Borissoff et al., 2011). Recent studies have shown that platelets express more active receptor glycoprotein (GP) VI dimers in stroke patients (Induruwa et al., 2022). Another study combined cell physiology and phosphoproteomics approaches to analyze the downstream signaling mechanism of the immunotyrosine activation motif (ITAM) platelet collagen receptor GPVI. The results inferred more than 300 signaling relationships between effectors (i.e., FcRg, Syk, PLCg2, PKCd, DAPP1) in the platelet GPVI/ITAM response (Babur et al., 2020). Following initial activation, platelets release thromboxane A2 (TxA2) and ADP, which mediate other platelets' recruitment, activation, and aggregation, culminating in three-dimensional aggregation (Jurk and Kehrel, 2005; Mackman et al., 2007). Thrombin produces fibrin during coagulation or thrombosis, and the fibrinogen receptor GP2b/3a mediates and forms platelet aggregation. However, in a specific pathological condition, the megakaryocyte-platelet-hemostatic axis (MPHA) becomes disturbed, resulting in dysregulated platelet activation and aggregation. This leads to uncontrolled clot formation, cerebrovascular embolism, and the development of IS (Cemin et al., 2011). A recent study found that platelet aggregation is mediated by the endoplasmic reticulum oxidoreductin 1α (Ero1α), protein disulfide isomerase (PDI), and glutathione (GSH) electron transport system on the platelet surface. At the platelet surface, Ero1α constitutively oxidizes PDI and further regulates platelet aggregation in a glutathione-dependent manner (Wang L. et al., 2022). In general, platelet attachment and activation through the GPIb–vWF–GPVI axis and FXII constitute a significant pathological mechanism of acute IS and promote a detrimental inflammatory response.

Reperfusion therapy could assist in restoring blood flow after IS, thereby minimizing brain tissue damage. However, the immune system may still sustain an inflammatory response after recanalization (Alawieh et al., 2020). The interaction of thrombotic and inflammatory mechanisms drives the progression of neuronal damage in IS (Nieswandt et al., 2011). The primary determinant of platelet-mediated inflammation is the platelet adhesion receptors, which can be classified into selectins, integrins, leucine-rich glycoproteins and immunoglobulin-type receptors (Mezger et al., 2015). Atypical platelet function links the cascade of thrombotic reactions to innate immunity through a fundamentally

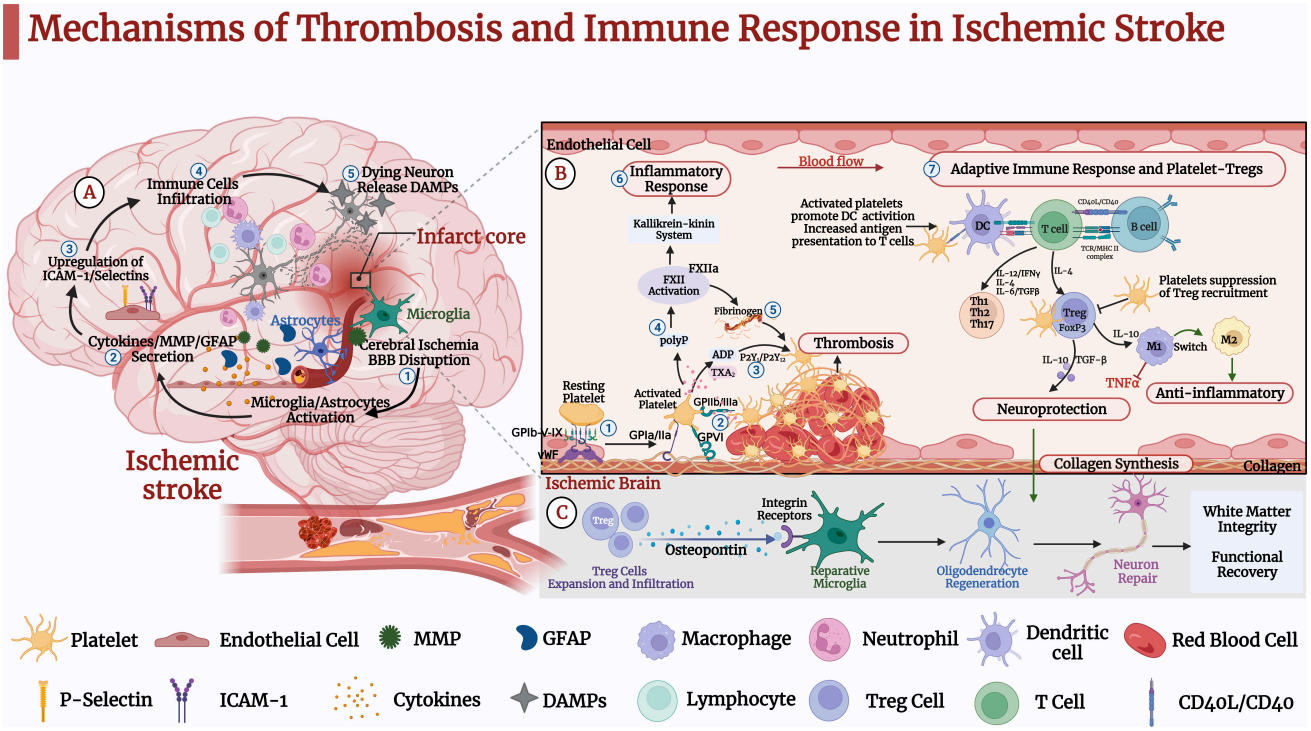

FIGURE 1 | Mechanisms of thrombosis and immune response in ischemic stroke (IS). **(A)** ① IS causes oxidative stress and excitotoxicity in the acute phase, activating microglia and astrocytes. ② IS leads to the secretion of cytokines, matrix metalloproteinase (MMP), and glial fibrillary acidic protein (GFAP). ③ Pro-inflammatory factors further lead to upregulation of intercellular cell adhesion molecule (ICAM-1) and selectins on endothelial cells. ④ Blood-derived inflammatory cells such as neutrophils, macrophages, and lymphocytes infiltrate the ischemic brain tissue. ⑤Dead neurons release danger-associated molecular patterns (DAMPs), activating microglia and peripheral immune cells and leading to pro-inflammatory factors that further activate microglia and astrocytes. These pathological events further lead to neuronal death and brain damage. **(B)** Platelet-Tregs Interaction. ① At the site of vascular embolic injury, platelets bind to vWF immobilized on collagen *via* the platelet glycoprotein GP Ib-IX-V receptor complex, GPVI and GP Ia/IIa receptors, and bind to exposed collagen to activate adhesion. ② Platelets' activation functionally upregulates GP IIb/IIIa. ③ Activated platelets release dense granules-ADP, α granules-fibrinogen, vWF, and factor-V, polyphosphates. ④ Polyphosphates activate coagulation factor XII (FXII). ⑤ Activated platelets aggregate *via* fibrinogen and vWF. ⑥ In addition to triggering thrombosis through fibrin generation, FXIIa promotes activation of the kallikrein-kinin system and initiates a signaling cascade response, which induces endothelial cell injury, vascular edema, and pro-inflammatory cytokine expression, further induces glial activation, inflammatory response, and ultimately neuronal death. ⑦ Activated platelets promote the activation of monocytes and dendritic cells (DCs) and enhance the adaptive immune response. T lymphocytes interact with activated platelets *via* CD40/CD40L to form a solid thrombus. One mechanism by which platelets-derived CD40L can promote atherosclerosis is through inhibiting the migration of Tregs to thrombus sites. Tregs inhibit the expression of adhesion molecules in endothelial and the production of pro-inflammatory cytokines. In addition, it secretes TGF-β and IL-10, promoting collagen synthesis and exerting neuroprotective effects. **(C)** Tregs secrete osteopontin to promote tissue-reparative microglial reactions, thereby promoting oligodendrocyte regeneration as well as remyelination, neuronal repair and behavioral recovery.

different mechanism. Activated platelets mediate thrombo-inflammation and engage in leukocyte recruitment (Franks et al., 2010). Additionally, other chemicals released by platelets are capable of mediating the kallikrein-kinin pathway, which produces pro-inflammatory bradykinin, causes endothelial cell injury, and leads to cerebrovascular edema and neuronal damage (Dobrivojević et al., 2015; Rawish et al., 2020). Meanwhile, IS activates circulating neutrophils and T cells, leading to a sterile inflammatory response. Platelets coordinate immune cells infiltrating into the brain parenchyma, causing neuronal damage (Konsman et al., 2007). All phases of the IS cascade involve inflammatory signals, from early injury events triggered by cerebral ischemia to the later regenerative processes of neural tissue repair. As the ischemic cascade progresses, neurons rapidly become dysfunctional or die under hypoxic-ischemic conditions, causing activation of the immune system (Lipton, 1999; Kono and Rock, 2008).

IMMUNOLOGICAL RESPONSE AFTER ISCHEMIC STROKE

After an IS attacks, damaged neurons activate the immune system. While, the over-activated immune system drives the death of neurons. Recent evidence suggests that immune cells, including neutrophils, macrophages, B cells, T cells, and dendritic cells, infiltrate brain tissue after blood-brain barrier disruption (BBB) (Jian et al., 2019). The innate immune system makes the earliest immune response to acute IS *via* pattern recognition of Toll-like receptors (TLRs) and Nod-like receptors (NLRs) (Chamorro et al., 2012). Further, it activates downstream

mitogen-activated protein kinase (MAPK) and nuclear factor-kB pathways to produce pro-inflammatory cytokines, reactive oxygen species (ROS), and chemokines, exacerbating post-ischemic inflammation (An et al., 2014). In distinction, the adaptive immune response is relatively delayed in IS. In animal models, neutrophils first migrate to the brain parenchyma after IS, followed by macrophages and natural killer cells, and finally by T and B lymphocyte infiltration. Relevant evidence suggests that adaptive immune responses primarily coordinate T and B lymphocytes and antigen-presenting cells to reduce severe inflammation, and limit the development of ischemic pathology (Gan et al., 2014; Hammond et al., 2014; Fu et al., 2015). A multicenter clinical trial evaluated that the immunomodulator (fingolimod and alteplase) effectively reduced brain injury in patients after acute IS, with suppressed lesion growth from day 1 to day 7 and better recovery at 90 days postoperatively. Patients treated with fingolimod combined with alteplase had lower circulating lymphocytes, smaller lesion volumes (10.1 vs. 34.3 mL; $P = 0.04$), less bleeding (1.2 vs. 4.4 mL; $P = 0.01$), and reduced neurological deficits measured by stroke scale (4 vs. 2; $P = 0.02$) (Zhu et al., 2015). Studies have shown that fingolimod reduces the number of circulating lymphocytes in IS, helps prevent local activation of microglia or macrophages, and controls early infiltration of lymphocytes into brain tissue (Schwab et al., 2005; Massberg and von Andrian, 2006). *In vitro* experiments, the interaction of macrophages with activated platelets enhanced the secretion of pro-inflammatory cytokines, suggesting that activated platelets exacerbate the activation of pro-inflammatory macrophages. In addition, a study found that collagen-activated platelets lead to increased release of interleukin (IL-10) and decreased secretion of tumor necrosis factor alpha (TNF-α) by releasing large amounts of prostaglandin E2 (PGE2) (Linke et al., 2017). In addition to interactions with the innate immune system, platelets interact with dendritic cells (DCs) via the CD40-CD154 axis to promote adaptive immunity (Cognasse et al., 2022). Correlative evidence suggests that immunodeficient Rag1 (–/–), CD4 + T-cell (–/–), and CD8 + T-cell (–/–) mice develop smaller infarct volumes and less leukocyte-platelet adhesion than wild-type mice (Yilmaz et al., 2006). Recent research has shown that mice lacking CD84 (a member of signaling lymphocyte activating molecule) exhibited reduced infiltration of CD4 + T cells, decreased thrombotic activity, and neurological injury after experimental stroke (Schuhmann et al., 2020). Therefore, an in-depth study of the interaction between the platelet-immune system and ischemic brain areas is essential to realize the full potential of immunotherapy in stroke.

TREGS IN ISCHEMIC STROKE

Tregs are an essential subpopulation of T cells that secrete immunosuppressive cytokines and maintain immune homeostasis or limit inflammatory additive injury by inhibiting self-reactive immunity (Sakaguchi, 2000; Duffy et al., 2018). Tregs can be classified into various subtypes such as CD4 + CD25 + Tregs, Tr1, and Th3 cells based on their surface markers, cytokines produced, and mechanism of action. Natural Tregs are usually characterized by CD25 + CD4 + and co-express transcription factor P3 (Foxp3) (Spitz et al., 2016). Currently, FOXP3 + Tregs are the cell line known to maintain immune tolerance, and almost all ongoing clinical trials using cell therapy to induce immune tolerance use CD4 + FOXP3 + Tregs (Ferreira et al., 2019). The inflammatory cascade in IS disrupts the integrity of the BBB. High expression of C-C chemokine receptor 5 (CCR5) on Tregs activates calcium signaling, helping Tregs interfacing with ischemic endothelium and interacting with neutrophils or macrophages (Zhang et al., 2020). Tregs can regulate multiple immune pathways in the pathology of IS through the secretion of cytokines, cytolysis, and receptor pathways. For example, Tregs induce immunosuppression through the production of IL-10 and TGF-β. In addition, Tregs maintain homeostasis of the immune system by decreasing the negative effects of excessive inflammation to prevent brain ischemia and promote neurological repair. Although the exact mechanism by which Tregs regulate IS remains controversial, current relevant studies *in vitro* or *in vivo* suggest that Tregs may be a novel target for IS immunotherapy (Wang H. et al., 2022). In 2009, Liesz et al. (2009b) first investigated the action of Tregs in cerebral ischemia and found that mice lacking Tregs had a significantly larger infarct size than controls at day 7 after permanent middle cerebral artery occlusion. Tregs prevent secondary infarction by inhibiting excessive pro-inflammatory cytokines production and regulating the invasion of lymphocytes or microglia in ischemic brain tissue. In addition, related studies have shown that IL-10 can mediate the protective effects of Tregs after stroke (Planas and Chamorro, 2009). Recent studies have shown that Tregs produce dual regulatory proteins with low affinity for epidermal growth factor receptor (EGFR) ligands to inhibit the proliferation of neurotoxic astrocytes. Furthermore, pathway analysis revealed an enormous enrichment of pathway genes involved in neuroactive ligand-receptor interactions in Tregs (Ito et al., 2019). An animal experiment elucidated the protective effect of IL-2/IL-2Ab (antibody) complexes on the prognosis of IS by expanding the number of Tregs. Results showed that IL-2/IL-2Ab significantly reduced brain infarct volume and suppressed neuroinflammatory responses in mice. Then, the injection of diphtheria toxin (DT) into transgenic mice (DTR mice) to achieve Tregs clearance revealed that the deletion of Tregs eliminated the neuroprotective effect of IL-2/IL-2Ab. Adoptive transfer of Tregs collected from IL-2/IL-2Ab-treated mice showed more effective neuroprotection, suggesting that IL-2/IL-2Ab effectively increased Tregs' numbers and enhanced function (Zhang et al., 2018).

In addition, a related study also found that increasing Tregs *in vivo via* the JES-6-1/IL-2 complex also reduced neuroinflammatory damage. It confirms that Tregs may promote neurological recovery after IS or prevent recurrent stroke. Li et al. (2013) evaluated the potential and neuroprotective mechanisms of Tregs in an IS model by combined cell-specific deletion, knockout mice, and bone marrow chimeras for Tregs-neutrophils co-culture *in vitro*. Findings suggest that in the early stages of ischemia, adoptive transfer of Tregs

reduces infiltration of peripheral inflammatory cells into the injured brain, decreases brain inflammation, and alleviates the impaired BBB integrity. A recent study combining single-cell RNA sequencing and flow cytometry methods found that Tregs began to infiltrate mouse brain tissue 1–5 weeks after experimental stroke. Experimental selective reduction of Tregs impeded oligodendrocyte and white matter repair and functional recovery after stroke. Transcriptome analysis showed that brain-infiltrating Tregs exert potent immunomodulatory effects on monocytes and other immune cells. In addition, Treg-derived bone bridge proteins enhance microglia repair activity via integrin receptors, thereby promoting oligodendrocyte formation and white matter repair (Shi et al., 2021). These results suggest a significant role for Tregs in regulating neuroinflammation, predicting that it may be a promising target for IS.

Tregs have beneficial effects on neural repair after IS, but some studies have shown that they can have the opposite or even no effect (Kleinschnitz et al., 2013). The reason for the inability of Tregs to play an active role may be related to the degree of brain damage (Hug et al., 2009; Liesz et al., 2009a), the timing of Tregs' analysis (Liesz et al., 2009b; Kleinschnitz et al., 2013; Na et al., 2015; Schuhmann et al., 2015), and inflammatory conditions (Danese and Rutella, 2007). Tregs can play different roles at different stages of IS, and current studies on Tregs migration or proliferation have shown that Tregs have significant anti-IS effects. Therefore, the appropriate timing, dose, and injection site for Tregs expansion need further investigation.

PLATELET-TREGS INTERACTION ORCHESTRATES INFLAMMATION

As mentioned earlier, platelets are actively involved in immune cell recruitment and host defense in addition to hemostatic function. Related studies have shown that platelets directly influence adaptive immune responses by secreting CD40 and CD40L molecules and partner with a continuous subpopulation of immune cells to coordinate the onset and regression of inflammation (Henn et al., 1998; Lam et al., 2015; Maouia et al., 2020). A previous report found that blocking platelet CD40L may preserve the natural Tregs response, which is a potentially novel mechanism to explain the putative suppressing effects of antiplatelet drugs (Moura and Tjwa, 2010). A study of the kinetic mechanisms by which platelets affect CD4 + T cell responses showed that platelets enhance Tregs responses by promoting the proliferation of FoxP3 + T cells (Zhu et al., 2014). The differentiation of Tregs requires the participation of TGFβ, and a high concentration of TGF-β inhibits IL-23R expression in favor of Foxp3 Tregs (Zhou et al., 2008). Large amounts of TGFβ are stored in platelets and released upon activation at levels approximately 50-fold higher than those released by activated CD4 + T cells. In addition, platelet factor 4 (PF4) significantly promotes Tregs' differentiation of αCD3/cd28-stimulated CD4 + T cells (Gerdes et al., 2011). One study applied a super-agonist to elucidate the role of Tregs, showing that antibody-mediated Tregs amplification enhanced stroke size and worsened functional outcomes. This suggests that Tregs promote thrombo-inflammatory lesion growth in the acute phase of IS (Schuhmann et al., 2015). The potential of immunomodulatory function is well established, including expansion of Tregs to limit early post-stroke inflammatory cytotoxicity. In addition, testing potential therapeutic approaches using different ischemic models may better approximate the clinical heterogeneity of stroke. Multiple stroke models allow for appropriate modeling of systemic immune changes in all aspects of stroke (Veltkamp et al., 2015). A previous study has shown that platelets promote the resolution of lung inflammation by directly recruiting Tregs into the lung and transcriptionally reprogramming alveolar macrophages to an anti-inflammatory phenotype. This study is the first to demonstrate that platelet MHC I mediates direct and critical regulation of CD8 + T cells, thus breaking the traditional notion that CD8 + T cells are primarily regulated by classical antigen-presenting cells, such as dendritic cells and monocytes. In addition, DQ-OVA was firstly used as a tool protein to demonstrate that platelets can actively endocytose and hydrolyze exogenous antigens, further supporting the crucial regulatory role of platelets. With the widespread application of cellular immunotherapy, the immune regulation induced by platelets will provide new ideas for future T-cell therapy (Kapur and Semple, 2021; Rossaint et al., 2021). This study indicates that platelets orchestrate Tregs and send signals to the macrophages. As the inflammation progresses, platelet-Tregs interaction can affect T cell migration which helps inflammation subside and prevents further tissue damage in IS. A recent study on trauma found that GPIIb/IIIa regulates the interaction between CD4 + Tregs and platelets-, fibrinogen-, and PAR4-dependent pathways (Bock et al., 2022). This provides some reference value to investigate the mechanism of platelet-Tregs interaction in IS.

CONCLUSION

Most IS have thromboembolism of the cerebral vessels, and a critical cellular mediator leading to thrombosis is platelets (Jackson, 2011). There are various types of antiplatelet drugs in clinical therapeutic applications, acting on different stages of platelet thrombosis process of adhesion and aggregation and inhibiting relevant receptors or enzymes to achieve antiplatelet effects. Nevertheless, some studies have highlighted that targeting the pathological mechanisms and pathways of IS may be invalid with a single classical antiplatelet agent (Kleinschnitz et al., 2007; Kraft et al., 2015). If innate and adaptive immune cells are over-activated after IS, it could lead to secondary damage and impede neural repair in the brain (An et al., 2014). In addition to novel compounds that impede thrombosis, recent studies have been conducted on novel immunomodulators to treat acute IS (Alawieh et al., 2020). After IS, the immune response involves the central immune cells, peripheral immune cells, BBB, vascular endothelial cells, and various inflammatory molecules. In the past decades, several efforts have tried to find new targets through antiplatelet or immunotherapy to treat IS. Early targeted treatment of thrombo-inflammation during recanalization may be a promising approach. However, most current studies on Thrombo-inflammation are limited to the role of platelets in

innate immune responses, such as platelets expressing multiple antigen recognition receptors, platelets regulating the activation and differentiation of monocytes, and platelets interacting with neutrophils. In addition, studies related to the regulation of platelets and T cells and the synergistic effect of platelets and Tregs are still lacking. With the development of gene-editing technologies, platelets can be edited *in vitro*, or generated *in vitro* from megakaryocytes according to their nucleus-free nature, showing a broad prospect as a tool cell for immunotherapy of IS.

AUTHOR CONTRIBUTIONS

All authors listed have made a substantial, direct, and intellectual contribution to the work, and approved it for publication.

FUNDING

This work was supported by the National Natural Science Foundation of China (31960178, 82074421, 82160923, 82160924, 8207153176, and 82160924), the Applied Basic Research Programs of Science and Technology Commission Foundation of Yunnan Province (2019FA007), the Joint Project of Applied Basic Research of Yunnan University of Chinese Medicine and Yunnan Provincial Science and Technology Department [2019FF002(–001)], Yunnan Provincial Department of Education Science Research Fund Project (2021Y456), the Key Realm R&D Program of Guangdong Province (2019B030335001), the China Postdoctoral Science Foundation (2018M631105), and the Yunnan Provincial Academician and Expert Workstation (202005AF150017, 202105AF150037, and 2019IC051).

REFERENCES

Alawieh, A. M., Langley, E. F., Feng, W., Spiotta, A. M., and Tomlinson, S. (2020). Complement-Dependent Synaptic Uptake and Cognitive Decline after Stroke and Reperfusion Therapy. *J. Neurosci.* 40, 4042–4058. doi: 10.1523/JNEUROSCI.2462-19.2020

An, C., Shi, Y., Li, P., Hu, X., Gan, Y., Stetler, R. A., et al. (2014). Molecular dialogs between the ischemic brain and the peripheral immune system: dualistic roles in injury and repair. *Prog. Neurobiol.* 115, 6–24. doi: 10.1016/j.pneurobio.2013.12.002

Babur, Ö, Melrose, A. R., Cunliffe, J. M., Klimek, J., Pang, J., Sepp, A.-L. I., et al. (2020). Phosphoproteomic quantitation and causal analysis reveal pathways in GPVI/ITAM-mediated platelet activation programs. *Blood* 136, 2346–2358. doi: 10.1182/blood.2020005496

Bock, M., Bergmann, C. B., Jung, S., Biberthaler, P., Heimann, L., and Hanschen, M. (2022). Platelets differentially modulate CD4+ Treg activation via GPIIa/IIIb-, fibrinogen-, and PAR4-dependent pathways. *Immunol. Res.* 70, 185–196. doi: 10.1007/s12026-021-09258-5

Borissoff, J. I, Spronk, H. M. H., and ten Cate, H. (2011). The hemostatic system as a modulator of atherosclerosis. *N. Engl. J. Med.* 364, 1746–1760. doi: 10.1056/NEJMra1011670

Campbell, B. C. V., De Silva, D. A., Macleod, M. R., Coutts, S. B., Schwamm, L. H., Davis, S. M., et al. (2019). Ischaemic stroke. *Nat. Rev. Dis. Primers* 5:70. doi: 10.1038/s41572-019-0118-8

Cemin, R., Donazzan, L., Lippi, G., Clari, F., and Daves, M. (2011). Blood cells characteristics as determinants of acute myocardial infarction. *Clin. Chem. Lab. Med.* 49, 1231–1236. doi: 10.1515/CCLM.2011.183

Chamorro, Á, Meisel, A., Planas, A. M., Urra, X., van de Beek, D., and Veltkamp, R. (2012). The immunology of acute stroke. *Nat. Rev. Neurol.* 8, 401–410. doi: 10.1038/nrneurol.2012.98

Cognasse, F., Duchez, A. C., Audoux, E., Ebermeyer, T., Arthaud, C. A., Prier, A., et al. (2022). Platelets as Key Factors in Inflammation: Focus on CD40L/CD40. *Front. Immunol.* 13:825892. doi: 10.3389/fimmu.2022.825892

Crunkhorn, S. (2018). Opening the therapeutic window. *Nat. Rev. Drug Discov.* 17, 467–467. doi: 10.1038/nrd.2018.98

Danese, S., and Rutella, S. (2007). The Janus Face of CD4+CD25+ Regulatory T Cells in Cancer and Autoimmunity. *CMC* 14, 649–666. doi: 10.2174/092986707780059599

Dobrivojević, M., Špiranec, K., and Sinđić, A. (2015). Involvement of bradykinin in brain edema development after ischemic stroke. *Pflug. Arch. Eur. J. Physiol.* 467, 201–212. doi: 10.1007/s00424-014-1519-x

Duffy, S. S., Keating, B. A., Perera, C. J., and Moalem-Taylor, G. (2018). The role of regulatory T cells in nervous system pathologies. *J. Neurosci. Res.* 96, 951–968. doi: 10.1002/jnr.24073

Feigin, V. L., Brainin, M., Norrving, B., Martins, S., Sacco, R. L., Hacke, W., et al. (2022). World Stroke Organization (WSO): Global Stroke Fact Sheet 2022. *Int. J. Stroke* 17, 18–29. doi: 10.1177/17474930211065917

Ferreira, L. M. R., Muller, Y. D., Bluestone, J. A., and Tang, Q. (2019). Next-generation regulatory T cell therapy. *Nat. Rev. Drug Discov.* 18, 749–769. doi: 10.1038/s41573-019-0041-4

Franks, Z. G., Campbell, R. A., Weyrich, A. S., and Rondina, M. T. (2010). Platelet-leukocyte interactions link inflammatory and thromboembolic events in ischemic stroke: Franks et al. *Ann. N. Y. Acad. Sci.* 1207, 11–17. doi: 10.1111/j.1749-6632.2010.05733.x

Fu, Y., Liu, Q., Anrather, J., and Shi, F.-D. (2015). Immune interventions in stroke. *Nat. Rev. Neurol.* 11, 524–535. doi: 10.1038/nrneurol.2015.144

Furie, B., and Furie, B. C. (2008). Mechanisms of Thrombus Formation. *N. Engl. J. Med.* 359, 938–949. doi: 10.1056/NEJMra0801082

Gan, Y., Liu, Q., Wu, W., Yin, J.-X., Bai, X.-F., Shen, R., et al. (2014). Ischemic neurons recruit natural killer cells that accelerate brain infarction. *Proc. Natl. Acad. Sci. U.S.A.* 111, 2704–2709. doi: 10.1073/pnas.1315943111

GBD 2019 Stroke Collaborators (2021). Global, regional, and national burden of stroke and its risk factors, 1990-2019: a systematic analysis for the Global Burden of Disease Study 2019. *Lancet Neurol.* 20, 795–820. doi: 10.1016/S1474-4422(21)00252-0

Gerdes, N., Zhu, L., Ersoy, M., Hermansson, A., Hjemdahl, P., Hu, H., et al. (2011). Platelets regulate CD4+ T-cell differentiation via multiple chemokines in humans. *Thromb. Haemost.* 106, 353–362. doi: 10.1160/TH11-01-0020

Ghoshal, K., and Bhattacharyya, M. (2014). Overview of Platelet Physiology: Its Hemostatic and Nonhemostatic Role in Disease Pathogenesis. *Sci. World J.* 2014, 1–16. doi: 10.1155/2014/781857

Hammond, M. D., Taylor, R. A., Mullen, M. T., Ai, Y., Aguila, H. L., Mack, M., et al. (2014). CCR2+Ly6Chi Inflammatory Monocyte Recruitment Exacerbates Acute Disability Following Intracerebral Hemorrhage. *J. Neurosci.* 34, 3901–3909. doi: 10.1523/JNEUROSCI.4070-13.2014

Henn, V., Slupsky, J. R., Gräfe, M., Anagnostopoulos, I., Förster, R., Müller-Berghaus, G., et al. (1998). CD40 ligand on activated platelets triggers an inflammatory reaction of endothelial cells. *Nature* 391, 591–594. doi: 10.1038/35393

Hubbard, W. B., Dong, J., Cruz, M. A., and Rumbaut, R. E. (2021). Links between thrombosis and inflammation in traumatic brain injury. *Thromb. Res.* 198, 62–71. doi: 10.1016/j.thromres.2020.10.041

Hug, A., Dalpke, A., Wieczorek, N., Giese, T., Lorenz, A., Auffarth, G., et al. (2009). Infarct Volume is a Major Determiner of Post-Stroke Immune Cell Function and Susceptibility to Infection. *Stroke* 40, 3226–3232. doi: 10.1161/STROKEAHA.109.557967

Induruwa, I., McKinney, H., Kempster, C., Thomas, P., Batista, J., Malcor, J.-D., et al. (2022). Platelet surface receptor glycoprotein VI-dimer is overexpressed in stroke: The Glycoprotein VI in Stroke (GYPSIE) study results. *PLoS One* 17:e0262695. doi: 10.1371/journal.pone.0262695

Ito, M., Komai, K., Mise-Omata, S., Iizuka-Koga, M., Noguchi, Y., Kondo, T., et al. (2019). Brain regulatory T cells suppress astrogliosis and potentiate neurological recovery. *Nature* 565, 246–250. doi: 10.1038/s41586-018-0824-5

Jackson, S. P. (2011). Arterial thrombosis–insidious, unpredictable and deadly. *Nat. Med.* 17, 1423–1436. doi: 10.1038/nm.2515

Jian, Z., Liu, R., Zhu, X., Smerin, D., Zhong, Y., Gu, L., et al. (2019). The Involvement and Therapy Target of Immune Cells After Ischemic Stroke. *Front. Immunol.* 10:2167. doi: 10.3389/fimmu.2019.02167

Johnston, S. C., Easton, J. D., Farrant, M., Barsan, W., Conwit, R. A., Elm, J. J., et al. (2018). Clopidogrel and Aspirin in Acute Ischemic Stroke and High-Risk TIA. *N. Engl. J. Med.* 379, 215–225. doi: 10.1056/NEJMoa1800410

Jurk, K., and Kehrel, B. E. (2005). Platelets: physiology and biochemistry. *Semin. Thromb. Hemost.* 31, 381–392. doi: 10.1055/s-2005-916671

Kapur, R., and Semple, J. W. (2021). Platelets instruct T reg cells and macrophages in the resolution of lung inflammation. *J. Exp. Med.* 218:e20210754. doi: 10.1084/jem.20210754

Kim, J. S., Kim, Y.-J., Ahn, S.-H., and Kim, B. J. (2018). Location of cerebral atherosclerosis: why is there a difference between East and West? *Int. J. Stroke* 13, 35–46. doi: 10.1177/1747493016647736

Kleinschnitz, C., Kraft, P., Dreykluft, A., Hagedorn, I., Göbel, K., Schuhmann, M. K., et al. (2013). Regulatory T cells are strong promoters of acute ischemic stroke in mice by inducing dysfunction of the cerebral microvasculature. *Blood* 121, 679–691. doi: 10.1182/blood-2012-04-426734

Kleinschnitz, C., Pozgajova, M., Pham, M., Bendszus, M., Nieswandt, B., and Stoll, G. (2007). Targeting Platelets in Acute Experimental Stroke: impact of Glycoprotein Ib, VI, and IIb/IIIa Blockade on Infarct Size, Functional Outcome, and Intracranial Bleeding. *Circulation* 115, 2323–2330. doi: 10.1161/CIRCULATIONAHA.107.691279

Kono, H., and Rock, K. L. (2008). How dying cells alert the immune system to danger. *Nat. Rev. Immunol.* 8, 279–289. doi: 10.1038/nri2215

Konsman, J. P., Drukarch, B., and Van Dam, A.-M. (2007). (Peri)vascular production and action of pro-inflammatory cytokines in brain pathology. *Clin. Sci.* 112, 1–25. doi: 10.1042/CS20060043

Koupenova, M., Clancy, L., Corkrey, H. A., and Freedman, J. E. (2018). Circulating Platelets as Mediators of Immunity, Inflammation, and Thrombosis. *Circ. Res.* 122, 337–351. doi: 10.1161/CIRCRESAHA.117.310795

Koupenova, M., Kehrel, B. E., Corkrey, H. A., and Freedman, J. E. (2017). Thrombosis and platelets: an update. *Eur. Heart J.* 38, 785–791. doi: 10.1093/eurheartj/ehw550

Kraft, P., Schuhmann, M. K., Fluri, F., Lorenz, K., Zernecke, A., Stoll, G., et al. (2015). Efficacy and Safety of Platelet Glycoprotein Receptor Blockade in Aged and Comorbid Mice With Acute Experimental Stroke. *Stroke* 46, 3502–3506. doi: 10.1161/STROKEAHA.115.011114

Lam, F. W., Vijayan, K. V., and Rumbaut, R. E. (2015). "Platelets and Their Interactions with Other Immune Cells," in *Comprehensive Physiology*, ed. R. Terjung (Hoboken: Wiley), 1265–1280. doi: 10.1002/cphy.c140074

Li, P., Gan, Y., Sun, B.-L., Zhang, F., Lu, B., Gao, Y., et al. (2013). Adoptive regulatory T-cell therapy protects against cerebral ischemia: T-Cell Therapy for Ischemia. *Ann. Neurol.* 74, 458–471. doi: 10.1002/ana.23815

Liesz, A., Suri-Payer, E., Veltkamp, C., Doerr, H., Sommer, C., Rivest, S., et al. (2009b). Regulatory T cells are key cerebroprotective immunomodulators in acute experimental stroke. *Nat. Med.* 15, 192–199. doi: 10.1038/nm.1927

Liesz, A., Hagmann, S., Zschoche, C., Adamek, J., Zhou, W., Sun, L., et al. (2009a). The Spectrum of Systemic Immune Alterations After Murine Focal Ischemia: immunodepression Versus Immunomodulation. *Stroke* 40, 2849–2858. doi: 10.1161/STROKEAHA.109.549618

Linke, B., Schreiber, Y., Picard-Willems, B., Slattery, P., Nüsing, R. M., Harder, S., et al. (2017). Activated Platelets Induce an Anti-Inflammatory Response of Monocytes/Macrophages through Cross-Regulation of PGE 2 and Cytokines. *Mediat. Inflamm.* 2017, 1–14. doi: 10.1155/2017/1463216

Lipton, P. (1999). Ischemic Cell Death in Brain Neurons. *Physiol. Rev.* 79, 1431–1568. doi: 10.1152/physrev.1999.79.4.1431

Mackman, N., Tilley, R. E., and Key, N. S. (2007). Role of the extrinsic pathway of blood coagulation in hemostasis and thrombosis. *Arterioscler. Thromb. Vasc. Biol.* 27, 1687–1693. doi: 10.1161/ATVBAHA.107.141911

Maouia, A., Rebetz, J., Kapur, R., and Semple, J. W. (2020). The Immune Nature of Platelets Revisited. *Transfus. Med. Rev.* 34, 209–220. doi: 10.1016/j.tmrv.2020.09.005

Massberg, S., and von Andrian, U. H. (2006). Fingolimod and Sphingosine-1-Phosphate — Modifiers of Lymphocyte Migration. *N. Engl. J. Med.* 355, 1088–1091. doi: 10.1056/NEJMp068159

Mezger, M., Göbel, K., Kraft, P., Meuth, S. G., Kleinschnitz, C., and Langer, H. F. (2015). Platelets and vascular inflammation of the brain. *Hamostaseologie* 35, 244–251. doi: 10.5482/HAMO-14-11-0071

Morrell, C. N., Pariser, D. N., Hilt, Z. T., and Vega Ocasio, D. (2019). The Platelet Napoleon Complex-Small Cells, but Big Immune Regulatory Functions. *Annu. Rev. Immunol.* 37, 125–144. doi: 10.1146/annurev-immunol-042718-041607

Moura, R., and Tjwa, M. (2010). Platelets suppress Treg recruitment. *Blood* 116, 4035–4037. doi: 10.1182/blood-2010-09-303396

Na, S.-Y., Mracsko, E., Liesz, A., Hünig, T., and Veltkamp, R. (2015). Amplification of Regulatory T Cells Using a CD28 Superagonist Reduces Brain Damage After Ischemic Stroke in Mice. *Stroke* 46, 212–220. doi: 10.1161/STROKEAHA.114.007756

Nieswandt, B., Kleinschnitz, C., and Stoll, G. (2011). Ischaemic stroke: a thrombo-inflammatory disease?: ischaemic stroke: a thrombo-inflammatory disease? *J. Physiol.* 589, 4115–4123. doi: 10.1113/jphysiol.2011.212886

Planas, A. M., and Chamorro, A. (2009). Regulatory T cells protect the brain after stroke. *Nat. Med.* 15, 138–139. doi: 10.1038/nm0209-138

Powers, W. J. (2020). Acute Ischemic Stroke. *N. Engl. J. Med.* 383, 252–260. doi: 10.1056/NEJMcp1917030

Rawish, E., Nording, H., Münte, T., and Langer, H. F. (2020). Platelets as Mediators of Neuroinflammation and Thrombosis. *Front. Immunol.* 11:548631. doi: 10.3389/fimmu.2020.548631

Rossaint, J., Thomas, K., Mersmann, S., Skupski, J., Margraf, A., Tekath, T., et al. (2021). Platelets orchestrate the resolution of pulmonary inflammation in mice by T reg cell repositioning and macrophage education. *J. Exp. Med.* 218:e20201353. doi: 10.1084/jem.20201353

Rubenstein, D. A., and Yin, W. (2018). "Platelet-Activation Mechanisms and Vascular Remodeling," in *Comprehensive Physiology*, ed. R. Terjung (Hoboken: Wiley), 1117–1156. doi: 10.1002/cphy.c170049

Sacco, R. L., Kasner, S. E., Broderick, J. P., Caplan, L. R., Connors, J. J. B., Culebras, A., et al. (2013). An updated definition of stroke for the 21st century: a statement for healthcare professionals from the American Heart Association/American Stroke Association. *Stroke* 44, 2064–2089. doi: 10.1161/STR.0b013e318296aeca

Sakaguchi, S. (2000). Regulatory T cells: key controllers of immunologic self-tolerance. *Cell* 101, 455–458. doi: 10.1016/s0092-8674(00)80856-9

Schuhmann, M. K., Kraft, P., Stoll, G., Lorenz, K., Meuth, S. G., Wiendl, H., et al. (2015). CD28 Superagonist-Mediated Boost of Regulatory T Cells Increases Thrombo-Inflammation and Ischemic Neurodegeneration during the Acute Phase of Experimental Stroke. *J. Cereb. Blood Flow Metab.* 35, 6–10. doi: 10.1038/jcbfm.2014.175

Schuhmann, M. K., Stoll, G., Bieber, M., Vögtle, T., Hofmann, S., Klaus, V., et al. (2020). CD84 Links T Cell and Platelet Activity in Cerebral Thrombo-Inflammation in Acute Stroke. *Circ. Res.* 127, 1023–1035. doi: 10.1161/CIRCRESAHA.120.316655

Schwab, S. R., Pereira, J. P., Matloubian, M., Xu, Y., Huang, Y., and Cyster, J. G. (2005). Lymphocyte Sequestration Through S1P Lyase Inhibition and Disruption of S1P Gradients. *Science* 309, 1735–1739. doi: 10.1126/science.1113640

Shi, L., Sun, Z., Su, W., Xu, F., Xie, D., Zhang, Q., et al. (2021). Treg cell-derived osteopontin promotes microglia-mediated white matter repair after ischemic stroke. *Immunity* 54, 1527–1542.e8. doi: 10.1016/j.immuni.2021.04.022

Spitz, C., Winkels, H., Bürger, C., Weber, C., Lutgens, E., Hansson, G. K., et al. (2016). Regulatory T cells in atherosclerosis: critical immune regulatory function and therapeutic potential. *Cell. Mol. Life Sci.* 73, 901–922. doi: 10.1007/s00018-015-2080-2

Stanzione, R., Cotugno, M., Bianchi, F., Marchitti, S., Forte, M., Volpe, M., et al. (2020). Pathogenesis of Ischemic Stroke: role of Epigenetic Mechanisms. *Genes* 11:E89. doi: 10.3390/genes11010089

Veltkamp, R., Na, S.-Y., and Liesz, A. (2015). Response to Letter Regarding Article, "Amplification of Regulatory T Cells Using a CD28 Superagonist Reduces Brain Damage After Ischemic Stroke in Mice.". *Stroke* 46:e52. doi: 10.1161/STROKEAHA.114.008106

Wang, H., Ye, J., Cui, L., Chu, S., and Chen, N. (2022). Regulatory T cells in ischemic stroke. *Acta Pharmacol. Sin.* 43, 1–9. doi: 10.1038/s41401-021-00641-4

Wang, L., Wang, X., Lv, X., Jin, Q., Shang, H., Wang, C., et al. (2022). The extracellular Ero1α/PDI electron transport system regulates platelet function by increasing glutathione reduction potential. *Redox Biol.* 50:102244. doi: 10.1016/j.redox.2022.102244

Yilmaz, G., Arumugam, T. V., Stokes, K. Y., and Granger, D. N. (2006). Role of T Lymphocytes and Interferon-γ in Ischemic Stroke. *Circulation* 113, 2105–2112. doi: 10.1161/CIRCULATIONAHA.105.593046

Zhang, H., Xia, Y., Ye, Q., Yu, F., Zhu, W., Li, P., et al. (2018). In Vivo Expansion of Regulatory T Cells with IL-2/IL-2 Antibody Complex Protects against Transient Ischemic Stroke. *J. Neurosci.* 38, 10168–10179.

Zhang, J., Liu, G., Chen, D., Wang, Z., Chen, D., Liu, Y., et al. (2020). The combination of C C chemokine receptor type 5(CCR5) and Treg cells predicts prognosis in patients with ischemic stroke. *J. Neuroimmunol.* 349:577404. doi: 10.1016/j.jneuroim.2020.577404

Zhou, L., Lopes, J. E., Chong, M. M. W., Ivanov, I. I., Min, R., Victora, G. D., et al. (2008). TGF-β-induced Foxp3 inhibits TH17 cell differentiation by antagonizing RORγt function. *Nature* 453, 236–240. doi: 10.1038/nature06878

Zhu, L., Huang, Z., Stålesen, R., Hansson, G. K., and Li, N. (2014). Platelets provoke distinct dynamics of immune responses by differentially regulating CD4 + T-cell proliferation. *J. Thromb. Haemost.* 12, 1156–1165. doi: 10.1111/jth.12612

Zhu, Z., Fu, Y., Tian, D., Sun, N., Han, W., Chang, G., et al. (2015). Combination of the Immune Modulator Fingolimod With Alteplase in Acute Ischemic Stroke: A Pilot Trial. *Circulation* 132, 1104–1112. doi: 10.1161/CIRCULATIONAHA.115.016371

Conflict of Interest: The authors declare that the research was conducted in the absence of any commercial or financial relationships that could be construed as a potential conflict of interest.

frontiers | Frontiers in Cellular Neuroscience

TYPE Original Research
PUBLISHED 19 July 2022
DOI 10.3389/fncel.2022.911973

OPEN ACCESS

EDITED BY
Zhang Pengyue,
Yunnan University of Traditional Chinese Medicine, China

REVIEWED BY
Sachchida Nand Rai,
University of Allahabad, India
Changmeng Cui,
Jining Medical University, China
Baojian Xue,
The University of Iowa, United States

*CORRESPONDENCE
Zongmao Zhao
zzm692017@sina.com

†These authors have contributed equally to this work

SPECIALTY SECTION
This article was submitted to Cellular Neuropathology, a section of the journal Frontiers in Cellular Neuroscience

RECEIVED 03 April 2022
ACCEPTED 27 June 2022
PUBLISHED 19 July 2022

CITATION
Sun Z, Li Q, Li X, Shi Y, Nan C, Jin Q, Wang X, Zhuo Y and Zhao Z (2022) Casein kinase 2 attenuates brain injury induced by intracerebral hemorrhage via regulation of NR2B phosphorylation.
Front. Cell. Neurosci. 16:911973.
doi: 10.3389/fncel.2022.911973

Casein kinase 2 attenuates brain injury induced by intracerebral hemorrhage via regulation of NR2B phosphorylation

Zhimin Sun[1,2†], Qiyao Li[1†], Xiaopeng Li[1,3†], Yunpeng Shi[1], Chengrui Nan[1], Qianxu Jin[1], Xiaoyan Wang[1,4], Yayu Zhuo[1] and Zongmao Zhao[1*]

[1]Department of Neurosurgery, The Second Hospital of Hebei Medical University, Shijiazhuang, China, [2]Department of Neurosurgery, The Third Hospital of Shijiazhuang City, Shijiazhuang, China, [3]Department of Neurosurgery, The First Hospital of Handan City, Handan, China, [4]Department of Neurosurgery, Hebei General Hospital, Shijiazhuang, China

Objective: Intracerebral hemorrhage (ICH) is a common cerebrovascular disease with high incidence, disability, and mortality. Casein kinase 2 (CK2) is a serine/threonine kinase with hundreds of identified substrates and plays an important role in many diseases. This study aimed to explore whether CK2 plays protective roles in ICH-induced neuronal apoptosis, inflammation, and oxidative stress through regulation NR2B phosphorylation.

Methods: CK2 expression level of brain tissues taken from ICH patients was determined by immunoblotting. Neurons from embryonic rat and astrocytes from newborn rats were cultured and treated by Hemoglobin chloride (Hemin). The proliferation of astrocytes, the apoptosis and oxidative stress of neurons and the inflammatory factors of astrocytes were detected. CK2 expression was determined in ICH model rats. The effects of CK2 overexpression plasmid (pc-CK2) on neurobehavioral defects and brain water content in ICH rats were observed.

Results: CK2 expression in ICH patients was down-regulated. Overexpression of CK2 promoted the astrocyte proliferation, inhibited neuronal apoptosis, and reduced astrocyte-mediated inflammation. *N*-methyl-D-aspartate receptor 2B (NR2B) reversed the effects of pc-CK2 on neurons and astrocytes. CK2 phosphorylated NR2B at the S1480 site, down-regulated the expression of NR2B and interfered with the interaction between NR2B and postsynaptic density protein 95 (PSD95). *In vivo* experiments showed that the expression of CK2 decreased and the expression of NR2B increased in ICH rats. Furthermore, pc-CK2 attenuated neurobehavioral defects, brain water content and neuronal damage in ICH rats.

Conclusion: CK2 phosphorylated NR2B, down-regulated the expression of NR2B, interfered with the interaction between NR2B and PSD95, alleviated

inflammatory reactions, inhibited neuronal apoptosis and oxidative stress after ICH. CK2 and NR2B may be new potential therapeutic targets for the treatment of ICH. However, the limitation of this study is that we only investigated the regulation of NR2B by CK2.

KEYWORDS

intracerebral hemorrhage, NR2B, apoptosis, inflammation, oxidative stress

Introduction

Intracerebral hemorrhage (ICH) is caused by non-traumatic brain parenchymal vascular rupture and accounts for about 15 ∼ 20% of the total stroke cases. The mortality of ICH at the early stage is very high, and most survivors have severe sequelae such as motor cognitive and language impairment (Chen et al., 2018; Wilkinson et al., 2018; Marques et al., 2019). The etiology of ICH mainly includes cerebrovascular dysfunctions during pathological conditions such as hypertension, hyperlipidemia, diabetes, aging, smoking and drinking, etc. ICH induces a huge economic and social burden due to the increased incidence in young patients (Qureshi et al., 2001; Whiteley et al., 2012). However, there is no effective treatment for ICH with high mortality and disability (Murthy et al., 2017; Imai et al., 2021).

Clinical and animal studies have shown that ICH is closely related to inflammation, oxidative stress, neuronal apoptosis and blood brain barrier (BBB) damage after hematoma formation (Lee et al., 2017; Lan et al., 2019; Selim and Norton, 2020). Rapid accumulation of blood in the brain parenchyma, elevated intracranial pressure, and damaged neurons and glial cells may lead to an increase in neurotransmitter release, neuron membrane depolarization, and mitochondrial dysfunction (MacLellan et al., 2008). Subsequently, along with coagulation reaction, thrombin generation and decomposition of hemoglobin, glial cells are activated, which releases pro-inflammatory factors and causes excessive inflammatory response (Selim and Norton, 2020). At the same time, an increase in BBB permeability and blood-derived cerebral edema may also occur. All of these factors lead to serious neurological defects in patients, such as sensorimotor disorders, consciousness disorders, and even respiratory dysfunction (Zhu et al., 2018). These events lead to the deterioration of the prognosis of the ICH. In addition, the interruption of cerebral blood flow during cerebral hemorrhage result in severe neuronal damage. In the early stage of hemorrhage, the apoptosis proteins of caspase family in nerve cells of the central ischemic area are activated significantly to trigger apoptosis and irreversible damage of neurons (Sekerdag et al., 2018). Up to date, the main approach for clinical prevention and treatment of ICH is controlling hypertension and other risk factors. Thus, it is urgent to find new targets that play a vital role in the pathological mechanism of ICH.

Casein kinase2 (CK2) is a highly conserved phosphorylated serine/threonine kinase widely distributed in various eukaryotes with a variety of physiological functions (Filhol et al., 2004). CK2 is a hetero-tetramer composed of 2 α catalytic subunits and 2 β regulatory subunits. CK2 plays an important role in the regulation of hundreds of identified substrates and can use both ATP and GTP as phosphate donor kinases (Bolanos-Garcia et al., 2006; Dominguez et al., 2011). Studies have shown that mice with global knockout CK2α or CK2β cannot survive in the second trimester of pregnancy (Moreno-Romero et al., 2008; Landesman-Bollag et al., 2011; Abi Nahed et al., 2020), suggesting that CK2 plays a key role in their development. In addition, CK2 is involved in important biological processes such as circadian rhythm (Allada and Meissner, 2005), inflammation (Singh and Ramji, 2008), and cancer (Seldin et al., 2008; Dominguez et al., 2009). CK2 also plays an important role in cell processes, including cell proliferation and growth (Litchfield, 2003), cell survival (Ahmad et al., 2008), cell cycle progression (Padilla-Benavides et al., 2020), cell apoptosis and transcription (Meggio and Pinna, 2003; St-Denis and Litchfield, 2009), cell differentiation (Guerra and Issinger, 1999; Dietz et al., 2009), cell metabolism (Kramerov et al., 2008), etc. CK2 increases *N*-methyl-D-aspartate receptor (NMDAR) activity by upregulating *N*-methyl-D-aspartate receptor 2A (NR2A) and phosphorylating NR2B on S1480 at presynaptic and postsynaptic sites in the hypothalamus of spontaneous hypertension rat (SHR), which is a key factor in paraventricular nucleus of hypothalamus (PVN) presympathetic neuron over-excitability in hypertension (Ye et al., 2012). In ischemic brain injury, reduced CK2 expression induces a transfer of P47phox, P67phox and Rac1 to the cell membrane, resulting in activation of nicotinamide adenine dinucleotide phosphate (NADPH) oxidase, which in turn increases the production of reactive oxygen species (ROSs) and the up-regulation of NOX, mediating the death of neurons (Kim et al., 2009). However, the changes of CK2 mRNA and protein levels and the role of CK2 after ICH remain unclear.

Brain hemorrhage leads to a rapid increase in glutamate levels, which activates NMDAR, thereby damaging neurons.

NMDAR plays a crucial role in excitatory synaptic transmission and plasticity. The functional NMDAR usually consists of two NR1 subunits and two NR2 (NR2A-D) subunits (Lee et al., 2014). The NR2B subunit determines many of the functional properties of NMDAR. Multiple amino acid sites at the end of NR2B that can be phosphorylated play different roles in NMDAR-mediated injury. Phosphorylation of NR2B at the S1303 site exacerbates ischemia-induced neuronal death (Tu et al., 2010). Phosphorylation at the Tyr1472 site interferes with the binding of NR2B and adapter2 (AP2) protein leading to increased expression of NR2B on the cell membrane (Lavezzari et al., 2003). The phosphorylation of NR2B at S1480 site affects the binding of NR2B to PZD domain, which promotes the intracellular transfer of NMDA receptor and down-regulates the expression of NR2B (Chung et al., 2004). It has been shown that the NR2B subunit plays a key role in promoting neuronal death under ischemic conditions (Vieira et al., 2016). In addition, the PDZ ligand on the NR2B subunit binds to the PDZ structural domain of the scaffolding protein (PSD-95) to form the NR2B-PSD95 complex, which regulates downstream synaptic signaling and participates in NMDA receptor-mediated neuroexcitation and neurotoxicity (Lai et al., 2011). Therefore, in this study, we determined whether NR2B, NR2B phosphorylation and the NR2B-PSD95 complex play an important role in the regulation of cerebral hemorrhage by CK2.

This study aimed to explore whether CK2 plays protective roles in ICH-induced neuronal apoptosis, inflammation, and oxidative stress through regulation NR2B phosphorylation. First, we investigated whether CK2 is involved in the progression of ICH injury using patient samples, rat ICH model and cultured primary neurons and astrocytes. The potential neuroprotective mechanisms of CK2 *in vitro* and *in vivo* were further explored. In this study, we found that CK2 reduced inflammatory response, neuronal apoptosis, and oxidative stress levels after ICH through regulating NR2B phosphorylation, and subsequently changing NR2B expression and the level of NR2B-PSD95 complex. To our knowledge, this is the first study showing that CK2 protects brain tissue from damage caused by ICH.

Materials and methods

Patient tissue sample

In this study, the brain tissue specimens and clinical data of 10 healthy controls and 10 patients with ICH were collected and analyzed. All patients in this study were informed and signed consents according to the guidelines approved by the Ethics Committee of the second Hospital of Hebei Medical University. The inclusion criteria of the ICH group were 18–80 years old, without gender restriction, in accordance with the diagnostic criteria of ICH confirmed by CT, and no other autoimmune diseases. The National Institutes of Health Stroke scale (NIHSS) was 11.05 ± 3.46. The control group had no cerebral hemorrhagic disease and no history of neurological or neuropsychiatric diseases. The specimens were collected with the informed consent of the patient's family. After the brain tissue was removed, it was frozen in liquid nitrogen immediately. The brain tissues of all patients in the control group and cerebral hemorrhage group were used for mRNA and protein levels analysis.

Cultured neurons and astrocytes *in vitro*

On the 20th day of pregnancy, the fetal rats were taken by laparotomy, their brain tissue was taken out and put in ice-cold Hank's balanced salt solutions. Their cortex was collected and cut into small pieces of 1 × 1 × 3 mm. Then, the solution containing trimmed brain tissue blocks was shook at 37°C for 15 min, and the medium containing 10% fetal bovine serum (FBS) was added to terminate digestion. The tissue suspension was centrifuged at 1000 rpm for 2 min and the supernatant was removed and the pellets were re-suspended in a complete culture medium consisting of DMEM/high glucose, 10% FBS (Gibco, United States) and 1% penicillin-streptomycin solution (HyClone, United States). The neurons were placed in a 96-well plate coated with poly-lysine with a cell density of 5×10^5/ml. The cells were incubated at 37°C and 5% CO_2 for 4 h and then the complete medium was replaced with neural basic medium (Thermo, 2110304, United States), and half of the medium was changed with fresh medium every 3 days. In order to culture astrocytes, newborn rats within 24 h were anesthetized with isoflurane and the brain was removed under aseptic condition and placed in CMF-HBSS. Under anatomical microscope, the cerebral hemisphere was removed, meninges and blood vessels and other connective tissue were removed, and the tissue was cut into small pieces as finely as possible. These small pieces were immersed in trypsin solution to which DNase had been added. The solution was cultured at 37°C for 5 min, and the solution was ground repeatedly with a pipette until most of the chunks disappeared. The cell suspension was collected in the colloid medium (sciencell, 1801, United States) through the cell filter. The cells were centrifuged with 1,000 *g* for 2 min, the supernatant was discarded, and the cell particles were re-suspended in colloid medium. 2.5×10^6 cells were cultured in T25cm^2 flask and changed to fresh medium 24 h later. The culture medium was changed every 3 days. After 7–10 days, the astrocytes covered the bottom of the bottle. The bottle was shaken, the supernatant was removed, and the cells were passaged growing at the bottom of the culture bottle. The neurons and astrocytes cultured in 96-well plates were

treated with different concentrations of hemoglobin (Hemin) (Meilunbio, MB4829, Dalian, China). After 24 h, the cell viability was determined by CCK-8. The 20 μmol/L of Hemin was selected to establish the cell model of ICH *in vitro* (Levy et al., 2002). Follow-up experiments were performed at 24 h after the establishment of cell ICH model by Hemin.

CCK8 assay

According to the instructions of CCK kit (ZOMANBIO, ZP328, Beijing, China), CCK-8 assay was carried out to determine the cell proliferation ability or inhibition rate. The cells were cultured in 96-well plate and treated respectively by each group. The blank groups were used as controls. At the end of the treatment, the culture medium was replaced with 10% CCK-8 solution and incubated for 2 h, then the absorbance at 450 nm was measured and the cell viability of each group was calculated.

Western blot

The total protein was extracted from the striatum tissue around the hematoma and the cells of each group, and the concentration was determined by BCA. SDS-PAGE gel was made by dispensing gel kit (ZOMANBIO, ZD304A-1, Beijing, China). 20μg protein of each sample was loaded on SDS-PAGE. The protein was separated by electrophoresis and transferred to PVDF membrane (Roche, 03010040001, Switzerland). 5% milk blocked non-specific antigen for 1.5 h, and the membrane was incubated with appropriate diluted primary antibody overnight at 4°C. The main antibodies were used as follows: CK2 (Abcam, ab76040, 1:2000), NR2B (Cell Signaling, #14544, 1:500), NR2B (Tyr 1472) (Cell Signaling, #4208, 1:500), NR2B (phospho S1303) (Abcam, ab81271, 1:500), NR2B (phospho S1480) (Abcam, ab73014, 1:500), Caspase3 (GeneTex, GTX86952, 1:500), GAPDH (ABclonal, AC001, 1:50000). The PVDF membrane was incubated with fluorescent secondary antibody (ROCKLAND,611-145-002) at room temperature for 2 h the next day, and the Odyssey infrared laser scanning imaging system (LI-COR, United States) was used to image and store the PVDF membrane. The Photoshop software was used to measure the grayscale value of the stripe. The average optical density of the target protein was calculated with the gray value of GAPDH as the internal reference.

Relative CK2 activity measurement

The CycLex CK2 Kinase Assay/Inhibitor Screening Kit (MBL International Cat#CY-1170, Japan) was used to measure CK2 activity in brain lysates and cell lysates according to the manufacturer's instructions.

Cell transfection

To transfect CK2 and NR2B, primary cortical neurons and astrocytes were cultured in a 24-well petri dish. Gene overexpression lentivirus was purchased from Hanheng Biological Company (Shanghai, China). According to the manual of lentivirus, MOI = 200 was taken, and the corresponding volume of virus solution (volume of virus solution = MOI × number of cells/virus titer) was added, and the volume of culture medium was made up after 4 h. After 24 h, the culture medium was changed to complete medium and continued culture. Puromycin screening was carried out 48 h later, and 48 h after drug addition, puromycin was removed and fresh medium was replaced. When these petri dishes were full of cells, follow-up experiments were carried out.

RT-PCR

Total RNA was extracted using RNA extraction kit (Takara, Dalian, China) and the concentration of RNA was measured. Reverse transcription of RNA into cDNA using PrimeScript RT kit (Takara). cDNA was used as a template and the instructions provided by SYBR® Premix Ex TapTM II Kit (Takara) were followed for RT-qPCR. With GAPDH as the internal reference, the relative expression of the gene was calculated by $^{-\Delta\Delta Ct}$ method.

Transferase-mediated nick end labeling assay

According to the instructions of Meilun One Step transferase-mediated nick end labeling (TUNEL) Apoptosis Assay Kit (TRITC) (Meilunbio MA0224, Dalian, China), after the neurons of each group were fixed and permeated, the neurons were exposed to TUNEL detection solution for 1 h under the condition of avoiding light at 37°C. After PBS washing, the neurons were stained with DAPI (Sigma, D9542, United States) for 15 min at room temperature, and the photos were taken under fluorescence microscope (Leica, Germany). TUNEL staining showed that the nucleus was red and DAPI staining showed that the nucleus was blue. The percentage of TUNEL/DAPI was measured by ImageJ software to quantify apoptosis.

Enzyme-linked immunosorbent assay (ELISA)

The culture supernatant of astrocytes in each group was collected and the precipitate was removed by centrifugation. According to the ELISA detection kit (ABclonal, RK00029;

RK00020, China), the levels of tumor necrosis factor (TNF)-α and interleukin (IL)-6 in the supernatant were detected.

Oxidative stress detection

In order to detect reactive oxygen species (ROS), neuronal cells were cultured in 96-well petri dishes at 37? for 30 min, and Highly Sensitive DCFH-DA Dye (ROS Assay Kit -Highly Sensitive DCFH-DA-Dye, DOjinDO, R252) was added to each petri dish. After HBSS cleaned the petri dish, the fluorescence microscope (Leica, Germany) was used to take pictures. The fluorescence intensity and the relative content of ROS were measured by ImageJ software. In order to detect glutathione (GSH), superoxide dismutase (SOD) and oxidation marker malondialdehyde (MDA), the culture supernatants of neurons in each group were collected. The contents of GSH, MDA and SOD were detected by kit (Jiangsu Nanjing Jiancheng Institute of Biological Engineering, A006-2-1; A003-4-1; A001-3). Each reaction solution was added to a 96-well plate, and the absorbance at 405 nm was measured on a microplate reader, and the GSH content was calculated. The absorbance value at 530 nm was measured to calculate the MDA content. The absorbance at 450 nm was measured and the content of SOD was calculated. The experiment was repeated three times.

Co-immunoprecipitation

In order to determine the effects of Hemin and pc-CK2 on the interaction between NR2B and PSD95, we collected brain samples and samples of neurons and astrocytes from each group of rats for experiments. After homogenizing the samples, cool low osmotic buffers (1 mmol/L CaCl2, 20 mmol/L Tris, pH 7.4, 1 mmol/L MgCl2 and protease inhibitor mixture) were prepared for membrane preparation. The supernatant was centrifuged at 21,000 *g* for 30 min. The particles were re-suspended and dissolved in immunoprecipitation buffer (mixture of protease inhibitors, 0.5%NP-40, 250 mmol/L NaCl, 50 mmol/L Tris, pH 7.4), and the soluble fraction was pre-combined with protein G beads overnight at 4°C to pre-bind to rat anti-NR2B antibodies(Cell Signaling, #14544, 1:50). As a control, protein G beads were bound to rat immunoglobulin G (IgG) in advance. The immunoprecipitation samples were washed for three times, and then immunoblotting was performed with anti-PSD95 antibody (HUABIO, ET1602-20, 1:3000).

Animal and intracerebral hemorrhage model

The Sprague-Dawley (SD) male rats (age 8–10 weeks, weight 280–320 g) were obtained from the *Invivo* Biotech Co. td (Shijiazhuang, China). The rats were randomly placed in cages and fed with normal food, and the temperature (23 ± 1°C) and humidity (55 ± 2%) were controlled. All animal uses and research programs have been approved by the Ethics Committee of the Second Affiliated Hospital of Hebei Medical University. These rats were divided into Sham group, Sham + PC-CK2 group, ICH group, ICH + PC-NC group and ICH + PC-CK2 group. According to the study of GaryA. Rosenberg, MD (Rosenberg et al., 1990), the rat model of ICH was established by injecting collagenase into the striatum. Rats were anesthetized by intraperitoneal injection of 1% pentobarbital sodium (40 mg/kg) and fixed on the stereotactic frame (NeuroStar company, Germany). A skull hole of 1 mm in diameter was drilled at the posterior 0.24 mm of the anterior fontanelle and 3 mm on the right side of the midline, and 1 μ l collagenase (0.3 U/μl, type IV, Sigma-Aldrich, V900893) was injected into the right striatum (0.2 μ l/min) through the PE tube (62204, Shenzhen RWD Life Technology Co., Ltd.) with a microinjection pump (KDS310 American KDS Co., Ltd.). During the operation, the rats were placed on a heating blanket to maintain their body temperature at 37 ± 0.5°C. The animals in the sham operation group were only injected with 1 μl normal saline without collagenase IV. Three days before modeling, the right striatum of rats in Sham + pc-CK2 group, ICH + pc-CK2 group and ICH + pc-NC group were microinjected with lentivirus overexpression vectors pcDNA-CK2 and pcDNA NC (Hanheng Biology, Shanghai, China). The lentivirus titer was 1 × 108 U/mL, the injection dose was 0.1 ml, and the needle was retained for 5 min after injection.

Neurobehavioral score

Forelimb placement test, corner turn test and Bederson score were used to evaluate the neurological function within 10 days after the establishment of ICH model by collagenase. In the forelimb placement test, when the beard of the rats was rubbed with the edge of the table corner, the healthy rats could immediately put the ipsilateral forelimb above the table corner, while the contralateral motor function of ICH rats was impaired and might not be able to complete this action. Each animal was tested 10 times, and the percentage of times of correct placement of the forelimb was recorded (Hartman et al., 2009). During Corner Turn Test, the rats were placed in a 30-degree corner, and in order to get away from the corner, the rats could turn left or right, which was recorded, including only fully upright turns along either wall (that is, excluding abdominal pleats or horizontal turns). Repeated this 10 times to calculate the percentage of the right turn (Hua et al., 2002). Another behavioral test involved was the Bederson score, which was divided into four grades: no neurological impairment, (1) the contralateral forepaw could not be fully extended in the tail suspension test, (2) the forelimb's ability to resist contralateral thrust decreased, and (3) turned the contralateral circle (Bederson et al., 1986).

Determination of brain water content

Rats were anesthetized with pentobarbital (60 mg/kg) and the brains were dissected quickly. Three samples were obtained from the brain: ipsilateral hemisphere, contralateral hemisphere and cerebellum. The brain samples were immediately weighed on the electronic analytical balance (Sartorius, China) to obtain wet weight. The brain sample was then dried at 100°C for 24 h to obtain dry weight. The calculation formula is as follows: (wet weight-dry weight)/wet weight × 100%.

Statistical analysis

All the results came from at least three independent experiments. Statistical analysis was carried out with GraphPad Prism8 software. To determine the single comparison between the two groups, Student's *t*-test, One-way analysis of variance or Two-way ANOVA was used to compare the differences between multiple groups. All data are expressed by mean ± standard error, and a *p*-value of less than 0.05 was considered to be statistically significant.

Results

CK2 expression level was decreased in patients with intracerebral hemorrhage

In order to determine the CK2 expression levels in ICH patients, we measured the CK2 protein and mRNA levels in the brain tissues of 10 ICH patients. CK2 protein and mRNA levels were significantly lower in ICH tissues than those in control tissues ($P < 0.0001$; **Figures 1A,B**).

Changes of CK2 activity and protein level and NR2B phosphorylation level in brain tissue of intracerebral hemorrhage rats

In ICH rats induced by injection of collagenase IV into the striatum, CK2 activity was measured in tissue taken from damaged cerebral cortex and striatum and undamaged contralateral hemisphere at 24 h after the establishment of ICH model by collagenase. The CK2 activity of the two hemispheres in the sham operation control group was similar, but compared with the contralateral hemisphere, the CK2 activity in the ipsilateral hemisphere decreased significantly after ICH ($P < 0.0001$; **Figure 2A**). Furthermore, the levels of CK2 protein in the tissue around the hematoma was measured at 12, 24, 48, and 72 h after the establishment of ICH model by collagenase. The results showed that compared with the control group, CK2 protein was decreased after hemorrhage, especially at 24 h ($P < 0.001$; **Figure 2B**). The level of NR2B and its phosphorylation sites increased after ICH, especially at 24 h ($P < 0.0001$; **Figure 2C**).

Overexpression of CK2 alleviates brain injury in intracerebral hemorrhage rats

We further verified the effect of overexpression of CK2 on neurological function ICH rats. **Figure 3A** verified that CK2

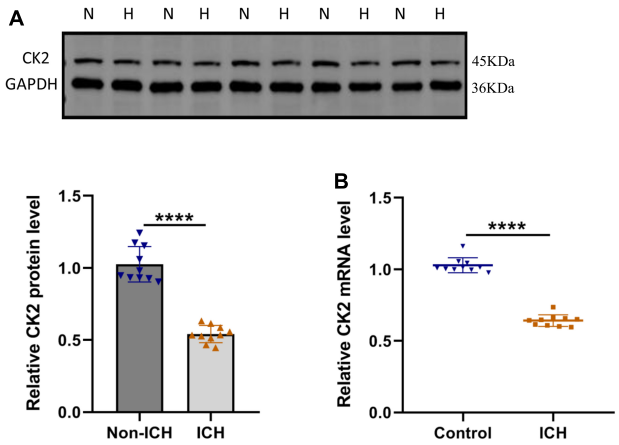

FIGURE 1
CK2 was downregulated in patients with intracerebral hemorrhage. **(A)** Representative blots and summary data show CK2 protein level in the brain tissues from ICH patients or non-hemorrhagic controls ($n = 10$). **(B)** Relative mRNA levels of CK2 were analyzed ($n = 10$). The experiment was repeated three times independently. Data were shown as mean ± SD and he values between groups were compared by Student's *t*-test. ****$P < 0.0001$.

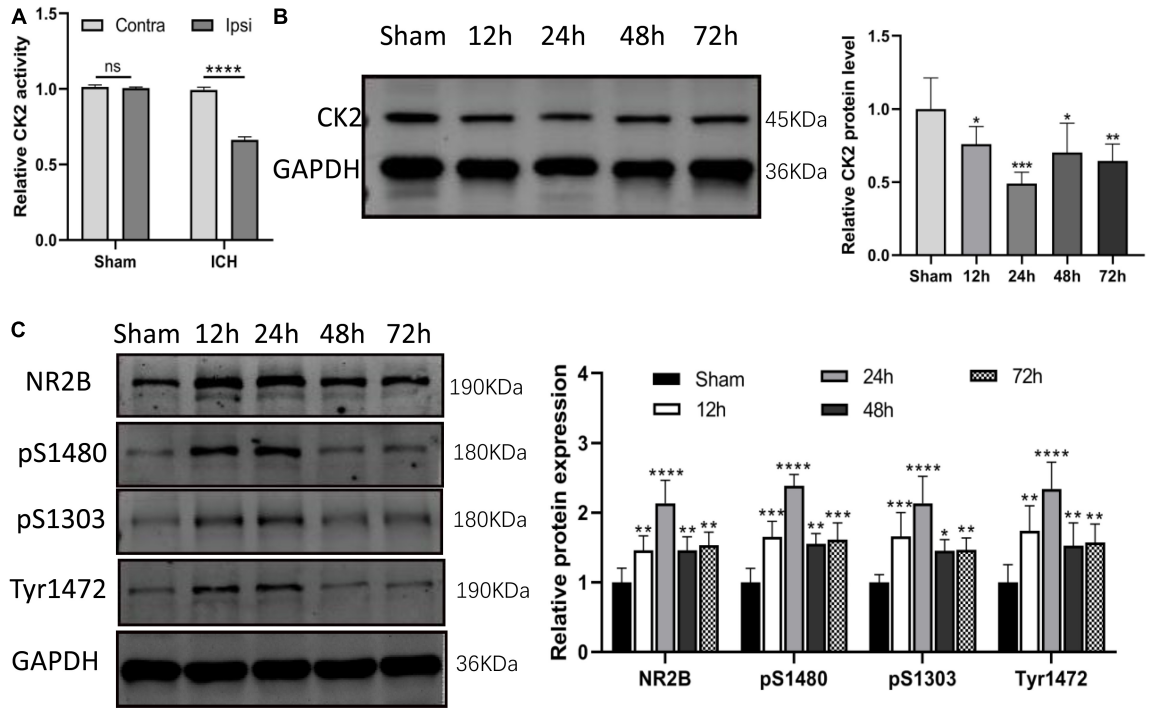

FIGURE 2
CK2 was downregulated in the brain tissues of ICH rats. **(A)** The CK2 activity in ipsilateral and contralateral hemisphere of sham and ICH groups (n = 3). **(B)** Expression of CK2 were determined 12, 24, 48, and 72 h after ICH in rats using Western blot. **(C)** Expression of NR2B, NR2B phosphorylation sites S1480, S1303, and Tyr1472 were determined 12, 24, 48, and 72 h after ICH in rats using Western blot (n = 6). Data were expressed as mean ± SD. *p < 0.05, **p < 0.01, ***p < 0.001, ****p < 0.0001.

was overexpressed by pcCK2 viral vector (P < 0.0001). The neurological function score was determined by Bederson scale, forelimb placement, and rotation angle tests. ICH + pc-NC rats showed a severe neurological impairment, which indicated that cortical and striatal functions were impaired and motor and sensory coordination was weakened. Pc-CK2 treatment significantly alleviated neurobehavioral impairment in ICH rats (all P < 0.001; Figure 3B). Compared with sham-operated rats, the brain water content in ICH group was increased (P < 0.001; Figure 3C), while pc-CK2 treatment decreased brain water content (P < 0.001; Figure 3C). Western Blot was used to detect the level of NR2B and its phosphorylation sites proteins, compared with ICH + pc-NC group, the expression level of NR2B protein in ICH + pc-CK2 group decreased (P = 0.0342; Figure 3D), on the contrary, the phosphorylation level of NR2B at S1480 site increased (P = 0.0259; Figure 3D). In addition, the level of NR2B-PSD95 complex decreased (detected by CO-IP; P = 0.0163; Figure 3E) and the level of apoptotic protein caspase3 decreased (P = 0.0017; Figure 3D). Thus, overexpression of CK2 significantly alleviated the neurological dysfunction in ICH rats, and reduced the neuronal injury in ICH rats by phosphorylating NR2B at S1480 site, down-regulating the expression of NR2B and interfering with the interaction between NR2B and PSD95.

The overexpression of CK2 enhanced the proliferation and activation of astrocytes and inhibited the apoptosis of neurons

In order to further understand the mechanisms of ICH and to explore effective targets for the treatment, we cultured neurons and astrocytes *in vitro* (Figure 4A). CCK8 experiment showed that with the extension of culture time, the OD value of cells increased, and the proliferation ability of astrocytes reached the peak on the 14th day (Figure 4B). In our cultures, the purity of neurons was more than 95%, and the positive expression of glial fibrillary acidic protein (GFAP) in astrocytes was higher than 95% (Figure 4C). Then, we treated neurons and astrocytes with Hemin, and detected the protein expression of CK2 and the activity of CK2. In the cells treated with Hemin, the expression of CK2 was lower than that of the control cells (P = 0.0065; P = 0.0439; Figure 4D), and the enzyme activity of CK2 was lower than that of the control cells (P < 0.001; P = 0.0011; Figure 4E).

In order to explore the role of CK2 overexpression in neurons and glial cells, we transfected pc-CK2 into neurons and glial cells treated with Hemin. RT-qPCR and Western Blot were used to confirm the transfection efficiency (P < 0.001,

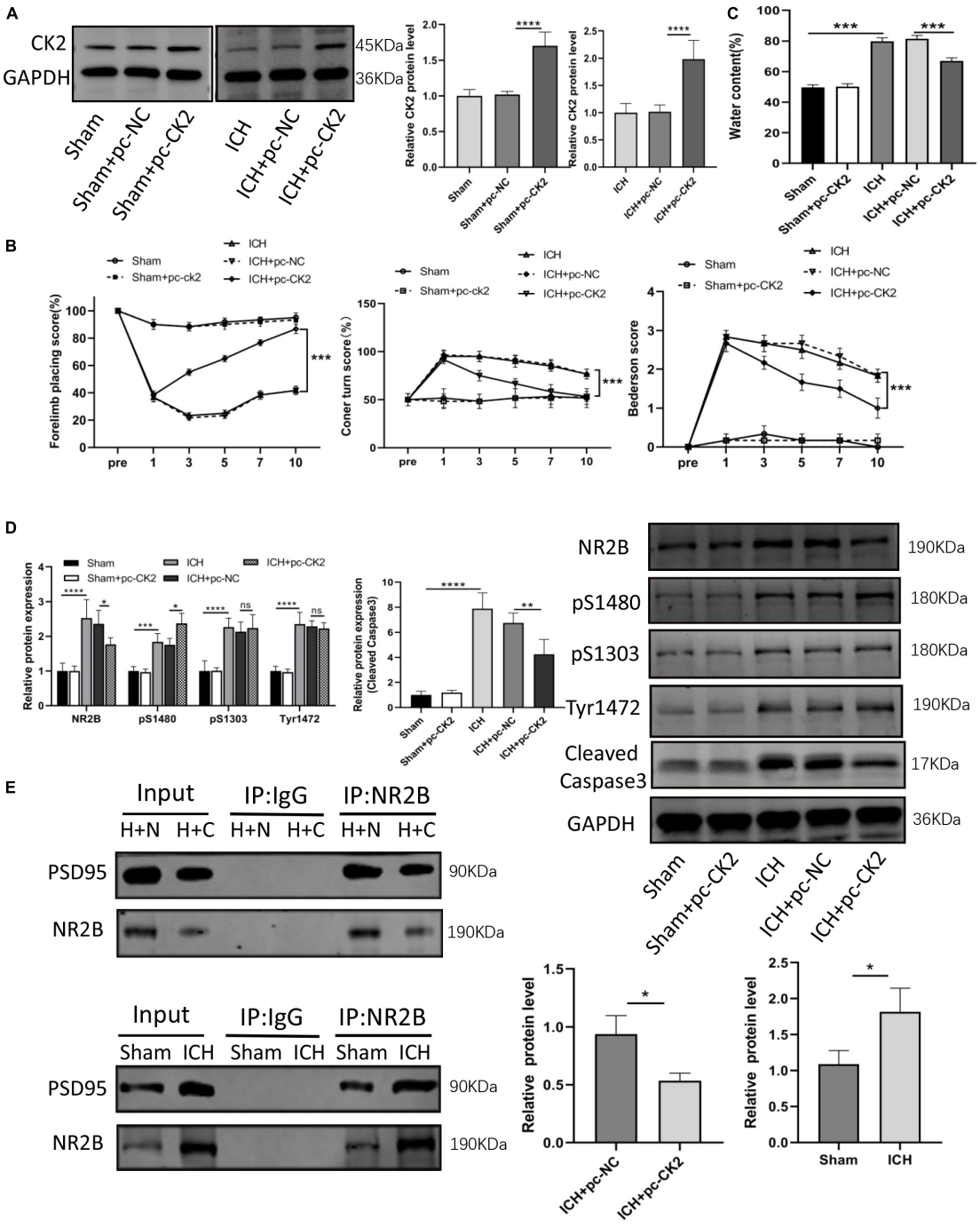

FIGURE 3
Overexpression of CK2 alleviated brain injury in ICH rats. pcDNA-CK2 and pcDNA-NC were transfected into ICH rats. **(A)** Expression of CK2 was detected using Western blot ($n = 6$). **(B)** Neurologic score was determined by the Forelimb placing test, corner turn test and Bederson score. **(C)** Analysis of brain edema. **(D)** Expression of cleaved caspase3, NR2B, NR2B phosphorylation sites S1480, S1303, and Tyr1472 were determined in rats using Western blot ($n = 6$). **(E)** Representative gel images and quantification of co-immunoprecipitation (co-IP) show the level of NR2B-PSD95 complex in rat brain tissues ($n = 3$). Data were expressed as mean ± standard deviation. *$p < 0.05$, **$p < 0.01$, ***$p < 0.001$, ****$p < 0.0001$.

Figure 5A; $P = 0.0052$, $P = 0.0014$, Figure 5B). We used CCK8 method to detect the proliferation of glial cells overexpressing CK2 and found that compared with the cells treated with Hemin + pc-NC, the cells treated with Hemin + pc-CK2 had a stronger ability of proliferation ($P < 0.0001$; Figure 5C). Then, we quantified the viability of CK2 overexpression

10.3389/fncel.2022.911973

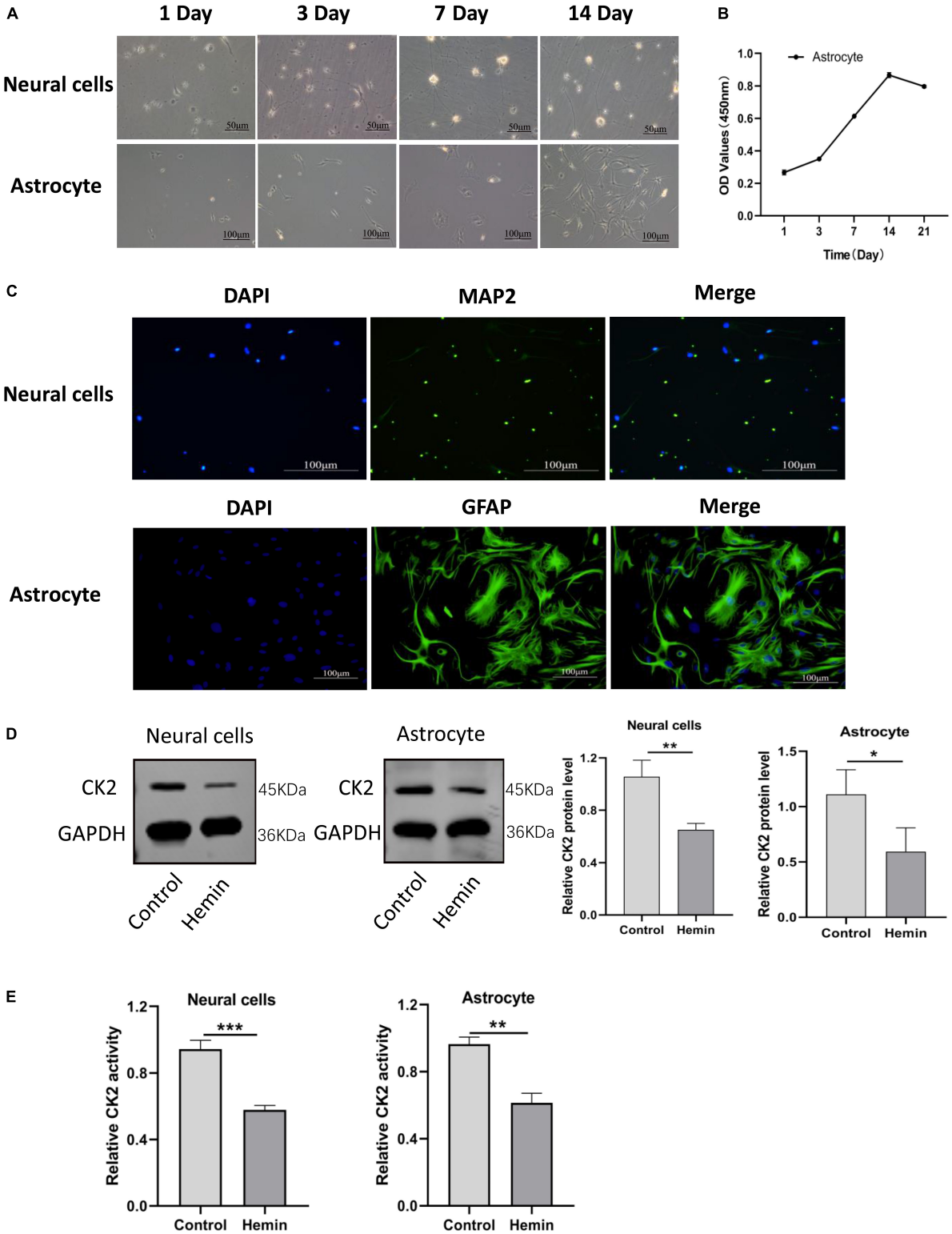

FIGURE 4
CK2 activity and expression levels were decreased in cultured neurons and astrocytes treated by hemin. **(A)** Morphological changes in neurons and astrocytes were observed. **(B)** Proliferation ability of astrocytes was detected using CCK8 assay. **(C)** Neurons and astrocytes were identified using immunofluorescence. **(D)** Hemin treatment decreased CK2 protein expressions levels in cultured neurons and astrocytes. **(E)** Hemin treatment decreased enzyme activity of CK2 in cultured neurons and astrocytes. The cell experiment was repeated three times independently. Data were expressed as mean ± SD. $*p < 0.05$, $**p < 0.01$, $***P < 0.001$.

neurons by CCK8 method, and detected the apoptosis of CK2 overexpression neurons by TUNEL staining. The results showed that compared with Hemin + pc-NC treatment, Hemin + pc-CK2 treatment significantly increased viability of neurons ($P < 0.0001$; **Figure 5D**). Compared with Hemin + pc-NC treated cells, Hemin + pc-CK2 treated cells had lower apoptosis rate ($P < 0.001$; **Figure 5E**). Thus, CK2 overexpression enhanced the proliferation and activation of glial cells and inhibited neuronal apoptosis.

The overexpression of CK2 reduced the inflammatory response of astrocytes and the oxidative stress of neurons

Neuroinflammation is a promising therapeutic target for hemorrhagic brain injury. We used ELISA to detect the levels of TNF-α and interleukin (IL)-6 in astrocytes. Compared with Hemin + pc-NC treated cells, Hemin + pc-CK2-treated cells showed decreased TNF-α and IL-6 levels (all $P < 0.0001$; **Figure 6A**). Inflammation could lead to oxidative stress in cells. We used fluorescence probe DCFH-DA to determine the content of reactive oxygen (ROS). After CK2 overexpression, the fluorescence of neurons treated with Hemin was decreased significantly ($P < 0.001$; **Figure 6B**). In addition, the levels of GSH, SOD, and MDA were detected by colorimetry. Compared with Hemin + pc-NC treated cells, Hemin + pc-CK2-treated cells showed increased levels of GSH and SOD and decreased levels of MDA ($P < 0.001$, **Figure 6C**; $P = 0.0016$, **Figure 6D**; $P < 0.001$, **Figure 6E**). Thus, CK2 overexpression reduced cellular inflammation and oxidative stress.

CK2 overexpression reduced cell inflammation, apoptosis and oxidative stress by affecting the level of NR2B phosphorylation and NR2B-PSD95 complex

We determined the level of NR2B and its phosphorylation were detected in hemin-treated neurons and astrocytes. NR2B expression and its phosphorylation in Hemin-treated cells was higher than that in control cells (all $P < 0.001$; **Figure 7A**). Compared with Hemin + pc-NC treated neurons and astrocytes, the expression of NR2B protein in Hemin + pc-CK2 treated neurons and astrocytes decreased ($P = 0.0414$, $P = 0.0049$; **Figure 7A**), on the contrary, the phosphorylation level of NR2B at S1480 site increased ($P = 0.0084$, $P < 0.001$; **Figure 7A**). Subsequently, we further detected the level of NR2B-PSD95 complex and found that the level of NR2B-PSD95 complex in Hemin + pc-CK2 group was lower than that in Hemin + pc-NC group ($P = 0.0040$, $P = 0.0155$; **Figure 7B**). These results suggested that pc-CK2 protect neurons and astrocytes against injury induced by Hemin through affecting the expression of NR2B protein and its phosphorylation level at S1480 site and interfering with the interaction between NR2B and PSD95. In addition, we transfected pc-NR2B into Hemin + pc-CK2-treated cells, and used RT-qPCR and WB experiments to confirm the transfection effect ($P < 0.001$, **Figure 7C**; $P = 0.0046$, $P = 0.0029$, **Figure 7D**). Compared with cells treated with Hemin + pc-CK2, the levels of TNF-α and IL-6, apoptosis rate and ROS levels of cells treated with Hemin + pc-CK2 + pc-NR2B were increased ($P < 0.001$, **Figures 7E,F**; $P = 0.0083$, **Figure 7G**). Thus, NR2B reversed the inflammatory, apoptotic and oxidative stress responses alleviated by CK2 overexpression after hemorrhagic injury.

Discussion

Intracerebral hemorrhage is an acute cerebrovascular disease with high morbidity, disability, and mortality. Up to date, the main treatment is to relieve the compression of hematoma on brain tissue, while no effective treatment to improve its prognosis exists (Murthy et al., 2017; Wilkinson et al., 2018). Primary and subsequent secondary brain injuries in ICH are often accompanied by varying degrees of nerve cell necrosis, apoptosis, inflammation and oxidative stress (Lan et al., 2019; Selim and Norton, 2020). The mechanism of nerve cell death and the expression of related regulatory genes remain unclear. Thus, information about pathogenesis including apoptosis, inflammatory response, oxidative stress and the regulatory mechanism of gene expression after ICH may provide new targets for treatment of ICH (Lan et al., 2019; Selim and Norton, 2020).

The brain tissue around the hematoma is subjected to compression and ischemia after ICH, and many cellular and molecular mechanisms are involved in neuronal damage (Lee et al., 2017). Specific mechanisms include the activation of excitatory amino acids and their receptors, persistent neuronal depolarization, release of inflammatory factors and activation of protein kinases (MacLellan et al., 2008). In the clinical samples of cerebral hemorrhage, we found that the expression of casein kinase CK2 was significantly down-regulated. Previous studies have shown that the inactivation of CK2 in mouse brain after cerebral ischemia increases the production of ROSs and the death of neurons by increasing the activity of NADPH oxidase (Kim et al., 2009). CK2 is a key regulator of NADPH oxidase and a neuroprotective agent after brain oxidative stress injury (Kim et al., 2009). The upregulation of synaptic *N*-methyl-D-aspartate receptor 2A (GluN2A) and the increase of NMDAR activity mediated by CK2 are the key factors for the hyperexcitability of hypothalamic paraventricular nucleus neurons (Ye et al., 2012). In addition, CK2 plays an important role in cellular processes,

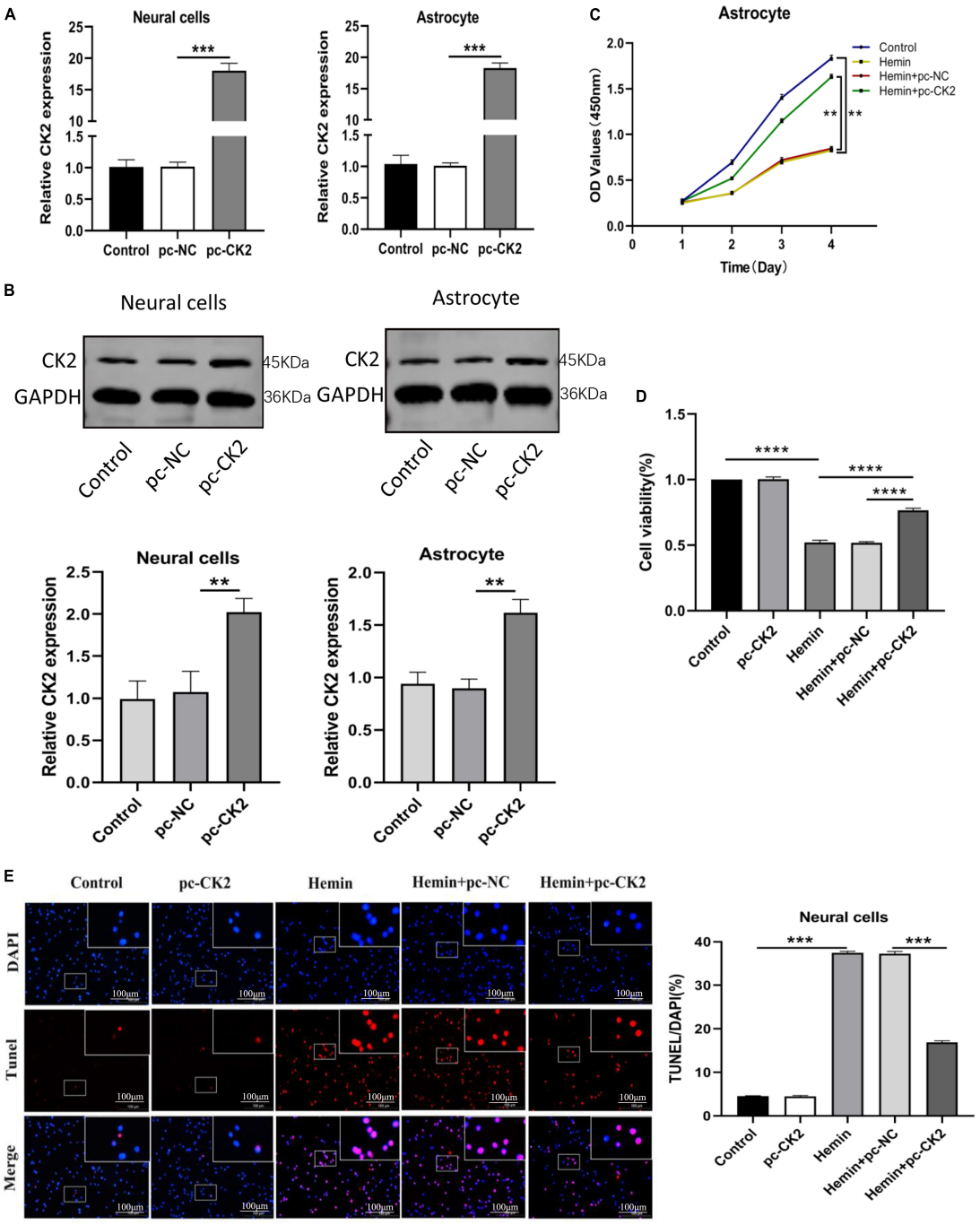

FIGURE 5
Overexpression of CK2 facilitated the proliferation of astrocytes, and inhibited apoptosis of neurons. pc-CK2 was transfected into Hemin-treated neurons and astrocytes. **(A)** Expressions of CK2 in cells were detected using RT-qPCR. **(B)** CK2 expression was detected using Western blot. **(C)** Proliferation ability of astrocytes was detected using CCK8 assay. **(D)** The viability of neurons was quantified by CCK8 assay. **(E)** Cell apoptosis was measured using TUNEL staining. The cell experiment was repeated three times independently. Data were expressed as mean ± SD. $^{**}p < 0.01$, $^{***}p < 0.001$, $^{****}p < 0.0001$.

important biological processes and development (Litchfield, 2003; Allada and Meissner, 2005; Moreno-Romero et al., 2008; Seldin et al., 2008; Singh and Ramji, 2008; Dominguez et al., 2009).

We found in ICH rats that CK2 activity in the ipsilateral hemisphere decreased significantly after ICH. In addition, NR2B expression levels were increased and the CK2 expression was decreased in ICH rats, and these changes reached a peak at 24 h

10.3389/fncel.2022.911973

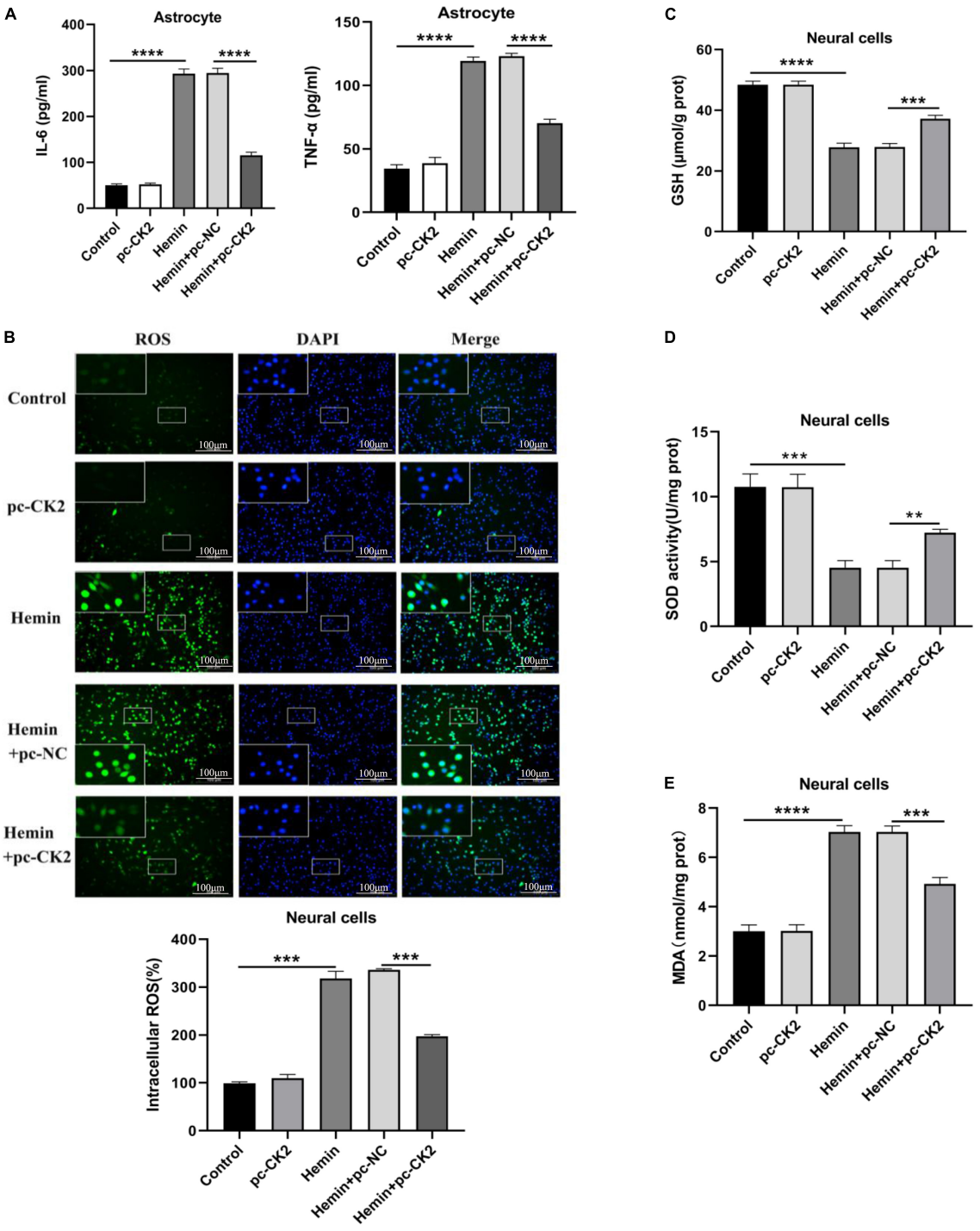

FIGURE 6
Overexpression of CK2 reduced cellular inflammation and alleviated oxidative stress. pc-CK2 was transfected into Hemin-treated neurons and astrocytes. **(A)** Levels of TNF-α and IL-6 in astrocytes were detected using ELISA. **(B)** Content of ROS was determined by fluorescence probe DCFH-DA. **(C–E)** Contents of GSH, SOD, and MDA were detected using the kits. The cell experiment was repeated three times independently. Data were expressed as mean ± SD. $^{**}p < 0.01$, $^{***}p < 0.001$, $^{****}p < 0.0001$.

after ICH. These data suggests that CK2 plays a regulatory role in hemorrhagic brain injury by affecting NR2B. Subsequent *in vivo* experiments further verified the effect of CK2 on ICH rats. Overexpression of CK2 alleviated neurobehavioral defects, brain water content and neuronal damage in ICH rats (Figures 3B,C). In addition, we found that CK2 overexpression decreased NR2B

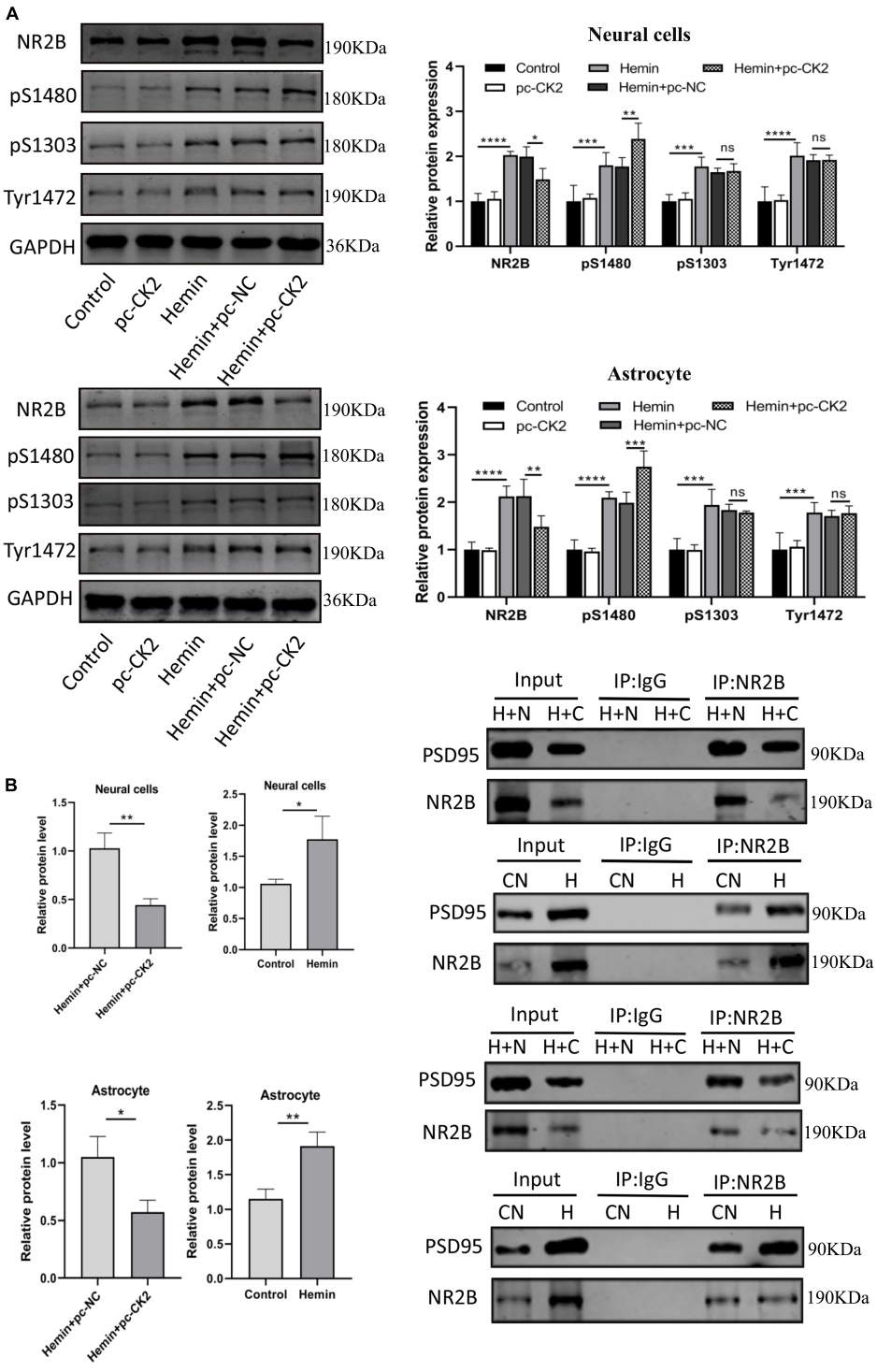

FIGURE 7
(Continued)

expression in ICH rats, up-regulated the phosphorylation level of NR2B at S1480 site, and decreased the level of NR2B-PSD95 complex. Furthermore, we found that CK2 overexpression reduced the neuronal apoptosis as indicated by a reduction of apoptotic protein caspase 3. In addition, NR2B protein level and its phosphorylation status at S1480 show the same trend in the ICH rat model (Figure 2C) but respond differently toward CK2 overexpression in ICH rats (Figure 3D). This may be

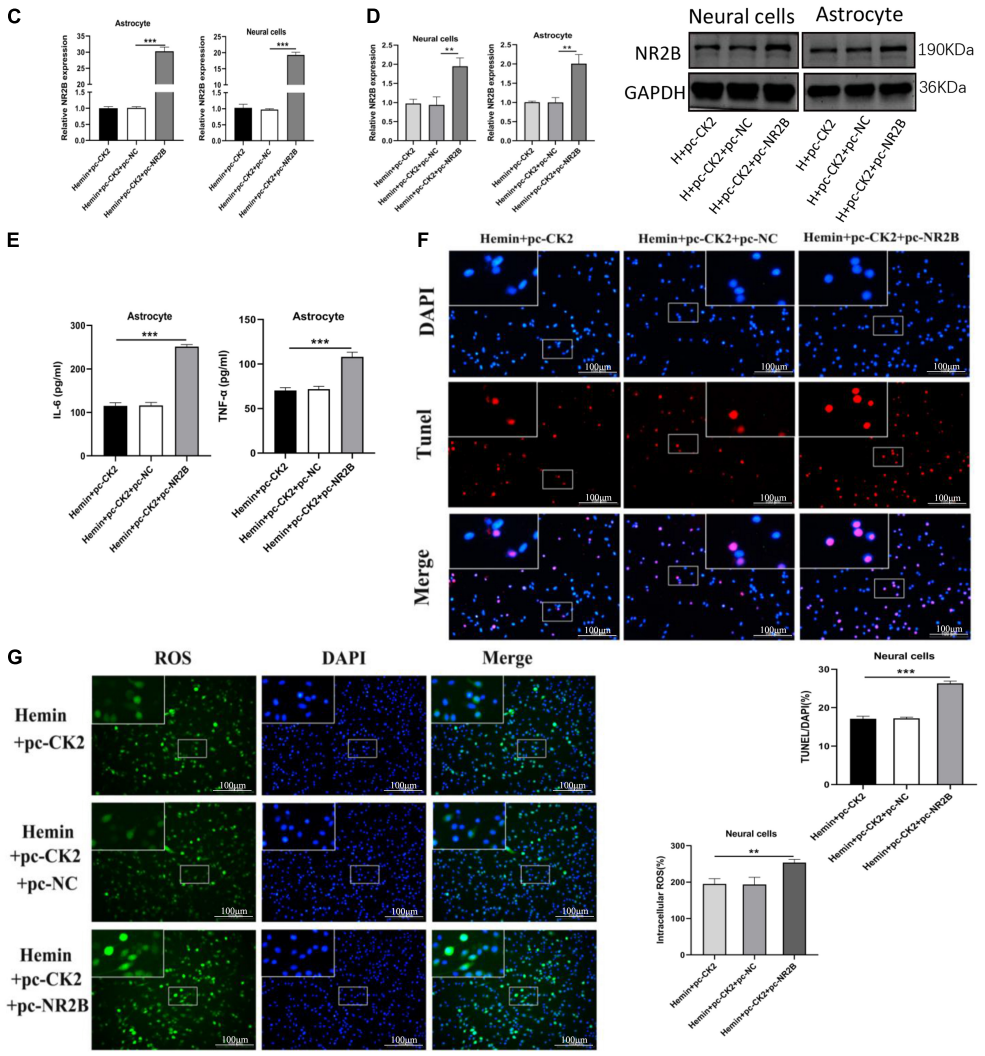

FIGURE 7
CK2 overexpression reduced cell inflammation, apoptosis and oxidative stress through changing NR2B phosphorylation level and NR2B-PSD95 complex. pc-NR2B was transfected into Hemin + pc-CK2 treated neurons and astrocytes. **(A)** Expression of NR2B, NR2B phosphorylation sites S1480, S1303, and Tyr1472 were determined in cells using Western blot. **(B)** Representative gel images and quantification of co-immunoprecipitation (co-IP) show the level of NR2B-PSD95 complex in cells. **(C)** Expressions of NR2B in cells were detected using RT-qPCR. **(D)** NR2B expression was detected using Western blot. **(E)** Levels of TNF-α and IL-6 in astrocytes were detected using ELISA. **(F)** Cell apoptosis was measured using TUNEL assay. **(G)** Content of ROS was determined by fluorescence probe DCFH-DA. The cell experiment was repeated three times independently. Data were expressed as mean ± standard deviation. $^{**}p < 0.01$, $^{***}p < 0.001$, $^{****}p < 0.0001$.

due to the fact that the phosphorylation of NR2B at the S1480 site may be affected by other kinases after cerebral hemorrhage (Chung et al., 2004).

To further determine the role of CK2 in ICH, we established a cell model of ICH by treating cultured primary neurons and astrocytes with Hemin. The expression level of CK2 protein and enzyme activity of CK2 in Hemin-treated cells were lower than in control cells. After ICH, the accumulation of blood leads to the increase of local pressure and the destruction of normal anatomical structure, and neurons are first affected by local compression and insufficient blood flow (MacLellan et al., 2008). Astrocytes are the most abundant cell types in brain tissue. They can provide nutrition for neurons, regulate cerebral blood flow, maintain the blood-brain barrier and regulate the level of extracellular glutamate. During brain injury, astrocytes are activated to produce neurotrophic factors and absorb excessive glutamine, thereby protecting neurons and reducing neuronal damage (Pan et al., 2016). In this study, we transfected lentivirus carrying CK2 gene (pc-CK2) into neurons and astrocytes treated with Hemin. The overexpression of CK2 enhanced the proliferation and activation of astrocytes and inhibited the apoptosis of neurons. It has been reported that inflammation plays a key role in the initiation, progression and recovery of ICH, and anti-inflammatory therapy reduces

hemorrhagic brain injury and promote cell survival in ICH (Lee et al., 2017; Lan et al., 2019; Selim and Norton, 2020). In addition, oxidative stress leads to neuronal apoptosis (MacLellan et al., 2008). Thus, inflammation and oxidative stress are effective interventional targets to treat ICH. Recent evidence suggests that CK2 plays an important role in controlling inflammation. For example, in patients with ulcerative colitis and Crohn's disease, CK2 can promote wound healing by inhibiting apoptosis under inflammatory conditions (Koch et al., 2013). CK2 activity inhibits the inflammatory response of myeloid cells. CK2 deficiency increases recruitment, activation and drug resistance of inflammatory myeloid cells after systemic Listeria monocytogenes (Lm) infection (Larson et al., 2020). In this study, we demonstrated that the overexpression of CK2 could reduce the inflammatory response of astrocytes and the oxidative stress of neurons.

Intracerebral hemorrhage leads to the release of a large number of endogenous molecules, including glutamate, Ca^{2+}, thrombin, hemoglobin, iron and IL-6, etc. (Iacobucci and Popescu, 2017; Marques Macedo and Gama Marques, 2020). The rapid increase of glutamate level in damaged brain tissue activates NMDAR to damage neurons. For many diseases, including cerebral hemorrhage, NMDAR plays an important role in excitatory synaptic transmission and plasticity in different brain regions (Lau and Zukin, 2007; Li et al., 2008). Functional NMDAR usually consists of two NR1 subunits and two NR2 (NR2A-D) subunits (Lee et al., 2014). NR2B subunit plays an important role in NMDAR-mediated injury. Several phosphorylated amino acid sites at NR2B subunit terminal can quickly regulate the opening rate of NMDAR and its expression on the cell membrane, and further affect its function. For example, the phosphorylation of NR2B at S1303 site can increase the opening rate of NMDAR and aggravate the neuronal death caused by ischemia (Tu et al., 2010). Phosphorylation of Tyr1472 site interferes with the binding of NR2B and AP2 proteins, resulting in an increase in the expression of NR2B on the cell membrane (Lavezzari et al., 2003). The phosphorylation of NR2B at S1480 site affects the binding of NR2B to PZD domain, which promotes the intracellular transfer of NMDA receptor and down-regulates the expression of NR2B (Chung et al., 2004). In this study, the levels of NR2B and its phosphorylated proteins in both *in vivo* and *in vitro* ICH models were significantly higher than those in the control group. CK2 overexpression treatment could down-regulate the expression of NR2B protein, up-regulate the phosphorylation level of NR2B at S1480 site, and decrease the level of NR2B-PSD95 complex. On the contrary, overexpression of CK2 had no effect on the phosphorylation of NR2B at S1303 and Tyr1472 sites. These results suggest that CK2 protects against hemorrhagic injury by affecting the expression of NR2B protein and its phosphorylation level at S1480 site and interfering with the interaction between NR2B and PSD95. In addition, we overexpressed NR2B in Hemin-pc-CK2-treated cells, and then assessed TUNEL apoptosis staining, ROS levels, and inflammatory cytokines TNF-α and IL-6 levels. As expected, NR2B reversed the cellular inflammation, apoptosis and oxidative stress reduced by CK2 overexpression after hemorrhagic injury.

Our results are the first study to show that CK2 plays a protective role in ICH-induced neuronal apoptosis, inflammation and oxidative stress through the regulation of NR2B phosphorylation. However, the limitation of this study is that we only investigated the regulation of NR2B by CK2. The regulation of CK2 in brain hemorrhage is a complex network involving multiple genes. In this study, we did not determine whether the nuclear factor (NF)-kB or NF-E2 related factor 2 (Nrf2) pathway is involved in the role of CK2 in cerebral hemorrhage. In addition, we did not investigate whether CK2 has other functions in brain hemorrhage, such as improving blood-brain barrier permeability and affecting autophagy. Therefore, we could not determine the possibility that other pathways are involved in the role of CK2 in cerebral hemorrhage, which deserves further investigation in future studies. In addition, the exact mechanism of CK2 effect on NR2B was not elucidated. Whether CK2-mediated phosphorylation of NR2B S1480, is regulated by other kinases or dependent on NMDAR's own activity needs to be further explored.

Conclusion

Our study provides new evidence to reveal the role of CK2-mediated NR2B phosphorylation in inflammatory response, neuron apoptosis and oxidative stress after hemorrhagic brain injury. This new information greatly improves our understanding of the molecular mechanism in the pathogenesis of ICH. Our findings indicate that CK2 and NR2B may be new potential therapeutic targets for the treatment of ICH.

Data availability statement

The original contributions presented in this study are included in the article/supplementary material, further inquiries can be directed to the corresponding author.

Ethics statement

The studies involving human participants were reviewed and approved by the Ethics Committee of the second Hospital of Hebei Medical University. The patients/participants provided their written informed consent to participate in this study. The animal study was reviewed and approved by the Ethics Committee of The Second Hospital of Hebei Medical University.

Author contributions

ZS and ZZ designed the study and wrote the manuscript. ZS, QL, XL, YS, CN, QJ, and XW performed the behavioral testing and experiments and analyzed the data. ZS, XL, YZ, and ZZ contributed to revising the manuscript. All authors read and approved the final manuscript.

Funding

This research was supported by the National Key R&D Program Intergovernmental Cooperation on International Scientific and Technological Innovation of the Ministry of Science and Technology of China (2017YFE0110400), the National Natural Science Foundation of China (81870984), Special Project for the Construction of Hebei Province International Science and Technology Cooperation Base (193977143D), Government funded Project on Training of Outstanding Clinical Medical Personnel and Basic Research Projects of Hebei Province in the Year of 2019, the Provincial Natural Science Foundation of Hebei (H2021206027), and the Provincial Natural Science Foundation of Hebei (H2021206003).

Conflict of interest

The authors declare that the research was conducted in the absence of any commercial or financial relationships that could be construed as a potential conflict of interest.

Publisher's note

All claims expressed in this article are solely those of the authors and do not necessarily represent those of their affiliated organizations, or those of the publisher, the editors and the reviewers. Any product that may be evaluated in this article, or claim that may be made by its manufacturer, is not guaranteed or endorsed by the publisher.

References

Abi Nahed, R., Reynaud, D., Lemaitre, N., Lartigue, S., Roelants, C., Vaiman, D., et al. (2020). Protein kinase CK2 contributes to placental development: physiological and pathological implications. *J. Mol. Med.* 98, 123–133. doi: 10.1007/s00109-019-01855-0

Ahmad, K. A., Wang, G., Unger, G., Slaton, J., and Ahmed, K. (2008). Protein kinase CK2–a key suppressor of apoptosis. *Adv. Enzyme Regul.* 48, 179–187. doi: 10.1016/j.advenzreg.2008.04.002

Allada, R., and Meissner, R. A. (2005). Casein kinase 2, circadian clocks, and the flight from mutagenic light. *Mol. Cell. Biochem.* 274, 141–149. doi: 10.1007/s11010-005-2943-1

Bederson, J. B., Pitts, L. H., Tsuji, M., Nishimura, M. C., Davis, R. L., and Bartkowski, H. (1986). Rat middle cerebral artery occlusion: evaluation of the model and development of a neurologic examination. *Stroke* 17, 472–476. doi: 10.1161/01.STR.17.3.472

Bolanos-Garcia, V. M., Fernandez-Recio, J., Allende, J. E., and Blundell, T. L. (2006). Identifying interaction motifs in CK2beta–a ubiquitous kinase regulatory subunit. *Trends Biochem. Sci.* 31, 654–661. doi: 10.1016/j.tibs.2006.10.005

Chen, G., Leak, R. K., Sun, Q., Zhang, J. H., and Chen, J. (2018). Neurobiology of stroke: research progress and perspectives. *Prog. Neurobiol.* 163-164, 1–4. doi: 10.1016/j.pneurobio.2018.05.003

Chung, H. J., Huang, Y. H., Lau, L. F., and Huganir, R. L. (2004). Regulation of the NMDA receptor complex and trafficking by activity-dependent phosphorylation of the NR2B subunit PDZ ligand. *J. Neurosci.* 24, 10248–10259. doi: 10.1523/JNEUROSCI.0546-04.2004

Dietz, K. N., Miller, P. J., and Hollenbach, A. D. (2009). Phosphorylation of serine 205 by the protein kinase CK2 persists on Pax3-FOXO1, but not Pax3, throughout early myogenic differentiation. *Biochemistry* 48, 11786–11795. doi: 10.1021/bi9012947

Dominguez, I., Degano, I. R., Chea, K., Cha, J., Toselli, P., and Seldin, D. C. (2011). CK2alpha is essential for embryonic morphogenesis. *Mol. Cell. Biochem.* 356, 209–216. doi: 0.1007/s11010-011-0961-8

Dominguez, I., Sonenshein, G. E., and Seldin, D. C. (2009). Protein kinase CK2 in health and disease: CK2 and its role in Wnt and NF-kappaB signaling: linking development and cancer. *Cell. Mol. Life Sci.* 66, 1850–1857. doi: 10.1007/s00018-009-9153-z

Filhol, O., Martiel, J. L., and Cochet, C. (2004). Protein kinase CK2: a new view of an old molecular complex. *EMBO Rep.* 5, 351–355. doi: 10.1038/sj.embor.7400115

Guerra, B., and Issinger, O. G. (1999). Protein kinase CK2 and its role in cellular proliferation, development and pathology. *Electrophoresis* 20, 391–408. doi: 10.1002/(SICI)1522-2683(19990201)20:2<391::AID-ELPS391>3.0.CO;2-N

Hartman, R., Lekic, T., Rojas, H., Tang, J., and Zhang, J. H. (2009). Assessing functional outcomes following intracerebral hemorrhage in rats. *Brain Res.* 1280, 148–157. doi: 10.1016/j.brainres.2009.05.038

Hua, Y., Schallert, T., Keep, R. F., Wu, J., Hoff, J. T., and Xi, G. (2002). Behavioral tests after intracerebral hemorrhage in the rat. *Stroke* 33, 2478–2484. doi: 10.1161/01.STR.0000032302.91894.0F

Iacobucci, G. J., and Popescu, G. K. (2017). NMDA receptors: linking physiological output to biophysical operation. *Nat. Rev. Neurosci.* 18, 236–249. doi: 10.1038/nrn.2017.24

Imai, T., Matsubara, H., and Hara, H. (2021). Potential therapeutic effects of Nrf2 activators on intracranial hemorrhage. *J. Cereb. Blood Flow Metab.* 41, 1483–1500. doi: 10.1177/0271678X20984565

Kim, G. S., Jung, J. E., Niizuma, K., and Chan, P. H. (2009). CK2 is a novel negative regulator of NADPH oxidase and a neuroprotectant in mice after cerebral ischemia. *J. Neurosci.* 29, 14779–14789. doi: 10.1523/JNEUROSCI.4161-09.2009

Koch, S., Capaldo, C. T., Hilgarth, R. S., Fournier, B., Parkos, C. A., and Nusrat, A. (2013). Protein kinase CK2 is a critical regulator of epithelial homeostasis in chronic intestinal inflammation. *Mucosal Immunol.* 6, 136–145.

Kramerov, A. A., Saghizadeh, M., Caballero, S., Shaw, L. C., Li Calzi, S., Bretner, M., et al. (2008). Inhibition of protein kinase CK2 suppresses angiogenesis and hematopoietic stem cell recruitment to retinal neovascularization sites. *Mol. Cell. Biochem.* 316, 177–186. doi: 10.1007/s11010-008-9831-4

Lai, T. W., Shyu, W. C., and Wang, Y. T. (2011). Stroke intervention pathways: NMDA receptors and beyond. *Trends Mol. Med.* 17, 266–275. doi: 10.1016/j.molmed.2010.12.008

Lan, X., Han, X., Liu, X., and Wang, J. (2019). Inflammatory responses after intracerebral hemorrhage: from cellular function to therapeutic targets. *J. Cereb. Blood Flow Metab.* 39, 184–186.

Landesman-Bollag, E., Belkina, A., Hovey, B., Connors, E., Cox, C., and Seldin, D. C. (2011). Developmental and growth defects in mice with combined deficiency

of CK2 catalytic genes. *Mol. Cell. Biochem.* 356, 227–231. doi: 10.1007/s11010-011-0967-2

Larson, S. R., Bortell, N., Illies, A., Crisler, W. J., Matsuda, J. L., and Lenz, L. L. (2020). Myeloid Cell CK2 Regulates Inflammation and Resistance to Bacterial Infection. *Front. Immunol.* 11:590266. doi: 10.3389/fimmu.2020.590266

Lau, C. G., and Zukin, R. S. (2007). NMDA receptor trafficking in synaptic plasticity and neuropsychiatric disorders. *Nat. Rev. Neurosci.* 8, 413–426. doi: 10.1038/nrn2153

Lavezzari, G., McCallum, J., Lee, R., and Roche, K. W. (2003). Differential binding of the AP-2 adaptor complex and PSD-95 to the C-terminus of the NMDA receptor subunit NR2B regulates surface expression. *Neuropharmacology* 45, 729–737. doi: 10.1016/S0028-3908(03)00308-3

Lee, C. H., Lu, W., Michel, J. C., Goehring, A., Du, J., Song, X., et al. (2014). NMDA receptor structures reveal subunit arrangement and pore architecture. *Nature* 511, 191–197. doi: 10.1038/nature13548

Lee, M. J., Cha, J., Choi, H. A., Woo, S. Y., Kim, S., Wang, S. J., et al. (2017). Blood-brain barrier breakdown in reversible cerebral vasoconstriction syndrome: implications for pathophysiology and diagnosis. *Ann. Neurol.* 81, 454–466.

Levy, Y. S., Streifler, J. Y., Panet, H., Melamed, E., and Offen, D. (2002). Hemin-induced apoptosis in PC12 and neuroblastoma cells: implications for local neuronal death associated with intracerebral hemorrhage. *Neurotox. Res.* 4, 609–616. doi: 10.1002/ana.24891

Li, D. P., Yang, Q., Pan, H. M., and Pan, H. L. (2008). Pre- and postsynaptic plasticity underlying augmented glutamatergic inputs to hypothalamic presympathetic neurons in spontaneously hypertensive rats. *J. Physiol.* 586, 1637–1647. doi: 10.1113/jphysiol.2007.149732

Litchfield, D. W. (2003). Protein kinase CK2: structure, regulation and role in cellular decisions of life and death. *Biochem. J.* 369, 1–15. doi: 10.1042/BJ20021469

MacLellan, C. L., Silasi, G., Poon, C. C., Edmundson, C. L., Buist, R., Peeling, J., et al. (2008). Intracerebral hemorrhage models in rat: comparing collagenase to blood infusion. *J. Cereb. Blood Flow Metab.* 28, 516–525. doi: 10.1038/sj.jcbfm.9600548

Marques Macedo, I., and Gama Marques, J. (2020). Catatonia secondary to anti-N-methyl-D-aspartate receptor (NMDAr) encephalitis: a review. *CNS Spectr.* 25, 475–492. doi: 10.1017/S1092852919001573

Marques, B. L., Carvalho, G. A., Freitas, E. M. M., Chiareli, R. A., Barbosa, T. G., Di Araujo, A. G. P., et al. (2019). The role of neurogenesis in neurorepair after ischemic stroke. *Semin. Cell Dev. Biol.* 95, 98–110. doi: 10.1016/j.semcdb.2018.12.003

Meggio, F., and Pinna, L. A. (2003). One-thousand-and-one substrates of protein kinase CK2? *FASEB J.* 17, 349–368. doi: 10.1096/fj.02-0473rev

Moreno-Romero, J., Espunya, M. C., Platara, M., Arino, J., and Martinez, M. C. (2008). A role for protein kinase CK2 in plant development: evidence obtained using a dominant-negative mutant. *Plant J.* 55, 118–130. doi: 10.1111/j.1365-313X.2008.03494.x

Murthy, S. B., Gupta, A., Merkler, A. E., Navi, B. B., Mandava, P., Iadecola, C., et al. (2017). Restarting Anticoagulant Therapy After Intracranial Hemorrhage: A Systematic Review and Meta-Analysis. *Stroke* 48, 1594–1600. doi: 10.1161/STROKEAHA.116.016327

Padilla-Benavides, T., Haokip, D. T., Yoon, Y., Reyes-Gutierrez, P., Rivera-Perez, J. A., and Imbalzano, A. N. (2020). CK2-Dependent Phosphorylation of the Brg1 Chromatin Remodeling Enzyme Occurs during Mitosis. *Int. J. Mol. Sci.* 21:923. doi: 10.3390/ijms21030923

Pan, Q., He, C., Liu, H., Liao, X., Dai, B., Chen, Y., et al. (2016). Microvascular endothelial cells-derived microvesicles imply in ischemic stroke by modulating astrocyte and blood brain barrier function and cerebral blood flow. *Mol. Brain* 9:63. doi: 10.1186/s13041-016-0243-1

Qureshi, A. I., Tuhrim, S., Broderick, J. P., Batjer, H. H., Hondo, H., and Hanley, D. F. (2001). Spontaneous intracerebral hemorrhage. *N. Engl. J. Med.* 344, 1450–1460. doi: 10.1056/NEJM200105103441907

Rosenberg, G. A., Mun-Bryce, S., Wesley, M., and Kornfeld, M. (1990). Collagenase-induced intracerebral hemorrhage in rats. *Stroke* 21, 801–807. doi: 10.1161/01.STR.21.5.801

Sekerdag, E., Solaroglu, I., and Gursoy-Ozdemir, Y. (2018). Cell Death Mechanisms in Stroke and Novel Molecular and Cellular Treatment Options. *Curr. Neuropharmacol.* 16, 1396–1415. doi: 10.2174/1570159X16666180302115544

Seldin, D. C., Lou, D. Y., Toselli, P., Landesman-Bollag, E., and Dominguez, I. (2008). Gene targeting of CK2 catalytic subunits. *Mol. Cell. Biochem.* 316, 141–147. doi: 10.1007/s11010-008-9811-8

Selim, M., and Norton, C. (2020). Perihematomal edema: implications for intracerebral hemorrhage research and therapeutic advances. *J. Neurosci. Res.* 98, 212–218. doi: 10.1002/jnr.24372

Singh, N. N., and Ramji, D. P. (2008). Protein kinase CK2, an important regulator of the inflammatory response? *J. Mol. Med.* 86, 887–897. doi: 10.1007/s00109-008-0352-0

St-Denis, N. A., and Litchfield, D. W. (2009). Protein kinase CK2 in health and disease: from birth to death: the role of protein kinase CK2 in the regulation of cell proliferation and survival. *Cell. Mol. Life Sci.* 66, 1817–1829. doi: 10.1007/s00018-009-9150-2

Tu, W., Xu, X., Peng, L., Zhong, X., Zhang, W., Soundarapandian, M. M., et al. (2010). DAPK1 interaction with NMDA receptor NR2B subunits mediates brain damage in stroke. *Cell* 140, 222–234. doi: 10.1016/j.cell.2009.12.055

Vieira, M. M., Schmidt, J., Ferreira, J. S., She, K., Oku, S., Mele, M., et al. (2016). Multiple domains in the C-terminus of NMDA receptor GluN2B subunit contribute to neuronal death following in vitro ischemia. *Neurobiol. Dis.* 89, 223–234.

Whiteley, W. N., Slot, K. B., Fernandes, P., Sandercock, P., and Wardlaw, J. (2012). Risk factors for intracranial hemorrhage in acute ischemic stroke patients treated with recombinant tissue plasminogen activator: a systematic review and meta-analysis of 55 studies. *Stroke* 43, 2904–2909.

Wilkinson, D. A., Pandey, A. S., Thompson, B. G., Keep, R. F., Hua, Y., and Xi, G. (2018). Injury mechanisms in acute intracerebral hemorrhage. *Neuropharmacology* 134, 240–248.

Ye, Z. Y., Li, L., Li, D. P., and Pan, H. L. (2012). Casein kinase 2-mediated synaptic GluN2A up-regulation increases N-methyl-D-aspartate receptor activity and excitability of hypothalamic neurons in hypertension. *J. Biol. Chem.* 287, 17438–17446. doi: 10.1074/jbc.M111.331165

Zhu, W., Gao, Y., Wan, J., Lan, X., Han, X., Zhu, S., et al. (2018). Changes in motor function, cognition, and emotion-related behavior after right hemispheric intracerebral hemorrhage in various brain regions of mouse. *Brain Behav. Immun.* 69, 568–581.

frontiers | Frontiers in Cellular Neuroscience

TYPE Review
PUBLISHED 02 September 2022
DOI 10.3389/fncel.2022.982881

OPEN ACCESS

EDITED BY
Zhang Pengyue,
Yunnan University of Traditional Chinese Medicine, China

REVIEWED BY
Lei Jiang,
Hannover Medical School, Germany
Fei Yan,
Shenzhen Institute of Advanced Technology (CAS), China
Rong Jing,
Yanan University Affiliated Hospital, China

*CORRESPONDENCE
Jie Jia
shannonjj@126.com

SPECIALTY SECTION
This article was submitted to Cellular Neuropathology, a section of the journal Frontiers in Cellular Neuroscience

RECEIVED 30 June 2022
ACCEPTED 12 August 2022
PUBLISHED 02 September 2022

CITATION
Jia J (2022) Exploration on neurobiological mechanisms of the central–peripheral–central closed-loop rehabilitation. *Front. Cell. Neurosci.* 16:982881. doi: 10.3389/fncel.2022.982881

Exploration on neurobiological mechanisms of the central–peripheral–central closed-loop rehabilitation

Jie Jia[1,2,3,4,5]*

[1]Department of Rehabilitation Medicine, Huashan Hospital, Fudan University, Shanghai, China, [2]National Center for Neurological Disorders, Shanghai, China, [3]National Clinical Research Center for Aging and Medicine, Huashan Hospital, Fudan University, Shanghai, China, [4]National Regional Medical Center, Fujian, China, [5]The First Affiliated Hospital of Fujian Medical University, Fujian, China

Central and peripheral interventions for brain injury rehabilitation have been widely employed. However, as patients' requirements and expectations for stroke rehabilitation have gradually increased, the limitations of simple central intervention or peripheral intervention in the rehabilitation application of stroke patients' function have gradually emerged. Studies have suggested that central intervention promotes the activation of functional brain regions and improves neural plasticity, whereas peripheral intervention enhances the positive feedback and input of sensory and motor control modes to the central nervous system, thereby promoting the remodeling of brain function. Based on the model of a central–peripheral–central (CPC) closed loop, the integration of center and peripheral interventions was effectively completed to form "closed-loop" information feedback, which could be applied to specific brain areas or function-related brain regions of patients. Notably, the closed loop can also be extended to central and peripheral immune systems as well as central and peripheral organs such as the brain–gut axis and lung–brain axis. In this review article, the model of CPC closed-loop rehabilitation and the potential neuroimmunological mechanisms of a closed-loop approach will be discussed. Further, we highlight critical questions about the neuroimmunological aspects of the closed-loop technique that merit future research attention.

KEYWORDS

central–peripheral–central, closed-loop rehabilitation, stroke, neuro-immune communication, rehabilitation intervention

Introduction

Concept and development of the theory of central–peripheral–central closed-loop rehabilitation

Proposed in 2016 (Jia, 2016), the CPC closed-loop rehabilitation theory refers to the assessment and therapy consisting of central rehabilitation methods and peripheral procedures. In this novel rehabilitation model, brain plasticity and rehabilitation efficacy following brain injury can be bidirectionally boosted with positive feedback. Related devices can combine input and output capabilities; for example, in the context of a brain–computer interface (BCI), a "closed loop" often refers to the provision of different kinds of feedback, such as proprioceptive feedback and tactile feedback, to the user through vision or other sensory modalities, but can more generally include feedback through any of the artificial input channels.

Long-term rehabilitation is essential for patients with motor dysfunction following a stroke to enable re-learning of motor function and conversion of motor capacity to daily living (Bernhardt et al., 2020). Motor rehabilitation tools for stroke patients mainly focus on peripheral intervention in early years, which include the traditional four major techniques based on the theory of cortical plasticity, which are the Bobath, Brunnstrom, proprioceptive neuromuscular facilitation, and Rood techniques (Huseyinsinoglu et al., 2012; Chen and Shaw, 2014), and new techniques derived from them, such as occupational therapy, compulsory movement therapy, bilateral interventions, anti-spasticity therapy, biofeedback techniques, and electrical stimulation techniques. However, a Cochrane systematic review (French et al., 2016; Legg et al., 2017) reported that the effectiveness of conventional rehabilitation treatment for motor dysfunction in stroke patients is poor, the quality of clinical studies is low, and the rehabilitation effect in many cases is still not evident after the above treatments. With the progression of medical–industrial integration, attempts were made to rehabilitate patients for whom peripheral interventions were ineffective by directly stimulating neural activity in the brain through a top–down approach. Instead of generating feedback through training of the affected limb, this approach employs various evoked modalities to generate central stimulation of the brain injury area to activate neural activity in the relevant brain regions and promote recovery of the patient's motor function. The central stimulation modalities currently used for stroke motor dysfunction rehabilitation are mainly non-invasive stimulation, including transcranial direct current stimulation (tDCS), transcranial magnetic stimulation (TMS), mirror therapy (MT), mental imagery (MI), BCI, and transcranial ultrasound stimulation (TUS). Systematic reviews have reported that non-invasive stimulation is effective in improving motor function and daily activities in stroke patients, but its mechanism of action remains controversial (Kang et al., 2016).

Neither top–down nor bottom–up interventions can create a closed-loop effect of stimulation for patients' rehabilitation. However, the CPC treatment model proposed by the team in 2016 theoretically suggests a closed-loop rehabilitation of CPC for motor dysfunction in stroke (Jia, 2016). The closed-loop rehabilitation theory (**Figure 1**) refers to the combination of the aforementioned central interventions with peripheral interventions to form a positive feedback loop and promote motor function rehabilitation in stroke patients.

Based on the "CPC closed-loop" rehabilitation theory that Jia proposed previously (Jia, 2016), Jia's team have explored novel application paradigms for stroke rehabilitation. In 2018, we stimulated the spastic muscle groups of the upper limbs after stroke through repetitive peripheral magnetic stimulation (rPMS) and found that rPMS could reduce the spastic state of the upper limb muscles in patients and observed central brain wave changes by electroencephalography (EEG; Chen et al., 2020b). In the same year, we used tDCS combined with upper limb functional electrical stimulation training and found that this intervention technique, which is based on closed-loop rehabilitation theory, could promote the rehabilitation of upper limb motor function in stroke patients (Shaheiwola et al., 2018). Another main application paradigm is camera-based mirror therapy visual feedback (camMVF), which has been proved to enhance limb and brain functions for stroke recovery. In 2018, we also verified the effect of camMVF for improving upper limb function after stroke (Ding et al., 2018). In 2019, we further determined that camMVF-based priming could improve the motor and daily functions of stroke and enhance brain network segregation (Ding et al., 2019). In 2021, we found that camMVF had a priming effect on robot-assisted training to facilitate rehabilitation for people with stroke (Rong et al., 2021). Additionally, we put forward the concept of "associated MT" (Zhuang et al., 2021), a novel paradigm based on camMVF, which could achieve a bimanual cooperation task under camMVF circumstances.

Considering the closed-loop BCI, we have performed several studies to explore its feasibility and clinical and sub-clinical efficacy. Since 2012, we have tested the effects of BCI in the recovery of upper limb motor function and cognitive function after stroke (Li et al., 2012a,b). In 2013, we found that neurofeedback-based BCI could improve the upper limb motor function of stroke patients and enhanced the event-related desynchronization (ERD) intensity of the ipsilesional hemisphere (Li et al., 2013). During 2014 and 2015, we reported some BCI schemes and strategies (Li et al., 2014; Liu et al., 2014; Xia et al., 2015). After that, in 2016, we again explored the clinical effects of electrical stimulation-based and exoskeleton-based BCI on stroke patients (Chen et al., 2016; Li et al., 2016). In 2017, we reviewed the application progress of BCI

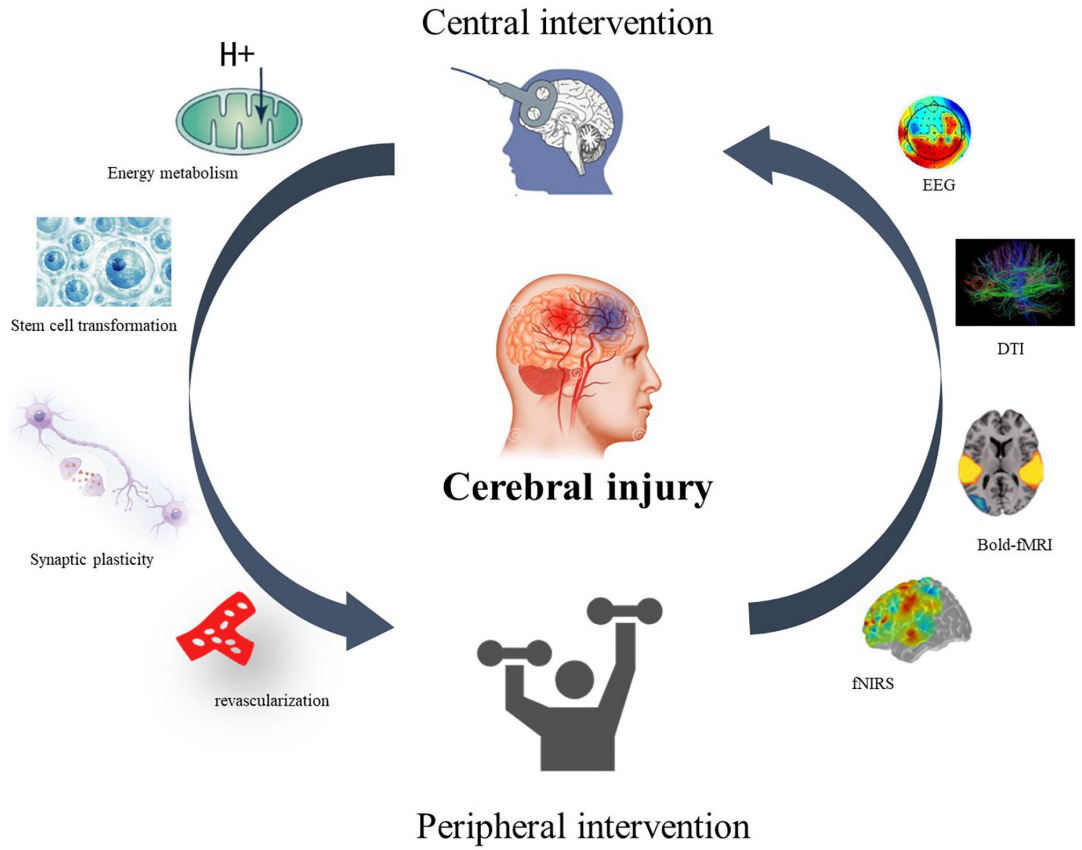

FIGURE 1
Closed-loop rehabilitation theory. A central–peripheral closed-loop intervention model for motor dysfunction after stroke. The therapeutic effect and mechanism can be reflected by EEG, neuroimaging, cerebral blood oxygen content, synaptic remodeling, energy metabolism, and stem cell transformation.

in hand functional rehabilitation of stroke patients (Jia, 2017). In 2018, we proposed a fast way to detect BCI-inefficient users by using physiological features from EEG signals (Shu et al., 2018b). In 2019, we used tactile stimulation to enhance BCI performance and peripheral magnetic stimulation to decrease upper limb spasticity to expand the scope of BCI application (Shu et al., 2018a; Chen et al., 2020b). Moreover, in 2020, we confirmed the clinical efficacy of BCI training on stroke patients with upper limb dysfunction in both sub-acute and chronic stages, and we explored the closed-loop brain activation changes in sensorimotor rhythm (Chen et al., 2020a; Miao et al., 2020). In 2021, we proposed an inter- and intra-subject transfer calibration scheme for improving feedback performance of the closed-loop BCI training (Cao et al., 2020). In the same year, we compared the differences between motor attempt and motor imagery tasks, which are commonly used in a closed-loop BCI system (Chen et al., 2021). In 2022, we further demonstrated the relationships between sensorimotor rhythm during motor attempt/imagery tasks and upper limb motor impairment in stroke (Chen et al., 2022), which may support the clinical application of the closed-loop BCI system. To sum up, we have explored the closed-loop application of BCI in both the clinic and brain region activations and will move forward to examining its closed-loop brain mechanism.

Clinical significance of central–peripheral–central closed-loop rehabilitation theory (stroke)

Numerous studies have found that the efficacy of combined intervention techniques based on the closed-loop theory of CPC rehabilitation is significantly greater than that of central- or peripheral-only interventions, which provides new ideas for the rehabilitation of motor dysfunction in stroke.

First, closed-loop neuromodulation can be tailored to each person's brain function. The CPC closed-loop rehabilitation theory allows for consideration of individual variability in the excitability and connectivity of brain networks. Second, the time course of dynamic changes amid brain function reorganization

during stroke rehabilitation based on the closed-loop technology can be taken into account (Grefkes and Ward, 2014). Third, since the modifiability of neurons and networks is a function of their recent activity, which critically determines the direction, extent, and duration of plasticity in neural networks (Müller-Dahlhaus and Ziemann, 2015). This can be used to time the stimulation appropriately by applying a closed-loop brain stimulation method.

Introduction of possible mechanisms of central–peripheral–central closed-loop rehabilitation

Central interventions can improve synaptic plasticity around the injured brain regions and increase the efficiency of synaptic remodeling, while peripheral interventions may induce synapse formation while promoting the establishment of functional synapses. The closed-loop rehabilitation theoretical technique formed by the organic combination of both can further strengthen synaptic plasticity and the remodeling ability through positive feedback, thus promoting functional recovery.

The CPC closed-loop may function on the basis of the brain's neuronal plasticity. In the context of closed-loop BCI training, the Hebbian theory is a typical neural mechanism used to explain the changes in the neural system.

Emerging studies about "closed-loop" neuroscience have increased in recent years. "Closed-loop" refers to the complex brain feedback loops and sensorimotor interactions between the brain and environment (Zrenner et al., 2016). As the biofeedback of neural activity, neurofeedback is the basis of "closed-loop" neuroscience, which provides participant neural activation feedback for self-regulation (Sitaram et al., 2017). "Closed-loop" rehabilitation strategies—for example, non-invasive brain stimulation (NIBS), which directly stimulates the brain—have become hot interventions for people with brain injuries, such as stroke (Hummel and Cohen, 2006; Kemps et al., 2022).

Combination strategies are more prevalent in modern rehabilitation than solo interventions. In the present review, based on "closed-loop" neuroscience, we put forward a "CPC closed-loop" rehabilitation strategy, which stresses the use of neurofeedback as a part of the multimodal intervention or adjuvant therapy. The "CPC closed-loop" rehabilitation strategy is a comprehensive intervention to restore neural repair during brain injury rehabilitation and facilitate the best limb function recovery possible. Animal studies have revealed that, after motor cortex injury, forelimb grasping training in rats could increase the projection from the injured cortex to the anterior horn of the spinal cord (Okabe et al., 2016). Exercise intervention can improve the activity of glial cells; strengthen the coupling between astrocytes, microglia, and neurons; and enhance the plasticity of neural function (Li et al., 2021). In addition, central interventions, such as tDCS (Elsner et al., 2020) and repetitive transcranial magnetic stimulation (rTMS; Kirton et al., 2008), have been proven to activate limb function in people with stroke. Hence, the rational combination of "central intervention" with "peripheral intervention" to form a closed-loop intervention model may further enhance limb function and improve the ability of synaptic plasticity. Based on the neurofeedback principle and combination strategies, we assume there are three closed-loop rehabilitation modes for brain injury recovery: large, small, and tiny closed-loop modes.

Closed-loop rehabilitation system

Large closed-loop rehabilitation mode

The closed-loop rehabilitation theory can organically combine traditional peripheral interventions and central interventions to form a 2-way transmission, which can select the appropriate treatment mode according to the degree of motor dysfunction of the patient. The complex composition of central and peripheral interventions increases the complexity of closed-loop rehabilitation intervention techniques guided by the closed-loop rehabilitation theory, and the different combinations of central intervention techniques combined with peripheral intervention techniques form new intervention techniques. Based on this, the large closed loop may undergo various forms of central and peripheral combinations, such as tDCS combined with task-oriented training, tDCS combined with functional electrical stimulation of the upper limbs, TMS combined with task-oriented training techniques, TMS combined with peripheral neuromuscular magnetic stimulation techniques (**Figure 2**), BCI combined with task-oriented training techniques, MT combined with upper limb task-oriented training techniques, MI combined with task-oriented training techniques, and other combinations.

For example, we used a closed-loop rehabilitation technique of transcranial direct current combined with functional electrical stimulation, and the Fugl-Meyer assessment for the upper extremity (FMA-UE) score, muscle tone modified Ashworth scale score, and Broetz hand function test result of upper limb motor function of stroke patients were significantly improved compared to those of the sham stimulation group; specifically, the mean value of FMA-UE was improved by 8.53 points vs. 4.60 points in the sham group, while the mean value of the Broetz hand function test was improved by 11.93 points vs. 6.33 points in the sham group, effectively improving patients' ability to perform activities of daily living and significantly shortening their inpatient rehabilitation period (Shaheiwola et al., 2018).

In a randomized controlled clinical trial using mirror therapy combined with task-oriented training, the technique

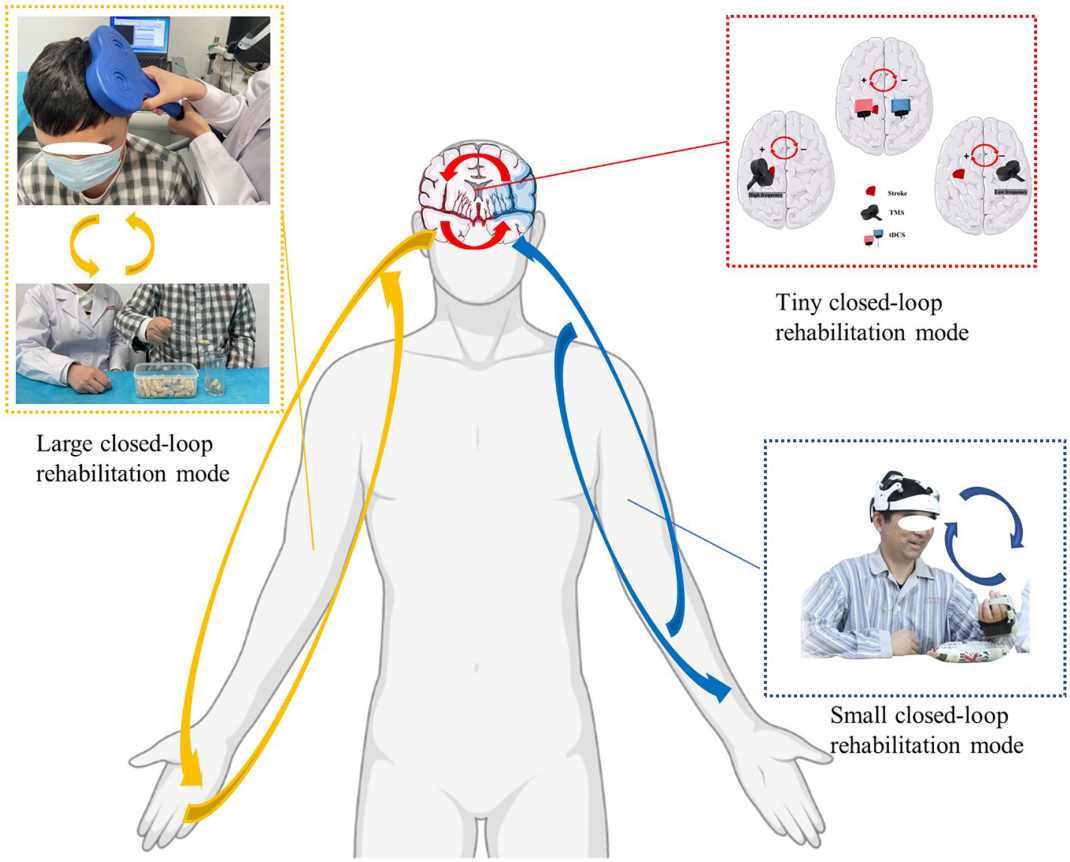

FIGURE 2
Closed-loop rehabilitation modes: large closed-loop rehabilitation mode, small closed-loop rehabilitation mode, and tiny closed-loop rehabilitation mode (The written informed consent was obtained from the individual for the publication of the image). Red arrow: tiny closed-loop rehabilitation mode, the modulation effect in the intra-hemisphere or the inter-hemisphere. Blue arrow: small closed-loop rehabilitation mode, an intervention strategy that relies on independent, comprehensive intervention that does not combine with peripheral interventions. Yellow arrow: large closed-loop rehabilitation mode, the different combinations of central intervention techniques combined with peripheral intervention technique.

protocol significantly improved upper limb motor function and functional independence compared to non-use of the closed-loop rehabilitation intervention technique. Specifically, the upper limb motor ability was improved by 17 points vs. 8.6 points in the conventional rehabilitation group, while functional independence was improved by 17.1 points vs. 6.2 points in the conventional rehabilitation group, with rehabilitation effects of 25.8 and 13.6%, which were 12.7 and 8.7% greater than the effects of conventional rehabilitation (Ding et al., 2019). The above study confirms that techniques based on the closed-loop rehabilitation theory help stroke patients to recover motor function.

Small closed-loop rehabilitation mode

The "closed loop" involves actions leading to consequences (future inputs into the brain) that are observable. Unlike the large closed-loop rehabilitation mode, the small closed-loop rehabilitation mode is an intervention strategy that relies on independent, comprehensive intervention that does not combine with peripheral interventions. This intervention can stimulate brain and limb function simultaneously. Moreover, unlike the tiny closed-loop rehabilitation mode, the intervention-based small closed-loop rehabilitation mode generally needs to test and guide patients before treatment to make them familiar with and cooperate with the training process. A critical aspect of the treatment is recommending that patients imagine actively and control their movements and feelings by using multimodal inputs like vision and hearing. The procedure also involves some cortical brain areas and brain networks, such as the prefrontal lobe and attention network (Deconinck et al., 2015). Therefore, small closed-loop strategies such as brain–machine interfaces (BMIs) and mirror visual feedback (MVF) generally require sensory priming and are system-regulation processes.

Many studies have regarded the BMI as a closed-loop device for patients requiring neurology rehabilitation,

such as those with a spinal cord injury (Jackson and Zimmermann, 2012). By integrating proprioceptive and visual feedback into the BMI, assistive devices, such as computers and robotic prosthetics, can be controlled by patients. People with paralysis using BMI can learn to control multiple neurons so that external devices and communication can be facilitated, which provides a therapeutic benefit by enhancing voluntary recruitment of surviving motor pathways (Birbaumer and Cohen, 2007; Daly and Wolpaw, 2008; Sitaram et al., 2017). There is promising evidence of BMI efficacy for people with stroke. In previous studies, we found that a BCI (**Figure 2**) with exoskeleton feedback was practical in sub-acute stroke patients, and patients who presented increasingly stronger or continuously strong activations (ERD) may obtain better motor recovery (Chen et al., 2020a). Further, the motor attempt task may provide better BCI accuracy but has similar activations in the cortex as the motor image task (Chen et al., 2021).

Another small closed-loop strategy is MVF, also called MT. In the past 20 years, MVF has emerged as a powerful tool to facilitate the recovery of disordered movement and to activate underactive brain areas after stroke (Pollock et al., 2014; Thieme et al., 2018; Zhuang et al., 2021). A mirror is placed in the median sagittal plane between 2 limbs, and the mirror side reflects the unaffected limb to avoid direct observation of the affected side. Participants are requested to move their bilateral limbs as far as possible while concentrating on the mirror side. Through this process, mirror visual illusion can be induced to activate the cortical cortex by MVF. Although MVF affects the sensorimotor cortex, the underlying specific mechanism of MVF is still unknown (Deconinck et al., 2015). Saleh et al. (2017) found that MVF could mediate contralesional parietal cortex modulation over the ipsilesional primary motor cortex in chronic stroke patients more effectively compared to the veridical feedback condition, which indicated the existence of network neurofeedback of MVF. MVF is a small closed loop that connects limb activities and brain activation. Based on a closed-loop strategy, we previously designed a novel camera-based MVF, through which participants could receive multiple sensory inputs. One of our studies revealed that camera-based MVF could improve motor recovery, daily function, and brain network segregation in sub-acute stroke patients (Ding et al., 2019).

Tiny closed-loop rehabilitation mode

A tiny closed-loop rehabilitation mode usually works on its own and leads to changes in the brain. The changes may exist in 1 of the 2 hemispheres of the brain, thus inducing intra-hemisphere neural plasticity. Changes existing in both hemispheres cause inter-hemisphere neural plasticity. Here, the "closed loop" can be explained as the modulation effect in the intra-hemisphere or the inter-hemisphere. Stimulations from both electricity and magnets can contribute to a closed-loop modulation effect on the brain.

Passive brain stimulation technologies, such as the tDCS and the TMS, are the main ways to form a tiny closed-loop rehabilitation mode (**Figure 2**). By applying an anode electrode and a cathode electrode on the brain, tDCS is able to activate or inhibit a hemisphere or specified brain region. As for tDCS, an inhibition from the cathode electrode and activation from the anode electrode form an inter-hemisphere modulation by upregulating the excitability of a hemisphere and downregulating excitability of the other hemisphere. By applying high- or low-frequency energy on the brain, TMS is able to activate or suppress the brain hemispheres. An inhibition comes from a low-frequency dosage, while an activation comes from a high-frequency dosage. This can also induce an inter-hemisphere change between the left and right hemispheres.

This phenomenon is usually detected by radiological technology like functional magnetic resonance imaging and electrophysiological techniques like EEG. Recent advances combining TMS with EEG are able to promote new brain stimulation protocols that are controlled by the EEG signal and thus "close the loop" around the brain in a very direct way, short-circuiting the motor–sensory loop (Bergmann et al., 2012).

Intervention means of closed-loop rehabilitation

Central interventions

Central nervous system (CNS) intervention is the technique that acts on the brain to modulate neuroplasticity, which plays an important role in promoting functional recovery after stroke. According to the active or passive form of patient participation, it can be divided into intrinsic and extrinsic central interventions. Intrinsic central interventions include MI, MT, and BCI, which require patients to actively issue instructions in the brain to activate the corresponding brain areas and circuits that promote neural remodeling. Extrinsic central intervention is further divided into invasive brain stimulation and NIBS. The former usually requires invasive operations on the patient, such as deep brain stimulation.

Due to the inconvenience of the deep brain stimulation operation, NIBS is more commonly applied in clinical practice. tDCS and TMS are typical methods of NIBS. tDCS can directly affect the excitability of neurons through currents, while TMS can generate reverse induced currents in the cortex by altering the magnetic field, balancing the excitability of the left and right hemispheres, and promoting functional remodeling. However, they cannot directly stimulate deep brain regions. TUS makes up for the defect and provides the possibility of precise intervention in deep brain regions, using the ultrasound energy to stimulate

brain tissue, which leads to a series of biological effects that promote recovery after stroke.

Non-invasive brain stimulation has been proven to modulate the process of neuroinflammation in stroke. Researchers (Zhang et al., 2020) found that tDCS (500 μA, 15 min, cathodal) could reduce high levels of neuron-specific enolase, caspase-3, and the Bax/Bcl-2 ratio in middle cerebral artery occlusion rats, which thereby contribute to the resistance of apoptosis and the inhibition of the activation of microglia and astrocyte at the acute phase of ischemic stroke. Furthermore, tDCS treatment significantly decreased the levels of pro-inflammatory cytokines such as interleukin (IL)-1β (Regner et al., 2020), IL-6 (Zhang et al., 2020), and tumor necrosis factor (TNF)-α (Callai et al., 2022) and increased the levels of anti-inflammatory cytokines such as IL-10 (Zhang et al., 2020) in cerebral ischemic penumbra, which can inhibit the neuroinflammatory response in cerebral ischemic penumbra and produce neuroprotective effects in the early stage of stroke. rTMS can significantly mitigate blood–brain barrier (BBB) permeabilization by preserving important BBB components from photothrombotic-induced degradation and decrease peripheral immune cell recruitment and infiltration to the peri-infarct cerebral vasculature by the downregulation of certain cytokines (CXCL10, CD54, CXCL9, and CCL5) (Zong et al., 2020). TUS can also inhibit the activation of microglia and astrocytes by normalizing the expression of inflammatory cytokines such as nuclear factor kappa B, TNF-α, and IL-1β (Zhou et al., 2021). Thus, the CNS interventions can ameliorate the neuroinflammation of stroke, which is induced by both CNS immunity and peripheral immunity.

Peripheral interventions

Peripheral interventions are a series of rehabilitation treatments that act on the trunk and limbs. They are mainly based on the natural recovery process after CNS injury and follow the general laws of neurodevelopment to promote the functional reconstruction of patients with CNS injury through repetitive training and enhanced motor control. Peripheral intervention techniques include neurodevelopmental techniques, such as Bobath, Brunnstrom, proprioceptive neuromuscular facilitation, and Rood techniques, and also include task-oriented training (TOT), functional electrical stimulation (FES), constraint-induced movement therapy, assistive technology, biofeedback therapy, and rehabilitation robots. These peripheral interventions promote CNS plasticity by continuously feeding sensory information to the CNS through external stimulation and reinforcing the correct motor patterns. However, single peripheral interventions are no longer sufficient to meet the rehabilitation needs of the growing number of patients with CNS injuries, and thus the intrinsic mechanisms and their application in combination with central interventions should be continuously explored. Studies (Zhang et al., 2013) have shown that exercise-based peripheral interventions can reduce the inflammation after reperfusion by inhibiting the activation of microglia and reactivating astrocytes, which subsequently reduce the expression of pro-inflammatory cytokines. It was also found that peripheral electrical stimulation promoted the resolution of ischemic edema and enhanced astrocyte activity in the marginal and distal septal regions of the infarct foci (Park et al., 2021).

Application of central–peripheral–central closed-loop rehabilitation in cerebral injury

The bulk of the research has proved that CPC closed-loop rehabilitation is more effective than single central or peripheral therapy in managing post-stroke dysfunctions, such as motor impairment, aphasia, and dysphagia, and treatment options include tDCS + FES, tDCS + electromyographic biofeedback, tDCS + TOT, rTMS + TOT, and so on (Wang et al., 2012; Baroni et al., 2022; **Figure 3**). This is reflected in both physiological indicators and clinical manifestations, including motor evoked potentials, the modified Ashworth scale, the Fugl–Meyer motor function assessment, the water drinking test, and so on (Shaheiwola et al., 2018; Muhle et al., 2021). In previous research, we found that tDCS combined with FES is more effective in improving upper limb function in severe chronic stroke patients than sham tDCS combined with FES (Shaheiwola et al., 2018). The effectiveness of this intervention paradigm was further validated by Salazar et al. (2020), who indicated that tDCS plus FES improved the movement cycle time, mean reaching velocity, and handgrip force of chronic post-stroke survivors with moderate or severe impairment. In addition, tDCS combined with FES gait training improved post-stroke patients' gait regularity better than a FES gait training intervention only (Mitsutake et al., 2021). In the treatment of stroke, some scholars have used our theoretical method (Yu et al., 2020; Yang et al., 2021). There is no best recommendation for CPC therapy. The combination therapy schemes used in animal experiments and clinical trials can be divided into the following categories: central intervention combined with conventional rehabilitation therapy, NMES, TOT, use of a rehabilitation robot, or acupuncture (Li et al., 2018; Xu et al., 2018; Zhao et al., 2022). These findings provide the evidence and potential of the CPC closed-loop theory.

In addition to synergistic therapy, central–peripheral combined therapy can also play a role in precise targeting and adjustment of stimulation time. In recent years, using EEG-based BCI technology to navigate other

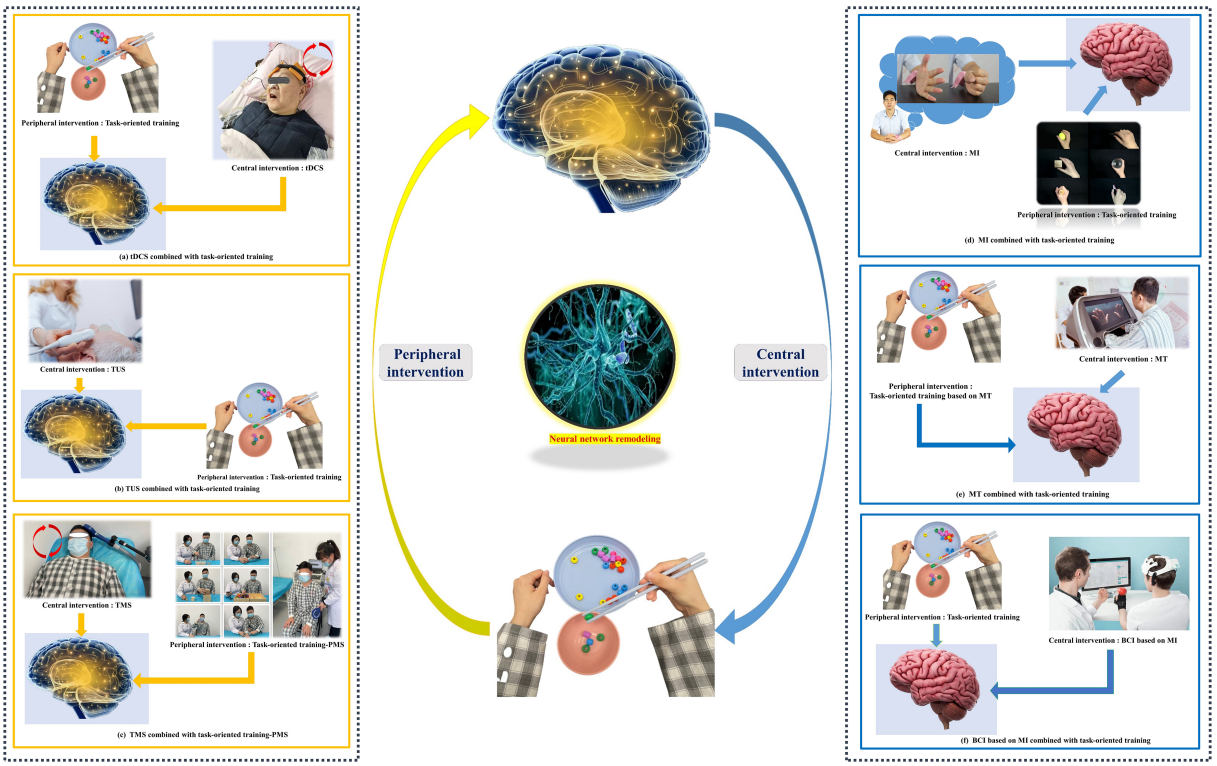

FIGURE 3
Common paradigms of the "closed-loop" rehabilitation strategy. **(a)** tDCS combined with task-oriented training. **(b)** TUS combined with task-oriented training. **(c)** TMS combined with task-oriented training-PMS. **(d)** MI combined with task-oriented training. **(e)** MT combined with task-oriented training. **(f)** BCI based on MI combined with task-oriented training. (Written informed consent was obtained from the individual for the publication of the image).

intervention technologies has gradually become a research hotspot. The current technology combinations are as follows: (1) EEG + rTMS, where rTMS stimulation target positioning is guided by task-state EEG analysis; (2) EEG/magnetoencephalography + tDCS, where EEG or magnetoencephalography tracking is used to guide timing and stimulus settings for tDCS; and (3) EEG + TUS, where navigation is performed through EEG to guide stimulation targets for TUS. In addition, therapeutic paradigms that guide central intervention by analyzing the periphery are also being explored.

Neuroimmunological mechanisms

Neuroplastic alterations or functional reorganization mediated by interhemispheric competition and vicariation models are the well-known recovery mechanisms of post-stroke rehabilitation. Numerous studies have established conclusively that the cerebral cortex displays spontaneous phenomena of neuroplasticity during brain injury (Dimyan and Cohen, 2011; Alia et al., 2017; Khan et al., 2017; Dabrowski et al., 2019). The disruption of neural networks does stimulate a reorganization of synaptic junctions that is highly sensitive to the appearance of damage (Li and Carmichael, 2006). Nevertheless, this reorganization suffers from the oversimplified or even incorrect rationale for CPC closed-loop rehabilitation due to limited beneficial effects after stroke. Actually, activation of brain-resident cells, such as microglia and astrocytes, and blood-borne immune cells, including periphery monocytes/macrophages and T lymphocytes, as well as the immunoreactive molecules they secrete are quickly engaged at the onset of brain injury (Iadecola et al., 2020). The crosstalk between the peripheral and CNS immune components mentioned above significantly correlates with functional recovery in patients with ischemic brain injury and stroke (**Figure 4**). More importantly, the immune response plays a bidirectional role in functional recovery in both the acute and chronic phases after stroke. Therefore, it is critical to understand the mechanisms of immune activation following stroke in order to implement rehabilitation interventions accordingly to different stages of disease in the CPC closed-loop rehabilitation. Here, we examine the role of CNS immunity and its complex interaction with peripheral immunity in closed-loop rehabilitation.

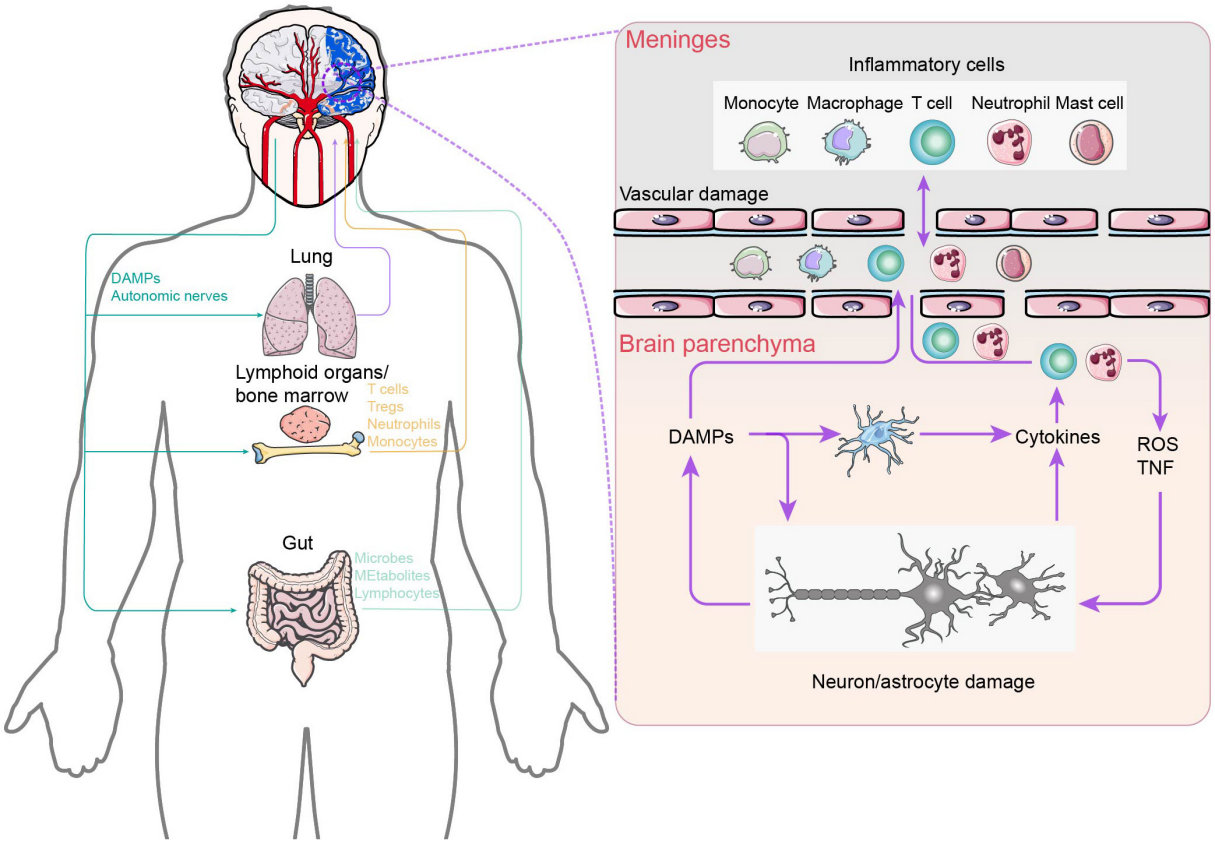

FIGURE 4
Central and peripheral immune response crosstalk in stroke. After ischemia, necrotic neuronal cells appear and release DAMPs due to intracellular adenosine triphosphate depletion and hypotonic hypoxia. On the one hand, DAMPs activate innate immune receptors on brain resident immune cells, leading to the release of cytokines and chemokines, which, in turn, promote additional neutrophil entry. Neutrophils damage the brain by producing reactive oxygen species and TNF. On the other hand, brain-derived DAMPs leak into the circulation and activate systemic immunity, mobilizing innate immune cells in lymphoid organs, the lungs, and the gut. Circulating peripheral immune cells subsequently extravasate into the brain parenchyma and meninges. In addition, the increase in gut permeability triggers bacteria and their metabolites to enter into the brain parenchyma. In the left part: Purple: Lung–Brain axis. Yellow: Lymphoid organs / bone marrow–Brain axis. Purple: Gut–Brain axis.

Central and peripheral immune response crosstalk

Immediately following cerebral ischemia, microglial activation occurs before necrotic neuronal cell appears due to intracellular adenosine triphosphate depletion and hypotonic hypoxia (Rupalla et al., 1998). Microglia features increased arborization, exploratory behavior, and ameboid transformation to prepare for phagocytizing dead cells and neutrophils. Subsequently, necrotic cells in the cerebral ischemia core secrete damage-associated molecular patterns (DAMPs) into the extracellular circulation to further activate brain resident immune cells mainly composed of microglia and astrocytes (Benakis et al., 2014). On the one hand, microglia suppress post-stroke inflammation by producing anti-inflammatory cytokines (IL-10, transforming growth factor β) and the neurotrophic factor IGF-1, removing cellular debris by phagocytosis and suppressing astrocyte activation, thus promoting angiogenesis and tissue re-organization (Lalancette-Hebert et al., 2007; Kawabori et al., 2015; Otxoa-de-Amezaga et al., 2019). On the other hand, cytokine profiles [IL-12 and interferon-γ for type 1 T helper (Th1) cells; IL-6, transforming growth factor β, and IL-23 for type 17 T helper (Th17) cells] secreted by activated microglia induce the generation of Th1 and Th17 cells to promote neuroinflammation (Wan, 2010; Martinez-Sanchez et al., 2018). Meanwhile, interferon-γ mainly produced by Th1 cells and IL-17 mainly produced by Th17 cells induce microglia to express IL-1β, IL-6, and TNF-α, which in turn induce the generation of Th1 and Th17 cells (Watanabe et al., 2016). In addition, stroke-induced activation of the sympathetic and parasympathetic nervous systems may mediate immunodepression after stroke. Ischemic injury immediately activates the sympathetic nervous system,

leading to the contraction and shrinkage of peripheral immune organs (Dorrance and Fink, 2015). The parasympathetic nervous system antagonizes the pathways that are activated by the sympathetic nervous system and then is suppressed following stroke. Some studies have demonstrated that splenic contractions prompt peripheral immune cells to migrate into the brain injury (Ajmo et al., 2008; Fathali et al., 2013). Thus, splenectomy prior to ischemic stroke or irradiation of the spleen following stroke significantly reduces infarct size as well as the number of neutrophils and activated microglia in the brain.

Gut–brain axis

For decades, researchers have studied the relationship between the gastrointestinal (GI) tract and the brain. The "gut–brain axis" refers to the specific linkage between the GI tract and the CNS, which consists of a bidirectional exchange between them. In other words, through the gut–brain axis, the gut and the brain communicate with each other (Socała et al., 2021). From an organ perspective, the brain represents the center and the gut represents the periphery. The brain–gut axis may profile the closed-loop pathway of the CPC theory.

Inflammatory signaling occurs in both the afferent ("gut-to-brain") and efferent ("brain-to-gut") directions across the gut–brain axis to relay the host's health status and stimulate regulatory responses that help to restore homeostasis or amplify inflammation in a context-dependent manner. Since the GI tract is in direct contact with antigens, intestinal microorganisms and their metabolites derived from food and the environment, in addition to the existence of physical barriers such as the gut–vascular barrier (Spadoni et al., 2015), the intestinal tract is also the place where the human body has the largest number of immune cells (Mowat and Agace, 2014). In the intestine, the innate and adaptive immune systems work together to respond quickly to intestinal damage *via* specific immune cell types, such as M cells (Lai et al., 2020), macrophages (Muller et al., 2014), mast cells (Reed et al., 2003), ILC2 cells (Klose et al., 2017), ILC3 cells (Talbot et al., 2020), B-cells (Rojas et al., 2019), CD4 T-cells (Yan et al., 2021), and CD8 T-cells (White et al., 2018). Besides immune cells, neurons and glial cells in the enteric nervous system also participate in intestinal immunity, and their dysfunction will alter the normal intestinal–brain communication and the control of the CNS over the intestine (Huh and Veiga-Fernandes, 2020). Under normal physiological conditions, the CNS is distinguished from its peripheral environment by the BBB. In addition, the CNS also contains a certain number of immune cells, such as microglia (Erny et al., 2015), astrocytes (Rothhammer et al., 2016), and natural killer cells (Sanmarco et al., 2021). Although meninx monocytes, neutrophils, and some subsets of B-cells are supplied directly from the skull and spinal marrow, these CNS-related immune cells are mainly derived from the periphery of the CNS (Cugurra et al., 2021). Complex interaction networks are formed between these immune and non-immune cells to regulate the inflammatory responses in the CNS and the GI tract (Agirman et al., 2021).

Recent studies have shown that the gut–brain axis regulates the allowed homeostasis of the body by mediating the transmission of inflammatory signals, which play an important role in an array of inflammatory diseases (Agirman et al., 2021). The transmission of inflammatory signals in the intestine–brain axis is bidirectional, and they can transmit inflammatory signals through 3 parallel but interconnected pathways: the systemic–humoral pathway, the cellular immune pathway, and the neuronal pathway. There is growing evidence that the gut microbiome is a major environmental factor that shapes the brain through the microbiome–gut–brain axis (Kelly et al., 2017; Mayer et al., 2022). This new perspective on gut and brain interactions has also been applied to the pathophysiology of several brain disorders that were previously attributed solely to pathophysiological processes that occurred within the brain. Calorie restriction provided long-term stroke rehabilitation benefits, in part by modulating gut microbiota (*Bifidobacterium* enrichment), which suggests the possibility of obtaining a favorable outcome in long-term stroke rehabilitation by fecal microbiota transplantation from calorie restriction–treated donors or *Bifidobacterium* supplementation (Huang et al., 2021). Research has shown that specific changes in the cecal microbiota of the Peptococcaceae and the Prevotellaceae are associated with the degree of injury in mice with brain injury. These effects are mediated by norepinephrine released by the autonomic nervous system and alter the production of cecal mucin and the number of goblet cells (Houlden et al., 2016). In addition, post-stroke gut microbiota dysbiosis promotes the proliferation of Th1 and Th17 cells in the intestine as well as the migration of gut-derived T-cells and monocytes to the ischemic brain, exacerbating neuroinflammation (Singh et al., 2016). As a bidirectional modulating system, it forms a closed-loop neuroimmune mechanism between the brain and the gut *via* neuroanatomical, immunological, and neuroendocrine pathways.

Lung–brain axis

The physiological changes caused by the interaction of microbial endocrinology and the external environment affect not only affect the gut but also the lungs (Bajinka et al., 2020). According to the findings of a few new studies, the lung microbiome may have an impact on the CNS. Five

potential mechanisms are known or predicted, as follows: direct microorganism translocation, effects of lung microbes on systemic immunity, nerves, the hypothalamic–pituitary–adrenal axis, and metabolic changes (Bell et al., 2019). This results in the formation of a closed-loop potential mechanism involving the lungs and brain.

The CNS autoimmune process is not only dependent on nerve tissue but also influenced by peripheral organs. According to research, smoking and pulmonary infection significantly increase the risk of developing multiple sclerosis (Olsson et al., 2017). Furthermore, previous research has shown that T-cells capable of causing CNS autoimmune reactions migrate into lung tissue before entering the CNS, where they settle and develop into pathogenic effector cells and long-term memory cells (Odoardi et al., 2012). Pulmonary microbiota disorders have a significant impact on CNS autoimmune responses. According to new research, using neomycin to transform the lung microbiota into a lipopolysaccharide-producing bacterial taxa can transform microglia into the gene-expression state of the type I interferon pathway, significantly inhibiting the pro-inflammatory response and relieving autoimmune symptoms (Hosang et al., 2022).

In the current study, focal ischemic stroke altered the respiratory pattern, caused histological lung damage and inflammation, and reduced the phagocytic capability of alveolar macrophages while leaving the pulmonary function unchanged. The mechanism underlying reduced phagocytic capability of alveolar macrophages appears to be related to serum release rather than BALF mediators. Furthermore, IL-6 gene expression was increased in macrophages and endothelial cells but not in epithelial cells isolated from stroke animals' lungs. These findings suggest the occurrence of dynamic crosstalk between the brain and lungs even after relatively mild/moderate brain injury caused by a stroke (Samary et al., 2018). A closed-loop pattern of the CPC might explain the potential link between the lungs and brain, but the mechanism of the central intervention to regulate lung function through neuroimmunology and peripheral interventions to regulate brain injury through changes in lung function is not clear for patients with brain injury.

Current challenges and future prospects

Closed-loop rehabilitation takes full advantage of central and peripheral intervention techniques that are applied simultaneously or sequentially to patients with brain injury, achieving a "1 + 1 > 2" synergistic therapeutic effect. Central interventions, such as MT and BCI—especially emerging non-invasive brain stimulation techniques (TMS, tDCS, and TUS)—facilitate the development of closed-loop rehabilitation. Numerous studies have further revealed the common mechanisms at play, including synaptic plasticity and functional reorganization mediated by the interhemispheric competition and vicariation models. Furthermore, we place emphasis on the role of CNS immunity and its complicated crosstalk with the peripheral immunity in closed-loop rehabilitation. This crosstalk has particular salience in post-stroke dysfunction, which triggers both beneficial and harmful immune processes. A major frontier in stroke research concentrates on understanding these interactions in order to develop new strategies to prevent and reduce the burden of stroke. Future work will focus on delineating precise clinical strategies for closed-loop rehabilitation based on non-invasive brain stimulation.

In addition, it would be reasonable to modulate the immune system toward beneficial post-stroke rehabilitation by precise non-invasive stimulation in view of data suggesting that this improves clinical outcomes. Furthermore, post-stroke immunodepression puts the patient at higher risk of infection, and clinical treatment strategies should be adjusted accordingly. Finally, the closed-loop rehabilitation of patients with stroke may be ameliorated by advances in specific areas, including exploration of whether modulating immune circuits can reduce the incidence of massive nerve damage or nerve cell death during acute stroke, whether immunity plays a role in different closed-loop systems, and whether bidirectional interventions to prevent post-stroke immunodepression or hyperimmune activation can reduce the risk of infection so as to avoid autoimmune responses against the brain. It is conceivable that future advances in bidirectional interventions will provide in-depth knowledge of closed-loop rehabilitation and that individualized brain stimulation will allow for notable enhancements in rehabilitation success.

We are remarkably sanguine that multimodal and personalized closed-loop rehabilitation will be part of the future of stroke and other brain diseases. Large, small, and tiny closed-loop rehabilitation modes can satisfy the treatment of different stages of disease accordingly, but more studies are needed to confirm which closed-loop mode best matches which stage of the disease. Note that further study on the mechanism will be more conducive to the clinical promotion of the system, especially in the area of the immune system. Additionally, future advances in non-invasive closed-loop systems should make rehabilitation interventions feasible and accessible to large numbers of individuals. Ideally, the non-invasive closed-loop technologies will have the ability to modulate precise brain region at millimeter spatial resolutions and in deep brain nuclear applications. Rather than TMS and tDCS, TUS accompanied by

high spatial resolution and deep transcranial penetration can be tailored to the patient's specific pathophysiology and disease severity, and then tracked by neuroimaging tools in real time. It is with such technological breakthroughs and an in-depth understanding of modulating mechanisms that we hope that this novel closed-loop rehabilitation will flourish to successfully improve the quality of life of patients with brain diseases.

Author contributions

The author confirms being the sole contributor of this work and has approved it for publication.

Funding

This study was supported by the National Key R&D Program of the Ministry of Science and Technology of the People's Republic of China (grant numbers: 2018YFC2002300 and 2018YFC2002301), National Natural Science Foundation of China (grant number: 91948302), and Innovative Research Group Project of National Natural Science Foundation of China (grant number: 82021002).

Acknowledgments

The author thanks Jie Zhu, Jieqiong Wang, Shugeng Chen, Shuo Xu, Jinyang Zhuang, Yifang Lin, Zewu Jiang, Zihang Chen, Yuxin Zhou, Chong Li, and Shuting Tu for assistance during the preparation of this manuscript.

Conflict of interest

The author declares that the research was conducted in the absence of any commercial or financial relationships that could be construed as a potential conflict of interest.

Publisher's note

References

Agirman, G., Yu, K. B., and Hsiao, E. Y. (2021). Signaling inflammation across the gut-brain axis. *Science* 374, 1087–1092. doi: 10.1126/science.abi6087

Ajmo, C. T. Jr., Vernon, D. O., Collier, L., Hall, A. A., Garbuzova-Davis, S., Willing, A., et al. (2008). The spleen contributes to stroke-induced neurodegeneration. *J. Neurosci. Res.* 86, 2227–2234. doi: 10.1002/jnr.21661

Alia, C., Spalletti, C., Lai, S., Panarese, A., Lamola, G., Bertolucci, F., et al. (2017). Neuroplastic changes following brain ischemia and their contribution to stroke recovery: Novel approaches in neurorehabilitation. *Front. Cell Neurosci.* 11:76. doi: 10.3389/fncel.2017.00076

Bajinka, O., Tan, Y., Abdelhalim, K. A., Özdemir, G., and Qiu, X. (2020). Extrinsic factors influencing gut microbes, the immediate consequences and restoring eubiosis. *AMB Express* 10:130. doi: 10.1186/s13568-020-01066-8

Baroni, A., Magro, G., Martinuzzi, C., Brondi, L., Masiero, S., Milani, G., et al. (2022). Combined effects of cerebellar tDCS and task-oriented circuit training in people with multiple sclerosis: A pilot randomized control trial. *Restor. Neurol. Neurosci.* 40:85-95. doi: 10.3233/rnn-211245

Bell, J. S., Spencer, J. I., Yates, R. L., Yee, S. A., Jacobs, B. M., and DeLuca, G. C. (2019). Invited review: From nose to gut - the role of the microbiome in neurological disease. *Neuropathol. Appl. Neurobiol.* 45, 195–215. doi: 10.1111/nan.12520

Benakis, C., Garcia-Bonilla, L., Iadecola, C., and Anrather, J. (2014). The role of microglia and myeloid immune cells in acute cerebral ischemia. *Front. Cell Neurosci.* 8:461. doi: 10.3389/fncel.2014.00461

Bergmann, T. O., Mölle, M., Schmidt, M. A., Lindner, C., Marshall, L., Born, J., et al. (2012). EEG-guided transcranial magnetic stimulation reveals rapid shifts in motor cortical excitability during the human sleep slow oscillation. *J. Neurosci.* 32, 243–253. doi: 10.1523/jneurosci.4792-11.2012

Bernhardt, J., Urimubenshi, G., Gandhi, D. B. C., and Eng, J. J. (2020). Stroke rehabilitation in low-income and middle-income countries: A call to action. *Lancet* 396, 1452–1462. doi: 10.1016/s0140-6736(20)31313-1

Birbaumer, N., and Cohen, L. G. (2007). Brain-computer interfaces: Communication and restoration of movement in paralysis. *J Physiol.* 579, 621–636. doi: 10.1113/jphysiol.2006.125633

Callai, E. M. M., Zin, L. E. F., Catarina, L. S., Ponzoni, D., Gonçalves, C. A. S., Vizuete, A. F. K., et al. (2022). Evaluation of the immediate effects of a single transcranial direct current stimulation session on astrocyte activation, inflammatory response, and pain threshold in naïve rats. *Behav. Brain Res.* 428:113880. doi: 10.1016/j.bbr.2022.113880

Cao, L., Chen, S., Jia, J., Fan, C., Wang, H., and Xu, Z. (2020). An inter- and intra-subject transfer calibration scheme for improving feedback performance of sensorimotor rhythm-based BCI rehabilitation. *Front. Neurosci.* 14:629572. doi: 10.3389/fnins.2020.629572

Chen, J. C., and Shaw, F. Z. (2014). Progress in sensorimotor rehabilitative physical therapy programs for stroke patients. *World J. Clin. Cases* 2, 316–326. doi: 10.12998/wjcc.v2.i8.316

Chen, S., Li, Y., Shu, X., Wang, C., Wang, H., Ding, L., et al. (2020b). Electroencephalography mu rhythm changes and decreased spasticity after repetitive peripheral magnetic stimulation in patients following stroke. *Front. Neurol.* 11:546599. doi: 10.3389/fneur.2020.546599

Chen, S., Cao, L., Shu, X., Wang, H., Ding, L., Wang, S. H., et al. (2020a). Longitudinal electroencephalography analysis in subacute stroke patients during intervention of brain-computer interface with exoskeleton feedback. *Front. Neurosci.* 14:809. doi: 10.3389/fnins.2020.00809

Chen, S., Shu, X., and Jia, J. (2016). Research on closed-loop-based brain computer interface for hand rehabilitation in stroke patients. *Chin. J. Rehabil. Med.* 31, 1189–1194. doi: 10.3969/j.issn.1001-1242.2016.11.003

Chen, S., Shu, X., Jia, J., Wang, H., Ding, L., He, Z., et al. (2022). Relation between sensorimotor rhythm during motor attempt/imagery and upper-limb motor impairment in stroke. *Clin. EEG Neurosci.* 53, 238–247. doi: 10.1177/15500594211019917

Chen, S., Shu, X., Wang, H., Ding, L., Fu, J., and Jia, J. (2021). The differences between motor attempt and motor imagery in brain-computer interface accuracy and event-related desynchronization of patients with hemiplegia. *Front. Neurorobot.* 15:706630. doi: 10.3389/fnbot.2021.706630

Cugurra, A., Mamuladze, T., Rustenhoven, J., Dykstra, T., Beroshvili, G., Greenberg, Z. J., et al. (2021). Skull and vertebral bone marrow are myeloid cell

reservoirs for the meninges and CNS parenchyma. *Science* 373:eabf7844. doi: 10.1126/science.abf7844

Dabrowski, J., Czajka, A., Zielinska-Turek, J., Jaroszynski, J., Furtak-Niczyporuk, M., Mela, A., et al. (2019). Brain functional reserve in the context of neuroplasticity after stroke. *Neural Plast.* 2019:9708905. doi: 10.1155/2019/9708905

Daly, J. J., and Wolpaw, J. R. (2008). Brain-computer interfaces in neurological rehabilitation. *Lancet Neurol.* 7, 1032–1043. doi: 10.1016/s1474-4422(08)70223-0

Deconinck, F. J., Smorenburg, A. R., Benham, A., Ledebt, A., Feltham, M. G., and Savelsbergh, G. J. (2015). Reflections on mirror therapy: A systematic review of the effect of mirror visual feedback on the brain. *Neurorehab. Neural Repair.* 29, 349–361. doi: 10.1177/1545968314546134

Dimyan, M. A., and Cohen, L. G. (2011). Neuroplasticity in the context of motor rehabilitation after stroke. *Nat. Rev. Neurol.* 7, 76–85. doi: 10.1038/nrneurol.2010.200

Ding, L., Wang, X., Chen, S., Wang, H., Tian, J., Rong, J., et al. (2019). Camera-based mirror visual input for priming promotes motor recovery, daily function, and brain network segregation in subacute stroke patients. *Neurorehabil. Neural Repair.* 33, 307–318. doi: 10.1177/1545968319836207

Ding, L., Wang, X., Guo, X., Chen, S., Wang, H., Jiang, N., et al. (2018). Camera-based mirror visual feedback: Potential to improve motor preparation in stroke patients. *IEEE Trans. Neural Syst. Rehabil. Eng.* 26, 1897–1905. doi: 10.1109/TNSRE.2018.2864990

Dorrance, A. M., and Fink, G. (2015). Effects of stroke on the autonomic nervous system. *Compr. Physiol.* 5, 1241–1263. doi: 10.1002/cphy.c140016

Elsner, B., Kugler, J., Pohl, M., and Mehrholz, J. (2020). Transcranial direct current stimulation (tDCS) for improving activities of daily living, and physical and cognitive functioning, in people after stroke. *Cochrane Database Syst. Rev.* 11:Cd009645. doi: 10.1002/14651858.CD009645.pub4

Erny, D., Hrabě de Angelis, A. L., Jaitin, D., Wieghofer, P., Staszewski, O., David, E., et al. (2015). Host microbiota constantly control maturation and function of microglia in the CNS. *Nat. Neurosci.* 18, 965–977. doi: 10.1038/nn.4030

Fathali, N., Ostrowski, R. P., Hasegawa, Y., Lekic, T., Tang, J., and Zhang, J. H. (2013). Splenic immune cells in experimental neonatal hypoxia-ischemia. *Transl. Stroke Res.* 4, 208–219. doi: 10.1007/s12975-012-0239-9

French, B., Thomas, L. H., Coupe, J., McMahon, N. E., Connell, L., Harrison, J., et al. (2016). Repetitive task training for improving functional ability after stroke. *Cochrane Database Syst. Rev.* 11:Cd006073. doi: 10.1002/14651858.CD006073.pub3

Grefkes, C., and Ward, N. S. (2014). Cortical reorganization after stroke: How much and how functional? *Neuroscientist* 20, 56–70. doi: 10.1177/1073858413491147

Hosang, L., Canals, R. C., van der Flier, F. J., Hollensteiner, J., Daniel, R., Flügel, A., et al. (2022). The lung microbiome regulates brain autoimmunity. *Nature* 603, 138–144. doi: 10.1038/s41586-022-04427-4

Houlden, A., Goldrick, M., Brough, D., Vizi, E. S., Lénárt, N., Martinecz, B., et al. (2016). Brain injury induces specific changes in the caecal microbiota of mice *via* altered autonomic activity and mucoprotein production. *Brain Behav. Immun.* 57, 10–20. doi: 10.1016/j.bbi.2016.04.003

Huang, J. T., Mao, Y. Q., Han, B., Zhang, Z. Y., Chen, H. L., Li, Z. M., et al. (2021). Calorie restriction conferred improvement effect on long-term rehabilitation of ischemic stroke *via* gut microbiota. *Pharmacol. Res.* 170:105726. doi: 10.1016/j.phrs.2021.105726

Huh, J. R., and Veiga-Fernandes, H. (2020). Neuroimmune circuits in inter-organ communication. *Nat. Rev. Immunol.* 20, 217–228. doi: 10.1038/s41577-019-0247-z

Hummel, F. C., and Cohen, L. G. (2006). Non-invasive brain stimulation: A new strategy to improve neurorehabilitation after stroke? *Lancet Neurol.* 5, 708–712. doi: 10.1016/s1474-4422(06)70525-7

Huseyinsinoglu, B. E., Ozdincler, A. R., and Krespi, Y. (2012). Bobath concept versus constraint-induced movement therapy to improve arm functional recovery in stroke patients: A randomized controlled trial. *Clin. Rehabil.* 26, 705–715. doi: 10.1177/0269215511431903

Iadecola, C., Buckwalter, M. S., and Anrather, J. (2020). Immune responses to stroke: Mechanisms, modulation, and therapeutic potential. *J Clin Invest.* 130, 2777–2788. doi: 10.1172/JCI135530

Jackson, A., and Zimmermann, J. B. (2012). Neural interfaces for the brain and spinal cord–restoring motor function. *Nat. Rev. Neurol.* 8, 690–699. doi: 10.1038/nrneurol.2012.219

Jia, J. (2016). "Central –Periphery –Center" closed loop rehabilitation: A new concept of hand function rehabilitation after stroke. *Chin. J. Rehabil. Med.* 31, 1180–1182. doi: 10.3969/j.issn.1001-1242.2016.11.001

Jia, S. C. J. (2017). Application of brain-computer interface in rehabilitation of hand function after stroke (review). *Chin. J. Rehabil. Theory Pract.* 23, 23–26. doi: 10.3969/j.issn.1006-9771.2017.01.006

Kang, N., Summers, J. J., and Cauraugh, J. H. (2016). Non-invasive brain stimulation improves paretic limb force production: A systematic review and meta-analysis. *Brain Stimul.* 9, 662–670. doi: 10.1016/j.brs.2016.05.005

Kawabori, M., Kacimi, R., Kauppinen, T., Calosing, C., Kim, J. Y., Hsieh, C. L., et al. (2015). Triggering receptor expressed on myeloid cells 2 (TREM2) deficiency attenuates phagocytic activities of microglia and exacerbates ischemic damage in experimental stroke. *J. Neurosci.* 35, 3384–3396. doi: 10.1523/JNEUROSCI.2620-14.2015

Kelly, J. R., Minuto, C., Cryan, J. F., Clarke, G., and Dinan, T. G. (2017). Cross talk: The microbiota and neurodevelopmental disorders. *Front. Neurosci.* 11:490. doi: 10.3389/fnins.2017.00490

Kemps, H., Gervois, P., Brône, B., Lemmens, R., and Bronckaers, A. (2022). Non-invasive brain stimulation as therapeutic approach for ischemic stroke: Insights into the (sub)cellular mechanisms. *Pharmacol. Ther.* 235:108160. doi: 10.1016/j.pharmthera.2022.108160

Khan, F., Amatya, B., Galea, M. P., Gonzenbach, R., and Kesselring, J. (2017). Neurorehabilitation: Applied neuroplasticity. *J. Neurol.* 264, 603–615. doi: 10.1007/s00415-016-8307-9

Kirton, A., Chen, R., Friefeld, S., Gunraj, C., Pontigon, A. M., and Deveber, G. (2008). Contralesional repetitive transcranial magnetic stimulation for chronic hemiparesis in subcortical paediatric stroke: A randomised trial. *Lancet Neurol.* 7, 507–513. doi: 10.1016/s1474-4422(08)70096-6

Klose, C. S. N., Mahlakõiv, T., Moeller, J. B., Rankin, L. C., Flamar, A. L., Kabata, H., et al. (2017). The neuropeptide neuromedin U stimulates innate lymphoid cells and type 2 inflammation. *Nature* 549, 282–286. doi: 10.1038/nature23676

Lai, N. Y., Musser, M. A., Pinho-Ribeiro, F. A., Baral, P., Jacobson, A., Ma, P., et al. (2020). Gut-innervating nociceptor neurons regulate Peyer's patch microfold cells and SFB levels to mediate *Salmonella* host defense. *Cell* 180, 33–49.e22. doi: 10.1016/j.cell.2019.11.014

Lalancette-Hebert, M., Gowing, G., Simard, A., Weng, Y. C., and Kriz, J. (2007). Selective ablation of proliferating microglial cells exacerbates ischemic injury in the brain. *J. Neurosci.* 27, 2596–2605. doi: 10.1523/JNEUROSCI.5360-06.2007

Legg, L. A., Lewis, S. R., Schofield-Robinson, O. J., Drummond, A., and Langhorne, P. (2017). Occupational therapy for adults with problems in activities of daily living after stroke. *Cochrane Database Syst. Rev.* 7:Cd003585. doi: 10.1002/14651858.CD003585.pub3

Li, F., Geng, X., Yun, H. J., Haddad, Y., Chen, Y., and Ding, Y. (2021). Neuroplastic effect of exercise through astrocytes activation and cellular crosstalk. *Aging Dis.* 12, 1644–1657. doi: 10.14336/ad.2021.0325

Li, F., Zhang, T., Li, B. J., Zhang, W., Zhao, J., and Song, L. P. (2018). Motor imagery training induces changes in brain neural networks in stroke patients. *Neural Regen. Res.* 13, 1771–1781. doi: 10.4103/1673-5374.238616

Li, M., Jia, J., Liu, Y., Wu, Y., and Liu, S. (2013). Effect of neural feedback rehabilitation training for upper extremity exercise function of stroke patients. *Chin. Manipul. Rehabil. Med.* 11, 11–14.

Li, M., Jia, J., Wu, Y., Liu, Y., Zhang, L., and Tang, C. (2016). Computer-guided electrical stimulation in upper limb rehabilitation after stroke. *Chin. J. Phys. Med. Rehabil.* 38, 409–413. doi: 10.3760/cma.j.issn.0254-1424.2016.06.003

Li, M., Liu, Y., Wu, Y., Liu, S., Jia, J., and Zhang, L. (2014). Neurophysiological substrates of stroke patients with motor imagery-based brain-computer interface training. *Int. J. Neurosci.* 124, 403–415. doi: 10.3109/00207454.2013.850082

Li, M. F., Jia, J., and Liu, Y. (2012a). Research on cognitive mechanism of motor Imagerytased brain compvter interface rehabilitation training for stroke patients with severe upper limb paralysis. *J. Chengdu Med. Coll.* 7, 519–523. doi: 10.3969/j.issn.1674-2257.2012.04.004

Li, M. F., Jia, J., Liu, Y., and Wu, Y. (2012b). Effect of motor imagery-based brain computer interface rehabilitation training on upper limb motor function for stroke patients. *Geriatr. Health Care* 18, 347–352. doi: 10.3969/j.issn.1008-8296.2012-06-08

Li, S., and Carmichael, S. T. (2006). Growth-associated gene and protein expression in the region of axonal sprouting in the aged brain after stroke. *Neurobiol. Dis.* 23, 362–373. doi: 10.1016/j.nbd.2006.03.011

Liu, Y., Li, M., Zhang, H., Wang, H., Li, J., Jia, J., et al. (2014). A tensor-based scheme for stroke patients' motor imagery EEG analysis in BCI-FES rehabilitation training. *J. Neurosci. Methods* 222, 238–249. doi: 10.1016/j.jneumeth.2013.11.009

Martinez-Sanchez, M. E., Huerta, L., Alvarez-Buylla, E. R., and Villarreal Lujan, C. (2018). Role of cytokine combinations on CD4+ T cell differentiation,

partial polarization, and plasticity: Continuous network modeling approach. *Front Physiol.* 9:877. doi: 10.3389/fphys.2018.00877

Mayer, E. A., Nance, K., and Chen, S. (2022). The gut-brain axis. *Annu. Rev. Med.* 73, 439–453. doi: 10.1146/annurev-med-042320-014032

Miao, Y., Chen, S., Zhang, X., Jin, J., Xu, R., Daly, I., et al. (2020). BCI-based rehabilitation on the stroke in sequela stage. *Neural Plast.* 2020:8882764. doi: 10.1155/2020/8882764

Mitsutake, T., Sakamoto, M., Nakazono, H., and Horikawa, E. (2021). The Effects of combining transcranial direct current stimulation and gait training with functional electrical stimulation on trunk acceleration during walking in patients with subacute stroke. *J. Stroke Cerebrovasc. Dis.* 30:105635. doi: 10.1016/j.jstrokecerebrovasdis.2021.105635

Mowat, A. M., and Agace, W. W. (2014). Regional specialization within the intestinal immune system. *Nat. Rev. Immunol.* 14, 667–685. doi: 10.1038/nri3738

Muhle, P., Labeit, B., Wollbrink, A., Claus, I., Warnecke, T., Wolters, C. H., et al. (2021). Targeting the sensory feedback within the swallowing network-reversing artificially induced pharyngolaryngeal hypesthesia by central and peripheral stimulation strategies. *Hum. Brain Mapp.* 42, 427–438. doi: 10.1002/hbm.25233

Muller, P. A., Koscsó, B., Rajani, G. M., Stevanovic, K., Berres, M. L., Hashimoto, D., et al. (2014). Crosstalk between muscularis macrophages and enteric neurons regulates gastrointestinal motility. *Cell* 158, 300–313. doi: 10.1016/j.cell.2014.04.050

Müller-Dahlhaus, F., and Ziemann, U. (2015). Metaplasticity in human cortex. *Neuroscientist* 21, 185–202. doi: 10.1177/1073858414526645

Odoardi, F., Sie, C., Streyl, K., Ulaganathan, V. K., Schläger, C., Lodygin, D., et al. (2012). T cells become licensed in the lung to enter the central nervous system. *Nature* 488, 675–679. doi: 10.1038/nature11337

Okabe, N., Shiromoto, T., Himi, N., Lu, F., Maruyama-Nakamura, E., Narita, K., et al. (2016). Neural network remodeling underlying motor map reorganization induced by rehabilitative training after ischemic stroke. *Neuroscience* 339, 338–362. doi: 10.1016/j.neuroscience.2016.10.008

Olsson, T., Barcellos, L. F., and Alfredsson, L. (2017). Interactions between genetic, lifestyle and environmental risk factors for multiple sclerosis. *Nat. Rev. Neurol.* 13, 25–36. doi: 10.1038/nrneurol.2016.187

Otxoa-de-Amezaga, A., Miro-Mur, F., Pedragosa, J., Gallizioli, M., Justicia, C., Gaja-Capdevila, N., et al. (2019). Microglial cell loss after ischemic stroke favors brain neutrophil accumulation. *Acta Neuropathol.* 137, 321–341. doi: 10.1007/s00401-018-1954-4

Park, E., Lyon, J. G., Alvarado-Velez, M., Betancur, M. I., Mokarram, N., Shin, J. H., et al. (2021). Enriching neural stem cell and anti-inflammatory glial phenotypes with electrical stimulation after traumatic brain injury in male rats. *J. Neurosci. Res.* 99, 1864–1884. doi: 10.1002/jnr.24834

Pollock, A., Farmer, S. E., Brady, M. C., Langhorne, P., Mead, G. E., Mehrholz, J., et al. (2014). Interventions for improving upper limb function after stroke. *Cochrane Database Syst. Rev.* 2014:Cd010820. doi: 10.1002/14651858.CD010820.pub2

Reed, D. E., Barajas-Lopez, C., Cottrell, G., Velazquez-Rocha, S., Dery, O., Grady, E. F., et al. (2003). Mast cell tryptase and proteinase-activated receptor 2 induce hyperexcitability of guinea-pig submucosal neurons. *J. Physiol.* 547, 531–542. doi: 10.1113/jphysiol.2002.032011

Regner, G. G., Torres, I. L. S., de Oliveira, C., Pflüger, P., da Silva, L. S., Scarabelot, V. L., et al. (2020). Transcranial direct current stimulation (tDCS) affects neuroinflammation parameters and behavioral seizure activity in pentylenetetrazole-induced kindling in rats. *Neurosci. Lett.* 735:135162. doi: 10.1016/j.neulet.2020.135162

Rojas, O. L., Pröbstel, A. K., Porfilio, E. A., Wang, A. A., Charabati, M., Sun, T., et al. (2019). Recirculating intestinal IgA-producing cells regulate neuroinflammation *via* IL-10. *Cell* 176, 610–624.e18. doi: 10.1016/j.cell.2018.11.035

Rong, J., Ding, L., Xiong, L., Zhang, W., Wang, W., Deng, M., et al. (2021). Mirror visual feedback prior to robot-assisted training facilitates rehabilitation after stroke: A randomized controlled study. *Front Neurol.* 12:683703. doi: 10.3389/fneur.2021.683703

Rothhammer, V., Mascanfroni, I. D., Bunse, L., Takenaka, M. C., Kenison, J. E., Mayo, L., et al. (2016). Type I interferons and microbial metabolites of tryptophan modulate astrocyte activity and central nervous system inflammation *via* the aryl hydrocarbon receptor. *Nat. Med.* 22, 586–597. doi: 10.1038/nm.4106

Rupalla, K., Allegrini, P. R., Sauer, D., and Wiessner, C. (1998). Time course of microglia activation and apoptosis in various brain regions after permanent focal cerebral ischemia in mice. *Acta Neuropathol.* 96, 172–178. doi: 10.1007/s004010050878

Salazar, A. P., Cimolin, V., Schifino, G. P., Rech, K. D., Marchese, R. R., and Pagnussat, A. S. (2020). Bi-cephalic transcranial direct current stimulation combined with functional electrical stimulation for upper-limb stroke rehabilitation: A double-blind randomized controlled trial. *Ann. Phys. Rehabil. Med.* 63, 4–11. doi: 10.1016/j.rehab.2019.05.004

Saleh, S., Yarossi, M., Manuweera, T., Adamovich, S., and Tunik, E. (2017). Network interactions underlying mirror feedback in stroke: A dynamic causal modeling study. *Neuroimage Clin.* 13, 46–54. doi: 10.1016/j.nicl.2016.11.012

Samary, C. S., Ramos, A. B., Maia, L. A., Rocha, N. N., Santos, C. L., Magalhães, R. F., et al. (2018). Focal ischemic stroke leads to lung injury and reduces alveolar macrophage phagocytic capability in rats. *Crit. Care* 22:249. doi: 10.1186/s13054-018-2164-0

Sanmarco, L. M., Wheeler, M. A., Gutiérrez-Vázquez, C., Polonio, C. M., Linnerbauer, M., Pinho-Ribeiro, F. A., et al. (2021). Gut-licensed IFNγ(+) NK cells drive LAMP1(+)TRAIL(+) anti-inflammatory astrocytes. *Nature* 590, 473–479. doi: 10.1038/s41586-020-03116-4

Shaheiwola, N., Zhang, B., Jia, J., and Zhang, D. (2018). Using tDCS as an add-on treatment prior to FES therapy in improving upper limb function in severe chronic stroke patients: A randomized controlled study. *Front. Hum. Neurosci.* 12:233. doi: 10.3389/fnhum.2018.00233

Shu, X., Chen, S., Yao, L., Sheng, X., Zhang, D., Jiang, N., et al. (2018b). Fast recognition of BCI-inefficient users using physiological features from EEG signals: A screening study of stroke patients. *Front. Neurosci.* 12:93. doi: 10.3389/fnins.2018.00093

Shu, X., Chen, S., Meng, J., Yao, L., Sheng, X., Jia, J., et al. (2018a). Tactile stimulation improves sensorimotor rhythm-based BCI performance in stroke patients. *IEEE Trans. Biomed. Eng.* doi: 10.1109/tbme.2018.2882075 [Epub ahead of print].

Singh, V., Roth, S., Llovera, G., Sadler, R., Garzetti, D., Stecher, B., et al. (2016). Microbiota dysbiosis controls the neuroinflammatory response after stroke. *J. Neurosci.* 36, 7428–7440. doi: 10.1523/jneurosci.1114-16.2016

Sitaram, R., Ros, T., Stoeckel, L., Haller, S., Scharnowski, F., Lewis-Peacock, J., et al. (2017). Closed-loop brain training: The science of neurofeedback. *Nat. Rev. Neurosci.* 18, 86–100. doi: 10.1038/nrn.2016.164

Socała, K., Doboszewska, U., Szopa, A., Serefko, A., Włodarczyk, M., Zielińska, A., et al. (2021). The role of microbiota-gut-brain axis in neuropsychiatric and neurological disorders. *Pharmacol. Res.* 172:105840. doi: 10.1016/j.phrs.2021.105840

Spadoni, I., Zagato, E., Bertocchi, A., Paolinelli, R., Hot, E., Di Sabatino, A., et al. (2015). A gut-vascular barrier controls the systemic dissemination of bacteria. *Science* 350, 830–834. doi: 10.1126/science.aad0135

Talbot, J., Hahn, P., Kroehling, L., Nguyen, H., Li, D., and Littman, D. R. (2020). Feeding-dependent VIP neuron-ILC3 circuit regulates the intestinal barrier. *Nature* 579, 575–580. doi: 10.1038/s41586-020-2039-9

Thieme, H., Morkisch, N., Mehrholz, J., Pohl, M., Behrens, J., Borgetto, B., et al. (2018). Mirror therapy for improving motor function after stroke. *Cochrane Database Syst. Rev.* 7:Cd008449. doi: 10.1002/14651858.CD008449.pub3

Wan, Y. Y. (2010). Multi-tasking of helper T cells. *Immunology* 130, 166–171. doi: 10.1111/j.1365-2567.2010.03289.x

Wang, R. Y., Tseng, H. Y., Liao, K. K., Wang, C. J., Lai, K. L., and Yang, Y. R. (2012). rTMS combined with task-oriented training to improve symmetry of interhemispheric corticomotor excitability and gait performance after stroke: A randomized trial. *Neurorehabil. Neural Repair* 26, 222–230. doi: 10.1177/1545968311423265

Watanabe, M., Masaki, K., Yamasaki, R., Kawanokuchi, J., Takeuchi, H., Matsushita, T., et al. (2016). Th1 cells downregulate connexin 43 gap junctions in astrocytes *via* microglial activation. *Sci. Rep.* 6:38387. doi: 10.1038/srep38387

White, J. P., Xiong, S., Malvin, N. P., Khoury-Hanold, W., Heuckeroth, R. O., Stappenbeck, T. S., et al. (2018). Intestinal dysmotility syndromes following systemic infection by flaviviruses. *Cell* 175, 1198–1212.e12. doi: 10.1016/j.cell.2018.08.069

Xia, B., Maysam, O., Veser, S., Cao, L., Li, J., Jia, J., et al. (2015). A combination strategy based brain-computer interface for two-dimensional movement control. *J. Neural Eng.* 12:046021. doi: 10.1088/1741-2560/12/4/046021

Xu, Y., Lin, S., Jiang, C., Ye, X., Tao, J., Wilfried, S., et al. (2018). Synergistic effect of acupuncture and mirror therapy on post-stroke upper limb dysfunction: A study protocol for a randomized controlled trial. *Trials* 19:303. doi: 10.1186/s13063-018-2585-8

Yan, Y., Ramanan, D., Rozenberg, M., McGovern, K., Rastelli, D., Vijaykumar, B., et al. (2021). Interleukin-6 produced by enteric neurons regulates the number and phenotype of microbe-responsive regulatory T cells in the gut. *Immunity* 54, 499–513.e5. doi: 10.1016/j.immuni.2021.02.002

Yang, W., Zhang, X., Li, Z., Zhang, Q., Xue, C., and Huai, Y. (2021). The effect of brain-computer interface training on rehabilitation of upper limb dysfunction after stroke: A meta-analysis of randomized controlled trials. *Front. Neurosci.* 15:766879. doi: 10.3389/fnins.2021.766879

Yu, P., Wang, Y., Yuan, J., Chen, J., Lei, Y., Han, Z., et al. (2020). Observation for the effect of rTMS combined with magnetic stimulation at Neiguan (PC6) and Sanyinjiao (SP6) points on limb function after stroke: A study protocol. *Medicine* 99:e22207. doi: 10.1097/md.0000000000022207

Zhang, K. Y., Rui, G., Zhang, J. P., Guo, L., An, G. Z., Lin, J. J., et al. (2020). Cathodal tDCS exerts neuroprotective effect in rat brain after acute ischemic stroke. *BMC Neurosci.* 21:21. doi: 10.1186/s12868-020-00570-8

Zhang, Y., Zhang, P., Shen, X., Tian, S., Wu, Y., Zhu, Y., et al. (2013). Early exercise protects the blood-brain barrier from ischemic brain injury *via* the regulation of MMP-9 and occludin in rats. *Int. J. Mol. Sci.* 14, 11096–11112. doi: 10.3390/ijms140611096

Zhao, C. G., Ju, F., Sun, W., Jiang, S., Xi, X., Wang, H., et al. (2022). Effects of training with a brain-computer interface-controlled robot on rehabilitation outcome in patients with subacute stroke: A randomized controlled trial. *Neurol. Ther.* 11, 679–695. doi: 10.1007/s40120-022-00333-z

Zhou, H., Meng, L., Xia, X., Lin, Z., Zhou, W., Pang, N., et al. (2021). Transcranial ultrasound stimulation suppresses neuroinflammation in a chronic mouse model of Parkinson's disease. *IEEE Transac. Biomed. Eng.* 68, 3375–3387. doi: 10.1109/tbme.2021.3071807

Zhuang, J. Y., Ding, L., Shu, B. B., Chen, D., and Jia, J. (2021). Associated mirror therapy enhances motor recovery of the upper extremity and daily function after stroke: A randomized control study. *Neural Plast.* 2021:7266263. doi: 10.1155/2021/7266263

Zong, X., Li, Y., Liu, C., Qi, W., Han, D., Tucker, L., et al. (2020). Theta-burst transcranial magnetic stimulation promotes stroke recovery by vascular protection and neovascularization. *Theranostics* 10, 12090–12110. doi: 10.7150/thno.51573

Zrenner, C., Belardinelli, P., Müller-Dahlhaus, F., and Ziemann, U. (2016). Closed-loop neuroscience and non-invasive brain stimulation: A tale of two loops. *Front. Cell Neurosci.* 10:92. doi: 10.3389/fncel.2016.00092

frontiers | Frontiers in Cellular Neuroscience

TYPE Original Research
PUBLISHED 04 January 2023
DOI 10.3389/fncel.2022.1077071

OPEN ACCESS

EDITED BY
Feng Zhang,
The Third Hospital of Hebei Medical University, China

REVIEWED BY
Kailiang Zhou,
The Second Affiliated Hospital and Yuying Children's Hospital of Wenzhou Medical University, China
Zhijian Wei,
Tianjin Medical University General Hospital, China
Zhisheng Ji,
Jinan University, China

*CORRESPONDENCE
Fei-Yue Lin
✉ feiyuelinsl@sina.com

SPECIALTY SECTION
This article was submitted to Cellular Neuropathology, a section of the journal Frontiers in Cellular Neuroscience

RECEIVED 22 October 2022
ACCEPTED 01 December 2022
PUBLISHED 04 January 2023

CITATION
Huang J-H, Chen Y-N, He H, Fu C-H, Xu Z-Y and Lin F-Y (2023) Schwann cells-derived exosomes promote functional recovery after spinal cord injury by promoting angiogenesis. *Front. Cell. Neurosci.* 16:1077071. doi: 10.3389/fncel.2022.1077071

Schwann cells-derived exosomes promote functional recovery after spinal cord injury by promoting angiogenesis

Jiang-Hu Huang[1], Yong-Neng Chen[1], Hang He[1], Chun-Hui Fu[2], Zhao-Yi Xu[1] and Fei-Yue Lin[1]*

[1]Department of Orthopedics, Fujian Provincial Hospital, Fujian Medical University, Fuzhou, China, [2]Fuzhou Maixin Biotech. Co., Ltd., Fuzhou, China

Exosomes are small vesicles that contain diverse miRNA, mRNA, and proteins that are secreted by multiple cells, and play a vital function in cell–cell communication. Numerous exosomes produced by cells have been demonstrated to be protective against spinal cord injury (SCI). This study aims to investigate the neuroprotective effect of Schwann cells-derived exosomes (SCs-Exos) on spinal cord injury. We found that SCs-Exos can be taken directly by brain-derived endothelial cells.3 (bEnd.3 cells) and promoted to proliferate, migrate, and form bEnd.3 tube. Additionally, our results showed that the pro-angiogenesis molecules, Integrin-β1, were highly expressed in SCs-Exos. Moreover, we used special shRNA technology to investigate the role of Integrin-β1 in mediating the effect of SCs-Exos-induced angiogenesis on bEnd.3 cells. We observed that the pro-angiogenic effect of SCs-Exos on bEnd.3 cells was suppressed by inhibiting the expression of integrin-β1 in SCs-Exos. In the SCI model, we found that SCs-Exos attenuated tissue damage and improved functional recovery after SCI. Using immunofluorescence staining, we observed that SCs-Exos treatment promoted angiogenesis in SCI, and integrin-β1 was required to promote angiogenesis. In conclusion, our results indicate that SCs-Exos promote angiogenesis by delivering integrin-β1 and may serve as a promising novel therapeutic agent for enhancing neurological functional recovery after SCI.

KEYWORDS

Schwann cells, exosomes, angiogenesis, integrin-β1, spinal cord injury

1. Introduction

Acute spinal cord injury (SCI), a condition frequently brought on by trauma, typically results in loss of movement and sensation, and places a huge burden on each patient's family and social society healthcare system (Carlson and Gorden, 2002). Numerous medications have been shown to be useful in treating SCI in animal models due to advances in science and technology, but none of them have been successful in

human clinical trials (Thuret et al., 2006). Therefore, it is critical to unravel the molecular mechanisms of SCI and develop new effective treatments for this devastating condition.

In the last decade, cell-based therapy has proven to be an effective treatment for SCI (Assinck et al., 2017). Schwann cells (SCs) are located in the peripheral nervous system. After SCI, SCs in the nerve roots could migrate to the injured site of the spinal cord (Takami et al., 2002). Spinal cord damage can be successfully treated by SCs transplantation, according to several studies (Takami et al., 2002; Oudega and Xu, 2006; Deng et al., 2015). Through the promotion of myelination and axonal regeneration, the transplantation of SCs exerts a protective impact following SCI (Deng et al., 2015). Immune rejection, however, limits the use of cell transplantation therapy (Assinck et al., 2017). According to a prior study, the therapeutic efficacy of SCs is mostly dependent on the neurotrophic factors and extracellular chemicals they produce (Oudega and Xu, 2006).

Recently, exosomes are a particular kind of extracellular vesicle that has attracted researchers' attention. Exosomes are small vesicles (30–150 nm) containing various types of miRNA, mRNA, and protein. It has been demonstrated to be present in a wide range of tissues and cells and is crucial for cell–cell communication (Dreyer and Baur, 2016). There are several benefits to using exosomes in the therapy of illnesses. First, the exosomes have a stable, two-layer membrane structure that resists degradation. Second, relative to cell transplantation, exosomes are safer with no immunological rejection. Due to their tiny size, exosomes do not readily obstruct microvessels as other cells do. Exosomes, third, are nanoscale vehicles that can cross the plasma membrane. Studies have shown that exosomes can cross the plasma membrane as well as the blood–brain barriers with less immunological rejection (Record et al., 2011; Dreyer and Baur, 2016). Therefore, exosome-based therapy for central nervous system (CNS) diseases has attracted great attention from researchers (Goetzl et al., 2015; Lee et al., 2016; Zhang et al., 2017; Zheng et al., 2019). Exosomes from SCs have significantly improved axonal regeneration in the sciatic nerve damage model by reducing the activity of the GTPase RhoA (Lopez-Verrilli et al., 2013). A study by Pan et al. (2022) found that Schwann cells-derived exosomes (SCs-Exos) have a positive effect on promoting functional recovery after spinal cord injury in rats. In our present study, we aimed to investigate whether SCs-Exos has a neuroprotective effect after SCI and elucidate the underlying mechanism.

2. Materials and methods

2.1. Animals

Adult male Sprague–Dawley (SD) rats (180–220 g) were provided by the Animal Center of Fujian Provincial Hospital (Fuzhou, China). All animal care and experimental procedures were approved by the Ethics Committee of Fujian Provincial Hospital (NO 2018-02-013). All animals were housed in individual cages in a temperature- and light-cycle-controlled environment and given free access to food and water.

2.2. Culture of rat SCs and identification

Following anesthesia with sodium pentobarbital (Sigma, St. Louis, MO, USA), the rats were sacrificed and immersed in 75% alcohol for 10 s for disinfection.

The sciatic nerve was removed under sterile conditions and washed with phosphate-buffered saline (PBS) two times, and cut into small pieces with ophthalmic scissors. The tissues were digested with 0.125% trypsin and 0.125% collagenase for 25 min followed by centrifuging at 1,500 rpm for 7 min. The supernatant was discarded, and 5 ml of PBS was added to suspend and wash the cells two times. Cells were collected and incubated in an incubator with 5% CO_2 at 37° for 24 h. The next day cells were treated with IgM class anti-Thy 1.1 antibodies (Serotec, Kidling, UK) and rabbit complement (Sigma-Aldrich, St. Louis, MO, USA) to eliminate fibroblasts. The culture medium was replaced with fresh medium supplemented with Dulbecco's modified eagle medium (DMEM)-10%, 20 mg/ml bovine pituitary extract (Invitrogen, Waltham, CA, USA), penicillin-streptomycin supplemented with 2 mM forskolin (Millipore, Burlington, MA, USA), and FBS-1%. After 7 days, SCs at the primary passage were detached with 0.25% EDTA–trypsin and passage. A routine cell culture method was then carried out, and the cells were identified by anti-S100 (rabbit 1:500, DakoCytomation, Santa Clara, CA, USA) and anti-P75 NTR (rabbit 1:500, Abcam, UK) immunostaining before the subsequent experiments according to previous description (Zheng et al., 2010).

2.3. Culture of bEnd.3 cells

The bEnd.3 cells (brain-derived endothelial cells.3) were obtained from the Type Culture Collection of the Chinese Academy of Sciences (Shanghai, China). Cells were cultured in Dulbecco's Modified Eagle's Medium (DMEM) (Sigma-Aldrich, St. Louis, MO, USA), containing 4,500 mg glucose/L, 10% FBS, and 1% penicillin-streptomycin. The medium was changed every 3 days. Cells were maintained in a cell culture incubator at 37°C, 5% CO2, and a humidified atmosphere.

2.4. The extraction and identification of exosomes

Schwann cells-derived exosomes were collected as previously described (Huang et al., 2017). After SCs were spread to the bottom of the cell culture flask for about 80%, were washed with PBS three times and the SCs serum-free medium was replaced, and the cells returned to the culture hood for 48 h.

The cells supernatant was collected, centrifuged at 1,000 × *g* for 10 min at 4°C to remove residual cells, and centrifuged at 4°C 1,000 × *g* for 20 min to remove cell debris. The resulting supernatant was filtered using a 0.22 μm filter (Millipore, Burlington, MA, USA). Then, the filtered supernatant was centrifuged at 100,000 × *g* for 70 min at 4°C to obtain the exosomes. The supernatant was removed, 500 μL of PBS was used to dissolve the SC-Exos, and transferred to a sterile EP tube for subsequent experiments. The total protein concentration of exosomes was quantified using a Bradford assay (BioRad, Hercules, CA, USA). Transmission electron microscopy (TEM), nanoparticle tracking analysis, and Western blotting were used to identify exosomes.

3. Oxygen glucose deprivation

After incubation with PBS, $SCs^{ctrlshRNA}$-Exos, or $SCs^{shIntegrin-\beta1}$-Exos, respectively, for 6 h, the bEnd.3 cells were then subjected to OGD. Briefly, the culture medium was replaced by glucose-free DMEM (Gibco, Hercules, CA, USA) and then placed into an anaerobic and humidified incubator, which was suffused with 94% N2, 1% O2, and 5% CO2 for 4 h at 37°C. Then, cells were washed two times with Roswell Park Memorial Institute (RPMI) 1,640 for two times and returned to a normal culture medium for 6 h to conduct further experiments.

3.1. Exosomes uptake by bEnd.3 cells

To determine exosome uptake by bEnd.3 cells, a green fluorescent dye (PKH67, Sigma-Aldrich, St. Louis, Mo, USA) was used to label exosomes, according to the previous study (Huang et al., 2017). The resuspended exosomes were then stained with PKH67 using a labeling kit (Sigma-Aldrich, St. Louis, Mo, USA). PKH67 dye was diluted in 100 μL diluent C to a final concentration of 8 μM. Then, 10 μg of exosomes in 20 μL DPBS were diluted with 80 μL diluent C, added to the dye solution, and incubated for 5 min while mixed with gentle pipetting. Then, the labeled exosomes were diluted to 1 ml with PBS and pelleted by ultracentrifugation at 100,000 × *g* for 1 h 10 min at 4°. Then, labeled exosome co-cultured with bEnd.3 cells for 3 h at 37°C. Next, the cells were fixed in 4% PFA for 15 min at RT. The cells were then washed with PBS three times, followed by stained nuclei with DAPI (1:500, Invitrogen, Waltham, CA, USA) for 5 min at RT. The signal was finally observed by a fluorescence microscope.

3.2. EdU test

The EdU test was used to determine how SCs-Exos affected the proliferation of bEnd.3 cells. Briefly, 1 × 105 cells were seeded by DMEM with 10% FBS supplemented for 24 h, then treated for 2 h with 10 m EdU-labeling reagent (1:1,000, Invitrogen, Waltham, CA, USA), followed by the addition of exosomes. The medium was removed and washed with PBS for 5 min two times. 30-min incubation in 4% PFA at room temperature (RT), 5-min incubation in glycine (2 mg/ml) at RT, and a 5-min wash in PBS. Cells were identified by following the manufacturer's instructions for using the ClickiT Edu Alexa Fluor 555 Imaging Kit (Invitrogen, Waltham, CA, USA). Cell nuclei were stained with 4′,6-diamidino-2-phenylindole (DAPI, 1:500, Invitrogen, Waltham, CA, USA) for 5 min at room temperature. In total, 10 randomly selected fields were examined with a fluorescence microscope to determine the percentage of cells that were EdU-positive.

3.3. The capillary network formation assay

After treated with PBS, SCs-Exos, $SCs^{ctrlshRNA}$-Exos, or $SCs^{shIntegrin-\beta1}$-Exos, respectively, for 4 h, and then OGD for 4 h, 1×10^5/well bEnd.3 cells were seeded at a density of 3/well on top of Matrigel in a 96-well plate. The cells were allowed to develop networks in culture for 6 h. Furthermore, an inverted microscope was used to see the tube creation. Image-Pro Plus 6.0 was utilized to quantitatively analyze the network architecture (Media Cybernetics, Rockville, MD, USA).

3.4. Transwell chamber migration assay

Brain-derived endothelial cells.3 cells pretreated with PBS, SCs-Exos, $SCs^{ctrlshRNA}$-Exos, or $SCs^{shIntegrin-\beta1}$-Exos, followed by OGD for 4 h. Cells of the bEnd.3 lines were cultured in serum-free media in the top chamber of a Matrigel-coated insert (BD, USA). The Transwell® plate wells were filled with a migration-inducing material. A total of 1×10^5 cells per well were placed in the top of the chambers. A total of 24 h later, cells remaining in the upper chambers were cleaned. Furthermore, 0.1% crystal violet was used to label the migrating cells, and an Olympus inverted microscope was utilized to tally the cell count.

3.5. siRNA

To investigate the effect of integrin-β1 in SCs-Exos-induced angiogenesis on bEnd.3 cells, the integrin-β1-specific shRNA (sh Integrin-β1, n387129) and Control siRNA were purchased from Thermo Fisher Scientific to repress the expression of integrin-β1 in bEnd.3 cells. Briefly, SCs were transfected with Integrin-β1 shRNA or control shRNA (ctrl shRNA) using Lipofectamine 2,000 (Thermo Fisher Scientific, Waltham, MA, USA) according to the manufacturer's instructions. The inhibition efficiency of this shRNA was measured by Western blotting and qRT-PCR after 48 h.

3.6. qRT-PCR

Total RNA was extracted from bEnd.3 cells with TRIzol (Invitrogen, Waltham, CA, USA). Then, the RNA was reverse-transcripted into cDNA using the PrimeScript RT reagent Kit (TaKaRa, Tokyo, Japan). Furthermore, qRT-PCR was performed with the SYBR Premix Ex Taq (TaKaRa, Tokyo, Japan) on an ABI PRISM® 7900HT System (Applied Biosystems, USA). Analyses of gene expression were performed by the delta–delta CT method. The GAPDH was used as an internal reference. The primers used in this study are as follows: Integrin-β1, F: 5′GTAACCAACCGTAGCAAA GGAACAGC-3′, R: 5′-ATGTCTGTGGCTCCCCTGATCTTA-3′; GAPDH: F: 5′-TGGGCTACACTGAGCACCAG-3′, and R: 5′-AAGTGGTCGTTGAGGGCAAT-3′.

4. Western blotting

The total proteins were obtained from cells or spinal cord issues. A BCA protein assay kit (Beyotime, Shanghai, China) was used to measure the protein concentrations. Furthermore, the proteins were separated by a 10% SDS/PAGE and transferred to the PVDF membranes (Millipore, Burlington, MA, USA). Next, the membranes were blocked in 5% non-fat milk at RT for 1 h. The membranes were then incubated with primary anti-Integrin-β1 (1:1,000, Abcam), anti-Integrin-α1 (1:1,000, Abcam), and anti-VEGF-A antibody (1:200, Abcam) at 4°C overnight. It was washed with PBS and incubated with anti-mouse IgG horseradish peroxidase-conjugated secondary antibody (1:2,000; Jackson) at RT for 1 h. Then, the bands were visualized using an ECL kit (Beyotime, China). The GAPDH served as an internal control.

4.1. Establishment of contusion SCI model in rats

Adult Sprague–Dawley rats (male, 180–220 g) were provided by the Animal Center of Fujian Provincial Hospital (Fujian, China). The animal experiments were performed in accordance with the Ethics Committee of Fujian Provincial Hospital. All procedures involving animals in this study were approved by the Ethics Committee of Fujian Provincial Hospital. All rats were housed in individual cages, in temperature and light-cycle-controlled environments, and they had unrestricted access to both food and water.

The rat contusion SCI model was established according to our previous study (Huang et al., 2017). Rats were anesthetized with sodium pentobarbital (Sigma, St. Louis, MO, USA), and routine skin preparation, disinfection, and paving. After the T10 spinous process as the center, the skin was cut in the median line, and the muscles were removed to reveal the T9-T11 spinous processes and lamina. The T10 spinous process and lamina were bitten and a circular area of approximately 3 mm in diameter centered on the spinal cord segment of T10 was revealed. Centered on the median blood vessel behind the spinal cord, 8 g striking rods were used to fall from the T10 spinal cord from a height of 4 cm. The injury to the spinal cord caused by the intramedullary hemorrhage was visible to the naked eye; in addition, the rat tail wiggled, and the lower limbs and the body retracted and fluttered. The wound was cleansed and the incision was closed in layers. The incision was exposed to complicated iodine disinfection (1 time per day for 3 days). Each rat's quadriceps were alternately injected with 4WU/time/day of penicillin for 3 days. In the Sham operation group, just a laminectomy was performed.

5. Experiment design

A total of 40 rats were randomly divided into four groups (n = 10 per group). In the Sham group, the rats were subjected to laminectomy only. In the Control group, the rats received SCI and then at 30 min after SCI, were treated with 0.5 ml of PBS by tail vein injection. In the SCI + $SCs^{ctrlshRNA}$-Exos group and the SCI + $SCs^{shIntegrin-\beta1}$-Exos group, the rats received SCI, and then at 30 min after SCI, were treated with 100 μg of exosomes precipitate in 0.5 ml of PBS by tail vein injection. At scheduled experiment time points, the rats were sacrificed after deep anesthesia. For subsequent experiments, 10 mm of spinal cord tissue, including the lesion center, was harvested.

6. Immunohistochemistry

On day 7 after SCI, we analyzed the presence of blood vessels in the spinal cord with an immunohistochemistry kit according to the manufacturer's protocol (Huang et al., 2020). After the spinal cord was harvested, the specimens were fixed with PFA for 24 h, and then dehydrated and embedded. Ten consecutive 10-μm transverse sections per millimeter along the spinal cord axis were cut and mounted onto charged microscope slides for primary rabbit anti-rat polyclonal CD31 antibody at 4°C overnight. Then, an immunohistochemistry kit was used for the staining. The nuclei were counterstained with hemalum. The positive-stained CD31 was quantified using Image-Pro Plus software 6.0 (Media Cybernetics, Rockville, MD, USA).

6.1. Immunofluorescence staining

To investigate the angiogenesis role of SCs-Exos on the spinal cord after SCI in rats, immunofluorescence staining was used for detecting the number of proliferating blood

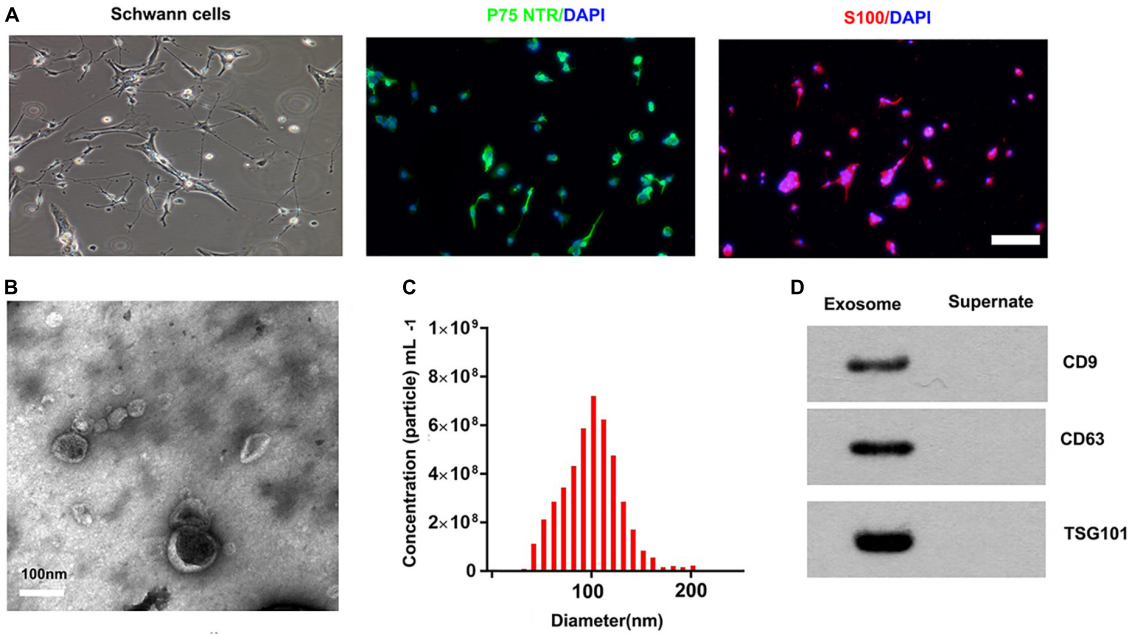

FIGURE 1
Characterization of SCs and derived exosomes. **(A)** Phase contrast image of the Schwann Cells (SCs). Immunofluorescence stain of the surfer markers-P75^{NTR} (green) and S100 (red) of SCs. Scale bar = 100 μm. **(B)** The Transmission electron micrograph of exosomes, Scale bar = 100 nm. **(C)** The nanoparticle tracking analysis of the exosomes. **(D)** The specific surface markers of exosomes, such as CD9, CD63, and TSG101 were then confirmed by Western blotting.

vessels in the spinal cord. On day 7 post-injury, the spinal cord was obtained. Then, the spinal cord was fixed with 4% paraformaldehyde at room temperature (RT) for 3 h. Moreover, it was incubated with 6% sucrose/PBS overnight. Then, the tissues were embedded in an optimal cutting temperature compound (OCT) (Sakura Finetek, USA). 5-μm-thick sections were then obtained in each group (n = 5/group). The frozen sections were air-dried for 15 min at room temperature, and the sections were blocked with 10% normal goat serum in PBS for 1 h at RT. Moreover, the sections were incubated with a mouse monoclonal CD31 antibody (1:100; Abcam) or a rabbit monoclonal proliferating cell nuclear antigen (PCNA) antibody (1:200; Abcam) overnight at 4°C. Washed with PBS, the sections were followed by incubation with the secondary antibodies Alexa Fluor 488 goat anti-rabbit IgG (H + L) (1:1,000, Jackson, USA) or Cy3 goat anti-mouse IgG (H + L) (1:1,000, Jackson, USA) for 30 min at RT. Washed with PBS 5 min × 3 times, the sections were incubated with DAPI working solution (CST, USA) at RT for 15 min. The numbers of CD31/PCNA co-staining positively in the spinal cord were counted in five randomly selected fields in the anterior horn of the gray matter in the spinal cord section per rat.

7. Behavioral assessment

The locomotor functional recovery of the rats post-SCI was accessed by the Basso, Beattie and Bresnahan (BBB) scores (Basso et al., 1995). Behavioral assessment was performed at 1, 3, 5, 7, 14, 21, and 28 days after SCI. The movement of the rats was observed by two independent and well-trained observers, and the score was recorded according to the BBB scores. In total, 5 min of the movement of each rat was observed and repeated three times. Finally, the average score of the two observers was analyzed.

7.1. Lesion identification by H&E staining

At 28 days post-SCI, after the behavioral assessment, the rats were anesthetized with sodium pentobarbital (Sigma, St. Louis, MO, USA) and transcardial perfusion with 4% PFA. A 10-mm-long spinal cord was obtained for HE staining, including the injury epicenter. The spinal cord tissues were embedded in paraffin. The longitudinal sections of the spinal cords were obtained with a thickness of 5 μm. Then, these sections were stained with H&E. The quantification of the cavity areas was accessed by Image-Pro Plus 6.0 (Media Cybernetics, Rockville, MD, USA).

8. Statistical analysis

All data were analyzed using SPSS (17.0; SPSS, Inc., Chicago, IL) statistical software. The data were shown as

means ± standard deviation (SD). The BBB scores were performed by repeated measures analysis of variance, followed by the Bonferroni *post-hoc* corrections. A one-way analysis of variance (ANOVA) was used to compare the means of multiple groups. Moreover, the means between the two groups were measured by an independent sample *t*-test. $P < 0.05$ was considered statistically significant.

9. Results

9.1. Characterization of SCs and derived exosomes

We used an immunofluorescence stain to confirm the surfer markers of SCs. Our results showed that the expression of $P75^{NTR}$ and S100 was positive in these cells (**Figure 1A**). The TEM, nanoparticle tracking analysis, and Western blotting were used to access exosomes. Under the transmission electron microscope, the exosomes were a biconcave hemispherical structure, with a size of about 100 nm (**Figure 1B**). The nanoparticle tracking analysis showed that the size of exosomes ranged from 30 to 200 nm, peaking at 85 nm (**Figure 1C**). The specific surface markers of exosomes, such as CD9, CD63, and TSG101, were expressed in exosomes as confirmed by Western blotting (**Figure 1D**).

9.2. The SC-Exos have pro-angiogenic effects on endothelial cells

To determine whether SCs-Exos could take up by bEnd.3 cells, we used PKH67 to label SCs-Exos. Then, added the labeled exosomes to the bEnd.3 cells. We observed that the PKH67 labeled exosomes were uptaken by endothelial cells and located in the cytoplasm of bEnd.3 cells (**Figure 2A**). These results revealed that bEnd.3 cells could take up SCs-Exos.

To assess the effect of SCs-Exos on the proliferation of bEnd.3 cells, the EdU test was performed. In the EdU test, there was a significantly higher percentage of EdU-positive cells in the SCs-Exos-treated groups than that in the Control group ($P < 0.01$; **Figures 2B, C**). The capillary network formation assay and transwell chamber migration assay were further conducted to access the pro-angiogenesis effects of SCs-Exos on bEnd.3 cells. In the capillary network formation assay, the number of total branch points and total tube length was higher in the SCs-Exos-treated groups than that in the Control group ($P < 0.01$; **Figures 2D–F**). Moreover, the migration of bEnd.3 cells in the SCs-Exos treated group was significantly greater than that in the Control group ($P < 0.01$; **Figures 2G, H**). These findings indicate that SC-Exos have pro-angiogenic effects on endothelial cells.

9.3. Identification of the pro-angiogenesis molecules in SCs-Exos

Previously the study has identified 433 proteins cargo in SCs-Exos using proteomics analysis (Basso et al., 1995). We found that several proteins were closely related to angiogenesis, so we used a Western blot to confirm whether the angiogenesis molecular was highly expressed in SCs-Exos. Our results showed that two pro-angiogenesis molecules, integrin-β1, and integrin-α1 were highly expressed in SCs-Exos (**Figures 3A, B**). We also found that another pro-angiogenesis molecule, VEGF-A was expressed in SCs-Exos, but the expression level was relatively low (**Figures 3A, B**).

9.4. Integrin-β1 is required for SCs-Exos to promote angiogenesis on endothelial cells

To investigate the effect of Integrin-β1 on SCs-Exos induced angiogenesis on bEnd.3 cells, we repressed Integrin-β1 expression using an Integrin-β1-specific siRNA. Integrin-β1 silenced shRNA (sh Integrin-β1), and control shRNA (ctrl shRNA) were transfected into SCs, respectively. Then, exosomes were extracted from these transfected SCs. Our results showed that the Integrin-β1 protein and mRNA expression of SCs-Exos was greatly repressed by Integrin-β1 siRNA ($P < 0.01$; **Figures 3C, D**). In the EdU test, there was a significantly lower percentage of EdU-positive cells in the $SCs^{shIntegrin-\beta1}$-Exos group than in the $SCs^{ctrlshRNA}$-Exos group ($P < 0.01$; **Figures 4A, D**). The capillary network formation assay results showed that the number of total branch points and total tube length was significantly lower in the $SCs^{shIntegrin-\beta1}$-Exos than in the $SCs^{ctrlshRNA}$-Exos group ($P < 0.01$; **Figures 4B, E, F**). In the transwell chamber migration assay, the migration of bEnd.3 cells in the $SCs^{shIntegrin-\beta1}$-Exos was significantly reduced than the $SCs^{ctrlshRNA}$-Exos group ($P < 0.01$; **Figures 4C, G**).

9.5. Exosomal Integrin-β1 mediated the promoted angiogenesis effect of SCs-Exos in the injured spinal cord after SCI

CD31 staining was performed to evaluate the presence of blood vessels in the spinal cord at day 7 post-SCI. The results showed that the number of blood vessels in the Control group was significantly decreased when compared to the Sham group ($P < 0.01$; **Figures 5A, B**). Furthermore, $SCs^{ctrlshRNA}$-Exos treatment significantly enhanced the number of blood vessels when compared with the Control group ($P < 0.05$; **Figures 5A, B**). But the pro-angiogenic effect was attenuated,

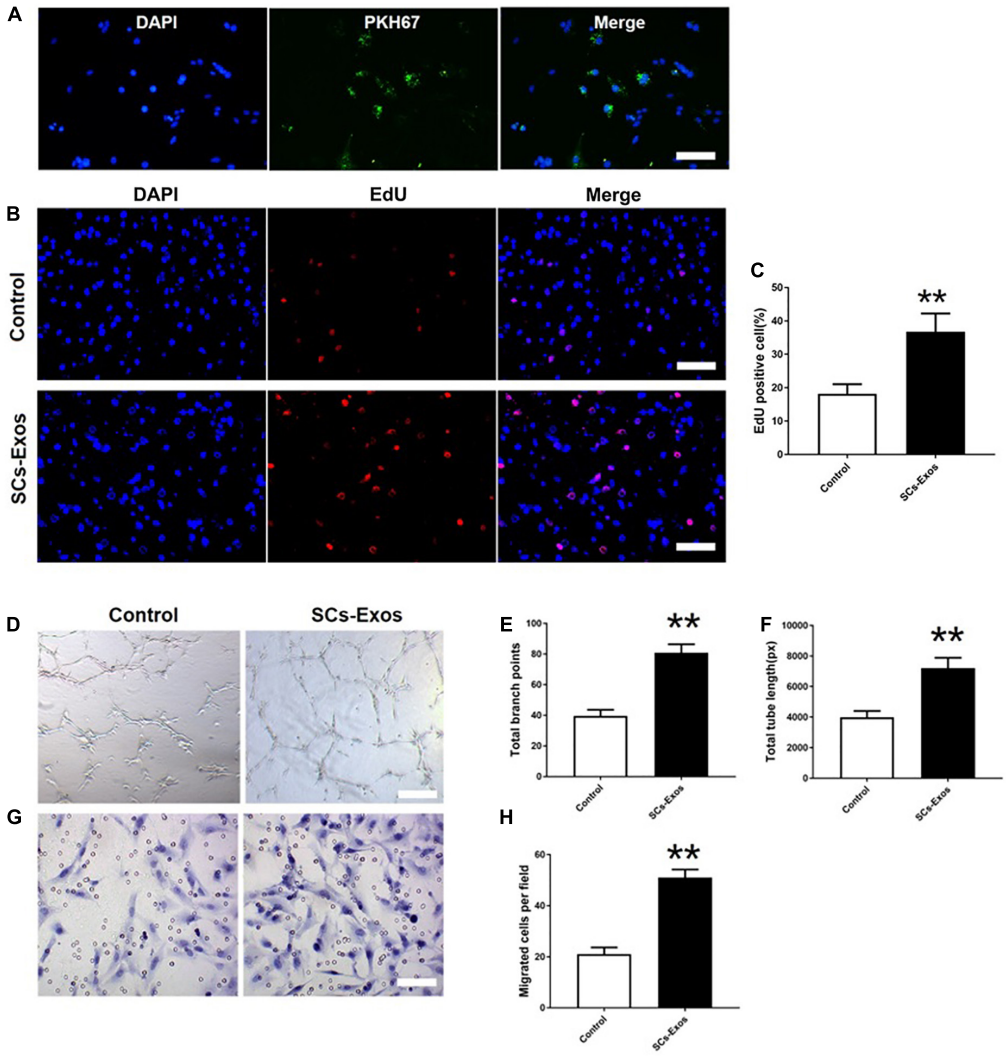

FIGURE 2
Schwann cells-derived exosomes enhance the angiogenic activities of Endothelial Cells. **(A)** Immunofluorescence images of PKH67-labeled exosomes taken up by bEnd.3 cells. Scale bar = 50 μm. **(B)** The proliferation of bEnd.3 cells was performed by the EdU test. **(C)** Quantitative analysis of EdU-positive cells in each group. **(D–F)** Tube formation and migration were measured by the capillary network formation assay and transwell chamber migration assay 6 h after seeding bEnd.3 cells pretreated with PBS, or SCs-Exos. Photomicrographs of tube-like structures and quantification of the tube number. **(G)** Photomicrographs of bEnd.3 cells that migrated through the Transwell® membrane. The bEnd.3 cells were stained with crystal violet. **(H)** Quantification of the number of the migrated bEnd.3 cells. The data are presented as mean ± SD. $^{**}p < 0.01$ SCs-Exos vs. Control group. $N = 5$ in each group. Scale bar = 500 μm.

once the Integrin-β1 was downregulated in $SCs^{shIntegrin-\beta1}$-Exos treated group than that in $SCs^{ctrlshRNA}$-Exos group ($P < 0.05$; Figures 5A, B). Immunofluorescence staining was employed to detect proliferating blood vessels in the spinal cord 7 days post-SCI after exosome therapy. The number of CD31/PCNA positive cells in the $SCs^{ctrlshRNA}$-Exos treated group was greater than that in the Control group ($P < 0.01$; Figures 6A, B). Similarly, the number of CD31/PCNA positive cells in $SCs^{shIntegrin-\beta1}$-Exos group was lower than that in $SCs^{ctrlshRNA}$-Exos group ($P < 0.01$; Figures 6A, B). These data suggest that Integrin-β1 present in SCs-Exos is responsible for promoting angiogenesis after SCI.

9.6. Exosomal Integrin-β1 mediates the protective effects of SCs-Exos on neurological functional recovery after SCI

H&E staining was used to detect the histopathological changes in the injuries spinal cord with the treatment of

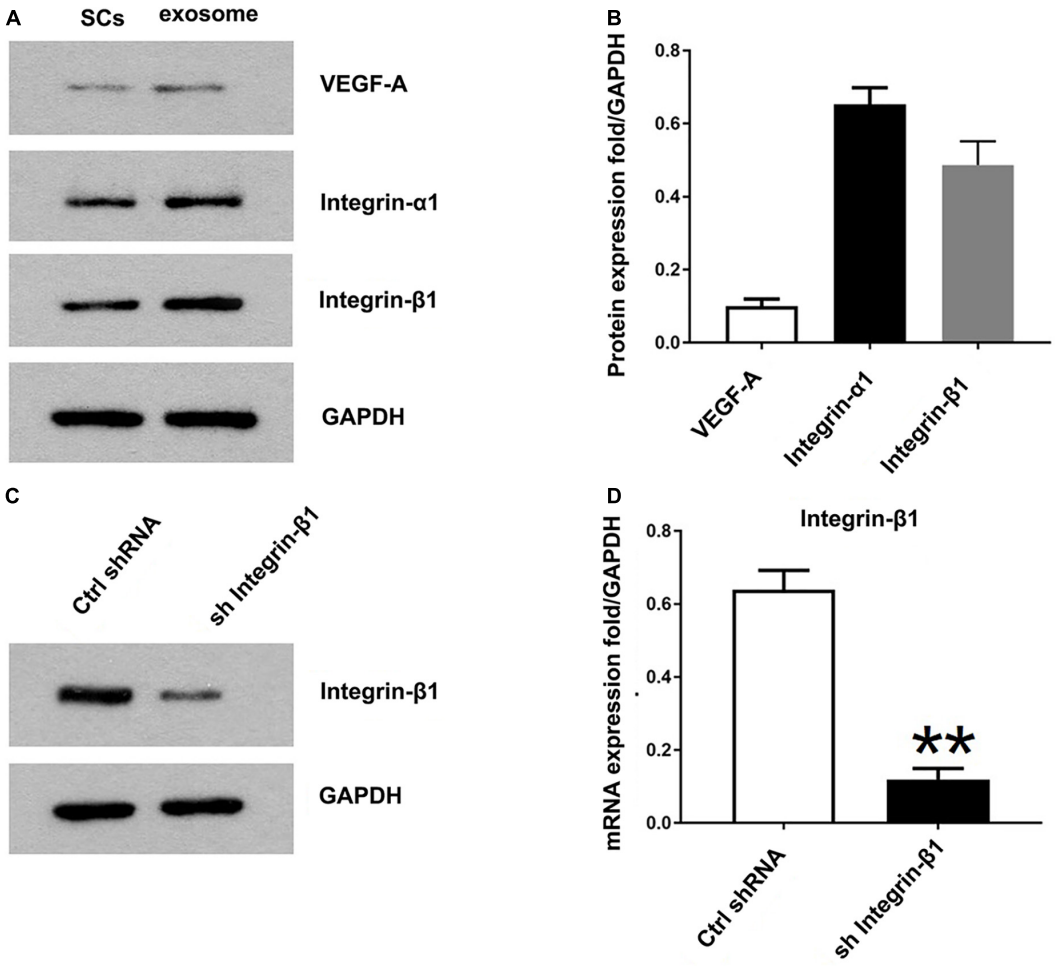

FIGURE 3
Identification of the pro-angiogenesis molecules in SCs-Exos and the inhibitory efficiency of integrin-β1 siRNA. **(A)** Western blotting was used to detect the protein level of VEGF-A, integrin-β1 and integrin-α1 in SCs and SCs-Exos. **(B)** The relative protein expression levels of VEGF-A, integrin-β1 and integrin-α1 in SCs-Exos **(C,D)**. Western blotting and qRT-PCR were performed to analyze the inhibitory efficiency of integrin-β1 siRNA. The data are presented as mean ± SD. $^{**}p < 0.01$ sh Integrin-β1 group vs. ctrl shRNA group. $N = 3$ in each group.

exosome after SCI at day 28 post-injury. A huge lesion area was observed in the Control group, and $SCs^{ctrl\,shRNA}$-Exos treatment significantly reduced the lesion area of the injured spinal cord ($p < 0.01$, Figures 7A, B). Moreover, the lesion area was larger in the $SCs^{shIntegrin-\beta1}$-Exos treated group than that in $SCs^{ctrl\,shRNA}$-Exos-treated group ($p < 0.01$, Figures 7A, B). The BBB scores were used to analyze the functional recovery after SCI. The results showed that the scores were 0 immediately after SCI in all groups, indicating that the SCI model in rats was produced successfully. Moreover, there was a spontaneous recovery of hind limb function in rats after SCI; the BBB score gradually increased in all treatment groups (Figure 8). At 14 days post-SCI, $SCs^{ctrl\,shRNA}$-Exos treatment group had higher BBB scores than that in the Control group and $SCs^{shIntegrin-\beta1}$-Exos group ($p < 0.05$, day 14, day 21, and day 28, Figure 8). Moreover, the BBB scores in the $SCs^{shIntegrin-\beta1}$-Exos group were significantly lower than that in the $SCs^{ctrl\,shRNA}$-Exos group since day 21 after SCI ($p < 0.05$, day 21, and day 28, Figure 8).

10. Discussion

Spinal cord injury is a catastrophic disease. Effective treatment strategies for promoting functional recovery after SCI are still lacking. In the present study, we investigated the protective role of SCs-derived exosomes on functional recovery after SCI for the first time. Our results demonstrated that SCs-Exos treatment significantly promoted the proliferation, migration, and tube formation of endothelial cells. Moreover, we further confirmed that integrin-β1 was involved in these pro-angiogenesis processes and mediated the pro-angiogenesis effect of SCs-Exos on endothelial cells. As presented in the SCI model,

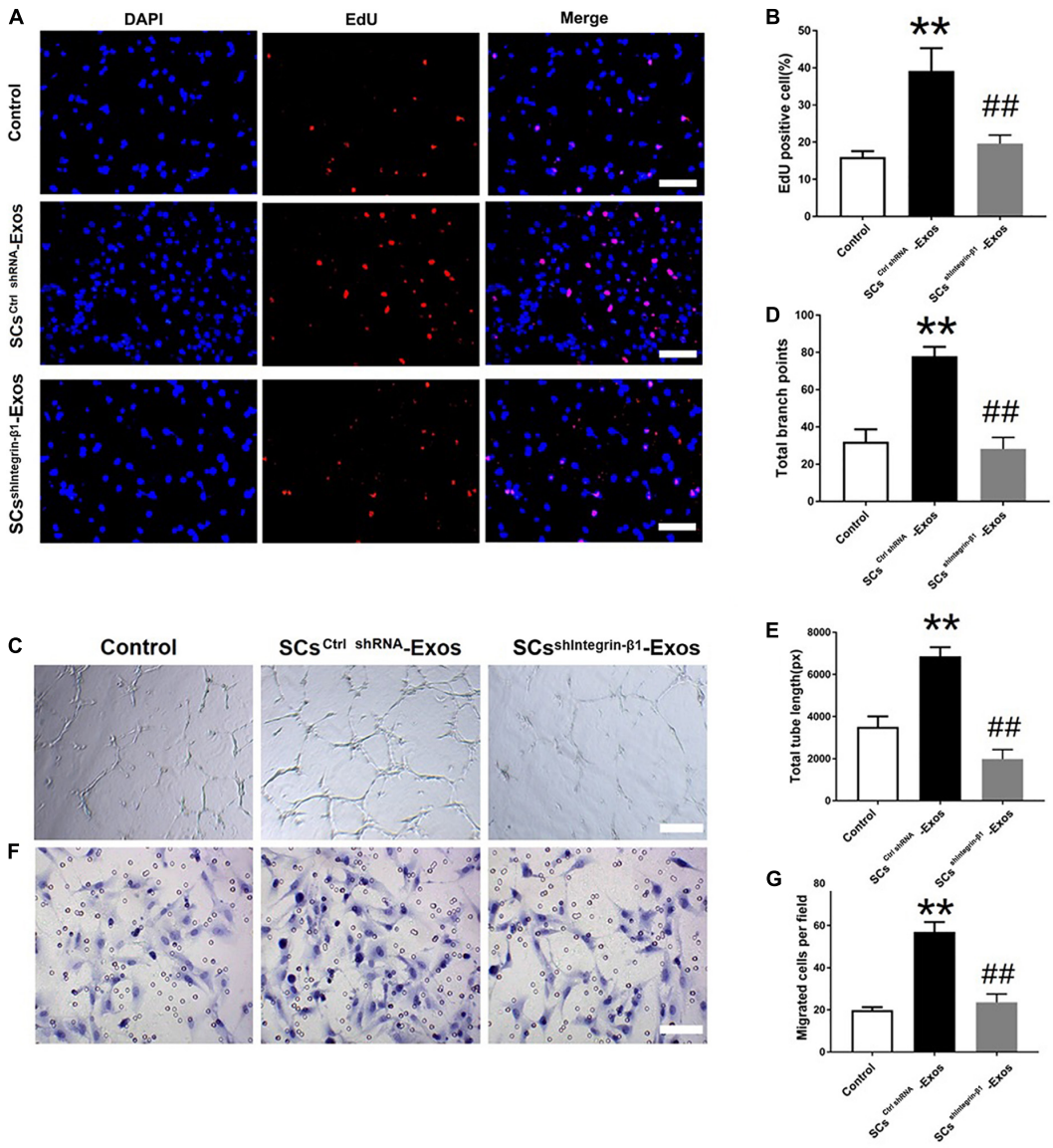

FIGURE 4
Integrin-β1 is required in mediating the role of SCs-Exos for promoting angiogenesis on Endothelial Cells. **(A)** The proliferation of bEnd.3 cells was performed by EdU test. **(D)** Quantitative analysis of EdU-positive cells in each group. **(B,E,F)** Tube formation and migration were measured by the capillary network formation assay and transwell chamber migration assay 6 h after seeding bEnd.3 cells pretreated with PBS, $SCs^{ctrlshRNA}$-Exos, or $SCs^{sh\ Integrin-\beta1}$-Exos. **(C)** Photomicrographs of tube-like structures and quantification of the tube number. Photomicrographs of bEnd.3 cells that migrated through the Transwell® membrane. The bEnd.3 cells were stained with crystal violet. **(G)** Quantification of the number of the migrated bEnd.3 cells. The data are presented as mean ± SD. $^{**}p < 0.01$ Control group vs. $SCs^{ctrlshRNA}$-Exos group, $^{\#\#}p < 0.01$ $SCs^{ctrlshRNA}$-Exos group vs. $SCs^{shIntegrin-\beta1}$-Exos group. $N = 5$ in each group. Scale bar = 500 μm.

SCs-derived exosomes enhanced microvascular density and pro-angiogenesis in the injured spinal cord after SCI. Furthermore, we observed that SCs-Exos treatment alleviated tissue damage of the spinal cord, and improved neurological functional recovery after SCI. Moreover, these protective effects of SCs-Exos on SCI were partly impaired by reducing the expression of integrin-β1 in exosomes cargo in SCs-Exos.

The pathophysiology of spinal cord injury is extremely complex and includes primary injury and secondary injury. Primary injury of the spinal cord was caused by immediate violence and cannot be avoided. Therefore, the focus of research is on how to reduce secondary injury of the spinal cord (Dumont et al., 2001). Studies have shown that the loss of vascular structure and the post-traumatic blood supply disturbance brought on by vascular dysfunction plays a significant role in exacerbating the spinal cord's secondary damage and the loss of neurological function (Crock et al., 2005; Martirosyan et al., 2011). In this study, we found that the density of the

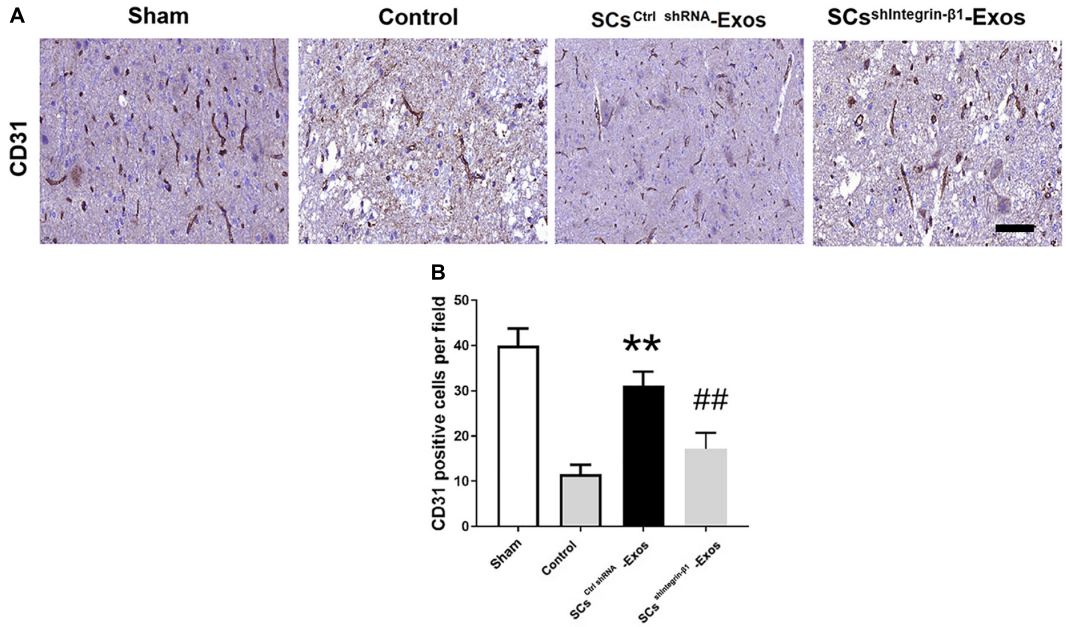

FIGURE 5
Exosomal Integrin-β1 of SCs-Exos promotes angiogenesis after SCI. **(A)** The presence of blood vessels in the spinal cord at day seven after SCI indifferent treated groups were analyzed by CD31. **(B)** Quantification of the number of CD31-positive cells in each group. The data are presented as mean ± SD. $^{**}p < 0.01$ Control group vs. $SCs^{ctrlshRNA}$-Exos group, $^{\#\#}p < 0.01$ $SCs^{ctrlshRNA}$-Exos group vs. $SCs^{sh\ Integrin-\beta1}$-Exos group. $N = 5$ in each group. Scale Bar = 50 μm.

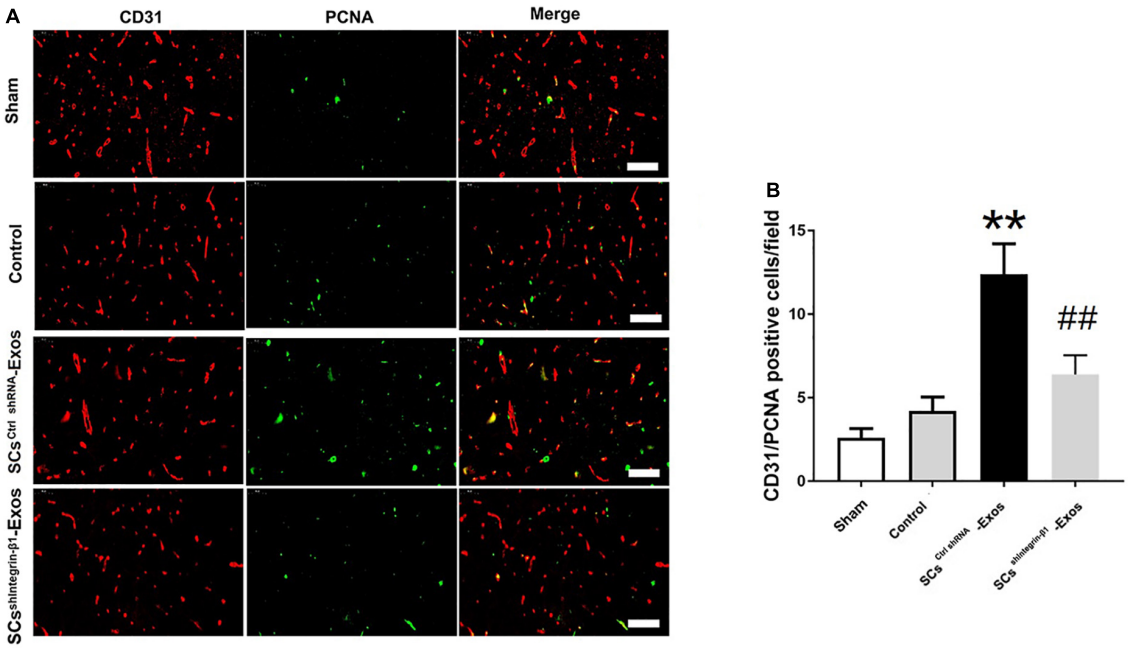

FIGURE 6
Exosomal Integrin-β1 of SCs-Exos promotes new blood vessel formation after SCI. The presence of proliferation of blood vessels in the spinal cord on day seven after SCI was analyzed by immunofluorescence staining. **(A)** Representative image of CD31-positive (Red) and PCNA-positive (Green) cells in the anterior horn of the spinal cord from each group at 7 days post-injury. **(B)** Quantitative analysis of CD31/PCNA-positive cells in the injured spinal cords from each group. The data are presented as mean ± SD. $^{**}p < 0.01$ Control group vs. $SCs^{ctrlshRNA}$-Exos group, $^{\#\#}p < 0.01$ $SCs^{ctrlshRNA}$-Exos group vs. $SCs^{shIntegrin-\beta1}$-Exos group. $N = 5$ in each group. Bar = 50 μm.

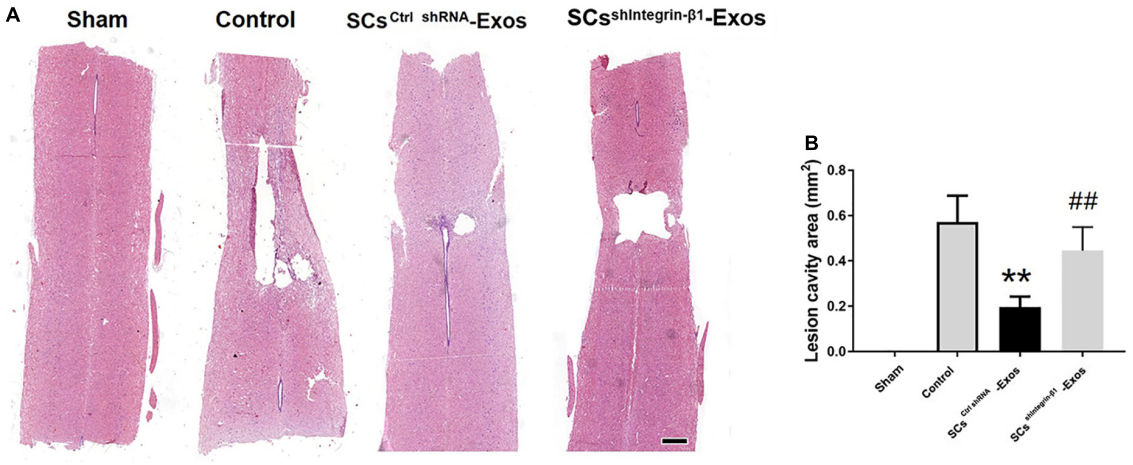

FIGURE 7
Exosomal Integrin-β1 of SCs-Exos attenuates tissue damage after SCI. **(A)** Representative H&E staining of lesion cavity of the spinal cord in each group. **(B)** Quantification of lesion cavity of each group. The data are presented as mean ± SD. $^{**}p < 0.01$ Control group vs. $SCs^{ctrlshRNA}$-Exos group, $^{\#\#}p < 0.01$ $SCs^{ctrlshRNA}$-Exos group vs. $SCs^{shIntegrin-\beta1}$-Exos group. $N = 5$ in each group. Scale bar = 1 mm.

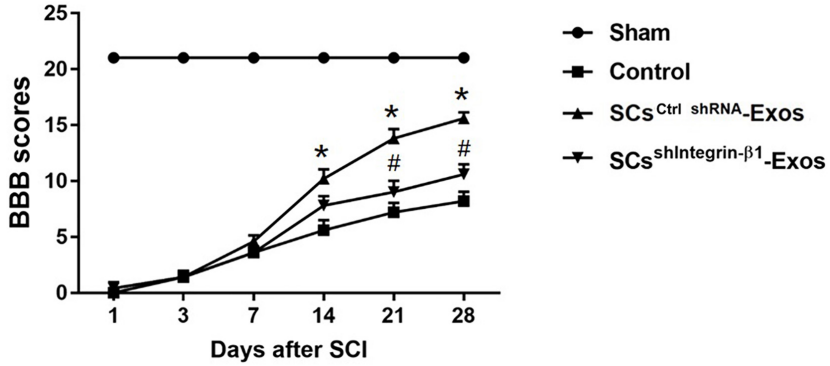

FIGURE 8
Exosomal Integrin-β1 of SCs-Exos improves neurological functional recovery after SCI. Functional recovery after SCI in rats was accessed by BBB scores, which ranged from Day 1 to Day 28 post-SCI. The data are presented as mean ± SD. $^{*}p < 0.05$ Control group vs. $SCs^{ctrlshRNA}$-Exos group, $^{\#}p < 0.05$ $SCs^{ctrlshRNA}$-Exos group vs. $SCs^{shIntegrin-\beta1}$-Exos group. $N = 5$ in each group. Scale bar = 1 mm.

microvascular in the spinal cord was decreased post-SCI, which was consistent with the previous report (Cao et al., 2017). However, the studies also demonstrated that the vessel could play a role in mediating nerve regeneration. A well vascular blood supply provides a sufficient nutrient substance for neural tissue survival. Therefore, how to reduce vascular damage and promote angiogenesis after SCI is crucial for promoting neurological functional recovery after SCI.

To date, multiple therapeutic interventions for promoting angiogenesis after SCI have been conducted. These treatments include proangiogenic factor administration, cell transplantation and gene therapy, and biomaterial implantation. The Schwann cells (SCs) are the glial cells of peripheral nerves, which can repair both peripheral nerve injury and CNS injury. The repair mechanism of SCs may be related to their secretion of cytokines and the extracellular matrix, which can improve the microenvironment of the injured site and promote angiogenesis and nerve regeneration (Takami et al., 2002; Webber and Zochodne, 2010; Lopez-Verrilli et al., 2013; Toft et al., 2013). Studies have shown that the transplantation of the Schwann cells can promote functional recovery after SCI, but the therapeutic effect was limited. The main reasons were due to its poor survival of SCs after transplantation and difficulty in crossing the blood–brain barrier in the injured spinal cord (Webber and Zochodne, 2010; Toft et al., 2013).

Exosomes have recently drawn a lot of attention from researchers for the treatment of CNS illnesses due to their tiny size and capacity to cross the blood–brain barrier (Braccioli et al., 2014; Zheng et al., 2019). Numerous studies have suggested that exosomes, which have a variety of roles including boosting

angiogenesis and controlling inflammation, are essential for the healing of SCI. All cells have the capacity to produce exosomes, which serve the same function as their parent cells. In our current study, the pro-angiogenesis role of exosomes derived from the Schwann cells (SCs-Exo) was investigated in SCI and *in vitro* cell models. We co-cultured SCs-Exo with bEnd.3 cells and found that SCs-Exos could take up by bEnd.3 cells, and the SCs-Exos treatment group significantly promoted endothelial cell proliferation and migration and increased tube formation. These results suggest that SCs-Exos have pro-angiogenic effects on endothelial cells, which may be used as a therapeutic agent for enhancing angiogenesis after SCI.

Exosomes comprise a variety of substances, including miRNAs, mRNAs, and proteins. These contents of exosomal cargo could be delivered to their recipient cells through intercellular communication (Dreyer and Baur, 2016). Due to the lipid bilayer, exosomal contents could be protected against external proteases and other enzymes, and are relatively stable. A study analyzed and found that SCs-Exos contained 433 proteins, including a variety of proteins related to nerve regeneration, inflammation, and angiogenesis. Among the angiogenesis-related proteins, integrin-β1 and integrin-α1 were found to be enriched and expressed in SCs-Exos content (Wei et al., 2019). Integrin-β1 plays an important role in the injury of various tissues and organs and controls VE-cadherin localization and blood vessel stability (Milner and Campbell, 2002; Mettouchi and Meneguzzi, 2006; Keely et al., 2009; Malan et al., 2010; Goto et al., 2016). In this study, we further explored the role of integrin-β1 in mediating the pro-angiogenesis effects of SCs-Exos following SCI. It has been reported that the contents of exosomes could be modified by multiple genetic engineering technologies (Didiot et al., 2016; Zhao et al., 2019). We generated integrin-β1-down expression SCS-Exos from sh integrin-β1-transfected SCs. We found that compared with $SCs^{ctrlshRNA}$-Exos, the level of integrin-β1 was downregulated in $SCs^{sh\ integrin-\beta1}$-Exos. And the proliferation, migration, and tube formation of bEnd.3 cells were inhibited in the $SCs^{sh\ integrin-\beta1}$-Exos group once the expression level of integrin-β1 was downregulated in the exosome derived from the genetically modified SCs. Our data also indicated that integrin-β1 can be transferred from SCs-Exos to bEnd.3 cells, and SCs-Exos exerted a pro-angiogenesis role on bEnd.3 cells partly by transferring integrin-β1.

We further investigated the role of SCs-Exos on the injured spinal cord after SCI and we injected SCs-Exos through the tail vein in the SCI model. We found that the microvascular density and the number of new blood vessel formations in the spinal cord tissue were significantly increased in the SCs-Exos-treated group, and the cavities of the spinal cord tissue in the SCs-Exo treatment group were significantly reduced compared with the Control groups, and the BBB score was significantly higher in SCs-Exo treatment groups than that in other injury groups. These demonstrated that SCs-Exo significantly improves angiogenesis, reduces tissue damage, and promotes the recovery of hindlimb function after SCI. These data also indicated that there is a close relationship between pro-angiogenesis and improved functional outcomes after SCI. However, these protective effects on the spinal cord were partly abolished when integrin-β1 was inhibited in SCs-Exo cargo. These results indicated that SCs-Exo exerted a pro-angiogenesis role on SCI partly due to its exosomal integrin-β1. However, this pro-angiogenesis effect of SCs-Exos was not completely blocked by integrin-β1 inhibition. This suggests that SCs-Exos also contain other molecules that play a role in promoting angiogenesis. Therefore, the role of other molecules in mediating the effect of SCs-Exos on promoting angiogenesis needs to be further investigated.

11. Conclusion

In conclusion, in the present study, we revealed that SCs-Exos treatment promoted proliferation, migration, and tube formation of endothelial cells, promoted angiogenesis, reduced tissue damage, and facilitated neurological function recovery after SCI, and integrin-β1 played a crucial role in mediating the role of SCs-Exos in this process. Therefore, the upregulation of integrin-β1 in SCs-Exos may serve as a new potential therapeutic strategy for the treatment of SCI.

Data availability statement

The original contributions presented in this study are included in the article/supplementary material, further inquiries can be directed to the corresponding author.

Ethics statement

The animal study was reviewed and approved by the Ethics Committee of Fujian Provincial Hospital (license no. K2018-02-012).

Author contributions

F-YL designed the study. J-HH, Y-NC, HH, and C-HF did the experiment and analyzed the data. J-HH and Z-YX analyzed the data and wrote the manuscript. All authors contributed to the article and approved the submitted version.

Funding

This work was supported by the High-level Hospital Foster Grants from Fujian Provincial Hospital, Fujian Province, China

(no. 2019HSJJ26) and the Foundation of Natural and Science of Fujian Province, China (no. 2020J011092).

Acknowledgments

We would like to thank C-HF for his technical support during the immunofluorescence staining procedure.

Conflict of interest

C-HF was employed by Fuzhou Maixin Biotech. Co., Ltd.

The remaining authors declare that the research was conducted in the absence of any commercial or financial relationships that could be construed as a potential conflict of interest.

Publisher's note

All claims expressed in this article are solely those of the authors and do not necessarily represent those of their affiliated organizations, or those of the publisher, the editors and the reviewers. Any product that may be evaluated in this article, or claim that may be made by its manufacturer, is not guaranteed or endorsed by the publisher.

References

Assinck, P., Duncan, G., Hilton, B., Plemel, J., and Tetzlaff, W. (2017). Cell transplantation therapy for spinal cord injury. *Nat. Neurosci.* 20, 637–647. doi: 10.1038/nn.4541

Basso, D., Beattie, M., and Bresnahan, J. (1995). A sensitive and reliable locomotor rating scale for open field testing in rats. *J. Neurotrauma* 12, 1–21. doi: 10.1089/neu.1995.12.1

Braccioli, L., van Velthoven, C., and Heijnen, C. (2014). Exosomes: A new weapon to treat the central nervous system. *Mol. Neurobiol.* 49, 113–119. doi: 10.1007/s12035-013-8504-9

Cao, Y., Zhou, Y., Ni, S., Wu, T., Li, P., Liao, S., et al. (2017). Three dimensional quantification of microarchitecture and vessel regeneration by synchrotron radiation microcomputed tomography in a rat model of spinal cord injury. *J. Neurotrauma* 34, 1187–1199. doi: 10.1089/neu.2016.4697

Carlson, G., and Gorden, C. (2002). Current developments in spinal cord injury research. *Spine J.* 2, 116–128. doi: 10.1016/S1529-9430(01)00029-8

Crock, H., Yoshizawa, H., Yamagishi, M., and Crock, M. (2005). Commentary on the prevention of paralysis after traumatic spinal cord injury in humans: The neglected factor–urgent restoration of spinal cord circulation. *Eur. Spine J.* 14, 910–914. doi: 10.1007/s00586-005-0924-4

Deng, L., Walker, C., and Xu, X. (2015). Schwann cell transplantation and descending propriospinal regeneration after spinal cord injury. *Brain Res.* 1619, 104–114. doi: 10.1016/j.brainres.2014.09.038

Didiot, M., Hall, L., Coles, A., Haraszti, R., Godinho, B., Chase, K., et al. (2016). Exosome-mediated delivery of hydrophobically modified siRNA for huntingtin mRNA silencing. *Mol. Ther.* 24, 1836–1847. doi: 10.1038/mt.2016.126

Dreyer, F., and Baur, A. (2016). Biogenesis and functions of exosomes and extracellular vesicles. *Methods Mol. Biol.* 1448, 201–216. doi: 10.1007/978-1-4939-3753-0_15

Dumont, R., Okonkwo, D., Verma, S., Hurlbert, R., Boulos, P., Ellegala, D., et al. (2001). Acute spinal cord injury, part I: Pathophysiologic mechanisms. *Clin. Neuropharmacol.* 24, 254–264. doi: 10.1097/00002826-200109000-00002

Goetzl, E., Boxer, A., Schwartz, J., Abner, E., Petersen, R., Miller, B., et al. (2015). Altered lysosomal proteins in neural-derived plasma exosomes in preclinical Alzheimer disease. *Neurology* 85, 40–47. doi: 10.1212/WNL.0000000000001702

Goto, K., Takemura, G., Takahashi, T., Okada, H., Kanamori, H., Kawamura, I., et al. (2016). Intravenous administration of endothelial colony-forming cells overexpressing integrin β1 augments angiogenesis in ischemic legs. *Stem Cells Transl. Med.* 5, 218–226. doi: 10.5966/sctm.2015-0096

Huang, J., Xu, Y., Yin, X., and Lin, F. (2020). Exosomes derived from miR-126-modified MSCs promote angiogenesis and neurogenesis and attenuate apoptosis after spinal cord injury in rats. *Neuroscience* 424, 133–145. doi: 10.1016/j.neuroscience.2019.10.043

Huang, J., Yin, X., Xu, Y., Xu, C., Lin, X., Ye, F., et al. (2017). Systemic administration of exosomes released from mesenchymal stromal cells attenuates apoptosis, inflammation, and promotes angiogenesis after spinal cord injury in rats. *J. Neurotrauma* 34, 3388–3396. doi: 10.1089/neu.2017.5063

Keely, S., Glover, L., MacManus, C., Campbell, E., Scully, M., Furuta, G., et al. (2009). Selective induction of integrin beta1 by hypoxia-inducible factor: Implications for wound healing. *FASEB J.* 23, 1338–1346. doi: 10.1096/fj.08-125344

Lee, M., Ban, J., Kim, K., Jeon, G., Im, W., Sung, J., et al. (2016). Adipose-derived stem cell exosomes alleviate pathology of amyotrophic lateral sclerosis in vitro. *Biochem. Biophys. Res. Commun.* 479, 434–439. doi: 10.1016/j.bbrc.2016.09.069

Lopez-Verrilli, M., Picou, F., and Court, F. (2013). Schwann cell-derived exosomes enhance axonal regeneration in the peripheral nervous system. *Glia* 61, 1795–1806. doi: 10.1002/glia.22558

Malan, D., Wenzel, D., Schmidt, A., Geisen, C., Raible, A., Bölck, B., et al. (2010). Endothelial beta1 integrins regulate sprouting and network formation during vascular development. *Development* 137, 993–1002. doi: 10.1242/dev.045377

Martirosyan, N., Feuerstein, J., Theodore, N., Cavalcanti, D., Spetzler, R., and Preul, M. (2011). Blood supply and vascular reactivity of the spinal cord under normal and pathological conditions. *J. Neurosurg. Spine* 15, 238–251. doi: 10.3171/2011.4.SPINE10543

Mettouchi, A., and Meneguzzi, G. (2006). Distinct roles of beta1 integrins during angiogenesis. *Eur. J. Cell Biol.* 85, 243–247. doi: 10.1016/j.ejcb.2005.09.010

Milner, R., and Campbell, I. (2002). Developmental regulation of beta1 integrins during angiogenesis in the central nervous system. *Mol. Cell. Neurosci.* 20, 616–626. doi: 10.1006/mcne.2002.1151

Oudega, M., and Xu, X. (2006). Schwann cell transplantation for repair of the adult spinal cord. *J. Neurotrauma* 23, 453–467. doi: 10.1089/neu.2006.23.453

Pan, D., Zhu, S., Zhang, W., Wei, Z., Yang, F., Guo, Z., et al. (2022). Autophagy induced by Schwann cell-derived exosomes promotes recovery after spinal cord injury in rats. *Biotechnol. Lett.* 44, 129–142. doi: 10.1007/s10529-021-03198-8

Record, M., Subra, C., Silvente-Poirot, S., and Poirot, M. (2011). Exosomes as intercellular signalosomes and pharmacological effectors. *Biochem. Pharmacol.* 81, 1171–1182. doi: 10.1016/j.bcp.2011.02.011

Takami, T., Oudega, M., Bates, M., Wood, P., Kleitman, N., and Bunge, M. (2002). Schwann cell but not olfactory ensheathing glia transplants improve hindlimb locomotor performance in the moderately contused adult rat thoracic spinal cord. *J. Neurosci.* 22, 6670–6681. doi: 10.1523/JNEUROSCI.22-15-06670.2002

Thuret, S., Moon, L., and Gage, F. (2006). Therapeutic interventions after spinal cord injury. *Nat. Rev. Neurosci.* 7, 628–643. doi: 10.1038/nrn1955

Toft, A., Tome, M., Barnett, S., and Riddell, J. (2013). A comparative study of glial and non-neural cell properties for transplant-mediated repair of the injured spinal cord. *Glia* 61, 513–528. doi: 10.1002/glia.22452

Webber, C., and Zochodne, D. (2010). The nerve regenerative microenvironment: Early behavior and partnership of axons and Schwann cells. *Exp. Neurol.* 223, 51–59. doi: 10.1016/j.expneurol.2009.05.037

Wei, Z., Fan, B., Ding, H., Liu, Y., Tang, H., Pan, D., et al. (2019). Proteomics analysis of Schwann cell-derived exosomes: A novel therapeutic strategy for central nervous system injury. *Mol. Cell. Biochem.* 457, 51–59. doi: 10.1007/s11010-019-03511-0

Zhang, Y., Chopp, M., Liu, X., Katakowski, M., Wang, X., Tian, X., et al. (2017). Exosomes derived from mesenchymal stromal cells promote axonal growth of cortical neurons. *Mol. Neurobiol.* 54, 2659–2673. doi: 10.1007/s12035-016-9851-0

Zhao, L., Jiang, X., Shi, J., Gao, S., Zhu, Y., Gu, T., et al. (2019). Exosomes derived from bone marrow mesenchymal stem cells overexpressing microRNA-25 protect spinal cords against transient ischemia. *J. Thorac. Cardiovasc. Surg.* 157, 508–517. doi: 10.1016/j.jtcvs.2018.07.095

Zheng, L., Ao, Q., Han, H., Zhang, X., and Gong, Y. (2010). Evaluation of the chitosan/glycerol-beta-phosphate disodium salt hydrogel application in peripheral nerve regeneration. *Biomed. Mater.* 5:35003. doi: 10.1088/1748-6041/5/3/035003

Zheng, M., Huang, M., Ma, X., Chen, H., and Gao, X. (2019). Harnessing exosomes for the development of brain drug delivery systems. *Bioconjug. Chem.* 30, 994–1005. doi: 10.1021/acs.bioconjchem.9b00085

frontiers | Frontiers in Cellular Neuroscience

TYPE Original Research
PUBLISHED 08 March 2023
DOI 10.3389/fncel.2023.1065873

OPEN ACCESS

EDITED BY
Yuchuan Ding,
Wayne State University, United States

REVIEWED BY
Guangtao Xu,
Jiaxing University Medical College, China
Yong Shen,
University of Science and Technology of China, China
Rasim Mogulkoc,
Selçuk University, Türkiye

*CORRESPONDENCE
Zhifeng Qi
✉ qizhifeng@xwh.ccmu.edu.cn
Yongmei Zhao
✉ zhaoym@ccmu.edu.cn

†These authors have contributed equally to this work

SPECIALTY SECTION
This article was submitted to Cellular Neuropathology, a section of the journal Frontiers in Cellular Neuroscience

RECEIVED 10 October 2022
ACCEPTED 15 February 2023
PUBLISHED 08 March 2023

CITATION
Li W, Yang X, Ding M, Shi W, Huang Y, An Q, Qi Z and Zhao Y (2023) Zinc accumulation aggravates cerebral ischemia/reperfusion injury by promoting inflammation.
Front. Cell. Neurosci. 17:1065873.
doi: 10.3389/fncel.2023.1065873

Zinc accumulation aggravates cerebral ischemia/reperfusion injury by promoting inflammation

Wei Li[1,2†], Xueqi Yang[1,2†], Mao Ding[1], Wenjuan Shi[1,2], Yuyou Huang[1], Qi An[1,2], Zhifeng Qi[1,2*] and Yongmei Zhao[1,2*]

[1]Institute of Cerebrovascular Diseases Research, Xuanwu Hospital of Capital Medical University, Beijing, China, [2]Beijing Geriatric Medical Research Center, Beijing, China

Intracellular zinc accumulation has been shown to be associated with neuronal death after cerebral ischemia. However, the mechanism of zinc accumulation leading to neuronal death in ischemia/reperfusion (I/R) is still unclear. Intracellular zinc signals are required for the production of proinflammatory cytokines. The present study investigated whether intracellular accumulated zinc aggravates I/R injury through inflammatory response, and inflammation-mediated neuronal apoptosis. Male Sprague–Dawley rats were treated with vehicle or zinc chelator TPEN 15 mg/kg before a 90-min middle cerebral artery occlusion (MCAO). The expressions of proinflammatory cytokines TNF-α, IL-6, NF-κB p65, and NF-κB inhibitory protein IκB-α, as well as anti-inflammatory cytokine IL-10 were assessed at 6 or 24 h after reperfusion. Our results demonstrated that the expression of TNF-α, IL-6, and NF-κB p65 increased after reperfusion, while the expression of IκB-α and IL-10 decreased, suggesting that cerebral ischemia triggers inflammatory response. Furthermore, TNF-α, NF-κB p65, and IL-10 were all colocalized with the neuron-specific nuclear protein (NeuN), suggesting that the ischemia-induced inflammatory response occurs in neurons. Moreover, TNF-α was also colocalized with the zinc-specific dyes Newport Green (NG), suggesting that intracellular accumulated zinc might be associated with neuronal inflammation following cerebral I/R. Chelating zinc with TPEN reversed the expression of TNF-α, NF-κB p65, IκB-α, IL-6, and IL-10 in ischemic rats. Besides, IL-6-positive cells were colocalized with TUNEL-positive cells in the ischemic penumbra of MCAO rats at 24 h after reperfusion, indicating that zinc accumulation following I/R might induce inflammation and inflammation-associated neuronal apoptosis. Taken together, this study demonstrates that excessive zinc activates inflammation and that the brain injury caused by zinc accumulation is at least partially due to specific neuronal apoptosis induced by inflammation, which may provide an important mechanism of cerebral I/R injury.

KEYWORDS

zinc, inflammation, middle cerebral artery occlusion, cerebral ischemia, apoptosis

1. Introduction

Zinc (Zn^{2+}) is essential for normal cellular functions and plays a signaling role in the brain (Qi et al., 2016; Mutlu and Baltaci, 2020; Alvarez et al., 2021). Zn^{2+} influx from the extracellular space and its mobilization from intracellular pools such as mitochondria, lysosomes, and cytosolic Zn^{2+} binding proteins lead to neuronal damage (Galasso and Dyck, 2007; Sensi et al., 2011). A growing number of basic and clinical experiments have suggested that cerebral ischemia/reperfusion (I/R) caused cellular injury resulting from activation of Zn^{2+} accumulation (Guo et al., 2019; Zhao et al., 2021; Manzanero et al., 2013). Removing Zn^{2+} with a specific Zn^{2+} chelator N,N,N′,N′-tetrakis (2-pyridylmethyl) ethylenediamine (TPEN) reduced Zn^{2+} accumulation in ischemic neurons, rescued them from cell death and improved functional outcomes (Qi et al., 2019). These findings implicate that Zn^{2+} acts as a critical mediator of neuronal death at high concentrations in the ischemic condition. In recent study, we showed that the overload of Zn^{2+} in mitochondria disrupted the function of mitochondria, resulting in reactive oxygen species generation and triggering cell death (Zhao et al., 2018; Qi et al., 2019). Reducing Zn^{2+} accumulation in mitochondria contributes to decreased cerebral ischemic injury by normobaric hyperoxia treatment (Dong et al., 2015). We also found that intracellular accumulated Zn^{2+} aggravates I/R injury through inducing endoplasmic reticulum stress (Zhao et al., 2022). However, the reason why Zn^{2+} produces severe brain damage remains to be elucidated.

Inflammation and immune responses have been proven to be crucial factors associated with stroke onset and progression (Lively et al., 2016; Li T. et al., 2022). In recent years, several cytokines have been proven especially promising as potential therapeutic targets for experimental ischemic stroke including the tumor necrosis factor-α (TNF-α), interleukin-6 (IL-6), and the anti-inflammatory cytokine-10 (IL-10; Zhang et al., 2017; Lambertsen et al., 2019). TNF-α is a proinflammatory factor and works as an initiation factor of inflammatory response. The expression of TNF-α is rapidly upregulated after cerebral ischemia, leading to neurotoxicity (Vila et al., 2000; Shen et al., 2022). As a nuclear transcription factor, nuclear factor kappa B (NF-κB) constitutes the most basic NF-κB signaling pathway with IκB and IκB kinase complex, which is involved in the regulation of inflammation (Chen et al., 1998; Berti et al., 2002). In I/R injury, NF-κB is activated by a variety of stimuli including TNF-α (Jarosz et al., 2017; Kang et al., 2019). Production of TNF-α and activation of NF-κB have been documented to play critical roles in the process of cerebral disease (Hussain et al., 2016). Besides, the activation of NF-κB is also regulated by IL-6 (Jarosz et al., 2017; Kang et al., 2019). IL-6 is a pleiotropic cytokine involved in many central nervous system disorders including stroke. The expression of IL-6 is most prominently identified in neurons in the peri-ischemic regions (Kumari et al., 2016; Rasmussen et al., 2019; Ridwan et al., 2021). In contrast to IL-6, IL-10 is a pleiotropic anti-inflammatory cytokine, which binds to IL-10 receptors to reduce inflammation and limit apoptosis (Chen et al., 2013). Therapeutic administration of IL-10 has been shown to be neuroprotective in experimental stroke and to limit post-stroke inflammation (Chen et al., 2013; Garcia et al., 2017).

The immune system, especially the inflammation, is markedly susceptible to changes of Zn^{2+} levels (Haase and Rink, 2014). Zn^{2+} induces the synthesis of DNA, RNA, and proteins to meet the desired immune response (Baltaci et al., 2019). Recent reports have indicated that Zn^{2+} homeostasis affects neuroinflammation in the brain (Baltaci et al., 2022). Intracellular Zn^{2+} signals are required for the production of proinflammatory cytokines IL-6 and TNF-α, which are also directly induced by incubation with high extracellular Zn^{2+} concentrations (Haase and Rink, 2014; Olechnowicz et al., 2018). Also, in type 2 diabetes mellitus patients, impaired Zn^{2+} homeostasis leads to uncontrolled expression of immune mediators, such as IL-6 and NF-κB, which simultaneously exacerbate the immune response (Bonaventura et al., 2015; Olechnowicz et al., 2018). Zn^{2+} is necessary for the activation of NF-κB signaling pathway, whereas chelating Zn^{2+} with membrane permeable Zn^{2+} specific chelator TPEN completely blocked this pathway (Wang et al., 2015; Jarosz et al., 2017). However, *in vitro*, Zn^{2+} augments monocyte adhesion to endothelial cells, and its deficiency increases the production of proinflammatory cytokines (Jarosz et al., 2017). Therefore, the relationship between Zn^{2+} and inflammation is still under debate, especially in cerebral I/R. The detailed relationship between Zn^{2+} accumulation and inflammation in cerebral I/R needs to be further studied.

To investigate the interaction between Zn^{2+} accumulation and inflammation in the ischemic brain, a rat model of focal cerebral I/R was used in this study. We hypothesize that Zn^{2+} accumulation could exert neurotoxicity effect by promoting inflammation responses in ischemic penumbra of middle cerebral artery occlusion (MCAO) rats. These results provide a novel mechanism for the toxic effect of Zn^{2+} on cerebral I/R injury.

2. Materials and methods

2.1. Rat model of focal cerebral ischemia/reperfusion

Male Sprague-Dawley (SD) rats (280–300 g) were purchased from SPF Biotechnology Co. (Beijing, China). Animal protocols for these studies were approved by the Institutional Animal Care and Use Committee of Xuanwu Hospital of Capital Medical University. The specific method we used to establish the right MCAO model in SD rats was described previously (Zhao et al., 2014). Briefly, rats were anesthetized with 2% isoflurane in N_2O:O_2 (70%:30%). MCAO was induced by the modified intraluminal filament method. The left common carotid artery, internal carotid artery, and external carotid artery branches were exposed by blunt dissection. A microscopic shear is then used to cut an incision in the external carotid artery stump, in which a 4–0 surgical nylon filament with a silicon-coated tip was inserted into the internal carotid artery approximately 18 mm beyond the carotid bifurcation, thereby occluding the origin of the middle cerebral artery. Rats were subjected to 90 min right MCAO followed by 6 or 24 h after reperfusion. Sham-operated rats underwent the same procedure without MCAO. A feedback temperature-controlled heating pad was used during and after surgery to maintain the rat's body temperature at 37°C ± 0.5°C. Rats were housed in individual cages with free access to food and water (12-h light/dark cycles at 22°C ± 2°C).

2.2. Experimental groups, drug administration, and tissue collection

Rats were assigned randomly to three groups: vehicle-treated sham-operated group, vehicle-treated MCAO group, and TPEN-treated MCAO group. Each group was further divided into two subgroups according to different reperfusion time (6 and 24 h; n = 6 in each subgroup). TPEN (15 mg/kg dissolved in 10% DMSO) was injected intraperitoneally 30 min before reperfusion. Physiological saline with 10% DMSO was used as control (Zhao et al., 2014).

Brains were harvested and cut into coronal sections with a thickness of 2 mm from 0 to 1.0 bregma. The ipsilateral side of the third slice was processed for Western blotting. The fourth to sixth slices were prepared for 20 μm frozen sections, which were then used for histological staining.

2.3. Immunofluorescence and cytosolic labile Zn^{2+} staining

Frozen sections of 20 μm thickness were fixed with 4% paraformaldehyde at room temperature for 10 min. After permeated by 0.5% Triton X-100 and blocked with goat serum, the sections were incubated at 4°C overnight either with the primary antibody against IL-6 (1:200, CST), or with the primary antibody against TNF-α (1:200, CST), NF-κB (1:200, CST), IL-10 (1:200, CST) with mouse monoclonal antibody against NeuN (1:100, CST) respectively. And then, sections were incubated with secondary antibody (1:200, Invitrogen) for 1 h at room temperature. The sections were sealed by dropping the tablet blocking agent containing 4′6-diamidino-2-phenylindole (DAPI).

For double staining of cytosolic labile Zn^{2+} with TNF-α, the sections were first incubated with zinc-specific dyes Newport Green (NG; N7991, Invitrogen) for 30 min in the dark as previously described (Zhao et al., 2014). After rinsing in PBS and fixed with 4% paraformaldehyde for 10 min, the sections were incubated with anti-TNF-α antibody (1:200, CST). After incubating with secondary antibody, the nuclei were stained with DAPI and fluorescence was measured with a Nikon fluorescence microscope.

For quantitative immunofluorescence, one in every four brain section samples was taken from a continuous series of sections prepared from brain tissue, a total of three sections were taken from each brain. Three areas were selected randomly in black rectangle of **Figure 1A** from each brain section under 200× magnification and the number of positively stained cells were counted.

2.4. Double staining of IL-6 and terminal deoxyribonucleotide transferase dUTP nick end labeling (TUNEL)

The frozen sections were incubated overnight with rabbit polyclonal antibody against IL-6 (1:200, CST). After incubating with secondary antibody (1:200, Invitrogen), a standard TUNEL procedure was performed (in situ Cell Death Detection Kit, POD, Roche Applied Science, Switzerland). The cell nucleus was stained with DAPI and images were acquired using a fluorescence microscope.

2.5. Western blotting analysis

Ipsilateral brain tissue slices collected 6 or 24 h after reperfusion were homogenized in RIPA buffer containing protease inhibitors. Protein concentration was determined by a BCA protein assay kit (Pierce, Rockford). Protein samples were separated by 10% SDS-polyacrylamide gel electrophoresis and subsequently transferred to 0.22 μm polyvinylidene difluoride membrane (Millipore). After blocking in 5% skimmed milk for 2 h at room temperature, the membrane was incubated overnight at 4°C with mouse monoclonal antibody against IκB-α (1:1,000; CST). The membrane was then incubated with peroxidase-conjugated goat anti-mouse IgG (1:2,000; Santa) for 1 h and developed with the Super Signal West Pico horseradish peroxidase substrate kit (Pierce). The membrane was re-probed with anti-β-actin antibody (1:4,000; Sigma-Aldrich), which served as a loading control. Expression levels were quantitated by measuring the optical density and expressing the value as a ratio relative to that of β-actin.

2.6. Statistical analysis

Data are expressed as mean ± standard errors of the mean (SEMs). Statistical analysis was performed using SPSS version 20.0 (SPSS). The Shapiro–Wilk normality test was used to analyze the normality of data. The data follows a normal distribution were assessed by one-way analysis of variance (ANOVA), followed by *post hoc* least significant difference/Tamhane T2 tests for multiple comparisons. If data did not pass the normality analysis, the data were analyzed using Kruskal-Wallis non-parametric tests. A value of $P < 0.05$ was considered statistically significant.

3. Results

3.1. TNF-α is colocalized with cytosolic labile Zn^{2+}/NeuN following cerebral I/R, and high level of TNF-α is suppressed by TPEN

To investigate the expression of TNF-α, an initiator of inflammatory response, in the ischemic penumbra following cerebral I/R injury and whether chelating Zn^{2+} could inhibit the expression of TNF-α, double immunofluorescence staining was performed by using TNF-α antibody and zinc-specific dye. **Figures 1B,C** showed that there were very few TNF-α and NG positive cells in the sham group, however, many TNF-α and NG positive cells were observed in the ischemic penumbra of MCAO rats at 6 and 24 h after reperfusion, indicating that cytosolic labile Zn^{2+} accumulation and TNF-α expression occur in the same cells of MCAO rats. Moreover, a drastic reperfusion time-dependent increase of TNF-α-positive cells were observable in the ischemic

10.3389/fncel.2023.1065873

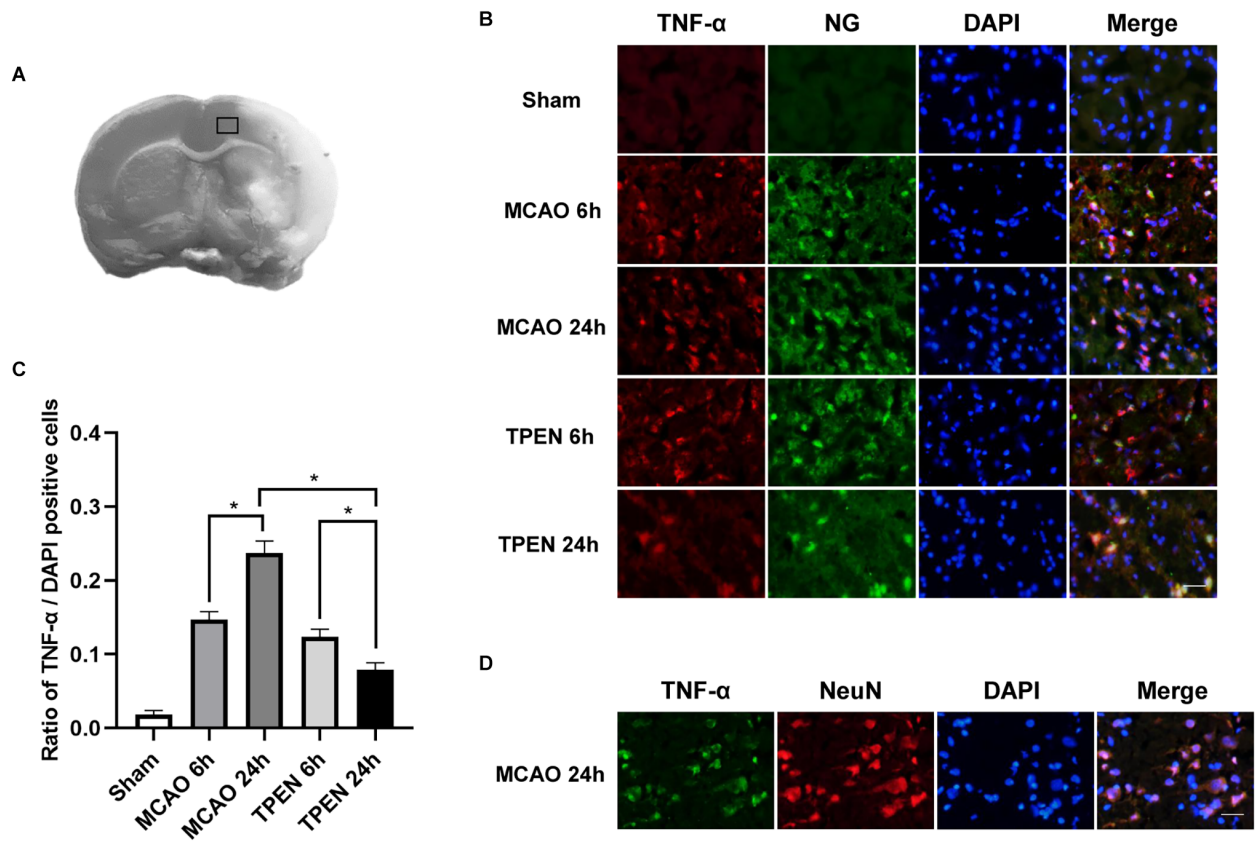

FIGURE 1
N,N,N′,N′-tetrakis (2-pyridylmethyl) ethylenediamine (TPEN) treatment suppresses the upregulation of inflammatory initiator TNF-α in neurons in ischemic penumbra of middle cerebral artery occlusion (MCAO) rats. **(A)** Brain tissues in black rectangle were observed for histological staining. **(B)** Representative double staining for TNF-α (red) and zinc-specific membrane permeable fluorescent dyes Newport Green (NG; green) in ischemic penumbra at 6 and 24 h after reperfusion. Nuclei were counterstained with 4′,6-diamidino-2-phenylindole (DAPI; blue). **(C)** Quantification of TNF-α-positive cells. Data are expressed as means ± SEMs (n = 6). *P < 0.05 vs. the indicated group. **(D)** Representative double staining for TNF-α (green) and neuron-specific nuclear protein (NeuN; red) in the ischemic penumbra of MCAO rats at 24 h after reperfusion. Bars = 20 μm.

penumbra at 6 and 24 h after reperfusion, indicating that TNF-α expression keeps on increasing after I/R (P < 0.05). TPEN treatment decreased the expression of TNF-α compared to the vehicle-treated MCAO group (P < 0.05). Besides, TNF-α-positive cells were displayed NeuN-positive in MCAO rats at 24 h after reperfusion (Figure 1D). These results indicate that ischemia-induced Zn^{2+} accumulation could increase TNF-α expression in neurons, which might aggravate I/R injury.

3.2. Chelating Zn^{2+} increases IκB-α expression following I/R injury

IκB-α is an inhibitor of NF-κB, which binds to and maintains NF-κB in an inactive state in the cytoplasm. Upon stimulation, IκB-α is rapidly downregulated, resulting in the nuclear translocation of NF-κB and initiation of target gene transcription (Traenckner et al., 1994). In order to explore whether Zn^{2+} accumulation influences the level of IκB-α, we measured the expression of IκB-α by Western blotting. The results showed a reperfusion time-dependent decrease of IκB-α expression in MCAO rats at 6 and 24 h after reperfusion (Figures 2A,B, P < 0.05). TPEN treatment increased the expression of IκB-α at 6 and 24 h after reperfusion as compared to the vehicle-treated MCAO group (P < 0.05), implying that Zn^{2+} accumulation promotes IκB-α degradation after cerebral ischemia.

3.3. Nuclear translocation of NF-κB increases in neurons after I/R injury and chelating Zn^{2+} by TPEN reduces the nuclear translocation of NF-κB in ischemic rats

The translocation of NF-κB from cytoplasm to nucleus is known to cause NF-κB activation (Zhang et al., 2005). Figure 3A showed that NF-κB-positive cells were colocalized with NeuN-positive cells in ischemic penumbra of MCAO rats, indicating that ischemia-induced inflammation occurs in neurons. Most of NF-κB p65 was localized in the neuron cytoplasm in the sham group. However, with the increase of reperfusion time, NF-κB p65 increasingly translocated to the neuronal nucleus in the ischemic penumbra of MCAO rats at 6 and 24 h after reperfusion (Figures 3A–C, P < 0.05), indicating that inflammatory cytokine NF-κB p65 is activated by I/R injury in ischemic neurons.

10.3389/fncel.2023.1065873

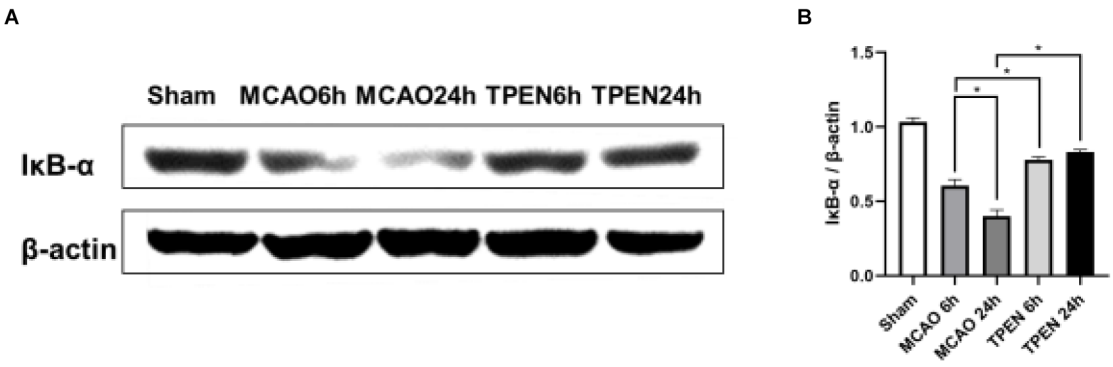

FIGURE 2
N,N,N′,N′-tetrakis (2-pyridylmethyl) ethylenediamine (TPEN) treatment suppresses the downregulation of inhibitory protein IκB-α of NF-κB in the ischemic hemisphere of middle cerebral artery occlusion (MCAO) rats. **(A,B)** Ipsilateral brain tissue at 6 and 24 h after reperfusion were examined for the expression of IκB-α by Western blotting, with β-actin used as a loading control. Data are expressed as means ± SEMs (n = 6). *P < 0.05 vs. the indicated group.

To investigate the interaction between cytosolic labile Zn^{2+} accumulation and inflammation, Zn^{2+} chelator TPEN was used to remove cytosolic labile Zn^{2+} in MCAO rats. The results showed that TPEN treatment significantly reduced the number of nuclear NF-κB p65-positive cells and the nuclear/cytoplasmic ratio of NF-κB p65 fluorescence intensity compared with the vehicle-treated MCAO group (P < 0.05). Taken together, these results indicate that Zn^{2+} accumulation after cerebral ischemia promotes nuclear translocation of NF-κB, which aggravates inflammatory response.

3.4. Inflammation-specific apoptosis is occurred in ischemic penumbra, and chelating Zn^{2+} by TPEN suppresses the expression of IL-6 in ischemic rats

To further gain insight into the effects of Zn^{2+} on inflammation, the expression of IL-6 in different groups was assessed by immunofluorescence. There were few IL-6-positive cells in the sham group. However, a drastic reperfusion time dependent increase of IL-6-positive cells was observed in the ischemic penumbra of MCAO rats at 6 and 24 h after reperfusion (**Figures 4A,B**, P < 0.05). TPEN treatment decreased IL-6-positive cells vs. vehicle-treated MCAO group (P < 0.05). Besides, IL-6-stained cells were displayed TUNEL-positive in MCAO rats at 24 h after reperfusion (**Figure 4C**). These results suggest that Zn^{2+} accumulation promotes inflammation responses by upregulating proinflammatory cytokines, leading to inflammation-specific apoptosis in ischemic rats.

3.5. Chelating Zn^{2+} increases the expression of anti-inflammatory cytokines in neurons in ischemic penumbra

To investigate the expression of anti-inflammatory cytokine IL-10 in neurons following cerebral I/R injury and whether chelating Zn^{2+} could affect the expression of IL-10, double immunofluorescence staining was performed by using IL-10 and NeuN antibodies. **Figures 5A,B** showed that IL-10-positive cells were colocalized with NeuN-positive cells, and there were a large number of IL-10 and NeuN-positive cells in the sham group, while a small number of IL-10 and NeuN-positive cells were observed in the ischemic penumbra of vehicle-treated MCAO rats, indicating that ischemia decreased the level of anti-inflammatory cytokine in neurons. TPEN treatment increased the expression of IL-10 after 90 min ischemia and 24 h reperfusion as compared to the vehicle-treated MCAO group (P < 0.05). These results suggest that Zn^{2+} accumulation decreases the expression of anti-inflammatory cytokines in ischemic neurons.

4. Discussion

In the present study, we investigated whether the Zn^{2+} induces ischemic brain injury by regulating inflammation. We demonstrated that a drastic reperfusion time-dependent increase of proinflammatory cytokines TNF-α, IL-6, and NF-κB p65 nuclear translocation in MCAO rats at 6 and 24 h after reperfusion, while IκB-α, the inhibitory protein of NF-κB, as well as the anti-inflammatory cytokines IL-10 decreased in the ischemic brain tissue of MCAO rats, indicating that cerebral I/R injury triggers inflammation. Importantly, TNF-α-positive cells were colocalized with Zn^{2+} indicator, NG. Treatment with Zn^{2+} chelator TPEN leads to a significant reduction in TNF-α, IL-6, NF-κB p65 expression and an increase in IκB-α and IL-10 expression, indicating that cytosolic labile Zn^{2+} accumulation promotes inflammation following I/R injury. Our results also revealed that TNF-α, NF-κB p65, and IL-10 were colocalized with NeuN-positive cells respectively, and IL-6-positive cells were largely colocalized with TUNEL, indicating that inflammation occurs in neurons of cerebral ischemic rats, which contributes to neuronal death of the brain after cerebral I/R. Taken together, the present study demonstrated that excessive Zn^{2+} accumulation following cerebral ischemia could activate inflammatory mediators and inflammation-mediated neuronal apoptosis, which is a novel mechanism of cerebral ischemic injury.

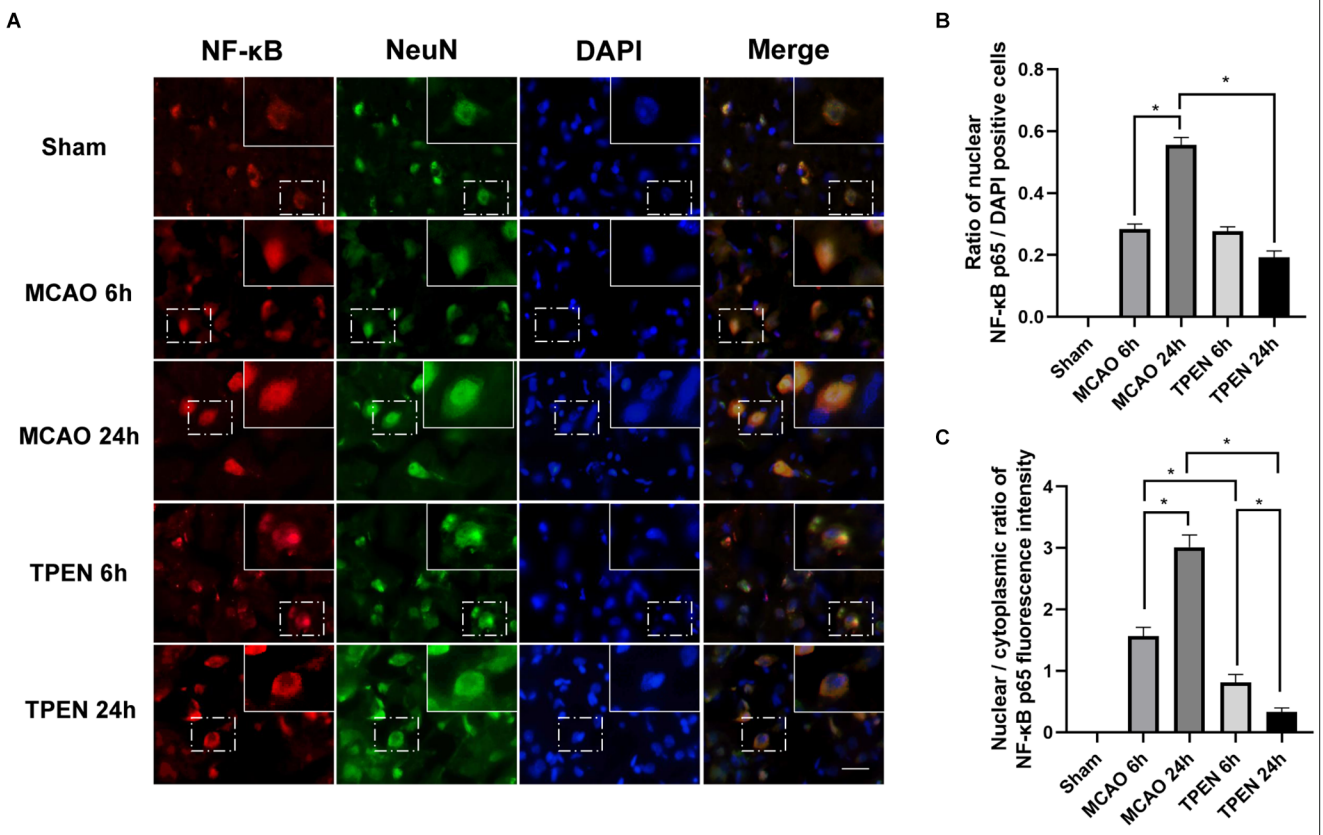

FIGURE 3
N,N,N′,N′-tetrakis (2-pyridylmethyl) ethylenediamine (TPEN) treatment suppresses the nuclear translocation of NF-κB p65 in neurons in the ischemic penumbra of middle cerebral artery occlusion (MCAO) rats. **(A)** Representative double staining for NF-κB p65 (red) and neuron-specific nuclear protein (NeuN; green) in ischemic penumbra at 6 and 24 h after reperfusion. Nuclei were counterstained with 4′,6-diamidino-2-phenylindole (DAPI; blue). Bar = 20 μm. The images in the dashed-line rectangles are magnified in the solid-line rectangles, showing the nuclear translocation of NF-κB p65 in the ischemic penumbra of MCAO rats. **(B)** The ratio of nuclear NF-κB p65-positive cells was determined. **(C)** The nuclear/cytoplasmic ratio of NF-κB p65 immunofluorescence intensity was determined. Data are expressed as means ± SEMs (n = 6). *P < 0.05 vs. the indicated group.

The inflammatory response was characterized by neutrophil accumulation and proinflammatory factors release (Zhou et al., 2023). It has been reported that neutrophils begin to enter the cerebral cortex through leptomeninges after 6 h of MCAO (Kim et al., 2019), followed by neuronal apoptosis at 24 h after reperfusion (Zhao et al., 2018). Therefore, the expression changes of proinflammatory cytokines and anti-inflammatory cytokine in ischemic rats were studied at 6 and 24 h after reperfusion in this study. TNF-α is a key mediator in neuronal immunomodulatory system, and its abnormal expression plays an important role in various pathological processes (Lambertsen et al., 2012; Li B. et al., 2022). In the present study, very few TNF-α-positive cells were observed in the brain of the sham group, whereas TNF-α-positive cells was gradually upregulated in the ischemic penumbra of MCAO rats at 6 and 24 h after reperfusion, indicating that cerebral I/R resulted in increased expression of TNF-α. Under physiological conditions, Zn^{2+} has been demonstrated to decrease the generation of TNF-α (Prasad et al., 2011; Prasad, 2012; Eddie-Amadi et al., 2022). However, high concentrations of Zn^{2+} in septic shock have been reported to promote the expression of endotoxin-induced TNF-α produced by human monocytes (von Bulow et al., 2007). Our previous study showed that intracellular accumulated Zn^{2+} induced cerebral I/R injury, and chelating Zn^{2+} significantly reduced ischemia-induced cerebral infarct (Zhao et al., 2018). In the present study, we found that TNF-α colocalized with NG and TPEN treatment significantly suppressed the expression of TNF-α in the ischemic penumbra of MCAO rats at 24 h after reperfusion, implying that chelating Zn^{2+} reduces ischemic injury by decreasing the expression of TNF-α in ischemic tissue. Therefore, we speculated that excessive Zn^{2+} accumulation following cerebral I/R might lead to the upregulation of TNF-α, which in turn promote inflammation-mediated brain damage.

NF-κB is a dimer redox-sensitive transcription factor consisting of p50 and p65, and its transcriptional activity is silenced by IκB (Perkins, 2007). Under normal conditions, the NF-κB complex binds to IκB and is sequestered in the cytoplasm. Matsui et al. found that NF-κB is activated after I/R injury in animals (Matsui et al., 2005). As a sequence-specific DNA binding protein, NF-κB was previously reported to be Zn^{2+} dependent (Zabel et al., 1991). Recent studies further reported that Zn^{2+} regulates the activation of NF-κB by acting on TNF-α transcription (Haase et al., 2008). Following stimulation with TNF-α, IκB kinase is activated. The NF-κB dimer becomes active when activated IκB kinase phosphorylates IκB, which leads to ubiquitination

10.3389/fncel.2023.1065873

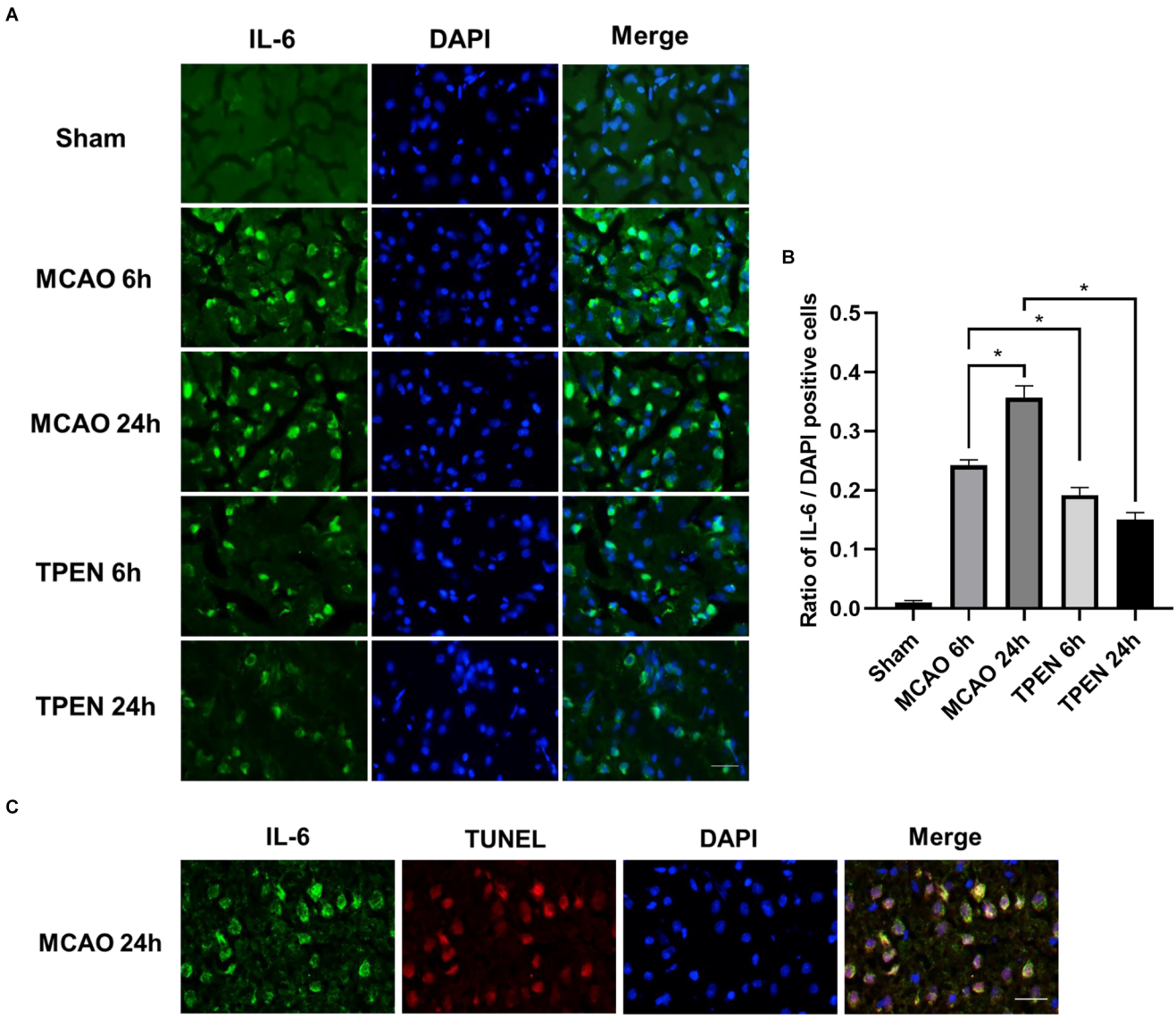

FIGURE 4
N,N,N′,N′-tetrakis (2-pyridylmethyl) ethylenediamine (TPEN) treatment suppresses the upregulation of proinflammatory cytokine IL-6 in the ischemic penumbra of middle cerebral artery occlusion (MCAO) rats, and IL-6-positive cells are colocalized with terminal deoxyribonucleotide transferase dUTP nick end labeling (TUNEL)-positive cells in the ischemic penumbra of MCAO rats. **(A)** Representative images of brain sections labeled with antibody against IL-6 (green). Nuclei were counterstained with 4′,6-diamidino-2-phenylindole (DAPI; blue). **(B)** Quantification of IL-6-positive cells. Data are expressed as means ± SEMs ($n = 6$). *$P < 0.05$ vs. the indicated group. **(C)** Representative double staining for IL-6 (green) and TUNEL-stained (red) in the ischemic penumbra of MCAO rats at 24 h after reperfusion. Bars = 20 μm.

and proteasomal degradation of IκB (Chen et al., 1998; Haase et al., 2008). Thus, in the present study, the decreased expression of IκB-α in MCAO rats at 6 and 24 h after reperfusion is possibly due to the increased expression of TNF-α. Chelating Zn^{2+} increased the IκB-α level in MCAO rats, suggesting that Zn^{2+} accumulation-induced increased TNF-α expression might lead to the degradation of IκB-α following cerebral I/R. With the degradation of IκB, NF-κB is released into the nucleus, leading to inflammatory response (Huang and Hung, 2013). In current study, we found that NF-κB p65-positive cells were colocalized with NeuN, NF-κB p65 mostly translocated to the neuronal nucleus in the ischemic penumbra of MCAO rats at 6 and 24 h after reperfusion, suggesting that NF-κB pathway is activated in neurons of ischemic rats. Moreover, nuclear NF-κB p65-positive cells were attenuated by TPEN treatment after reperfusion. Therefore, we speculated that excessive Zn^{2+} accumulation upregulates the expression of TNF-α, which in turn downregulates IκB, leading to the activation of NF-κB to promote neuronal apoptosis following I/R injury.

IL-6 is commonly regarded as a prominent mediator of the inflammatory response, which is involved in the elicitation of acute-phase inflammatory reactions/responses (Kumari et al., 2016; Rasmussen et al., 2019; Ridwan et al., 2021). During inflammatory response, IL-6 expression might be activated by

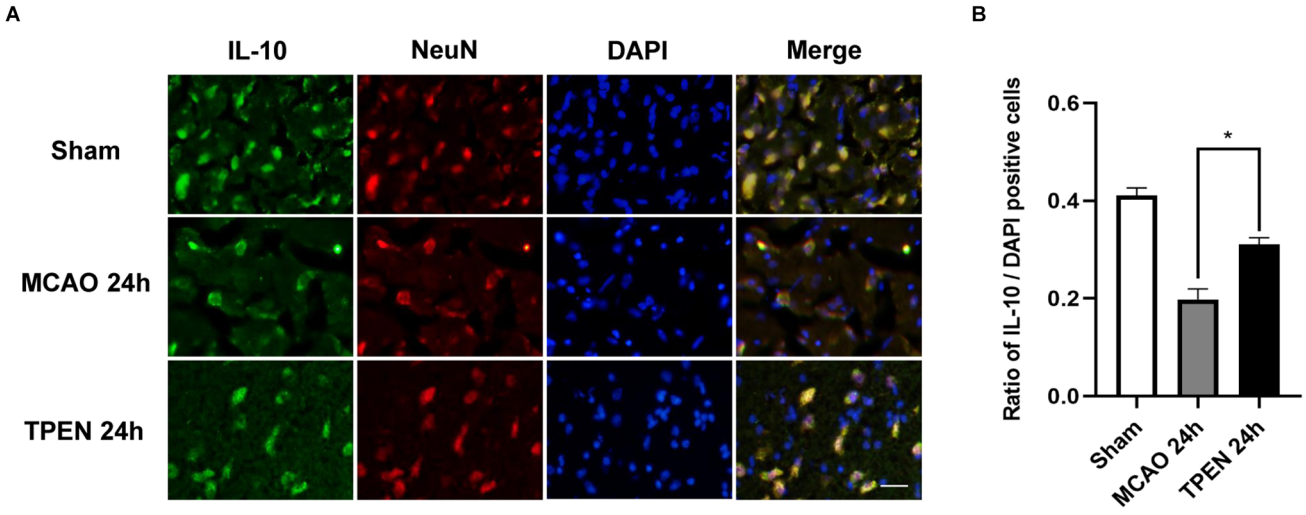

FIGURE 5
N,N,N′,N′-tetrakis (2-pyridylmethyl) ethylenediamine (TPEN) treatment suppresses the down-regulation of anti-inflammatory cytokine IL-10 in neurons in the ischemic penumbra of middle cerebral artery occlusion (MCAO) rats. **(A)** Representative double staining for IL-10 (green) and neuron-specific nuclear protein (NeuN; red) in ischemic penumbra at 24 h after reperfusion. Nuclei were counterstained with 4′,6-diamidino-2-phenylindole (DAPI; blue). Bar = 20 μm. **(B)** Quantification of IL-10-positive cells. Data are expressed as means ± SEMs (n = 6). *P < 0.05 vs. the indicated group.

TNF-α (Kumari et al., 2016; Hotter et al., 2019; Jenny et al., 2019; Lambertsen et al., 2019). Besides, it has been reported that Zn^{2+} levels affect IL-6 in DMBA-induced breast cancer in female rats (Gulbahce-Mutlu et al., 2021). In the present study, we found a reperfusion time-dependent increase in IL-6 expression in the ischemic penumbra of MCAO rats, which shows a similar trend with TNF-α. TPEN treatment decreased the expression of IL-6 in ischemic penumbra of MCAO rats at 6 and 24 h after reperfusion, indicating that inflammatory factor levels is associated with the reperfusion time in MCAO rats and the zinc-induced increased expression of TNF-α promotes the expression of IL-6, aggravating the inflammatory response of ischemic tissue. In addition, the results of this study showed that IL-6-positive cells were colocalized with TUNEL at 24 h after reperfusion, suggesting that Zn^{2+} accumulation exacerbates I/R injury through inflammatory response and inflammation-mediated neuronal apoptosis.

IL-10 inhibits the production of proinflammatory cytokines as shown by the development of hyper-inflammation and autoimmunity in IL-10-deficient mice (Frangogiannis et al., 2000; Yao et al., 2008; Jung et al., 2017). In animal models of cerebral ischemia, IL-10 significantly reduced infarct size and neurological deficits (Ooboshi et al., 2005; Jung et al., 2017). Our study found that IL-10-positive cells were largely colocalized with NeuN, and IL-10 expression decreased at 24 h after I/R compared with the sham group, indicating that along with the expression of proinflammatory factors increasing, the expression of anti-inflammatory factors decreased after cerebral ischemia. Besides, we found an obvious increase in IL-10 levels after TPEN treatment, suggesting that inhibition of Zn^{2+} accumulation has anti-inflammatory effect. Therefore, we speculated that high concentrations of Zn^{2+} might influence the expression of anti-inflammatory factors to promote inflammatory response, which in turn aggravates I/R neuronal injury. Although we demonstrated that ischemia-induced Zn^{2+} accumulation in MCAO rats could exacerbate cerebral I/R injury by promoting inflammation, further studies on the cellular and ionic mechanisms underlying the effects of Zn^{2+} on inflammatory factors should be investigated.

In summary, our results clearly demonstrated that cerebral I/R injury induced the upregulation of proinflammatory factors at 6 and 24 h post reperfusion, and downregulated anti-inflammatory factor at 24 h post reperfusion. More importantly, ischemia induced high concentration of Zn^{2+} caused inflammatory apoptosis in neurons, indicating that Zn^{2+} accumulation is an important inducement of inflammatory response and brain injury in ischemic stroke. Our study provided the evidence that Zn^{2+} accumulation following cerebral ischemia induced neuronal inflammation, and inflammation-mediated neuronal apoptosis, which provides an important mechanism of brain injury by Zn^{2+} following cerebral ischemia.

Data availability statement

The datasets presented in this study can be found in online repositories. The names of the repository/repositories and accession number(s) can be found in the article.

Ethics statement

The animal study was reviewed and approved by the Institutional Animal Care and Use Committee of Xuanwu Hospital of Capital Medical University.

Author contributions

WL: investigation, methodology, visualization, writing—original draft. XY: data curation, visualization, methodology, and investigation. MD: data curation, resources, and investigation. WS: investigation, writing—review and editing. YH: investigation, resources. QA: investigation. ZQ: supervision, writing—review and editing. YZ: conceptualization, supervision, resources, methodology, writing—review and editing. All authors contributed to the article and approved the submitted version.

Funding

This study was supported by grants from the National Natural Science Foundation of China (No. 81971095, 82271308).

Conflict of interest

The authors declare that the research was conducted in the absence of any commercial or financial relationships that could be construed as a potential conflict of interest.

Publisher's note

All claims expressed in this article are solely those of the authors and do not necessarily represent those of their affiliated organizations, or those of the publisher, the editors and the reviewers. Any product that may be evaluated in this article, or claim that may be made by its manufacturer, is not guaranteed or endorsed by the publisher.

References

Alvarez, E. O., Sacchi, O. J., and Ratti, S. G. (2021). The inorganic chemicals that surround us: role of tellurium, selenium and zinc on behavioural functions in mammals. *J. Neurorestoratol.* 9, 151–163. doi: 10.26599/jnr.2021.9040015

Baltaci, A. K., Mogulkoc, R., and Baltaci, S. B. (2019). Review: the role of zinc in the endocrine system. *Pak. J. Pharm. Sci* 32, 231–239.

Baltaci, S. B., Unal, O., Gulbahce-Mutlu, E., Gumus, H., Pehlivanoglu, S., Yardimci, A., et al. (2022). The role of zinc status on spatial memory, hippocampal synaptic plasticity and insulin signaling in icv-STZ-induced sporadic Alzheimer's-like disease in rats. *Biol. Trace Elem. Res.* 200, 4068–4078. doi: 10.1007/s12011-021-02999-2

Berti, R., Williams, A. J., Moffett, J. R., Hale, S. L., Velarde, L. C., Elliott, P. J., et al. (2002). Quantitative real-time RT-PCR analysis of inflammatory gene expression associated with ischemia-reperfusion brain injury. *J. Cereb. Blood Flow. Metab.* 22, 1068–1079. doi: 10.1097/00004647-200209000-00004

Bonaventura, P., Bonaventura, P., Benedetti, G., Albarède, F., and Miossec, P. (2015). Zinc and its role in immunity and inflammation. *Autoimmun. Rev.* 14, 277–285. doi: 10.1016/j.autrev.2014.11.008

Chen, F. E., Chen, F. E., Huang, D. B., Chen, Y. Q., and Ghosh, G. (1998). Crystal structure of p50/p65 heterodimer of transcription factor NF-κB bound to DNA. *Nature* 391, 410–413. doi: 10.1038/34956

Chen, H. G., Xie, K. L., Han, H. Z., Wang, W. N., Liu, D. Q., Wang, G. L., et al. (2013). Heme oxygenase-1 mediates the anti-inflammatory effect of molecular hydrogen in LPS-stimulated RAW 264.7 macrophages. *Int. J. Surg.* 11, 1060–1066. doi: 10.1016/j.ijsu.2013.10.007

Dong, W., Qi, Z., Liang, J., Shi, W., Zhao, Y., Luo, Y., et al. (2015). Reduction of zinc accumulation in mitochondria contributes to decreased cerebral ischemic injury by normobaric hyperoxia treatment in an experimental stroke model. *Exp. Neurol.* 272, 181–189. doi: 10.1016/j.expneurol.2015.04.005

Eddie-Amadi, B. F., Eddie-Amadi, B. F., Ezejiofor, A. N., Orish, C. N., and Orisakwe, O. E. (2022). Zinc and selenium mitigated heavy metals mixture (Pb, Al, Hg and Mn) mediated hepatic-nephropathy *via* modulation of oxido-inflammatory status and NF-kB signaling in female albino rats. *Toxicology* 481:153350. doi: 10.1016/j.tox.2022.153350

Frangogiannis, N. G., Mendoza, L. H., Lindsey, M. L., Ballantyne, C. M., Michael, L. H., Smith, C. W., et al. (2000). IL-10 is induced in the reperfused myocardium and may modulate the reaction to injury. *J. Immunol.* 165, 2798–2808. doi: 10.4049/jimmunol.165.5.2798

Galasso, S. L., and Dyck, R. H. (2007). The role of zinc in cerebral ischemia. *Mol. Med.* 13, 380–387.

Garcia, J. M., Stillings, S. A., Leclerc, J. L., Phillips, H., Edwards, N. J., Robicsek, S. A., et al. (2017). Role of interleukin-10 in acute brain injuries. *Front. Neurol.* 8:244. doi: 10.3389/fneur.2017.00244

Gulbahce-Mutlu, E., Gulbahce-Mutlu, E., Baltaci, S. B., Menevse, E., Mogulkoc, R., Baltaci, A. K., et al. (2021). The effect of zinc and melatonin administration on lipid peroxidation, IL-6 levels and element metabolism in DMBA-induced breast cancer in rats. *Biol. Trace Elem. Res.* 199, 1044–1051. doi: 10.1007/s12011-020-02238-0

Guo, M., Lu, H., Qin, J., Qu, S., Wang, W., Guo, Y., et al. (2019). Biochanin a provides neuroprotection against cerebral ischemia/reperfusion injury by Nrf2-mediated inhibition of oxidative stress and inflammation signaling pathway in rats. *Med. Sci. Monit.* 25, 8975–8983. doi: 10.12659/MSM.918665

Haase, H., and Rink, L. (2014). Zinc signals and immune function. *Biofactors* 40, 27–40. doi: 10.1002/biof.1114

Haase, H., Ober-Blöbaum, J. L., Engelhardt, G., Hebel, S., Heit, A., Heine, H., et al. (2008). Zinc signals are essential for lipopolysaccharide-induced signal transduction in monocytes. *J. Immunol.* 181, 6491–6502. doi: 10.4049/jimmunol.181.9.6491

Hotter, B., Hotter, B., Hoffmann, S., Ulm, L., Meisel, C., Fiebach, J. B., et al. (2019). IL-6 plasma levels correlate with cerebral perfusion deficits and infarct sizes in stroke patients without associated infections. *Front. Neurol.* 10:83. doi: 10.3389/fneur.2019.00083

Huang, W. C., and Hung, M. C. (2013). Beyond NF-κB activation: nuclear functions of IκB kinase α. *J. Biomed. Sci.* 20:3. doi: 10.1186/1423-0127-20-3

Hussain, T., Hussain, T., Tan, B., Yin, Y., Blachier, F., Tossou, M. C., et al. (2016). Oxidative stress and inflammation: what polyphenols can do for us. *Oxid. Med. Cell Longev.* 2016:7432797. doi: 10.1155/2016/7432797

Jarosz, M., Jarosz, M., Olbert, M., Wyszogrodzka, G., Młyniec, K., Librowski, T., et al. (2017). Antioxidant and anti-inflammatory effects of zinc. zinc-dependent NF-κB signaling. *Inflammopharmacology* 25, 11–24. doi: 10.1007/s10787-017-0309-4

Jenny, N. S., Jenny, N. S., Callas, P. W., Judd, S. E., McClure, L. A., Kissela, B., et al. (2019). Inflammatory cytokines and ischemic stroke risk: the REGARDS cohort. *Neurology* 92, e2375–e2384. doi: 10.1212/WNL.0000000000007416

Jung, M., Ma, Y., Iyer, R. P., DeLeon-Pennell, K. Y., Yabluchanskiy, A., Garrett, M. R., et al. (2017). IL-10 improves cardiac remodeling after myocardial infarction by stimulating M2 macrophage polarization and fibroblast activation. *Basic Res. Cardiol.* 112:33. doi: 10.1007/s00395-017-0622-5

Kang, R., Kang, R., Li, R., Dai, P., Li, Z., Li, Y., et al. (2019). Deoxynivalenol induced apoptosis and inflammation of IPEC-J2 cells by promoting ROS production. *Environ. Pollut.* 251, 689–698. doi: 10.1016/j.envpol.2019.05.026

Kim, S. W., Kim, S. W., Lee, H., Lee, H. K., Kim, I. D., Lee, J. K., et al. (2019). Neutrophil extracellular trap induced by HMGB1 exacerbates damages in the ischemic brain. *Acta Neuropathol. Commun.* 7:94. doi: 10.1186/s40478-019-0747-x

Kumari, N., Kumari, N., Dwarakanath, B. S., Das, A., and Bhatt, A. N. (2016). Role of interleukin-6 in cancer progression and therapeutic resistance. *Tumour Biol.* 37, 11553–11572. doi: 10.1007/s13277-016-5098-7

Lambertsen, K. L., Biber, K., and Finsen, B. (2012). Inflammatory cytokines in experimental and human stroke. *J. Cereb. Blood Flow Metab.* 32, 1677–1698. doi: 10.1038/jcbfm.2012.88

Lambertsen, K. L., Finsen, B., and Clausen, B. H. (2019). Post-stroke inflammation-target or tool for therapy. *Acta Neuropathol.* 137, 693–714. doi: 10.1007/s00401-018-1930-z

Li, B., Lu, Y., Wang, R., Xu, T., Lei, X., Jin, H., et al. (2022). MiR-29c inhibits TNF-α-induced ROS production and apoptosis in mouse hippocampal HT22 cell line. *Neurochem. Res.* 48, 519–536. doi: 10.1007/s11064-022-03776-w

Li, T., Zhao, J., and Gao, H. (2022). Depletion of Arg1-positive microglia/macrophages exacerbates cerebral ischemic damage by facilitating the inflammatory response. *Int. J. Mol. Sci.* 23:13055. doi: 10.3390/ijms232113055

Lively, S., Hutchings, S., and Schlichter, L. C. (2016). Molecular and cellular responses to interleukin-4 treatment in a rat model of transient ischemia. *J. Neuropathol. Exp. Neurol.* 75, 1058–1071. doi: 10.1093/jnen/nlw081

Manzanero, S., Santro, T., and Arumugam, T. V. (2013). Neuronal oxidative stress in acute ischemic stroke: sources and contribution to cell injury. *Neurochem. Int.* 62, 712–718. doi: 10.1016/j.neuint.2012.11.009

Matsui, N., Kasajima, K., Hada, M., Nagata, T., Senga, N., Yasui, Y., et al. (2005). Inhibiton of NF-κB activation during ischemia reduces hepatic ischemia/reperfusion injury in rats. *J. Toxicol. Sci.* 30, 103–110. doi: 10.2131/jts.30.103

Mutlu, E. G., and Baltaci, S. B. (2020). Zinc and melatonin supplementation ameliorates brain cortex tissue damage in DMBA-induced breast cancer in rats. *Bratislava Med. J.* 121, 749–752. doi: 10.4149/BLL_2020_122

Olechnowicz, J., Olechnowicz, J., Tinkov, A., Skalny, A., and Suliburska, J. (2018). Zinc status is associated with inflammation, oxidative stress, lipid and glucose metabolism. *J. Physiol. Sci.* 68, 19–31. doi: 10.1007/s12576-017-0571-7

Ooboshi, H., Ibayashi, S., Shichita, T., Kumai, Y., Takada, J., Ago, T., et al. (2005). Postischemic gene transfer of interleukin-10 protects against both focal and global brain ischemia. *Circulation* 111, 913–919. doi: 10.1161/01.CIR.0000155622.68580.DC

Perkins, N. D. (2007). Integrating cell-signalling pathways with NF-κB and IKK function. *Nat. Rev. Mol. Cell Biol.* 8, 49–62. doi: 10.1038/nrm2083

Prasad, A. S. (2012). Discovery of human zinc deficiency: 50 years later. *J. Trace Elem. Med. Biol.* 26, 66–69. doi: 10.1016/j.jtemb.2012.04.004

Prasad, A. S., Prasad, A. S., Bao, B., Beck, F. W., and Sarkar, F. H. (2011). Zinc-suppressed inflammatory cytokines by induction of A20-mediated inhibition of nuclear factor-κB. *Nutrition* 27, 816–823. doi: 10.1016/j.nut.2010.08.010

Qi, Z., Liang, J., Pan, R., Dong, W., Shen, J., Yang, Y., et al. (2016). Zinc contributes to acute cerebral ischemia-induced blood-brain barrier disruption. *Neurobiol. Dis.* 95, 12–21. doi: 10.1016/j.nbd.2016.07.003

Qi, Z., Qi, Z., Shi, W., Zhao, Y., Ji, X., Liu, K. J., et al. (2019). Zinc accumulation in mitochondria promotes ischemia-induced BBB disruption through Drp1-dependent mitochondria fission. *Toxicol. Appl. Pharmacol.* 377:114601. doi: 10.1016/j.taap.2019.114601

Rasmussen, R., Bache, S., Stavngaard, T., and Møller, K. (2019). Plasma Levels of IL-6, IL-8, IL-10, ICAM-1, VCAM-1, IFNγ and TNFα are not associated with delayed cerebral ischemia, cerebral vasospasm, or clinical outcome in patients with subarachnoid hemorrhage. *World Neurosurg.* 128, e1131–e1136. doi: 10.1016/j.wneu.2019.05.102

Ridwan, S., Grote, A., and Simon, M. (2021). Interleukin 6 in cerebrospinal fluid is a biomarker for delayed cerebral ischemia (DCI) related infarctions after aneurysmal subarachnoid hemorrhage. *Sci. Rep.* 11:12. doi: 10.1038/s41598-020-79586-3

Sensi, S. L., Sensi, S. L., Paoletti, P., Koh, J. Y., Aizenman, E., Bush, A. I., et al. (2011). The neurophysiology and pathology of brain zinc. *J. Neurosci.* 31, 16076–16085. doi: 10.1523/JNEUROSCI.3454-11.2011

Shen, Q. Q., Shen, Q. Q., Wang, W., Wu, H., and Tong, X. W. (2022). The effect of edaravone combined with DL-3-N-butylphthalide on the levels of tumor necrosis factor-alpha, interleukin-10, neuron-specific enolase and effect in patients with acute cerebral infarction. *J. Physiol. Pharmacol.* 73, 371–376. doi: 10.26402/jpp.2022.3.05

Traenckner, E. B., Wilk, S., and Baeuerle, P. A. (1994). A proteasome inhibitor prevents activation of NF-kappa B and stabilizes a newly phosphorylated form of I kappa B-alpha that is still bound to NF-kappa B. *EMBO J.* 13, 5433–5441. doi: 10.1002/j.1460-2075.1994.tb06878.x

Vila, N., Vila, N., Castillo, J., Dávalos, A., and Chamorro, A. (2000). Proinflammatory cytokines and early neurological worsening in ischemic stroke. *Stroke* 31, 2325–2329. doi: 10.1161/01.str.31.10.2325

von Bulow, V., Dubben, S., Engelhardt, G., Hebel, S., Plümäkers, B., Heine, H., et al. (2007). Zinc-dependent suppression of TNF-α production is mediated by protein kinase A-induced inhibition of Raf-1, IκB kinase β and NF-κB. *J. Immunol.* 179, 4180–4186. doi: 10.4049/jimmunol.179.6.4180

Wang, W. M., Liu, Z., Liu, A. J., Wang, Y. X., Wang, H. G., An, D., et al. (2015). The zinc ion chelating agent TPEN attenuates neuronal death/apoptosis caused by hypoxia/ischemia *via* mediating the pathophysiological cascade including excitotoxicity, oxidative stress and inflammation. *CNS Neurosci. Ther.* 21, 708–717. doi: 10.1111/cns.12428

Yao, L., Yao, L., Huang, K., Huang, D., Wang, J., Guo, H., et al. (2008). Acute myocardial infarction induced increases in plasma tumor necrosis factor-α and interleukin-10 are associated with the activation of poly(ADP-ribose) polymerase of circulating mononuclear cell. *Int. J. Cardiol.* 123, 366–368. doi: 10.1016/j.ijcard.2007.06.069

Zabel, U., Schreck, R., and Baeuerle, P. A. (1991). DNA binding of purified transcription factor NF-κB. Affinity, specificity, Zn^{2+} dependence and differential half-site recognition. *J. Biol. Chem.* 266, 252–260.

Zhang, B., Zhang, B., Gao, M., Shen, J., and He, D. (2017). Inhaled methane protects rats against neurological dysfunction induced by cerebral ischemia and reperfusion injury: PI3K/Akt/HO-1 pathway involved. *Arch. Med. Res.* 48, 520–525. doi: 10.1016/j.arcmed.2018.01.001

Zhang, W., Potrovita, I., Tarabin, V., Herrmann, O., Beer, V., Weih, F., et al. (2005). Neuronal activation of NF-κB contributes to cell death in cerebral ischemia. *J. Cereb. Blood Flow. Metab.* 25, 30–40. doi: 10.1038/sj.jcbfm.9600004

Zhao, H., Liu, D., Yan, Q., Bian, X., Yu, J., Wang, J., et al. (2021). Endoplasmic reticulum stress/Ca^{2+}-calmodulin-dependent protein kinase/signal transducer and activator of transcription 3 pathway plays a role in the regulation of cellular zinc deficiency in myocardial ischemia/reperfusion injury. *Front. Physiol.* 12:736920. doi: 10.3389/fphys.2021.736920

Zhao, Y., Pan, R., Li, S., Luo, Y., Yan, F., Yin, J., et al. (2014). Chelating intracellularly accumulated zinc decreased ischemic brain injury through reducing neuronal apoptotic death. *Stroke* 45, 1139–1147. doi: 10.1161/STROKEAHA.113.004296

Zhao, Y., Yan, F., Yin, J., Pan, R., Shi, W., Qi, Z., et al. (2018). Synergistic interaction between zinc and reactive oxygen species amplifies ischemic brain injury in rats. *Stroke* 49, 2200–2210. doi: 10.1161/STROKEAHA.118.021179

Zhao, Y., Zhao, Y., Ding, M., Yang, N., Huang, Y., Sun, C., et al. (2022). Zinc accumulation aggravates cerebral ischemia/reperfusion injury through inducing endoplasmic reticulum stress. *Neurochem. Res.* 47, 1419–1428. doi: 10.1007/s11064-022-03536-w

Zhou, Y., Medik, Y. B., Patel, B., Zamler, D. B., Chen, S., Chapman, T., et al. (2023). Intestinal toxicity to CTLA-4 blockade driven by IL-6 and myeloid infiltration. *J. Exp. Med.* 220:e20221333. doi: 10.1084/jem.20221333

Frontiers in
Cellular Neuroscience

Leading research in cellular mechanisms underlying brain function and development

Part of the world's most cited neuroscience journal series that advances our understanding of the cellular mechanisms underlying cell function in the nervous system across all species.

Discover the latest Research Topics

See more →

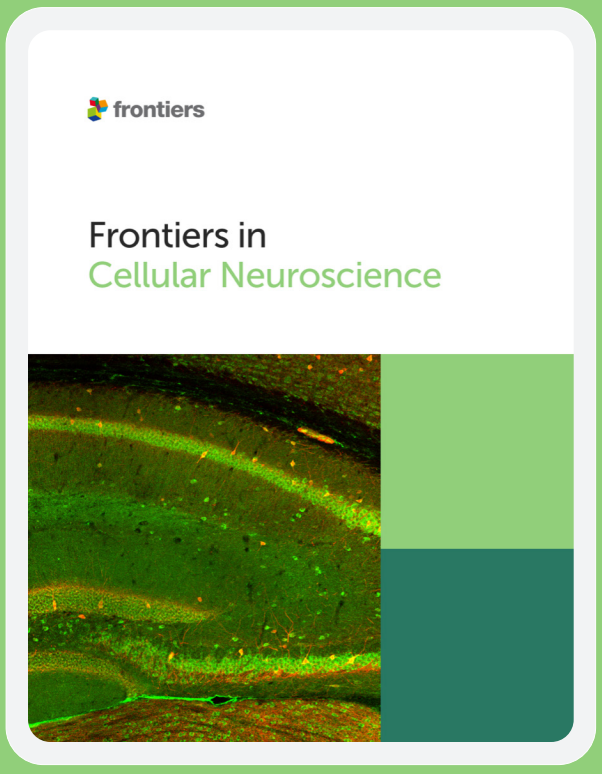

Frontiers

Avenue du Tribunal-Fédéral 34
1005 Lausanne, Switzerland
frontiersin.org

Contact us

+41 (0)21 510 17 00
frontiersin.org/about/contact